

**CLASSIFYING SINGLE-THREAD
RIVERS: A EUROPEAN
PERSPECTIVE**

QUEEN MARY UNIVERSITY OF LONDON
SCHOOL OF GEOGRAPHY


PRIMA WORO SEKARSARI

SUBMITTED IN PARTIAL FULFILLMENT OF THE REQUIREMENTS OF THE
DEGREE OF DOCTOR OF PHILOSOPHY

MARCH 2015

STATEMENT OF ORIGINALITY

I confirm that the work here presented is my own. Information derived from other sources is indicated in the thesis.

Signed:  _____

Date: 20 March 2015

PhD in River Science

Research for this thesis was conducted within the framework of SMART (Science for Management of Rivers and their Tidal systems), which is an Erasmus Mundus Joint Doctoral Programme (EMJD).

EMJDs aim to foster cooperation between higher education institutions and academic staff in Europe and third countries with a view to creating centres of excellence and providing a highly skilled 21st century workforce enabled to lead social, cultural and economic developments. All EMJDs involve mandatory mobility between the universities in the consortia and lead to the award of recognised joint, double or multiple degrees.

The SMART programme represents a collaboration among The University of Trento, Queen Mary University of London, and Freie University Berlin. Each doctoral student within the SMART programme has conformed to the following during their 3 years of study:

- (i) Supervision by a minimum of two supervisors in two institutions (their primary and secondary institutions).
- (ii) Study for a minimum period of 6 months at their secondary institution
- (iii) Successful completion of a minimum of 30 ECTS of taught courses
- (iv) Collaboration with an associate partner to develop a particular component / application of their research that is of mutual interest.
- (v) Submission of a thesis within 3 years of commencing the programme.

ABSTRACT

This thesis develops and tests a classification of ‘near-natural’ European single-thread rivers, which are free to adjust to fluvial processes. The research involves subdividing rivers along a continuum of geomorphological characteristics to assign river reaches to geomorphologically-meaningful classes according to their channel dimensions and forms, and floodplain characteristics.

The classification was developed and tested through three research components.

First, a preliminary classification was developed using information entirely derived from a new information system containing remotely-sensed imagery and digital terrain data: Google Earth. This research stage required the development of rules for identifying, extracting and standardising information from this source for a large sample of river reaches. 221 single-thread river reaches distributed across 75 European rivers were investigated. Analysis of the derived information resulted in the development of a classification comprising six classes of European single thread river.

Second, the robustness of the classification was explored including assessments of (i) the degree to which the classes were interpretable in relation to the geomorphic features they displayed; (ii) the degree to which sub-divisions of the six classes could be identified and justified; (iii) the accuracy of some specific types of information extracted from Google Earth; and (iv) the degree to which the six classes corresponded to expected gradients in two controlling variables: stream power and bed sediment calibre.

Thirdly, bar theory was applied to a sample of rivers representative of the six classes. Since bars are an important contributor to river channel form and dynamics, the correspondence of the bars in the six river classes to their expected distribution as indicated by bar theory, provided further confirmation of the robustness of the classification.

The outputs of the research are (i) a fully-tested classification of European single-thread rivers; and (ii) a demonstration of how Google Earth can provide valuable information for research in fluvial geomorphology. Some additional future research stages are proposed that could turn the classification into an operational tool in the context of river assessment and management.

CONTENTS

Statement of Originality	1
Abstract	3
Contents	5
Table of Figures	9
Table of Tables.....	15
Attribution Page	18
Acknowledgements	19
1 Chapter 1 Introduction	21
1.1 Rationale.....	21
1.2 River Classification	24
1.3 The Research	24
2 Chapter 2 Literature Review	26
2.1 Introduction	26
2.2 Channel patterns	26
2.2.1 Channel pattern classification	26
2.2.2 A channel style continuum.....	31
2.3 Single-thread rivers: planform and controlling factors	34
2.3.1 Characteristics of sinuous to fully meandering rivers.....	35
2.3.2 Key factors controlling meandering.....	46
2.4 Single-thread rivers: bars and other geomorphological features.....	49
2.5 Research questions	62
3 Chapter 3 A preliminary classification of single-thread European rivers using European data extracted from Google™ Earth.....	64
3.1 Introduction	64

3.2	Research Context.....	64
3.2.1	Geomorphological Classification of Rivers	64
3.2.2	Design and Measurement Quality	67
3.2.3	Geospatial Data	68
3.3	Methods	70
3.3.1	Site selection	71
3.3.2	Defining relevant geomorphological, vegetation, and channel geometry features to support consistent data extraction	75
3.3.3	Data extraction and preparation	89
3.3.4	Statistical analysis	97
3.4	Results	100
3.4.1	Principal Components Analysis (PCA).....	100
3.4.2	Agglomerative Hierarchical Cluster Analysis (AHC)	105
3.5	Discussion	116
3.5.1	Interpreting the River Classification	116
3.5.2	Google Earth as a Data Source for River Science.....	117
4	Chapter 4 Exploring the robustness of the classification	121
4.1	Introduction	121
4.2	Properties of the six classes of river	122
4.2.1	Geographical distributions of reaches within the six classes	122
4.2.2	Frequency distributions of channel and floodplain properties within the six river classes	124
4.3	Is subdivision of the 6 classes informative.....	132
4.4	Assessment of the accuracy of elevation data extracted from Google Earth .	138
4.5	Influence of the image selected on river reach classification.....	143
4.6	Impact of including additional variables from other data sources	149
4.6.1	River flow data.....	149
4.6.2	Sediment data	159
4.7	Summary	167

4.8	Application of the Classification to Restored River reaches in England	170
5	Chapter 5 Embedding theoretical morphodynamics ‘bar theory’ into the classification of single-thread rivers	176
5.1	Introduction	176
5.2	Methods	182
5.2.1	Problem formulation	182
5.2.2	Sediment load predictors	184
5.2.3	Linear solution	185
5.2.4	Input data.....	188
5.2.5	Assumptions.....	195
5.3	Implications of morphodynamic “Bar” Theory for single-thread rivers	196
5.3.1	Behaviour of the values of theoretical parameters across the five classes of river reach.....	196
5.3.2	Geomorphic and vegetation features observed within reaches associated with the three theoretical regimes	200
5.4	Sensitivity of outcomes to input variables	203
5.4.1	Choice of bar forming discharge value	203
5.4.2	Sediment predictors.....	206
5.5	Discussion and Conclusions	212
6	Chapter 6 Discussion	214
6.1	Introduction	214
6.2	Research results	214
6.2.1	Can a geomorphologically-interpretable classification of single-thread sinuous to meandering European rivers be compiled using data extracted from aerial imagery (Chapter 3)?.....	215
6.2.2	To what extent does the classification remain robust, when tested using data sets from other information sources (Chapter 4)?	219
6.2.3	To what extent does the classification based on information extracted from aerial imagery correspond to a classification of single-thread rivers based on theory (Chapter 5)?	221

6.3	Discussion of the Research Outcomes	222
6.3.1	Scientific Advances in Relation to Previous River Classification Research 222	
6.3.2	Links between the Google Earth classification and bar theory.....	232
6.3.3	The usefulness of the Google Earth classification and its potential application in Management.....	233
6.4	Limitations of the research	236
6.4.1	Google Earth as a data source	236
6.4.2	Thorough testing of the classification	237
6.5	Recommendations for future research.....	240
6.5.1	Increasing the size and quality of the data set.....	240
6.5.2	Increasing the complexity of the classification.....	240
6.5.3	Developing the classification into an applicable tool for river managers 240	
6.5.4	Applying the classification in practice.....	241
6.5.5	Linking the classification to theory.....	241
6.6	Conclusion.....	242
7	References	243
8	Appendix: Full data set extracted from Google Earth Images.....	260

TABLE OF FIGURES

Figure 1.1 Examples of European rivers of different planform. A. Narew, Poland; B. Frome, England; C. Towy, Wales; D. Loire, France; E. Tagliamento, Italy; F. Val Roseg, Switzerland.....	22
Figure 2.1 Classification of channel patterns (from Church, 2006, from Schumm, 1985 and Church, 1992).....	27
Figure 2.2 Classification of degree of meandering (from Kellerhals et al., 1976)	29
Figure 2.3 Alluvial river classification of single thread and related anabranching systems (from Nanson and Knighton, 1966).....	30
Figure 2.4 Values of channel slope and bankful discharge from various natural channels and a proposed threshold between braided and meandering channel planforms (from Leopold and Wolman, 1957).....	32
Figure 2.5 Discrimination of straight, meandering and braided channels and also the degree of braiding based on the ratios of slope:Froude number and depth:width (from Parker, 1976).....	33
Figure 2.6 Channel patterns in relation to gradients in grain size and unit stream power (from Kleinhans and Van den Berg, 2011)	34
Figure 2.7 Planimetric and cross sectional form of a meandering river (from Morisawa, 1985)	35
Figure 2.8 Meander geometry sketch (from Leopold et al., 1964)	37
Figure 2.9 Single-thread alluvial river patterns with classes categorized according to the distribution and degree of spatial variation in channel width (modified from Brice, 1975 by Lagasse, et al., 2004).....	38
Figure 2.10 Wave number distribution of bends for wider-at-bends (class C) and equi-width meandering channels (class B ₁) (from Lagasse et al., 2004)	39
Figure 2.11 Meandering patterns: (a) Degree of meandering; (b) Standard sketch of meander bends with key meander properties; (c) Quantifying meander path direction (θ) and change of curvature ($\Delta\theta$): (d) Planform geometry and spatial distribution of curvature (i) regular meander (from Langbein and Leopold, 1966) (ii) irregular meanders of the River Trent (from Ferguson, 1979)	40

Figure 2.12 Meander loop classification with flow direction from left to right (from Brice, 1974).....	41
Figure 2.13 Flow in a meander bend (Leopold and Wolman, 1960; Crosato, 2008).....	42
Figure 2.14 Meander neck cut off process (image credit: Bruce Railsback).....	45
Figure 2.15 Planform stability diagram plotting (a) data from rivers with sparse bank vegetation and (b) data from rivers with dense bank vegetation. (open symbols are meandering rivers and solid symbols are braided rivers; rivers in areas I and III are meandering and braided, respectively, regardless of bank vegetation, whereas rivers in area II will only meander if they have dense, deep-rooted bank vegetation) (from Millar, 2000).	49
Figure 3.1 A hierarchy of spatial scales, illustrating how the character of a river reach, including the geomorphic units that it contains, is influenced by processes cascading through larger spatial units now and in the past, and how the process cascade influences the future character of the reach (from Gurnell et al., 2014).	65
Figure 3.2 An example of three replicate reaches of River Dee, UK, and indicated by yellow, red and light blue lines from upstream to downstream.	72
Figure 3.3 A. Decision tree used to identify sites and reaches for analysis B. Decision tree used to refine the recorded feature set and to record individual features.....	74
Figure 3.4 An example of lateral bar	90
Figure 3.5 A. Instream chute feature B. Floodplain chute feature.....	91
Figure 3.6 A. Bar and B. Bench.....	91
Figure 3.7 Vegetation development.....	92
Figure 3.8 Classes of Riparian Vegetation Complexity.....	93
Figure 3.9 Bank-top Riparian Tree Distribution.....	93
Figure 3.10 AHC Dendrogram based on the scores of 221 river reaches on 10 geomorphologically-informative PCs (the emboldened numbers labelling each cluster correspond to those in the text and the number of reaches (<i>n</i>) in each cluster is indicated in italics).....	106
Figure 3.11 Scatter plot illustrating the scores of reaches within the eight clusters on PC1.1 and PC1.2.	109
Figure 3.12 Scatter plots of reach scores on PC1.1 against PC2.1 (top left), PC3.1 (top right), PC4.1 (bottom left) and PC4.2 (bottom right) coded by cluster membership ...	110
Figure 3.13 Scatter plots of reach scores on PC1.1 against PC5.1 (top left), PC5.2 (top right), PC6.1 (bottom left) and PC6.2 (bottom right) coded by cluster membership ...	111

Figure 3.14 Scatter plots of reach scores on PC1.2 against PC2.1 (top left), PC3.1 (top right), PC4.1 (bottom left) and PC4.2 (bottom right) coded by cluster membership ...	112
Figure 3.15 Scatter plots of reach scores on PC1.2 against PC5.1 (top left), PC5.2 (top right), PC6.1 (bottom left) and PC6.2 (bottom right) coded by cluster membership ...	113
Figure 3.16 Reach scores on aggregate PCs 1 and 2 coded according to cluster membership.....	114
Figure 3.17 Reach scores on aggregate PCs 1 and 3 coded according to cluster membership.....	114
Figure 3.18 Boxplots of emergent macrophyte stand and wood jam frequencies (standardised for reach dimensions) within each reach cluster.....	118
Figure 3.19 Summary of the relative properties of the reach clusters and some example river reaches	120
Figure 4.1 Geographical distributions of the studied reaches according to their class membership.....	123
Figure 4.2 Boxplots illustrating differences in three river dimension variables across the six classes of river reach: A and B: log ₁₀ baseflow channel width and log ₁₀ bankfull channel width; C and D: log ₁₀ baseflow channel slope and log ₁₀ bankfull channel slope; E and F: log ₁₀ baseflow channel sinuosity and log ₁₀ bankfull channel sinuosity	126
Figure 4.3 Boxplots of channel dimension ratios A: Baseflow:Bankfull Width; B: Baseflow:Bankfull Slope; C: Baseflow:Bankfull Sinuosity	127
Figure 4.4 Boxplots illustrating differences in the frequency of six channel bed features, standardised for channel width and reach length, across the six classes of river reach: A. pools; B. riffles; C: cascades; D. waterfalls plus steps; E: exposed boulders; F. bedrock exposures.....	128
Figure 4.5 Boxplots illustrating differences in the frequency of channel marginal bar and bench features, standardised for channel width and reach length, across the six classes of river reach: active (A) and stabilising (B) marginal bars; active (C) and stabilising (D) marginal benches.....	129
Figure 4.6 Boxplots illustrating differences in the frequency of channel-margin-transitional and floodplain features across the six classes of river reach: A. swamp-wetlands; B. water-filled depressions; C. connected side channels; D. dry depressions; E. ridges and swales; F. oxbows.	130

Figure 4.7 Boxplots illustrating differences in vegetation features across the six classes of reach: A. (Riparian) vegetation structure; B. Tree distribution along the bank tops; C. wood accumulations; D. (abundance of) emergent macrophytes.	131
Figure 4.8 Cluster dendrogram showing the original six classes / clusters with the number of reaches (n) contained in each (divided by thick red lines) and the first splits of each cluster (divided by the narrow red lines) with the number of reaches (n) contained in each split.....	133
Figure 4.9 Scatter plot comparing elevation estimates in m.a.s.l. extracted from Google Earth (vertical axes) and Lidar (horizontal axes) data for 25 reaches and 36 points	142
Figure 4.10 Box and whisker plots illustrating the elevation (m.a.s.l.) recorded within the six river classes for all reaches whose elevation was extracted from Google Earth.	142
Figure 4.11 Procedure used to calculate PC scores for the 12 new reaches within the original PCA spaces.	147
Figure 4.12 Changes in plotting position (from O to ×) of 12 reaches for which two images were analysed in relation to the first two PCs of the aggregate PCA and in comparison to the 221 rivers originally analysed.	148
Figure 4.13 Boxplots illustrating variation in discharges of different flood recurrence interval (daily flow data, annual maximum series) according to river class. (A) 2 year flood, (B) 5 year flood, (C) 10 year return period.....	156
Figure 4.14 Boxplots illustrating variations in stream power for discharges of different flood recurrence interval (daily flow data, annual maximum series) according to river class. (A) 2 year flood, (B) 5 year flood, (C) 10 year return period.	157
Figure 4.15 Boxplots illustrating variations in unit stream power for discharges of different flood recurrence interval (daily flow data, annual maximum series) according to river class. (A) 2 year flood, (B) 5 year flood, (C) 10 year return period.....	158
Figure 4.16 Boxplots illustrating bed sediment calibre estimates for British rivers in five of the six river classes. Upper graphs show D_{50} ; lower graphs D_{50B} (includes bedrock data and excludes Findhorn reach 3); left graphs are in phi units; right graphs are in mm.	166
Figure 4.17 PC scores of restored (X symbols) and control (O symbol) reaches in relation to PC1 and PC2 of the integrated PCA (note that the lengths of the axes are much shorter than in the graph representing the original 221 reaches: PC1 was previously plotted in the range -6 to +6 and PC2 in the range -7 to + 3.5).....	173

Figure 5.1 Theoretical regimes according the positioning of β , <i>width-to-depth ratio</i> to the threshold of β_c , <i>aspect ratio critical</i> and β_r , <i>aspect ratio resonant</i>	180
Figure 5.2 A. Amplification of Ω_r and Ω_i versus wavenumber λ , for a fixed θ and d_s and varying β and B. Marginal curve of bar amplification is produced at the crossing of Ω_r and $\Omega_i = 0$	187
Figure 5.3 Illustrative patterns of flow and bed deformation associated with the presence of bars (from Crosato, 2008).....	196
Figure 5.4 Boxplots illustrating channel dimension and sediment properties of reaches across five classes of single-thread river.....	197
Figure 5.5 Scatterplots of β to θ with different symbols identifying: A. Aggregate type (black = gravel, red = sand); B. Sediment predictors (red = Engelund and Hansen, black =Parker); C. Super-resonant and sub-resonant behaviour (red = super-resonant, black = sub-resonant).....	198
Figure 5.6 Boxplots illustrating variations in the values of the computed aspect ratios across the five classes of river reaches: A: aspect ratio, B: β critical, and C: β resonant.	199
Figure 5.7 A and B: Contrasts in A. the difference between the aspect ratio (β) and $\beta_{critical}$ and B. the difference between the aspect ratio (β) and $\beta_{resonant}$, across river classes 1, 3, 4, 5 and 6.....	200
Figure 5.8 Boxplots illustrating values of computed $\beta_{critical}$ (left) and $\beta_{resonant}$ (right) across the 5 investigated classes of river reach when computed using a daily discharge of: A. and D. (Q_2) – the 2 year return period event; B. and E. (Q_5) – the 5 year return period event; C. and F. (Q_{10}) – the 10 year return period event.....	204
Figure 5.9 Boxplots illustrating variation in the values of computed $\beta - \beta_{critical}$ (left) $\beta - \beta_{resonant}$ (right) across the 5 classes of river reaches when computed using discharge of A, D 2-year interval B, E 5-year interval and C, F 10-year interval.....	205
Figure 5.10 Boxplots illustrating variation in the values of Shields range across the 5 classes of river reaches when computed using a daily discharge of: A. 2-year recurrence interval; B. 5-year recurrence interval; and C. 10-year recurrence interval.....	206
Figure 5.11 Sensitivity of the morphodynamic regimes to the choice of different bed load predictors: A. $(\beta - \beta_r)/\beta_r$ B. $(\beta_r - \beta_c)/\beta_r$ C. $(\beta - \beta_c)/\beta_r$. The x-axis is Meyer-Peter Müller, and y-axis in black = Parker (1990) for gravel; red= Engelund and Hansen (1972) for sand.	207
Figure 5.12 Reach scores on aggregate “Google Earth” PC1 plotted against “bar theory” parameters: A. the difference between the aspect ratio (β) and $\beta_{resonant}$; B. the	

difference between the aspect ratio (β) and $\beta_{critical}$, according to morphodynamics regimes	213
Figure 6.1 Summary of the relative properties of the river classes and some example river reaches	218
Figure 6.2 Classification of channel patterns (from Church, 2006).....	226
Figure 6.3 Illustrations of classes of river channel based upon (i) their slope – sinuosity - cross profile - entrenchment (ratio of floodplain width to channel width), horizontally across the diagram, and (ii) their bed material calibre, vertically down the diagram. ..	227

TABLE OF TABLES

Table 1.1 System A and B River Typologies of the Water Framework Directive	23
Table 2.1 Bars and other geomorphic features of river channels and their floodplains (developed from Table 5.7 of Gurnell et al., 2014)	51
Table 3.1 Definitions of geomorphological and vegetation features of rivers and floodplain that were extracted from Google Earth images (yellow arrow/circle in images indicates the geomorphic features, flow direction is consistently from left to right or top to bottom of each image).....	76
Table 3.2 Definitions of channel dimensions that were extracted from Google Earth ..	88
Table 3.3 Aggregate Variables derived from the Raw Variables extracted from Aerial Imagery	96
Table 3.4 Groups of Raw (Table 3.1 and Aggregate Variables (Table 3.3)) subjected to Principal Components Analysis	98
Table 3.5 River Dimensions PCA: Eigenvalues, Variance Explained and Loadings (loadings greater than 0.7 are emboldened)	100
Table 3.6 Dimension Ratios PCA: Eigenvalues, Variance Explained and Loadings (loadings greater than 0.7 are emboldened)	101
Table 3.7 Channel Bed PCA: Eigenvalues, Variance Explained and Loadings (loadings greater than 0.7 are emboldened and those between 0.6 and 0.7 underlined).....	102
Table 3.8 Channel Bar and Bench PCA: Eigenvalues, Variance Explained and Loadings (loadings greater than 0.7 are emboldened and those between 0.6 and 0.7 underlined)	102
Table 3.9 Channel-margin-transitional and Floodplain PCA: Eigenvalues, Variance Explained and Loadings (loadings greater than 0.7 are emboldened and those between 0.6 and 0.7 underlined).....	103
Table 3.10 Vegetation PCA: Eigenvalues, Variance Explained and Loadings (loadings greater than 0.7 are emboldened and those between 0.6 and 0.7 underlined).....	104
Table 3.11 The 10 PCs selected from the 6 PCAs to describe geomorphologically-interpretable gradients in the 75 river data set	104

Table 3.12 Integrated PCA of the scores on the PCs listed in Table 3.11: Eigenvalues, Variance Explained and Loadings (loadings greater than 0.7 are emboldened and those between 0.6 and 0.7 underlined)	105
Table 3.13 Results of Kruskal-Wallis tests applied to the PC scores on the 10 PCs listed in Table 3.11, grouped according to AHC clusters 1, 2, 3A, 3B, 4, 6	108
Table 3.14 Upper and lower quartile values of channel bankfull width, slope and sinuosity of river reaches within each cluster and the degree to which each cluster shows significantly higher (pink shading) or lower (blue shading) than other clusters with respect to each of the 10 PCs.	115
Table 4.1 Groups of Raw and Aggregate Variables describing different properties of the river and its floodplain	125
Table 4.2 Statistically significant differences (Mann-Whitney U test, $P < 0.05$) in reach scores between sub-classes or splits of the original 6 river classes on the 10 PCs that underpin the cluster analysis. Significant differences between the scores on each cluster with Pink shaded cells indicate those subclasses that show statistically significantly larger scores on a particular PC.	134
Table 4.3 Statistically significant differences (Kruskal-Wallis tests) in reach scores within the 6 classes of river on each of the 10 PCs that underpin the classification. The shaded cells indicate classes that show significantly higher (pink) or lower (blue) reach scores than the other classes on each individual PC.	135
Table 4.4 Values of elevation for the same points extracted from Google Earth (nearest m) and Lidar data (nearest cm)	140
Table 4.5 Details of the 12 reaches for which a second image was analysed from a different year and/or different season	143
Table 4.6 Summary information on standardised variables extracted from the images listed in Table 4.5.....	145
Table 4.7 Gauging station names, codes, locations, record lengths and computed 2, 5, 10 year floods (annual series based on daily flows) for 55 rivers.....	150
Table 4.8 58 river reaches for which at least one RHS survey was available (RHS Ids are provided for all surveys that were analysed).....	161
Table 4.9 Spot-check observations of channel substrate calibre, with associated sample sizes and estimates of D_{50} (in phi and mm units) for 58 reaches of British rivers (substrate calibre classes: BE = bedrock; BO = boulder; CO = cobble; P = pebble; GP = gravel-pebble; G = gravel; SA = sand; SI = silt; CL = clay)	163

Table 4.10 Summary information on the four restored reaches selected for analysis (source: www.therrc.co.uk).....	170
Table 4.11 Summary of information extracted from Google Earth images for the 4 restored and 12 control reaches.....	171
Table 5.1 Sediment transport formula implemented on the mathematical analysis	185
Table 5.2 Summary properties of the 5 river classes investigated in this chapter.	189
Table 5.3 Reaches, observed / estimated values of D_{50} , width, slope, sinuosity, Q_2 , Q_5 , Q_{10} and derived estimates of the three parameters (β , θ , d_s) required in the analyses presented in this chapter.....	191
Table 5.4 The number of reaches analysed from each of classes 1, 3, 4, 5 and 6.....	194
Table 5.5 Abbreviations used to refer to the three morphodynamic regimes	200
Table 5.6 Results of Kruskal-Wallis (comparison of k samples) test applied to the geomorphic and vegetational units grouped according to the three regimes in Table 5.2	202
Table 5.7 Output of β_{cr} and β_r (computed using fixed values of θ_{10} and ds_{10}) in different sediment predictors (*MPM=Meyer-Peter Muller, EH= Engelund and Hansen)	208
Table 6.1 Floodplain types identified by Nanson and Croke (1992) that are associated with single-thread rivers.....	229

ATTRIBUTION PAGE

Firstly, I would like to greatly thank GoogleTM Earth which has generously provided the large archive of images across Europe from which I have extracted information. In collaboration with Google, there are companies who provided free and good resolution aerial imagery, they are:

Image Landsat, Infoterra Ltd and Bluesky, Getmapping plc, Digital Globe, IGN France, GeoBasis-DE/BKG, Cnes/Spot Image, Geoimage Austria, Eurosense/Geodis Slovakia, CNES/Austrum, MGGP Aero, Lantmaateriet/Metria, and Geodis Brno.

Secondly, I would like to thank the providers of daily discharge data. They are (1) The National River Flow Archive (NRFA) and (2) The Centre for Ecology and Hydrology (CEH) for British rivers, (3) 'Ministère de l'Ecologie et du Développement Durable' for French rivers, (4) 'Centro de Estudios Hidrográficos' for Spanish rivers.

Lastly, I would like to thank the Environment Agency, who provided the River Habitat Survey (RHS) data, which enabled me to approximate the average bed sediment size for some British rivers.

ACKNOWLEDGEMENTS

Firstly, I would like to thank my main supervisor, Prof. Angela Gurnell, who always conveys a spirit of adventure and excitement in exploring science. She has inspired me in so many ways to continually learn many new things and to easily become absorbed by new encounters. I have also been extremely lucky, that she cared so much and paid very detailed attention to every aspect of my work. Without her guidance and persistent help this dissertation would not have been possible.

I would also like to thank Dr. Guido Zolezzi as my second supervisor, who always shows enthusiasm in theoretical science. The topic has been motivating, yet challenging for me. I was also lucky that he was able to facilitate me with a SMART EMJD scholarship for the second half of the PhD.

I would like to thank Dr. Alex Henshaw as my third supervisor, for providing me with efficient ‘geomorphological’ technical suggestions, fruitful discussions and practical sources of information for this thesis.

I would like to thank Dr. Bob Grabowski for providing me with a tremendous amount of information for British rivers such as LiDAR data, River Habitat Survey data, etc., and also for our motivating discussion about statistical methods in geomorphology.

I would like to thank Dr. Judy England, who provided me with a placement in the Environmental Agency so that I can gain understanding of some recent restoration projects in the United Kingdom.

A big thank you to Dr. Harry Dixon and Dr. Matt Fry from National River Flow Archives who provided me with flow data for Scottish rivers, and Dr. Virginia Garofano Gomez and Jean-Philippe Belliard, for links to access Spanish and French river flow records, respectively.

I also would like to thank Simone Zen, for letting me use his matlab ‘bar theory’ code and his patience in explaining it to me so that I could proceed efficiently during my stay at the University of Trento. I would also like to thank Marco Redolfi for his motivating and enlightening explanations on the topic and his inspiring aptitude in discussing

research. Thanks to Davide Vanzo, for providing me with much information and his didactical instruction, Luca Adami and Umesh Singh for our exciting scientific conversations.

I must express my gratitude to my family, Robert, Triworo and Wisnu, for their support and encouragement of my scientific passion. I was very grateful for their financial aid during the first half of this PhD.

Again, I would also like to personally thank Jean-Philippe Belliard, who constantly encourages me to pursue river science up to the highest degree through SMART EMJD and who supports me in many ways during the process.

I would like to thank the SMART programme in providing this particular joint doctoral program that has enabled me to enrol in different institutions and to grasp an international and inter-disciplinary approach in the thesis, which is not common in a PhD program. Additionally, I would like to give a big thank you specifically to the SMART secretaries, Laura Martuscelli, Marina Rogato, Claudia Fraizingher, for their professional assistance in taking care of the many bureaucratic measures.

Lastly, I would like to thank all of the SMART doctoral candidates for both scientific and non-scientific discussions. It has been three colourful years of information sharing and helping each other, especially during my mobility periods.

CHAPTER 1

INTRODUCTION

1.1 Rationale

In the absence of significant human modification, rivers vary enormously in their form (e.g. Figure 1.1). This variation does not simply reflect the large changes in climate, sediment availability and vegetation that occur from one biogeographical region to another, but also to variations in controlling factors within biogeographical regions and within individual catchments. Variations occur in both space and time and provide the challenging context in which human activities take place and river management strategies are developed. As far as is possible, river restoration and management need to work with these natural variations in river morphodynamics as well as the needs of human populations, in order to achieve cost-effective and sustainable river management solutions.

This thesis aims to contribute to improving river management outcomes, by developing and testing a typology of naturally-functioning single-thread rivers in Europe that is both simple and applicable but also scientifically sound. In order to constrain the research to something that is achievable within a three year PhD programme:

1. The focus is on Europe (i) for practical reasons of data availability, (ii) for scientific reasons, in that Europe covers a large area that incorporates a variety of biogeographical regions which might be expected to contain rivers of many different forms and dynamics; (iii) for management reasons, in that the area of Europe within the European Union is subject to the requirements of the Water Framework Directive, where the currently-applied ‘hydromorphological’ river typologies (A and B) are remarkably simple and actually define *catchment* rather than *river* types, with only the optional factors of system B providing true ‘hydromorphological’ information on the river (Table 1.1).

2. The focus is on single-thread rivers, because this group of river types is most common within Europe, particularly in areas where population density is relatively high and thus river management is a pressing concern.
3. The focus is on classification because this provides a simple framework for identifying the type of river that is of interest and then considering its likely geomorphic features and dynamics in the context of current and future management options.

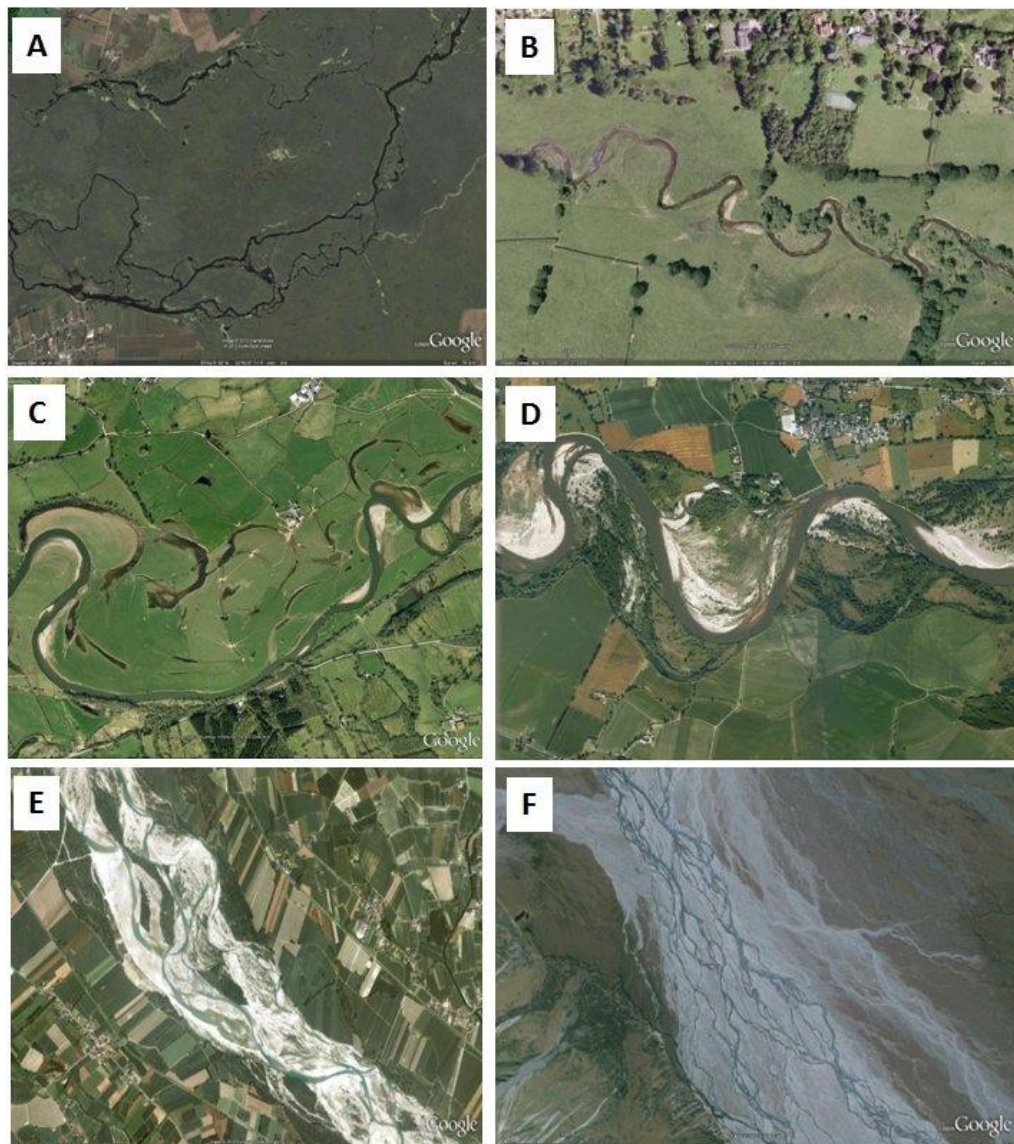


Figure 1.1 Examples of European rivers of different planform. **A.** Narew, Poland; **B.** Frome, England; **C.** Towy, Wales; **D.** Loire, France; **E.** Tagliamento, Italy; **F.** Val Roseg, Switzerland.

Table 1.1 System A and B River Typologies of the Water Framework Directive

SYSTEM A (Fixed typology)	Descriptors	SYSTEM B (Alternative characterisation)	Physical and chemical factors that determine the characteristics of the river or part of the river and hence the biological population structure and composition
Ecoregion	Ecoregions shown on map A in Annex XI	Obligatory factors	altitude
Altitude typology	high: >800 m mid-altitude: 200 to 800 m lowland: <200 m		latitude longitude geology size
Size typology (based on catchment area)	small: 10 to 100 km ² medium: >100 to 1 000 km ² large: >1 000 to 10 000 km ² very large: >10 000 km ²	Optional factors	distance from river source energy of flow (function of flow and slope) mean water width mean water depth mean water slope form and shape of main river bed river discharge (flow) category valley shape transport of solids acid neutralising capacity mean substratum composition chloride air temperature range mean air temperature precipitation
Geology typology	Calcareous Siliceous Organic		

A classificatory approach could be criticised in that it assigns rivers, which possess a continuum of forms and dynamics into discrete classes. However, if applied with care, the typology developed in this thesis should provide a useful tool that can contribute to understanding, designing, restoring and managing rivers in a European context.

1.2 River Classification

An individual river can vary significantly in character over time and from upstream to downstream, showing dramatic changes in pattern and dynamics over short distances. This spatial and temporal variability has long intrigued river engineers, geomorphologists and geologists (Schumm, 2005). Chapter 2 reviews research on this theme, considering various classifications of rivers - their forms, dynamics and controls – and commencing with the work of Leopold and Wolman (1957), who separated rivers into three classes: straight, meandering, braided.

Because of the focus of this research on single thread rivers, the literature review in Chapter 2 commences with a broad appraisal of all river types but then focuses on single thread types and particularly on meandering rivers. Since different styles of river are associated with different geomorphic features, the review concludes by tabulating some of the features that might be indicative of particular processes and styles of rivers, emphasising features that may be identifiable on aerial images, which form the main data source for the present research.

1.3 The Research

In order to build a typology of single-thread rivers that is applicable at European scale, the research depends upon secondary sources of information. Therefore, a major component of the research was to develop and apply methods that could extract robust and consistent data from secondary sources. The core data source was the Google Earth information system, since this offers (i) multi-temporal aerial imagery at European scale and thus detailed information on plan properties of rivers and their floodplains, and also (ii) topographic data that allows some information on the third dimension of river reaches to be extracted. In Chapter 3, a methodology is developed and then used to extract data from Google Earth on the properties of 221 river reaches of 75 European

rivers. This data set is analysed statistically to develop a six-category classification of European rivers.

In Chapter 4 the robustness of the classification is explored by (i) referring back to the raw data extracted from Google Earth to assess whether the classification is geomorphologically meaningful, whether splitting of the classes might be informative and, in the case of the elevation data, (ii) to check its accuracy in comparison with airborne Lidar data; (iii) using additional data on river flows and bed material to assess whether the classification relates in a meaningful way to these ‘control’ variables.

In Chapter 5, the classification developed in Chapter 3 is compared with a classification based on bar theory. This research tests whether interpretations based on the form of natural river reaches correspond to interpretations based on entirely theoretical considerations.

The thesis concludes in Chapter 6 with a summary of the research findings and its shortcomings, and some suggestions for further research.

CHAPTER 2

LITERATURE REVIEW

2.1 Introduction

This chapter reviews the published literature on river channel patterns or styles, with a particular emphasis on single-thread rivers. Following a broad overview of the range of channel patterns that have been identified in the literature (section 2.2), planform and controlling factors of these single-thread rivers are explored (section 2.3). Throughout sections 2.2 and 2.3, a range of geomorphic features are mentioned in relation to different river types, suggesting that recognising an assemblage of such features might form a basis for recognising different types of single-thread river. Therefore, section 2.4 lists and briefly describes some of the features that may be found within river channels and floodplains in a tabular format as a context for developing practical definitions for geomorphic feature extraction from different data sources. The chapter ends (section 2.5) with a perspective on the methodologies that have been employed by researchers whose work is mentioned in this review, and how those methodologies are adopted in the research reported in this thesis to address three broad research questions related to the development of a classification of single thread European rivers.

2.2 Channel patterns

2.2.1 Channel pattern classification

An early assessment of channel pattern types (defined as the river planform or pattern that would be viewed vertically from above the river) was proposed by Leopold and Wolman (1957). They placed meandering rivers as an intermediate river style between braided and relatively straight channels. Therefore, this early work recognized meandering rivers as a core pattern that changed to multi-thread braiding as river bank-full discharge and valley gradient increased.

Since Leopold and Wolman's early classification, the importance of hydraulic properties in controlling river channel patterns has become increasingly recognized, with the range of properties and channel patterns becoming more complex as research has progressed. Thus, it has become recognized that discharge and sediment load primarily control the size of the channel cross section. The importance of the channel width has also been recognized as a crucial element as channel form is influenced by bed and bank resistance to erosion, which in turn reflect sediment grain size as well as sediment load. This latter linkage was recognized by Schumm (1963) in his subdivision of river channels into suspended load, mixed load and bedload types that reflect increasing gradient and width to depth ratio, as well as decreasing sinuosity. Thus the broad channel style in terms of channel geometry and sinuosity reflects feedbacks between discharge, sediment calibre and load, channel gradient, width, depth and sinuosity.

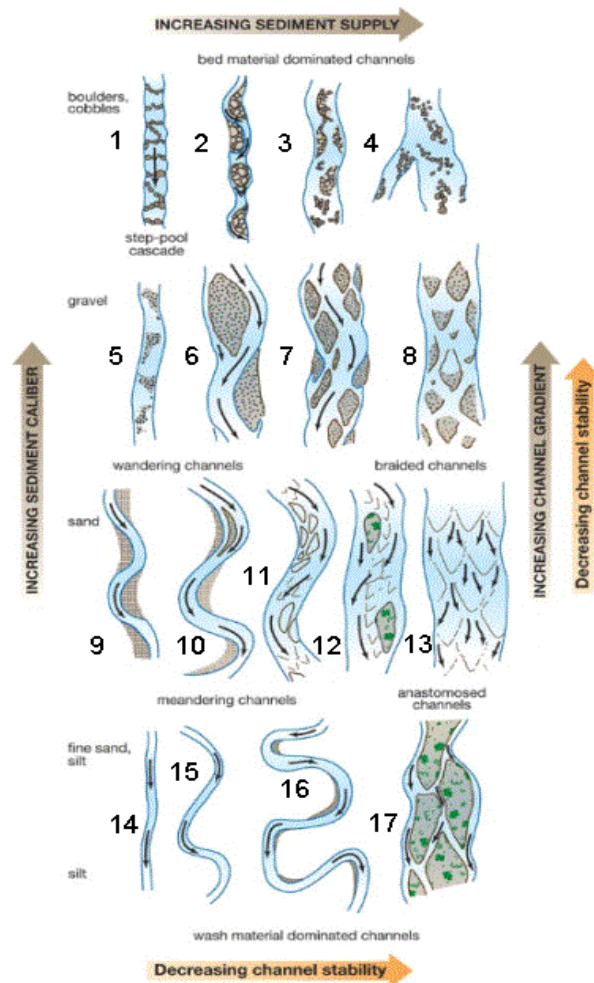


Figure 2.1 Classification of channel patterns (from Church, 2006, from Schumm, 1985 and Church, 1992)

Across all of the channel patterns that have been recognized so far in the literature, two of the original patterns defined by Leopold and Wolman (1957) persist. A single-thread, sinusoidal pattern is still described as meandering, whereas a multi-thread channel supporting multiple mid-channel bars is described as braiding. However Schumm (1981, 1985) and Church (2002) developed additional channel styles that describe gradual rather than abrupt transitions between these two basic types and define additional single-thread and multi-thread patterns that encompass a wider range in the controlling factors (Figure 2.1). Whilst Schumm's three types of load (sediment calibre) provide the fundamental discriminator between the 17 channel types (bed load—types 1-8; mixed load—9-13; and suspended load—types 14-17) displayed in Figure 2.1, gradient and sediment supply (a function of discharge and sediment sources) are also included as controlling factors. Figure 2.1 essentially describes a continuum of styles that can be broadly categorized into single-thread and multi-thread forms.

Single-thread channels include straight and sinuous channels. There are six types of straight channel displayed in Figure 2.1: those with (types 1, 2, 5) or without (type 14) exposed bedforms and with mobile alternating bars (types 6, 9). These grade into 4 types of sinuous channel: slightly sinuous channels of different stability (type 3, 15) and more sinuous, truly meandering channels of different stability (types 10, 16), where stability is essentially a function of sediment calibre (silty banks are more cohesive and stable than sandy-gravelly banks) and sinuosity is quantified (Kellerhals et al., 1976; Knighton, 1998) as:

$$\text{Sinuosity} = (\text{channel length})/(\text{straight-line valley length}) \quad (2.1)$$

Kellerhals et al. (1976) also defined three categories of degree of meandering: irregular meanders (Figure 2.2a); regular meanders with a clear repeating pattern and a maximum deviation angle of $<90^\circ$ (Figure 2.2b); and regular meanders with clear repeating pattern and maximum deviation angle of $>90^\circ$ (Figure 2.2c).

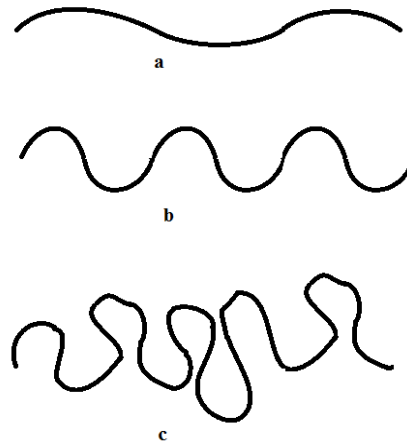


Figure 2.2 Classification of degree of meandering (from Kellerhals et al., 1976)

Multi-thread channels were represented by a single ‘braided’ class by Leopold and Wolman (1957) but these are represented in Figure 2.1 by three main types (7, 8, 13) that vary with sediment calibre and two main transitional, island-braided types (11, 12). Anastomosing rivers (17) form an additional type of multi-thread river (type 17), which consist of multiple channels divided by vegetated, stable islands with no exposed unvegetated bars.

Nanson and Knighton (1966) emphasized links between multi- and single- thread alluvial channels in more detail, implying that there is a multi-thread (anabranching) equivalent of straight, sinuous – meandering and braided patterns (Figure 2.3). They illustrate anastomosing channels as a stable form of straight channel, although a broader definition would classify all laterally-stable multi-thread (anabranching) channels as anastomosing.

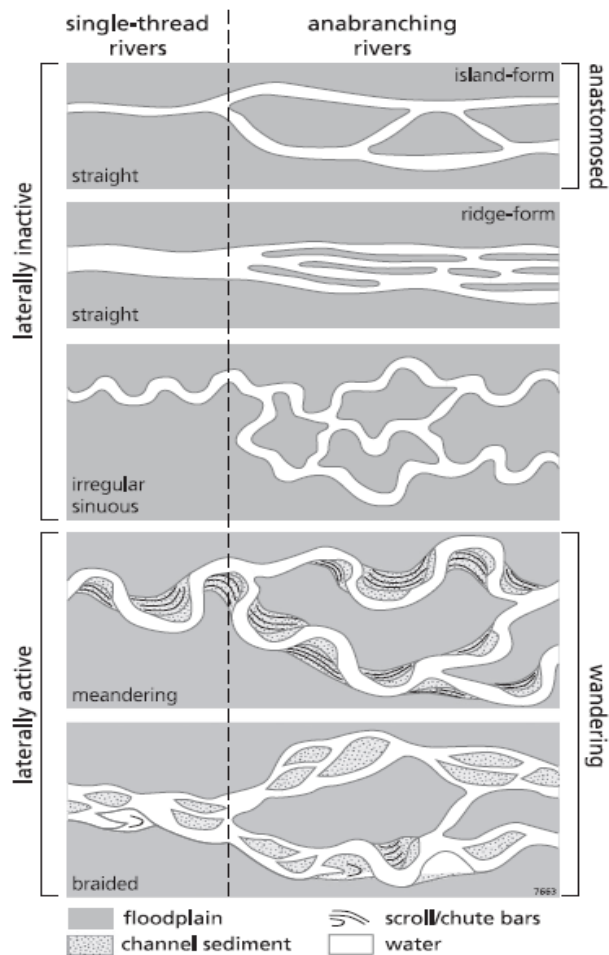


Figure 2.3 Alluvial river classification of single thread and related anabranching systems (from Nanson and Knighton, 1966)

Numerous other river channel planform classifications have been proposed, but they are generally based on one of two broad types of approach: qualitative analyses (e.g. Schumm, 1977; Mosley, 1987) or the estimation of empirically-based thresholds between river styles (e.g. Ferguson, 1987; Van den Berg, 1995). In the latter approaches, key river properties of gradient, discharge, sediment supply, calibre and cohesion have been identified, which are discussed further below. Moreover, although different channel pattern morphologies have been identified (e.g. Figure 2.1), all natural rivers exhibit physical characteristics across a continuous range. Thus, it is important to identify these physical characteristics and understand how they control river channel pattern, recognizing that in reality, rivers follow a continuum of forms rather than being attributable to distinct, rigid classes or types.

2.2.2 A channel style continuum

Despite their three-fold channel pattern classification, Leopold and Wolman (1957) recognized that a continuum of channel styles existed and they tried to locate a transitional zone across which single-thread meandering rivers graded into multi-thread braiding rivers by estimating a power function that linked average channel slope (s) and bankfull discharge (Q_b) (Figure 2.4 and equation (2.2)):

$$s = 0.006 Q_b^{-0.44} \quad (2.2)$$

Subsequent research based on laboratory experiments (Ackers and Charlton, 1970a; Schumm and Khan, 1972; Edgar, 1984) has proposed similar threshold relationships to the one defined by Leopold and Wolman (1957) and also a lower threshold separating straight and meandering channels. Subsequent research has also combined discharge and slope into an integrated index of stream power. Stream power is defined as γQs , where γ is a constant representing water density and gravitational acceleration, Q is a measure of channel-forming (e.g. bankfull) discharge, and s is the channel gradient, whereas unit or specific stream power is defined as $\gamma Qs/w$, where w is the channel width. These measures of stream power have been used to describe the succession of straight to meandering to braided channels along a stream power gradient (e.g. Ferguson, 1987; Carson, 1984). In these analyses, most anastomosing channels plot below the meandering-braided threshold defined in equation (2.2) and also below meandering channels in the plot; suggesting that, like straight channels, they occur at the low end of the flow strength / power continuum (Knighton and Nanson, 1993). Furthermore, Nanson and Croke (1992) separated laterally stable (straight and anastomosing), actively meandering, and braided rivers and floodplains, respectively, according to specific stream power ranges of <10, 10-60, 50-300 W/m².

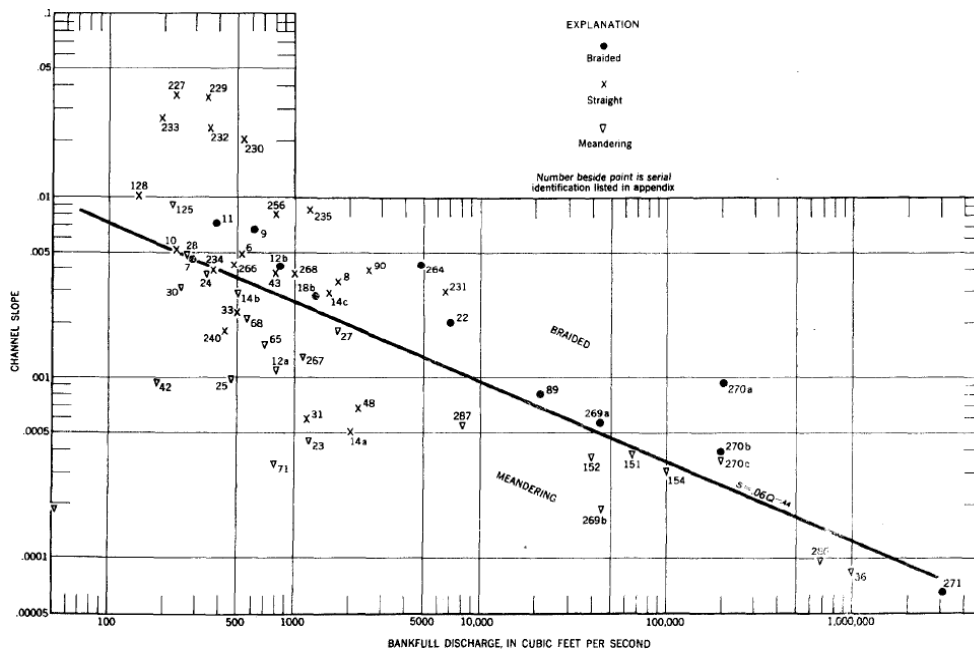


Figure 2.4 Values of channel slope and bankfull discharge from various natural channels and a proposed threshold between braided and meandering channel planforms (from Leopold and Wolman, 1957)

Despite being less easily quantified, sediments are also significant factors determining channel patterns. Schumm (1963) noted an increase in planform sinuosity (S) with an increase in the silt-clay content (M) of the channel boundary sediments:

$$S = 0.94 M^{0.25} \quad (2.3)$$

Bank resistance to erosion determines the ability of streams to shift laterally (Hickin and Nanson, 1984). Active meandering and braiding patterns evolve as a result of bank erosion, with active meandering developing as a result of bend development through bank erosion and deposition on opposing banks, and braiding resulting from channel widening and bend destruction. Straight, stable meandering and anastomosing rivers have been assumed to have stable banks because of their lack of lateral movement (Knighton and Nanson, 1993). Thus, Parker (1976) produced a regime diagram reflecting bank erodibility, which plots sites according to two ratios: width:depth and slope:Froude number (Figure 2.5), where the following equation separates braided from meandering – straight channels.

$$s = Fd/w \quad (2.4)$$

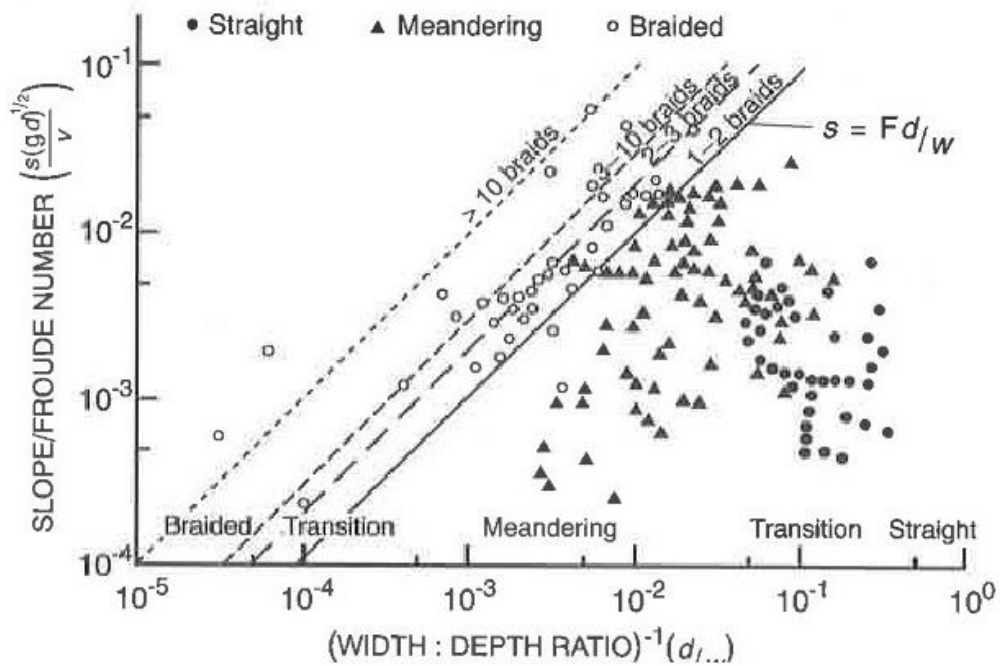


Figure 2.5 Discrimination of straight, meandering and braided channels and also the degree of braiding based on the ratios of slope:Froude number and depth:width (from Parker, 1976)

More recent research on identifying the threshold slope for these channel patterns has also demonstrated how bed material size (D_{50}) determines braided and single-thread channels. Van den Berg (1995) classified braided and sinuous channels ($S > 1.3$) using a plot of specific stream power against median grain size. This approach was extended by introducing a range of landforms associated with these channel styles: scroll bars, chute bars, and scrolled point bars (Figure 2.6).

The discriminator between predominantly braiding and meandering channels (ω_{bm}) was found to be:

$$\omega_{bm} = 900D_{50}^{0.42} \quad (2.5)$$

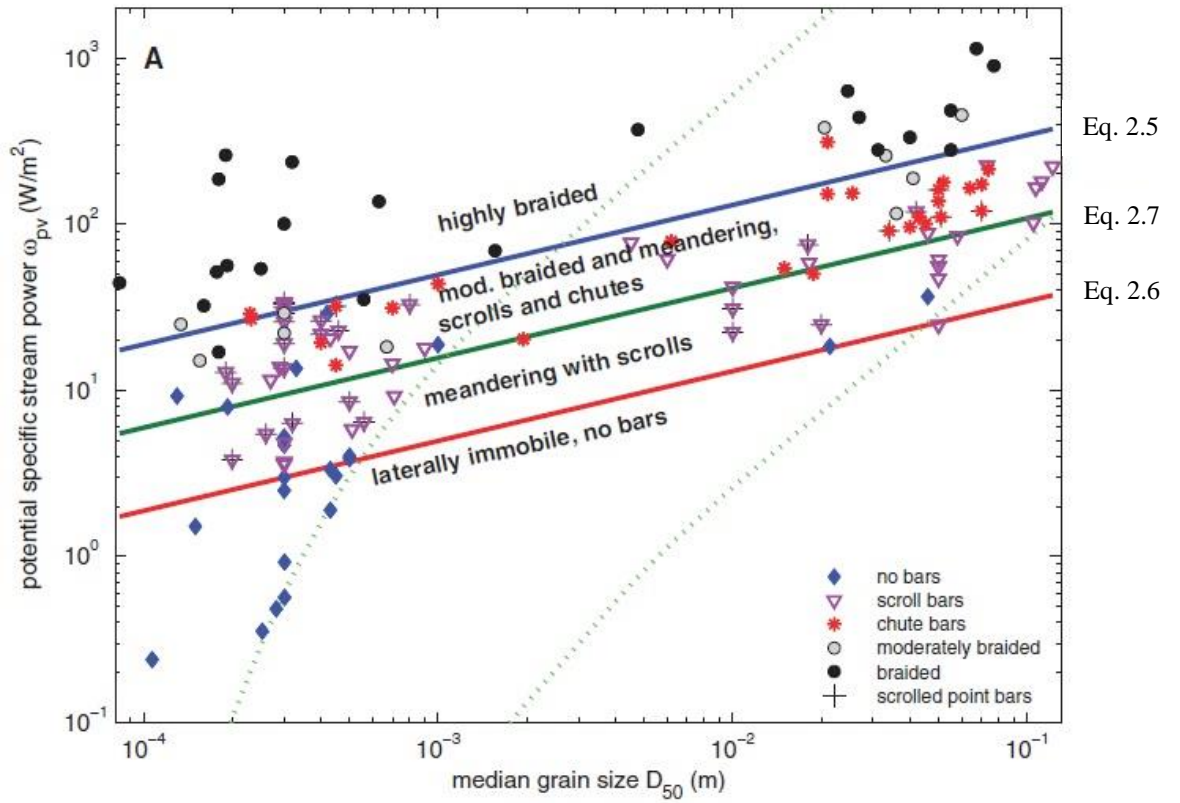


Figure 2.6 Channel patterns in relation to gradients in grain size and unit stream power (from Kleinhans and Van den Berg, 2011)

Whereas the discriminator for low energy stable channels occurs at an order of magnitude lower stream power, ω_{ia} (Makaske, et al., 2009) is defined as:

$$\omega_{ia} = 90D_{50}^{0.42} \quad (2.6)$$

A transition between meandering rivers characterized by scrolls and by scrolls and chutes is found between equations (2.5) and (2.6) and is defined as:

$$\omega_{sc} = \frac{90}{\sqrt{10}} D_{50}^{0.42} \approx 285 D_{50}^{0.42} \quad (2.7)$$

2.3 Single-thread rivers: planform and controlling factors

Single thread rivers form the focus of this thesis, so this section explores their planform and controlling factors in more detail from both theoretical and observational perspectives. In doing this, meandering rivers are a particular focus and a range of characteristic morphological features are also revealed that may relate to single thread

ivers of different types. Meandering rivers are a very common river planform characterised by planimetric evolution that involves meander migration, growth, and cutoffs. Well documented examples include the Amazon River (Puhakka et al. 1992), the Congo River (Peters, 1978), Yellow River (Wang et al., 2004), Ob River (Alabayan and Chalov, 1998), and Brahmaputra river (Coleman, 1969; Jagers, 2003). Within this class of river planform there are many variants and there are no well-developed morphological models capable of fully representing large-scale planimetric changes of this style of river.

2.3.1 Characteristics of sinuous to fully meandering rivers

The planimetric form of a meandering river is sinuous with successive inflection points and meander bends, whilst the longitudinal bed profile is characterized by alternation between pools and riffles or runs (Figure 2.7). Riffles (rough water surface characterized by standing waves) or runs (water surface characterized by ripples) are shallow zones with fast moving water that are mainly located at planform inflection points. Conversely, pools are deeper areas with a smooth water surface and relatively slow moving water (Crosato, 2008). The plan and geometry of meanders has been described and quantified by many researchers.

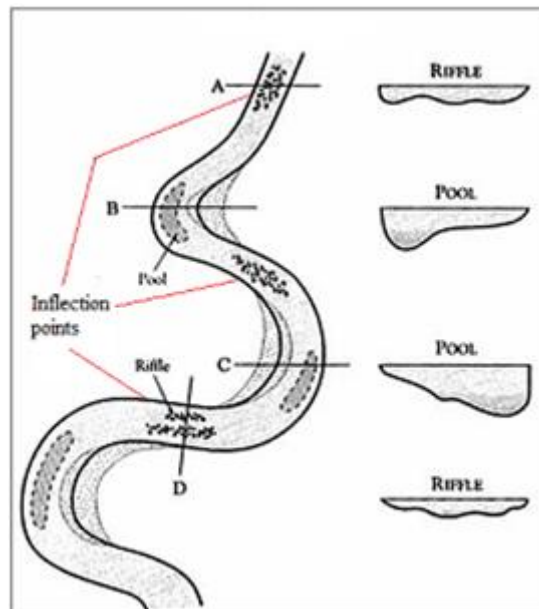


Figure 2.7 Planimetric and cross sectional form of a meandering river (from Morisawa, 1985)

a) Planimetry

Channel sinuosity (S) is the ratio between channel thalweg length (L_T) and valley length (L_0) (Rust, 1978):

$$S = L_T / L_0 \quad (2.8)$$

Brice (1984) proposed that meandering rivers have a sinuosity that exceeds 1.25, whereas Leopold et al. (1964) and Rosgen (1994) suggested a value exceeding 1.5. The latter threshold has become the most widely used definition, since meander river planimetry can be considered to consist of a series of opposing semicircles and thus a sinuosity $\pi/2 = 1.57$.

Meander wavelength (Figure 2.8) refers to a pair of opposing meander loops (Leopold et al., 1964). According to Friedkin's (1945) laboratory experiments, meander wavelength is influenced by the hydraulic river regime, sediment, valley slope and upstream and downstream conditions. Leopold and Wolman (1960) also noted the proportionality of wavelength to channel width, quantifying a ratio of 10.9 between meander wavelength (L) and the product of sinuosity (S) and channel width (B), whereas Garde and Raju (1977) suggested a value of 6:

$$L = (10.9 \text{ or } 6)SB \quad (2.9)$$

Wave number (λ) is a dimensionless meander property that is used in theoretical analyses of meandering, which expresses the ratio of reach-averaged width (W) to meander wavelength (L):

$$\lambda = \pi W / L \quad (2.10)$$

Camporeale et al. (2005) found from an analysis of 44 real river reaches that the width of the meander belt/amplitude (W) is approximately 40 to 50 times the spatially-averaged linear wavenumber (m) $\bar{\lambda}$:

$$W = (40 - 50)\bar{\lambda} \quad (2.11)$$

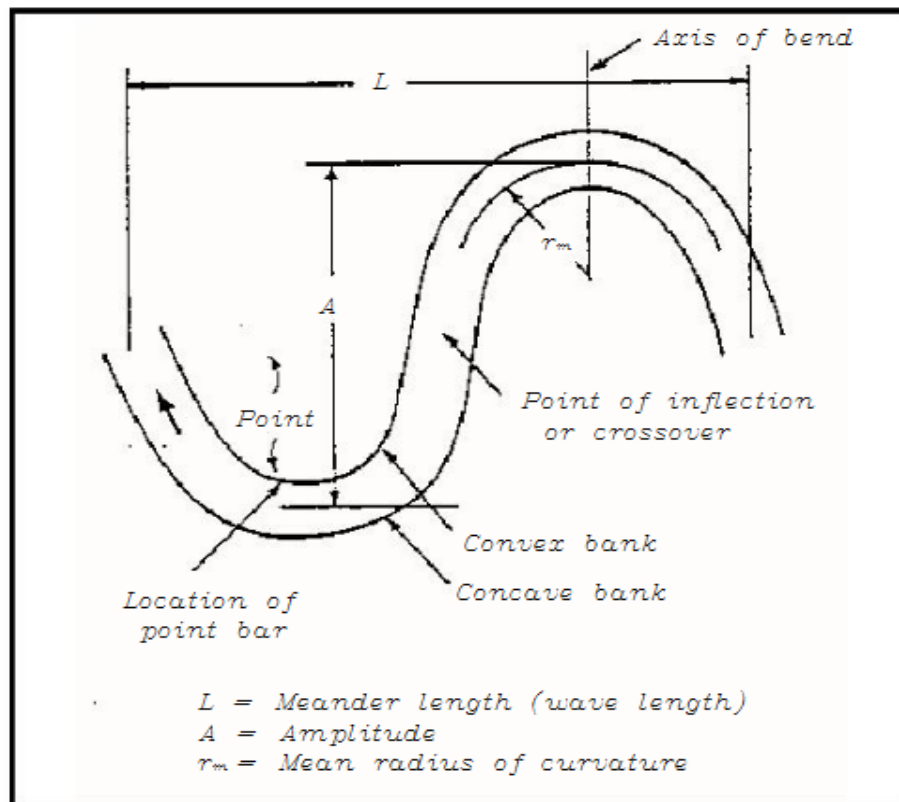


Figure 2.8 Meander geometry sketch (from Leopold et al., 1964)

Different styles of alluvial meandering show variations in the magnitude and character of channel width and curvature, where the highest degree of width oscillation occurs in association with transitional forms. Brice (1975) suggested a form-based river classification of meanders into nine typologies (Figure 2.9), of which five typologies show clear and regular oscillations (Luchi et al., 2011). The wider-at-bend streams show regular meandering for classes B2, C, D, G2 (Figure 2.9) and more irregular meandering for class E. Consequently, the spatial distribution of channel width is expected to play an important role in relation to meander evolution of wider-at-bend types in comparison with equiwidth types A, B1, G1, F (Zolezzi et al., 2012a)

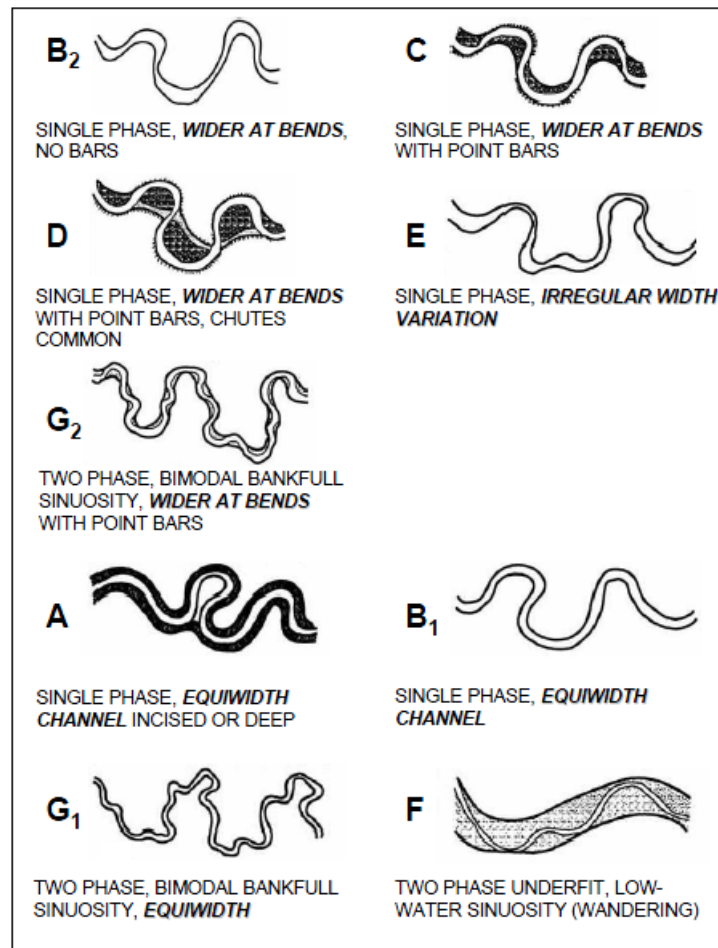


Figure 2.9 Single-thread alluvial river patterns with classes categorized according to the distribution and degree of spatial variation in channel width (modified from Brice, 1975 by Lagasse, et al., 2004)

Analysis by Brice (1982), which was refined by Lagasse et al. (2004), showed that wider-at-bends rivers exhibit higher migration rates in comparison with equal-width rivers, so linking form to lateral mobility. Using equation (2.10), Lagasse et al. (2004) computed the wave number λ for class B₁ (Figure 2.9, representing equiwidth meanders) and C (Figure 2.9, representing wider-at-bends meanders) to produce the distribution shown in Figure 2.10. The mean wave number for class B₁ is 0.21, and for class C is 0.26, and there are wide-ranging disparities in the wave number between the two classes across 99% of the probability range (Figure 2.10), indicating that meanders of wider-at-bends planforms tend to be shorter than equiwidth meander planforms for the same average river width (Luchi et al., 2011).

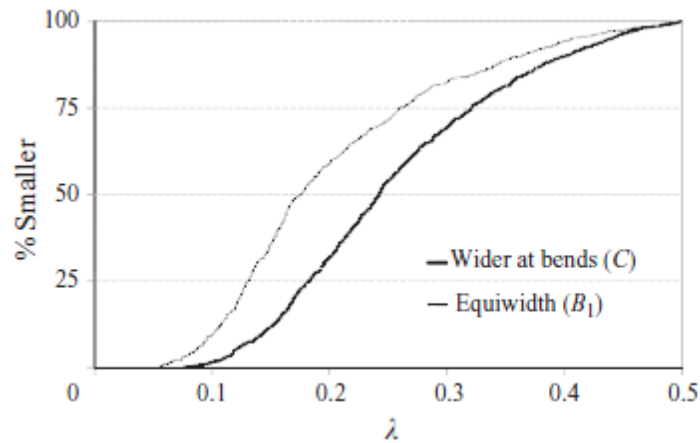


Figure 2.10 Wave number distribution of bends for wider-at-bends (class C) and equi-width meandering channels (class B_1) (from Lagasse et al., 2004)

In reality, meanders can be either regular or irregular (Figure 2.11A) and regularity may not be strictly preserved over distance, so that meanders may not be completely regular or solely random and there can be considerable variability between the two within and between meander systems (Ferguson, 1979).

b) Meander geometry

Meander geometry has been investigated using two methods. First is the traditional approach that is based on measures extracted for individual bends, such as meander wavelengths (λ) and radius of curvature (r_c), and then averaged over sequences of bends (Figure 2.11B). The second analyses series of meanders, investigating the stream trace as a spatial series of direction (θ) or direction change ($\Delta\theta$) with respect to distance (x) (Figure 2.11C and D).

Ferguson (1975, 1979) suggested the subdivision of meandering into three properties: a scale variable such as wavelength (λ or λ_*), sinuosity or wiggleness, and degree of irregularity. These and other morphometric variables can be estimated by the direction (θ) and change of direction/curvature ($\Delta\theta$) series (Howard and Hemberger, 1991).

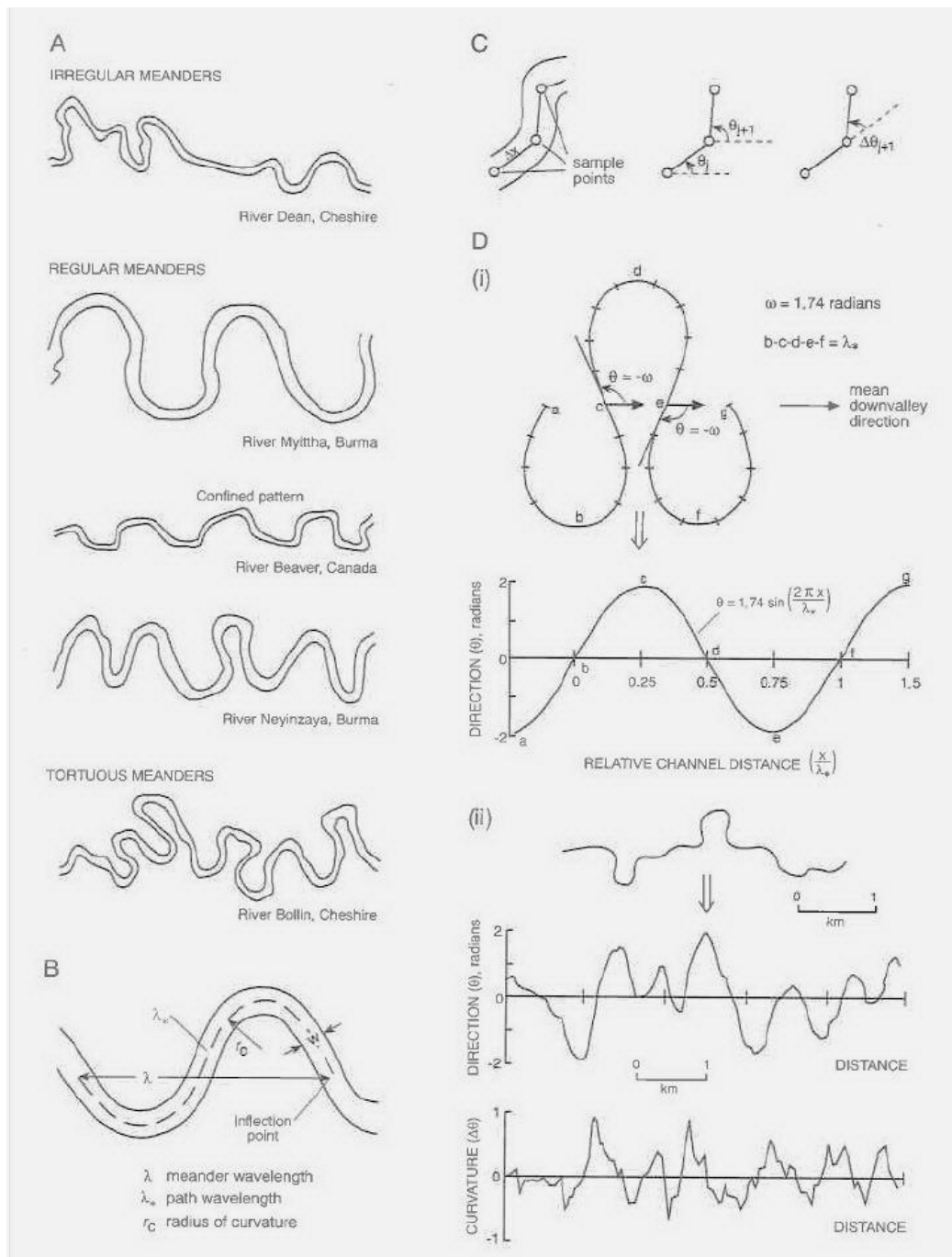


Figure 2.11 Meandering patterns: (a) Degree of meandering; (b) Standard sketch of meander bends with key meander properties; (c) Quantifying meander path direction (θ) and change of curvature ($\Delta\theta$); (d) Planform geometry and spatial distribution of curvature (i) regular meander (from Langbein and Leopold, 1966) (ii) irregular meanders of the River Trent (from Ferguson, 1979)

The preliminary stage of meanders generally exhibits periodic planform sequences through which the channel axis can be expressed by a sine-generated curve (Langbein and Leopold, 1964), which in its simplest form is:

$$\theta = \omega \sin k x \quad (2.12)$$

The channel direction (θ) is presented as a sinusoidal function of distance (x), ω is the angle formed between the channel section axis and down valley axis, and k is $2\pi/\lambda^*$ (see Figure 2.11D(i)).

Meander loops are individual meander bends (i.e. half a meander wavelength; Leopold et al., 1964) and four basic types have been identified (Figure 2.12): simple symmetrical, simple asymmetrical, compound symmetrical, and compound asymmetrical. A simple symmetrical loop is formed when a low symmetrical arc with constant curvature (increasing in height but decreasing in radius) grows and its length surpasses its radius. It becomes asymmetrical when the growth of a second arc is tangential to the first but also curved toward the same side of the stream. A simple loop becomes compound when the second arc is developed into a loop. Compound loops are considered to be deviant forms having indefinite radius and length. However, meandering patterns can be analysed by simple loops whose properties can be easily measured and treated statistically (Brice, 1974; Hooke and Harvey, 1983).

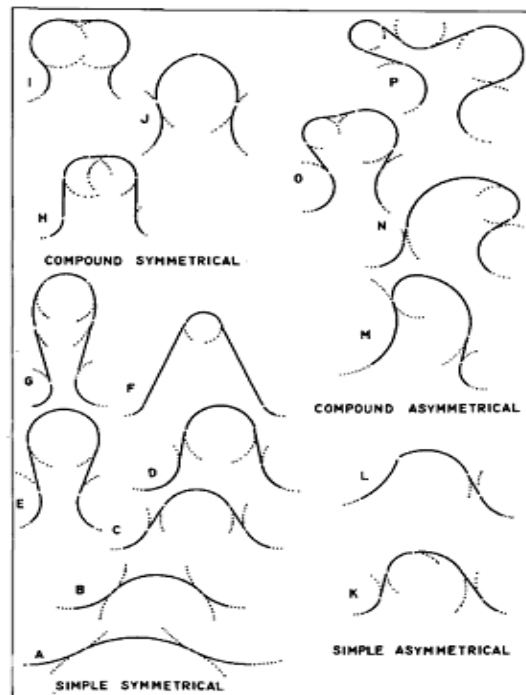


Figure 2.12 Meander loop classification with flow direction from left to right (from Brice, 1974)

c) Bend Flow

Flow patterns in meandering rivers are governed by the sequence of opposing bends (Figure 2.13). Primary flow is two-dimensional water flow (obtained from depth-averaging) and consists of longitudinal and transverse components. Secondary flow includes the components of primary flow and all the deviations from it. It is a feedback process between centrifugal force caused by channel curvature, vertical gradient of the main flow and transverse inclination of water surface layer (which leads to transverse pressure gradients) (Rozovskii, 1957; Kalkwijk and de Vriend, 1980, de Vriend, 1981).

Centrifugal force pushes the water toward the outer bank, resulting in a higher water level on that bank and a transverse pressure gradient which pushes the water toward the inner bank. The centrifugal force is stronger near the surface and weaker close to the river bed. In combination with the pressure gradient, it results in a transverse current. The current is directed towards the outer bank close to the water surface and inwards close to the bed. The current is vertical in a downward direction near the outer bank and upwards near the inner bank. This transverse circulation combines with longitudinal (downstream) flow to produce helical flow (Figure 2.13b) (Crosato, 2008).

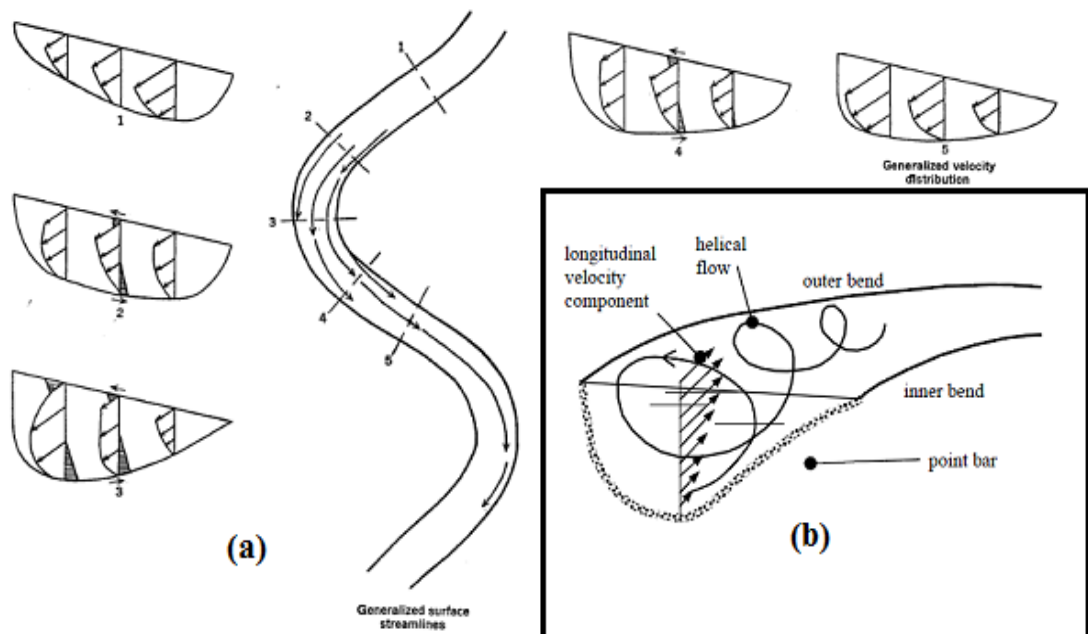


Figure 2.13 Flow in a meander bend (Leopold and Wolman, 1960; Crosato, 2008)

In relation to morphology, sediment is continuously carried towards the inner bank of the bend until an equilibrium condition between the drag force and gravitational force is established. This generates a triangular cross-sectional shape, with the deepest part towards the outer bank (pool) and the shallowest part towards the inner bank (point bar). Fully-developed bend flow cannot be reached in natural rivers, since channel geometry is not uniform along the longitudinal profile (Crosato, 2008).

d) Discharge

Rather than use the entire flow record, it is convenient to represent the discharge hydrograph by one or more simple indices of which the bankfull discharge (the discharge that fills the channel cross section without significant flooding of the flood plain) has been the most widely used (Leopold and Wolman, 1957; Ackers and Charlton, 1970b; Fredsøe, 1978; Hey and Thorne, 1986; Van den Berg, 1995). Bankfull discharge is a useful index of flow strength for meandering rivers. Since bankfull is not a frequent flow condition, it is best estimated from stage-discharge curves or as a 1.5 to 2 year return period 'instantaneous' peak discharge from a discharge time series (Williams, 1978; Parker, et al., 2007).

e) Sediment

As a result of selective transport and abrasion processes, sediment tends to fine downstream along rivers. Most meandering rivers are located in lowland areas and are characterized by relatively fine (sandy to silty) river beds, although numerous natural meandering rivers have gravel beds, when they are either close to the braiding transition or are controlled by strong erosional process (Parker and Andrews, 1985; Parker, 1991; Seal et al., 1998; Ferguson et al., 1998; Gasparini et al., 1999).

Owing to the selective transport process, coarse sediment and fine sediment may be found in the same cross section. Coarser sediment is located where velocity is higher, and finer sediment is located where velocity is lower. Normally, river bends present finer sediment (sand) in the inner bank and coarser sediment in the outer bank/pool. River sediment transport capacity varies through time. During falling river stages, only fine materials are conveyed in suspension and are deposited everywhere, even on the coarser deposits which had formed during the previous higher river stages. As a result during this stage, fine sediments are deposited in pools where they form a layer above coarser sediment. Sediment deposited on meandering banks is usually very fine and has high organic content. The latter supports vegetation growth during low flow and the presence of vegetation increases the quantity of fine sediment trapped on the banks.

This feedback process, which causes river bank accretion, is an important process in river meandering.

f) Channel Migration

Long term stationary meanders may display planimetric evolution that consists of a combination of translation and extension (Brice, 1984), known as channel migration. This process is based on sequences of bank erosion and accretion, which cause bank retreat and advance, respectively. As flow erodes the outer bank, causing local bank retreat, the eroded sediment deposits downstream at the inner bank (Friedkin, 1945), leading to point bar accretion and bank advance. The river remains meandering in planform because the bank advance process is counterbalanced with bank retreat in the opposite bank. If this does not occur, the river either becomes braided or anabranching or fills with silt and narrows.

Hooke (1980) compared historical bank retreat rates of rivers in Devon, UK with published data from rivers across the world, where data of mean river width, discharge, extension of drainage area, local radius of curvature and bank characteristics for a few of cross sections were reported.

Meander migration is a discontinuous process. High infrequent flows cause the channel to expand through bed erosion and raise channel margin elevations, while low frequent flows are associated with aggradation. Both processes reallocate the thalweg towards the eroding bank. Overall the meander migration process is governed by sequences of bank erosion and accretion accompanying series of high and low discharges and reinforced by the presence of riparian vegetation (Nanson and Hickin, 1983; Pizzuto, 1994).

The direction of upstream or downstream migration of meander bends depends on the position of pools with respect to the apex of bends, bend form and eroding bank characteristics. In most cases, the highest near bank velocity is located downstream from the bend apex, which causes meanders to shift in a downstream direction. However, there are some cases of upstream meander migration which theoretically occur in super-resonant conditions (Seminara et al., 2001; Lanzoni et al., 2005) with point bar development associated with the stalling of upstream coarse material (Requena et al., 2006).

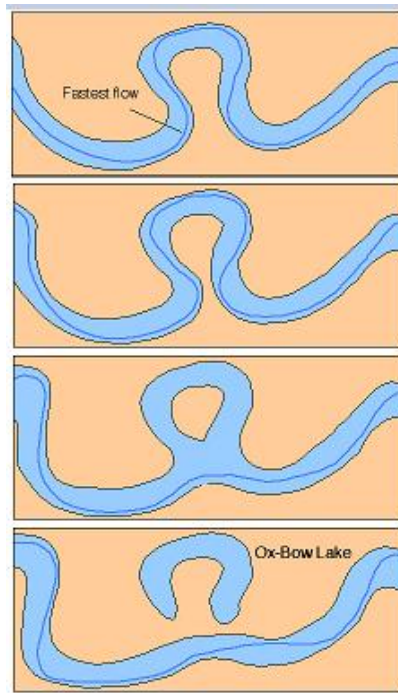


Figure 2.14 Meander neck cut off process (image credit: Bruce Railsback)

g) Cutoffs

Meander migration and cutoff processes are drivers of changes in channel morphology, sediment load and habitat qualities of alluvial floodplain rivers. Predicting and allowing for their occurrence is one of the greatest challenges for meandering river managers, and to allow a balance between ecological function, flood protection and water supply (Micheli and Larsen, 2011).

Meander neck cutoff (Figure 2.14) occurs when meander extension is discontinued by flow excavation of the upstream outer bank until it connects downstream. This leaves the old bend abandoned as the flow progressively moves into the newly connected channel until it becomes the main channel. The new channel is generally shorter, straighter, and steeper and supports faster flow velocities than the old bend (Jagers, 2003).

Cutoffs across the floodplain that are not at the neck of a meander are called chute cutoffs. These have longer flow diversions than neck cutoffs and are able to increase in size during sequences of floods until they can carry all of the channel flow. Chute cutoffs can develop from downstream or upstream (Jagers, 2003). Meander growth progressively decreases channel bed slope, whereas cutoffs decrease channel slope. Thus the spatial and temporal development of cutoffs causes the bed slope to remain

(dynamically) constant and can be considered a stabilizing phenomenon for meandering dynamics in the long-term.

Channel morphological adjustments were demonstrated after both neck and chute cutoffs on River Bollin and Dane, UK (Hooke, 1995). The occurrence of multiple cutoffs was investigated through historical images by Hooke (2004), who assumed that cutoffs are a part of a self-organizing (river) system and that they occur because the river has reached a critical state.

h) Channel width dynamics and curvature

Field observations of rivers with cohesive banks (Pizzuto and Meckelnburg, 1989) support the idea that meandering channel width is constant in time and space due to an equal rate of bank retreat and advance. The most well-known geometrical classification of single-channel river patterns (Brice, 1982) emphasizes differences in the degree and the nature of channel width and curvature variations, where curvature and width are seen as deviations from a straight equiwidth channel pattern. Relationships between channel curvature and width variations may occur due to counterbalanced feedback process, which finally resulting in a variety of meandering behaviour (Zolezzi et al., 2009). The mechanistic evolution of curvature in meanders has been well researched (Ferguson, 1973; Blondeaux and Seminara, 1985); but the morphodynamics of spatial width variations in single-thread channels are less well understood, and thus understanding of the role of spatial variations in channel width in meander morphodynamics is also limited. Figure 1.8 implies that there might be a systematical variation of channel width along the meander wavelength: equiwidth single-thread streams (Figure 1.8 A, B1, G1, F); wider-at-bend streams (Figure 1.8 B2, C, D, G2) and irregular width streams (Figure 1.8 E). According to Brice (1982), the highest morphological activity is relevant to local bend widening, with most stable meandering channels showing little variation in width. High meander migration rates are usually associated with wider-at-bend streams (Lagasse et al., 2004).

2.3.2 Key factors controlling meandering

Several factors control natural meandering both explicitly and implicitly: flow strength, sediment supply, bank erodibility and riparian vegetation.

a) Flow strength

Flow strength is defined as the capacity of the flowing water to convey sediment and erode river bed and banks. This term incorporates shear stress, flow velocity or

stream power, and temporal discharge variations, and it can be used to classify river types. In general, meandering rivers have lower flow strength than braided rivers.

b) Sediment supply

Meandering rivers are associated with the transport and deposition of significant quantities of fine (silt and clay) sediment, giving them generally cohesive bank even when they support a gravel bed, whereas braided rivers are characterized by sand and gravel and thus less cohesive banks. A relationship between channel pattern and sediment supply has been proposed by several authors (ASCE Task Committee, 1982). Braided rivers require a high sediment supply. When load decreases, rivers tend to become incised and start to meander (Schumm, 1981). Braiding is supported by bed aggradation, which occurs when bed material supply is larger than the river's ability to transport it (transport capacity). Stable meandering generally occurs when sediment supply is equal to or less than the river's transport capacity.

c) Bank erodibility

Meandering river and other sinuous single-thread rivers are considered to have banks of relatively low erodibility as a result of soil cohesion, but this may also be attributable to well-developed riparian vegetation. Because meandering river banks are relatively cohesive, bank material entrainment is comparatively smaller than in braided rivers. Because of high bank cohesion, bank recession generally result from toe erosion followed by bank failure on meandering rivers. Smith (1998) explored this in a laboratory flume containing a very sinuous meandering river with slowly-migrating thalweg. Cohesive sediment ensured that the banks were resistant to erosion and the laboratory experiment suggested that bank erosion resistance to erosion strongly controlled river pattern, particularly sinuosity. Natural rivers show similar behaviour, implying that erodible banks are a key characteristic of braided rivers whereas resistant cohesive banks are typical of meandering rivers (Simpson and Smith, 2000).

d) Riparian vegetation

The importance of riparian vegetation for channel morphology has been demonstrated across a wide range of timescales and across laboratory and field spatial scales.

Around 400 million years ago during the Silurian period, prior to the existence of plants with roots and rhizomes, alluvial rivers on Earth were predominantly braided (Pannekoek and Van Straaten, 1984). A shift from meandering to braided river deposits

during the Permian-Triassic period (251 million years ago) in South Africa was attributed by Ward et al. (2000) to the devastation of plants. Furthermore, Davies and Gibling (2009, 2010) noted that during the Paleozoic, rivers across the Earth's surface changed from predominantly braided to increasingly meandering forms as rooted vegetation capable of stabilizing river banks evolved. Laboratory experiment suggests the strong effect of vegetation presence on stream morphology, with a tendency to transform river pattern from multi- to single-thread (Gran and Paola, 2001). Flume experiments on braided rivers have shown how the presence of plants decreases the braid number (Kurabayashi and Shimizu, 2003) and how braided channels without vegetation transform into incised meandering as the banks become vegetated (Jang et al., 2003; Tal and Paola, 2005). Moreover, field observations indicate how riparian vegetation causes channel width to decrease (Eschner et al., 1983; Beeson and Doyle, 1995; Allmendinger et al., 2005). Importantly, Millar (2000) defined a bank stability criterion, incorporating riparian vegetation into the assessment of bank strength, that separates meandering from braiding channels and identifies channels where riparian vegetation is critical for maintaining a meandering rather than a braided pattern (Figure 2.15).

The specific effects of riparian vegetation on channel pattern, river bed degradation/aggradation and river bank erosion/accretion are: (1) vegetation canopy protection of the bank surface from high shear stresses and thus erosion; (2) vegetation canopy flow resistance increasing the trapping of sediment and thus bank accretion; and (3) root development and reinforcement stabilizing the accreting banks and enhancing their lateral development.

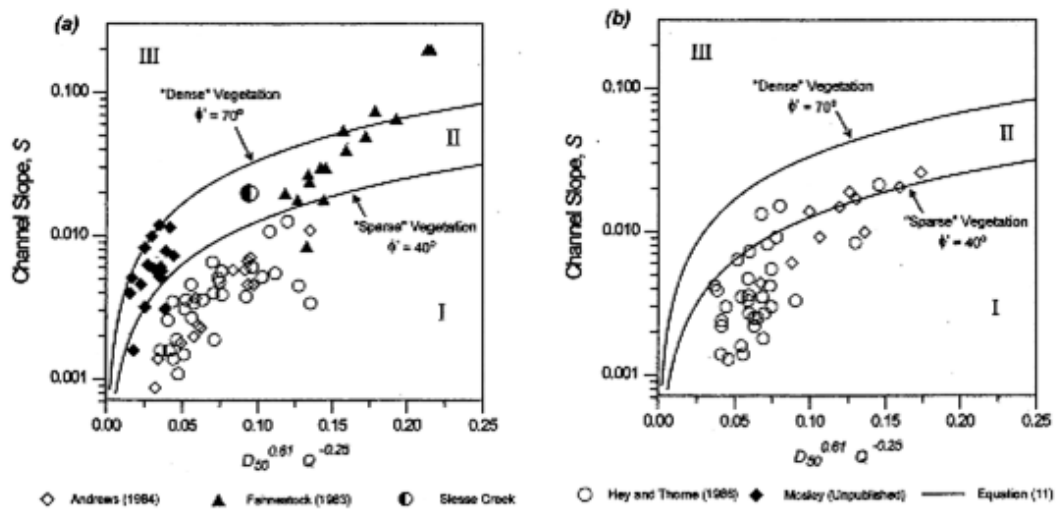


Figure 2.15 Planform stability diagram plotting (a) data from rivers with sparse bank vegetation and (b) data from rivers with dense bank vegetation. (open symbols are meandering rivers and solid symbols are braided rivers; rivers in areas I and III are meandering and braided, respectively, regardless of bank vegetation, whereas rivers in area II will only meander if they have dense, deep-rooted bank vegetation) (from Millar, 2000).

2.4 Single-thread rivers: bars and other geomorphological features

The preceding sections have considered the continuum of channel patterns that rivers may display, with a particular emphasis on single thread sinuous-meandering patterns (section 2.2); and then have focused on single-thread sinuous-meandering planforms and their controlling factors from both theoretical and descriptive-observational perspectives (section 2.3). Throughout these sections, a range of geomorphic features have been mentioned, which may allow discrimination between different river types, suggesting that recognising an assemblage of such features might also be the basis for classifying single-thread rivers. The presence and type of bars is particularly informative, since these are a fundamental feature of alluvial channels. ‘The presence of channel banks gives rise to a class of large-scale bed form called bars, the dimensions of which are controlled by the flow width as well as the depth’ (Bridge 2003, p141).

Bars are generally classified by their calibre/texture, shape and position within the river channel. Thus cobble, gravel, sand and silt bars may be discriminated, reflecting contrasts in river energy and thus capacity to transport different grain sizes as well as the supply of sediment of varying calibre to the fluvial system. In terms of shape, unit

bars are simple forms composed of one main depositional feature, whereas compound bars reflect multiple phases of deposition and reworking under a range of flow conditions and thus are comprised of multiple units (Smith, 1974, Brierley, 1996). Descriptions of bar position include side bars and mid-channel bars. Linking bar shape and position leads to the identification of specific types of side bar associated with river bends, particularly on meandering rivers (point and counterpoint bars positioned, respectively, on convex and concave banks), sequences of bars along opposing channel margins of straight or sinuous rivers (alternate bars), and the general term lateral bar which refers to any bank-attached bar along a river margin, particularly those not directly associated with river bends. A particular type of bank-attached bar that crosses the channel is the diagonal bar, which is often associated with the cross-over point of river meanders. Finally, there are mid-channel bars, which are not attached to the banks, and are distinguished according to their orientation and shape into longitudinal (main axis parallel to the banks), transverse (main axis at an angle to the banks) and complex.,including found on transitional, wandering and braided rivers, linguoid bars are often recognised as a characteristic bar shape. The classification of bars is an extremely complex subject (e.g. Bridge, 2003), that goes beyond the scope of this thesis, and so the above represents one simple approach to classification. However, different broad types of bar (calibre/texture, position, shape) have been associated with different river styles, as illustrated earlier in this chapter (e.g. Miall, 1977, Schumm, 1985, Church 2006), and some of these may be distinguishable from aerial imagery, which forms the primary data source for this thesis (see Chapter 2).

Bars can show associated geomorphic features (e.g. scrolls, chutes), can be separated by other bed features (e.g. pools, riffles) and can evolve into other geomorphic features, including benches, islands, and floodplain scrolls. Furthermore, in very steep and low gradient channels, the coarse and fine bed material (respectively) can present other prominent bed features such as steps, cascades, dunes and ripples. Table 2.1 lists and describes some simple bar types and other geomorphic features that may be relevant to distinguishing different river and floodplain types (particularly from aerial imagery). These will be extended and investigated further in the research presented in the following chapters of this thesis.

Table 2.1 Bars and other geomorphic features of river channels and their floodplains (developed from Table 5.7 of Gurnell et al., 2014)



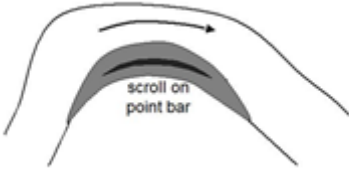
	Geomorphic feature	Description	Diagram	Formation/typical setting	Reference(s)
In-channel marginal bars	Side bar	Bank-attached bar, often distributed periodically along one and then the other side of channel to form alternate bars.	 <p>Plan view</p>	Typically found in sinuous channels and indicative of secondary current development and pool-riffle formation.	Church and Jones (1982)
	Point bar	Bank-attached arc-shaped bar developed along inside of river bends with bar surface towards channel and typically devoid of vegetation.	 <p>Plan view</p>	Point bars are characteristic of actively meandering streams and tend to extend into the channel and downstream, keeping roughly parallel with the eroding bankline.	Church and Jones (1982)
	Scroll bar	Elongated ridge-like bar formed along inside of meander bends, commonly on point bars. Often contain trees deposited on point bars during floods and may develop into vegetation-covered ridges.	 <p>Plan view</p>	Formed by deposition in the shear zone between the helical flow cell in the thalweg zone and flow in a separation zone adjacent to the convex bank of a bend.	Nanson (1980, 1981)

Table 2.1 (ctd.)

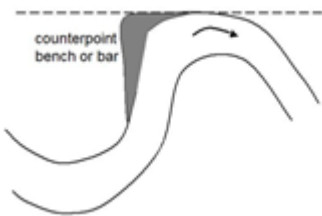
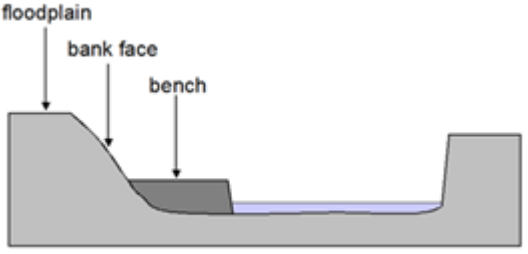
	Geomorphic feature	Description	Diagram	Formation/typical setting	Reference(s)
In-channel marginal bars	Counterpoint bar	Depositional feature consisting of typically finer sediment than that of point bars which develops in the separation zone formed against the upstream limb of the convex bank of tightly curving bends.	 <p>Plan view</p>	Often form on tight bends created when the river is constrained by the valley wall or a major terrace.	Hickin (1984); Lewin (1983); Page and Nanson (1982)
	Berm/bench	A step-like, sedimentary feature located against the bank face with a relatively flat upper surface and steep edge sloping towards the channel.	 <p>Profile view</p>	Formation occurs through aggradation and subsequent colonisation by vegetation of marginal bars.	Gurnell et al. (2012)

Table 2.1 (ctd.)

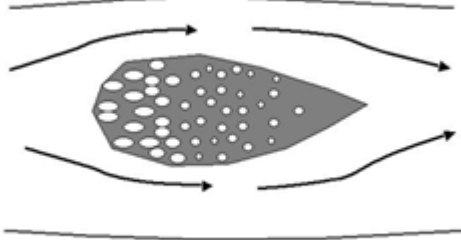
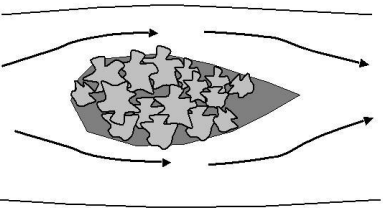
	Geomorphic feature	Description	Diagram	Formation/typical setting	Reference(s)
In-channel mid-channel bars	Mid-channel bar	Depositional sedimentary feature in the mid-channel region around which flow diverts. Many sub-types exist (e.g. transverse, medial, diagonal, etc.) but all are exposed during normal flow conditions and submerged during bankfull flows.	 <p style="text-align: center;">Plan view</p>	Formation can occur via a number of mechanisms ranging from a localised decline in competence leading to deposition of coarse material to chute cutoffs of point bars but presence indicative of high rates of sediment supply and transport.	Church and Jones (1982), Ashmore (1991)
	Island	Landform within the central channel region that is emergent at bankfull stage. Island surface is usually aggraded to floodplain level and covered by vegetation.	 <p style="text-align: center;">Plan view</p>	Formation can occur via a number of mechanisms including floodplain dissection and continued deposition of fine sediment on bar surfaces (often aided by vegetation).	Gurnell et al. (2001); Osterkamp (1998).

Table 2.1 (ctd.)

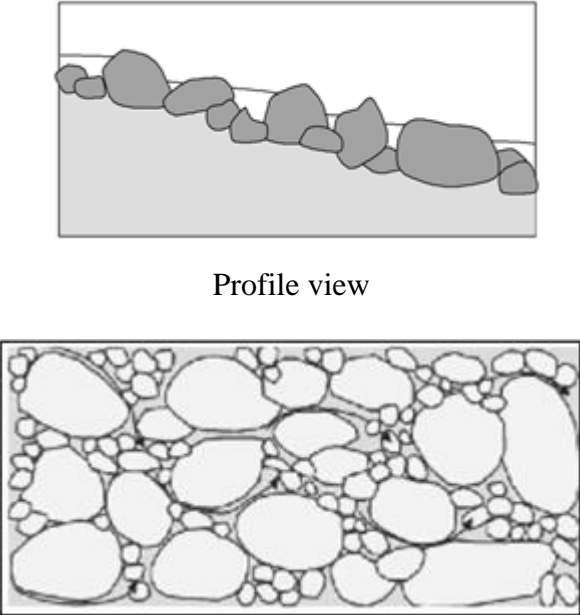
Geomorphic feature	Description	Diagram	Formation/typical setting	Reference(s)
Cascade	Non-alluvial features composed of large boulders that are partially emergent during low and intermediate flows with small (i.e. diameter less than channel width) intervening pools characterised by highly turbulent flow. No systematic lateral or longitudinal organisation.	 <p style="text-align: center;">Profile view</p> <p style="text-align: center;">Plan view</p>	Cascades are typically found in very steep and confined channels with high contemporary or historic coarse sediment supply rates.	Grant et al. (1990); Halwas and Church (2002)

Table 2.1 (ctd.)

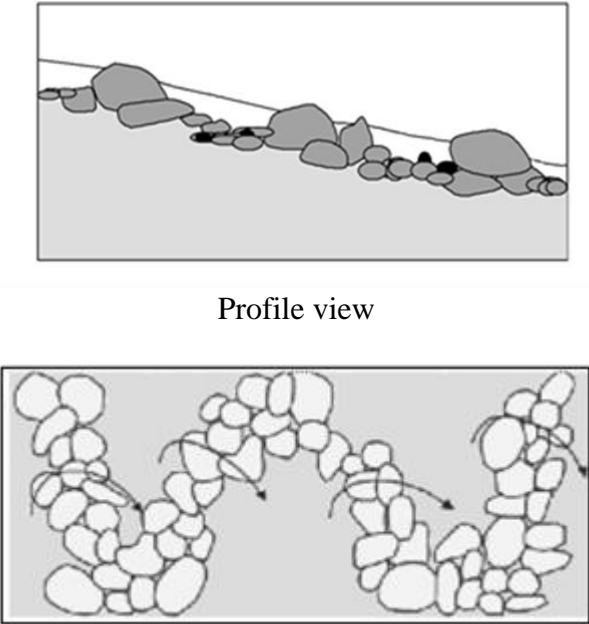
Geomorphic feature	Description	Diagram	Formation/typical setting	Reference(s)
Rapid	Semi-alluvial features in which boulders are organised into irregular lines oriented approximately perpendicular to the channel and that either partially or completely span the width of the channel. Small, shallow pools may be evident between the boulder lines but they are poorly developed.	 <p style="text-align: center;">Profile view</p> <p style="text-align: center;">Plan view</p>	Rapids are typically in steep and confined channels, but where gradients are lower than for cascades.	Grant et al. (1990); Halwas and Church (2002)

Table 2.1 (ctd.)

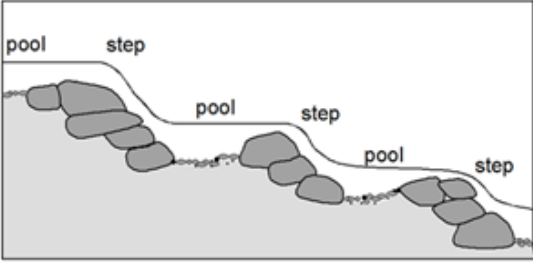
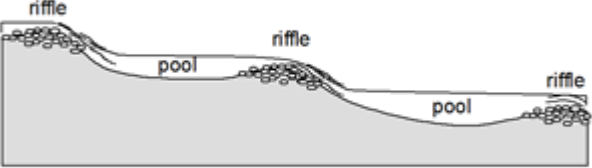
Geomorphic feature	Description	Diagram	Formation/typical setting	Reference(s)
Step	A channel-spanning linear accumulation of coarse sediment (typically boulders/cobbles). Usually associated with a distinct downstream pool that is scoured by water plunging over the step.	 <p style="text-align: center;">Profile view</p>	Sequences of steps and pools are steep upland channels with coarse beds. Step-pool sequence repeats with a mean spacing of 1-4 times the mean channel width.	Chin (2003); Halwas and Church (2002)
Riffle	Accumulations of coarse sediment (typically pebbles and cobbles) associated with rapid, shallow flow and disturbance of the water surface. Regularly interspersed by pools.	 <p style="text-align: center;">Profile view</p>	Characteristic feature of gravel bed meandering streams. Tend to occur at inflection points between meanders and pool-riffle sequence repeats with a mean spacing of 5-7 times the mean channel width, indicating initial formation is linked to large-scale turbulent eddy patterns.	Richards (1976)

Table 2.1 (ctd.)

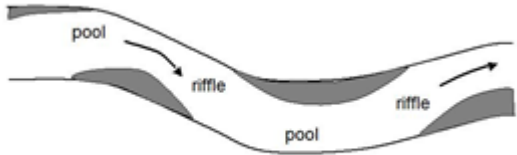
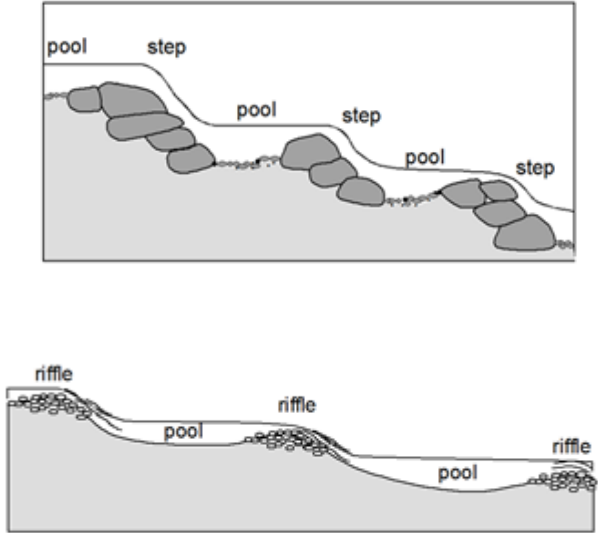
Geomorphic feature	Description	Diagram	Formation/typical setting	Reference(s)
		 <p style="text-align: center;">Plan view</p>		
Pool	<p>Topographic depression in the river bed associated with deep and tranquil flow. Often found alternating with either steps or riffles, giving rise to the characteristic undulating longitudinal profile of gravel bed rivers.</p>	 <p style="text-align: center;">Profile views</p>	<p>Either freely formed through the interaction of flow and sediment transport or forced by local obstructions (e.g. boulders, large wood, debris jams) that lead to flow convergence and associated scour or upstream ponding.</p>	<p>Bisson et al. (1982), Richards (1976), Grant et al. (1990), Chin (2003)</p>

Table 2.1 (ctd.)

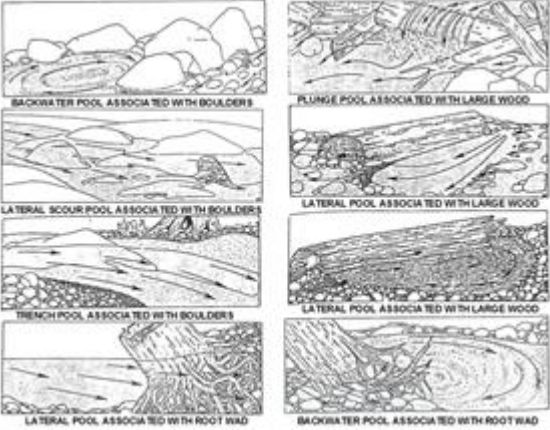

Geomorphic feature	Description	Diagram	Formation/typical setting	Reference(s)
		 <p style="text-align: center;">Examples of forced pools</p>		
Dune	Large depositional feature composed of fine sediment. Gives rise to undulating longitudinal bed profile in sand bed rivers.	 <p style="text-align: center;">Profile view</p>	Characteristic bedform of sand bed rivers formed through interaction of flow and sediment transport.	Simons and Richardson (1966)

Table 2.1 (ctd.)

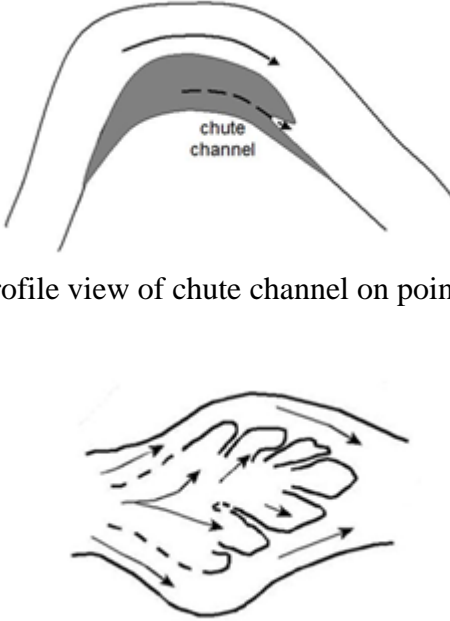
Geomorphic feature	Description	Diagram	Formation/typical setting	Reference(s)
Chute channel	Channels cut into bar deposits or floodplain areas. Typically dry during normal flow conditions.	 <p data-bbox="831 703 1375 735">Profile view of chute channel on point bar</p> <p data-bbox="801 1070 1404 1134">Profile view of chute channels on mid-channel bar</p>	Chute channels are formed where flow across a bar or floodplain surface leads to scour and incision of a channel.	Grenfell et al. (2012), Church and Jones (1982)

Table 2.1 (ctd.)


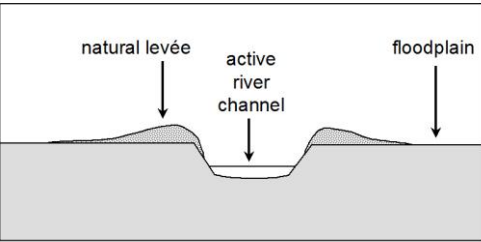
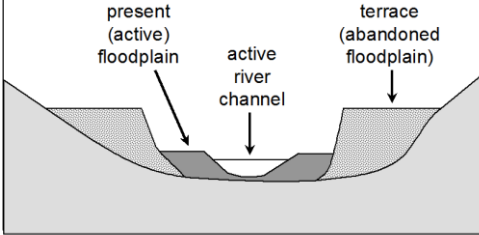
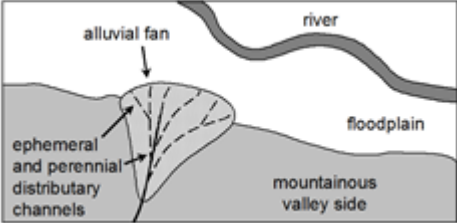
Geomorphologic feature	Description	Diagram	Formation/typical setting	Reference(s)
Ridges and swales	Linear, arcuate topographic high (ridges) and low (swales) points on floodplains.	 <p data-bbox="1039 751 1164 778">Plan view</p>	These features develop as old scroll bars integrate into floodplains as channels migrate.	Nanson and Croke (1992)
Levéé	Raised elongated asymmetrical ridge bordering the river channel composed of river-deposited sediment.	 <p data-bbox="981 1155 1236 1182">Cross-section view</p>	Formed by overbank deposits during floods.	Knighton (1998)

Table 2.1 (ctd.)

Geomorphic feature	Description	Diagram	Formation/typical setting	Reference(s)
Terrace	A relatively flat feature perched above the contemporary channel and/or floodplain.	 <p style="text-align: center;">Cross-section view</p>	Formed when a river incises into its floodplain, leaving the remnants at a height that is rarely inundated.	Knighton (1998)
Alluvial fan	Fan-shaped landform composed of sediments that fine rapidly with distance from the fan apex.	 <p style="text-align: center;">Plan view</p>	Formed by ephemeral or perennial streams emerging from steeply dissected terrain onto a valley floor. Typically associated with piedmont rivers.	Knighton (1998)

2.5 Research questions

The review presented in this chapter has shown that there are two basic approaches to recognising different river types. A top-down approach recognises river types from their (planform) patterns and then investigates their hydraulic and geomorphic properties in more detail. A bottom-up approach also recognizes a wide range of geomorphic and hydraulic features from which a river type can be deduced.

The review has also illustrated how these two approaches can be advanced through three broad research methodologies, which have been adopted by geologists, geomorphologists, and engineers investigating the character and controls of different types of river. The first methodology is qualitative and conceptual, whereby channel type is distinguished using geomorphic expert judgement (Schumm, 1985; Church, 1992, Rosgen, 1994) and pictorial representations describing the appearance of each type. A second, more quantitative methodology is to apply criteria extracted from empirical and experimental data from real rivers and flumes. Such information can be compiled from published sources (Kleinhans and van den Berg, 2011) or purpose-collected, original data sets (Leopold and Wolman, 1957; Parker, 1976; Ferguson, 1987; Carson, 1984). Geomorphological tools are mainly based on this type of methodology, whereby statistical evidence supports and verifies river behaviour. The last methodology is based on theory and modelling. In this approach, many simplifications of the main processes are incorporated in order to determine channel patterns by imposing known conditions and solving the problem mathematically (Blondeaux and Seminara, 1985; Tubino, 1991; Crosato, 1987). Unlike the statistical approach, this method usually has no observational data but relies on flume or field data for verification. Application of these three research methodologies have resulted in varying outcomes, and each has its own strength and weakness. One particular constraint for the second approach is the assembly of a large and internally-consistent data set for analysis.

In the present research the second and third methodologies are both adopted to develop and test a classification of single-thread European rivers. The research is facilitated by the extraction of a large, trans-European data set, mainly from a single data source: Google Earth. Data extraction is based on a set of rules developed for the purpose; is accomplished by a single operator; and is then tested for its consistency and robustness. The research is underpinned by three research questions which are investigated in the next three chapters of this thesis:

1. Can a geomorphologically-interpretable classification of single-thread sinuous to wandering European rivers be compiled using data extracted from aerial imagery (Chapter 3)?
2. To what extent does the classification remain robust, when tested using data sets from other information sources (Chapter 4)?
3. To what extent does the classification based on information extracted from aerial imagery correspond to a classification of single-thread rivers based on theory (Chapter 5)?

CHAPTER 3

A PRELIMINARY CLASSIFICATION OF SINGLE- THREAD EUROPEAN RIVERS USING EUROPEAN DATA EXTRACTED FROM GOOGLETM EARTH

3.1 Introduction

Chapter 2 introduced research on different river styles, the processes that control them, and how researchers have attempted to classify them. This chapter builds on that research by exploring the potential of a new information source, GoogleTM Earth, to provide information that can support a preliminary classification of naturally functioning single-thread European rivers. Section 3.2 briefly reviews past research on river classification (3.2.1); issues concerning measurement in geomorphology (3.2.2); and the potential of remotely-sensed data sources for providing quantitative information on river characteristics with a particular focus on Google Earth as data source (3.2.3). Section 3.3 presents the methods used to extract and analyse data from Google Earth. The results are presented in section 3.4, and are discussed in section 3.5

3.2 Research Context

3.2.1 Geomorphological Classification of Rivers

Fluvial systems can be viewed as being comprised of a hierarchy of spatial units from the catchment and its regional setting, via landscape units of different types (e.g mountains, piedmont areas, plains), to segments of the river network, and their contained river-floodplain reaches (Figure 3.1). These spatial units are linked by processes that transfer water and sediment through the fluvial system from headwaters to the river mouth, interacting with dynamic stores of sediment that are present as geomorphic units within river corridors, including floodplains and river channels. As a result of this process cascade, different styles of river channel and floodplain evolve at different locations within the river network and display different geomorphic features.

Furthermore, the style and geomorphic features of reaches are not static, but respond to changes in processes, including water flow; mobilisation, transport and deposition of sediment and the trapping and stabilisation of sediment by riparian and aquatic vegetation and large wood. These spatial scales, processes, forms and their temporal dynamics have been synthesised in a number of geomorphological and ecological frameworks (e.g. Frissell et al. (1986); Rosgen (1994), Montgomery and Buffington (1998); Montgomery (1999); Habersack (2000); Brierley and Fryirs (2005); Thorp et al. (2006); Beechie et al. (2010); Ibisate et al. (2011); Ollero et al. (2011); Rinaldi et al. (2013); Meitzen et al. (2013); Gurnell et al., 2014).

In the present research, the focus is on the reach scale and on identifying classes or types of river pattern that are observed at this scale, incorporating both river channel and floodplain forms and features. As illustrated in Figure 3.1, these river types reflect processes occurring through time and at larger spatial scales as well as within the reaches that are the focus of the present research.

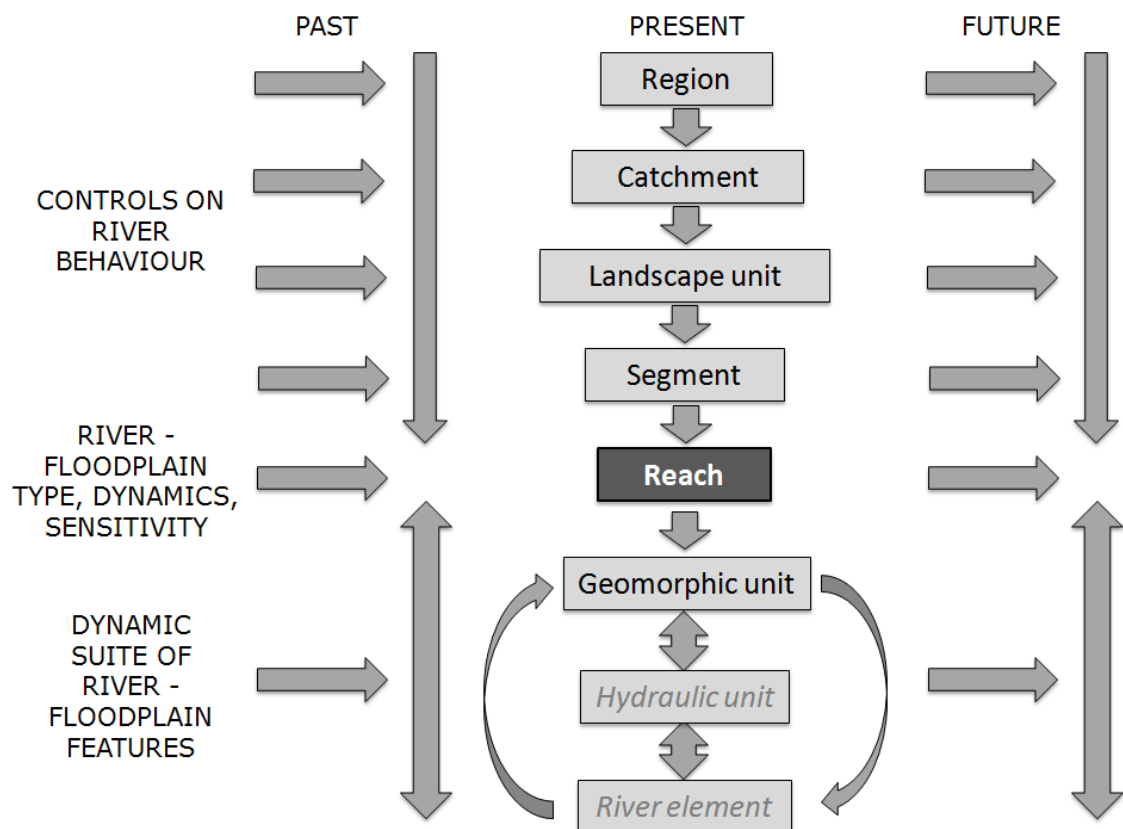


Figure 3.1 A hierarchy of spatial scales, illustrating how the character of a river reach, including the geomorphic units that it contains, is influenced by processes cascading through larger spatial units now and in the past, and how the process cascade influences the future character of the reach (from Gurnell et al., 2014).

In relation to the classification of river and floodplain types at the reach scale, the two pioneers of this field of research, Leopold and Wolman (1957), presented a quantitative basis for distinguishing three types of river channel pattern based upon the land surface channel slope and bankfull discharge: straight, meandering and braided. This early discrimination of three patterns based upon two variables has been extended by many researchers over the subsequent decades. Additional discriminatory variables and processes have been added, including (i) sediment transport control (suspended load, bedload dominated), which implicitly incorporates particle size, and (ii) bed stability (stable, eroding aggrading), which implicitly incorporates particle supply/budget (Schumm, 1963, 1977). These additions allowed variants of the original three-fold classification to be identified along gradients of discharge, slope, sediment calibre and dynamics, to which a further group of multi-thread channel patterns, anastomosing rivers was later added (Smoth and Smith, 1980; Knighton and Nanson, 1993). While, much of the research has been devoted to the properties of the main river channel, Nanson and Croke (1992) extended geomorphologically-based river classification into the floodplain, emphasising the interconnectedness between channel and floodplain, to propose a genetic classification of floodplains that linked floodplain and river types. In general, the focus of these classifications has been alluvial channels, many of which have well-developed floodplains. Steep, confined channels types have received less attention, limiting the application of the classifications.

In parallel with the above classifications, the concept of stream power was used as predictor of sediment transport (Bagnold, 1966). Stream power is estimated from the two variables that underpin much of the classificatory research (discharge and slope), although in this case the water surface slope is employed. It also links these two variables with sediment transport, and its applications have included the consideration of both bedload and suspended load (Bagnold, 1977), channel instability and bank erosion (Brookes, 1987), and the identification of thresholds between channel styles (Ferguson, 1981; Van den Berg, 1995). This work has incorporated measures of total and specific stream power, but neither are truly independent of channel type. Both incorporate channel or water surface slope, which depend partly on channel sinuosity, whereas specific stream power also depends on the channel width, which in turn reflects channel geometry. Nevertheless, stream power is recognized as a powerful variable to support geomorphological classification of rivers at different spatial scales because of

its strong association with channel processes and adjustment (National Rivers Authority, 1992; Kondolf, 1995; Newson, et al., 1998).

Another important dimension in attempts to classify rivers has been to adopt a spatially hierarchical analysis. Fluvial systems are naturally hierarchical, with larger units accommodating the smaller ones. Such a sequence of spatial units includes: landscape/regions, catchment, valley, channel reach, geomorphic/hydraulic units, microhabitats (Lotspeich, 1980; Amoros, et al., 1982; Frissel, et al., 1986). Generally, the smaller units are controlled by the properties and processes occurring in the larger units within which they are located, and not vice versa (Naiman, et al., 1992). Thus, the same region, climate, lithology, topography and land cover would constrain stream characteristics so that only a particular range of stream types or classes are feasible, and in turn, the stream type would constrain the range of smaller features that are present. This hierarchy of controls implies that one must consider more than local conditions to appreciate the controls on river types (Hynes, 1975).

3.2.2 Design and Measurement Quality

The consistency and precision of measurements is fundamental to the quality of the scientific outcomes that can be extracted from data sets. Variables need to be quantified in a consistent and rigorous manner. In many cases, solving the problem of what to measure and how to measure also helps the broader conceptualisation of what is to be studied, and in every case, quantification is an improvement on qualitative assessment (Goudie, 1990).

Establishing valid measurement techniques is a crucial step in any geomorphological study. A strong theoretical background and structure to the research helps to define the objects and features that need to be measured. The measurement procedures that are adopted should gather meaningful and consistent data to ensure that hypotheses can be tested rigorously. Therefore, the measurement procedure should be well defined with a clear set of guidelines and criteria that ensure the collection of consistent and reproducible measurements. In many cases, simple methods are preferable to complex ones, because they are more likely to produce consistent measurements even though those measurements may represent a compromise in the level of detail obtained. In this sense, precision (repeatability of the measurement) takes precedence over accuracy (proximity of the measurement to the 'true' value). This is particularly true of a complex field science like geomorphology (Harvey, 1969).

Decisions on measurement techniques need to be coupled with a broader ‘experimental’ design that dictates when and where measurements should be taken and how many measurements are needed to test the hypotheses of interest. Both are implicit components of scientific investigations, in which existing knowledge is explored; research questions are defined; an ‘experimental’ design is established to test those questions; measurements are taken according to the design; the data are analysed to test the research questions or hypotheses; and as a result the hypotheses are confirmed, modified or rejected. Relatively few geomorphological studies have a fully developed, well-grounded experimental design, instead giving most attention to methods of detailed measurement (Slaymaker, 1980). Even when design and measurement are given full and equal emphasis, Church (1984) argued that most field-based research merely constituted ‘case studies’, even though the empirically-based outcomes may contribute to the development of theory or conceptual models. He stressed the need for initial ‘exploratory’ experiments from which ‘confirmatory’ experiments could be devised and conducted, and then their outcomes tested on different sites, before field research could go beyond ‘case study’ status.

The present research attempts to address several of the above issues by placing emphasis on (a) obtaining simple, repeatable and precise measurements; (b) extracting those measurements from a large and ‘representative sample’ of single-thread rivers across Europe; in order to (c) propose a robust classification of European single-thread rivers that can subsequently be (d) explored, tested and validated or modified.

3.2.3 Geospatial Data

Fluvial geomorphological research is benefitting from the development of many new data acquisition techniques including geospatial methods (e.g. multi-spectral, radiometric, dGPS data sets) that provide high spatial and temporal resolution information for large areas, and geophysical methods (e.g. isotopic, microscopic, luminescence data sets) that allow a range of new properties of geomorphological phenomena to be quantified. Over the last 50 years, these methods have multiplied, increased in precision, and have become more widely available to support the investigation of river processes through field observations, experimental investigations and numerical methods (Thorndycraft, et al., 2008).

Early data acquisition in fluvial geomorphology was predominantly based upon qualitative field observations and subjective map interpretation. However, statistical testing has required quantitative data sets, which are increasingly derived from

laboratory analyses as well as field investigations. True laboratory experiments (e.g. flume based research) allow detailed examination of cause-and-effect relationships while controlling boundary conditions (e.g. gradient, sediment calibre, temperature, moisture) that cannot be controlled in the field (Goudie, 1990). The availability and quality / accuracy of these three information sources have constrained many geomorphological studies of river channel form and adjustment (e.g. Hooke and Kain, 1982).

Recent development of geospatial methods has eased the acquisition of data, particularly when multi-temporal data sets are required or where large-area spatial coverage is important. Global positioning (GPS), digital photogrammetry techniques, and high resolution ground and airborne remote sensing data sets (Airborne Laser Scanning, Synthetic Aperture Radar, Light Detection and Ranging) have revolutionised the quantity and quality of information available for geomorphological study. At the same time, these techniques and data sets can be acquired at increasingly reasonable costs, allowing their widespread use.

Google Earth is an information system through which a range of geospatial data sets can be accessed. The data held within the Google Earth information system is available under two different licenses: Google Earth, a free version with limited function, and Google Earth Pro (\$399 per year) with greater functionality for commercial use. Google Earth incorporates a virtual globe onto which geographical information acquired by Google is registered. This geographic information system provides geographic coordinates (latitude/longitude) based on the World Geodetic System 1984 (WGS 1984) datum and allows image data to be viewed through a 'General Perspective' projection (Google, 2013).

Through the Google Earth information system, data layers comprising multi-spectral satellite imagery (captured from satellite platforms), and aerial images (captured from aircraft) are registered to the same virtual globe and can be interrogated. The typical baseline resolution of Google Earth data varies across the Earth according to the availability of imagery within the information system (Google, 2013). Recent images are often of high spatial resolution across the European study area because of the availability of airborne imagery, with resolutions of up to 0.15-0.30 m for France, Germany, Switzerland, Italy, and the United Kingdom. However, where airborne imagery is not available, the highest spatial resolution of recent images is generally around 15 m. Historical imagery (usually back to year 2000, but sometimes to the mid

twentieth century) is available for most locations. In addition, digital elevation data are provided from NASA's Shuttle Radar Topography Mission (SRTM) to support 3D images (Farr, et al., 2007), and the elevation data can also be extracted as point elevations.

The present research explores the degree to which robust data sets describing river characteristics can be extracted from Google Earth and can then be analysed to derive a classification of single-thread rivers. The rationale for this research is that the Google Earth information system is freely available, it integrates a vast selection of images as well as digital elevation data, and provides tools to extract distance measurements. Thus, the Google Earth information system has the potential to support quantification of key river channel dimensions such as channel width, slope and sinuosity, as well as images from which channel and floodplain features can be assessed. Of course, the precision and accuracy of any extracted information is constrained by the accuracy of the dimensional data, the degree to which feature interpretation is feasible from aerial images, and the precision with which the various data sets have been registered to the virtual globe. Therefore, it is crucial to develop a set of definitions and rules by which robust data can be obtained.

The aims of this chapter are:

1. To assess the potential of the Google earth information system to provide robust data on river characteristics
2. To develop definitions and methods for extracting river characteristics from the Google Earth information system.
3. To analyse the extracted data in order to produce a classification of European single-thread rivers.

In chapter 4, additional data sets, notably river flow time series and information on bed material calibre will be introduced to refine the classification, and the robustness of the digital elevation data will be tested using some higher resolution data sources.

3.3 Methods

This section provides details of the methods used in the research including site selection (3.3.1); extraction of information from Google Earth (3.3.2); preparation of

data for analysis (3.3.3) and methods of data analysis (3.3.4). The stages described in sections 3.3.1 to 3.3.3 are shown schematically in Figure 3.3.

3.3.1 Site selection

Prior to selecting the study sites, a set of criteria were developed to guide site selection. These criteria required the selected sites:

- (i) To be morphologically intact and free to adjust. This was based on identifying sites that were unconfined by buildings, infrastructure and channel training structures such as embankments. Because of the widespread modification of European rivers, sites where up to 20 % of the channel length was affected by engineering structures were permitted. Moreover, any modifications that are not apparent from a plan image could not be recognised and thus many of the selected sites may have greater modification than was anticipated.
- (ii) To be located within 30 km of a known gauging station. This constraint was imposed to support the more detailed analyses presented in chapter 4.
- (iii) To be sufficiently long to support data extraction from up to three (replicate) reaches, ensuring capture of a substantial range of representative geomorphological features.

To ensure sufficient information for a robust statistical analysis, a minimum of 50 sites was required within which replicate reaches could be investigated (i.e. a minimum of 50 sites x 3 replicate reaches = 150 reaches).

To satisfy criterion (2) and contribute to satisfying criterion (1), the search started with a list of European gauging stations deemed to have a near natural flow regime (Stahl et al., 2010). This list emanated from the FRIEND programme and so was confined to the participating European countries, largely restricting the areas of Europe that could be investigated to northern and western Europe.

The river gauging sites were viewed within Google Earth. At each site, a search was conducted upstream and downstream to establish whether:

- (1) the imagery was of sufficient spatial resolution for analysis (i.e. baseflow channel width \gg 10 pixels);
- (2) to further satisfy criterion (1), whether the river appeared to be morphologically intact and free to adjust;

- (3) to satisfy criterion (3), whether a sufficiently long river length was available to identify at least three, replicate reaches for analysis. These were usually adjacent to one another (e.g. Figure 3.2),

The above procedure followed the decision tree illustrated in Figure 3.3A, and progressed until a large enough sample of rivers had been identified that were also widely distributed geographically and represented a variety of environmental conditions.

In the event, 75 sites were identified and for almost all of these, information was extracted for 3 (replicate) with a minimum reach length of 70 times the bankfull channel width.



Figure 3.2 An example of three replicate reaches of River Dee, UK, and indicated by yellow, red and light blue lines from upstream to downstream.

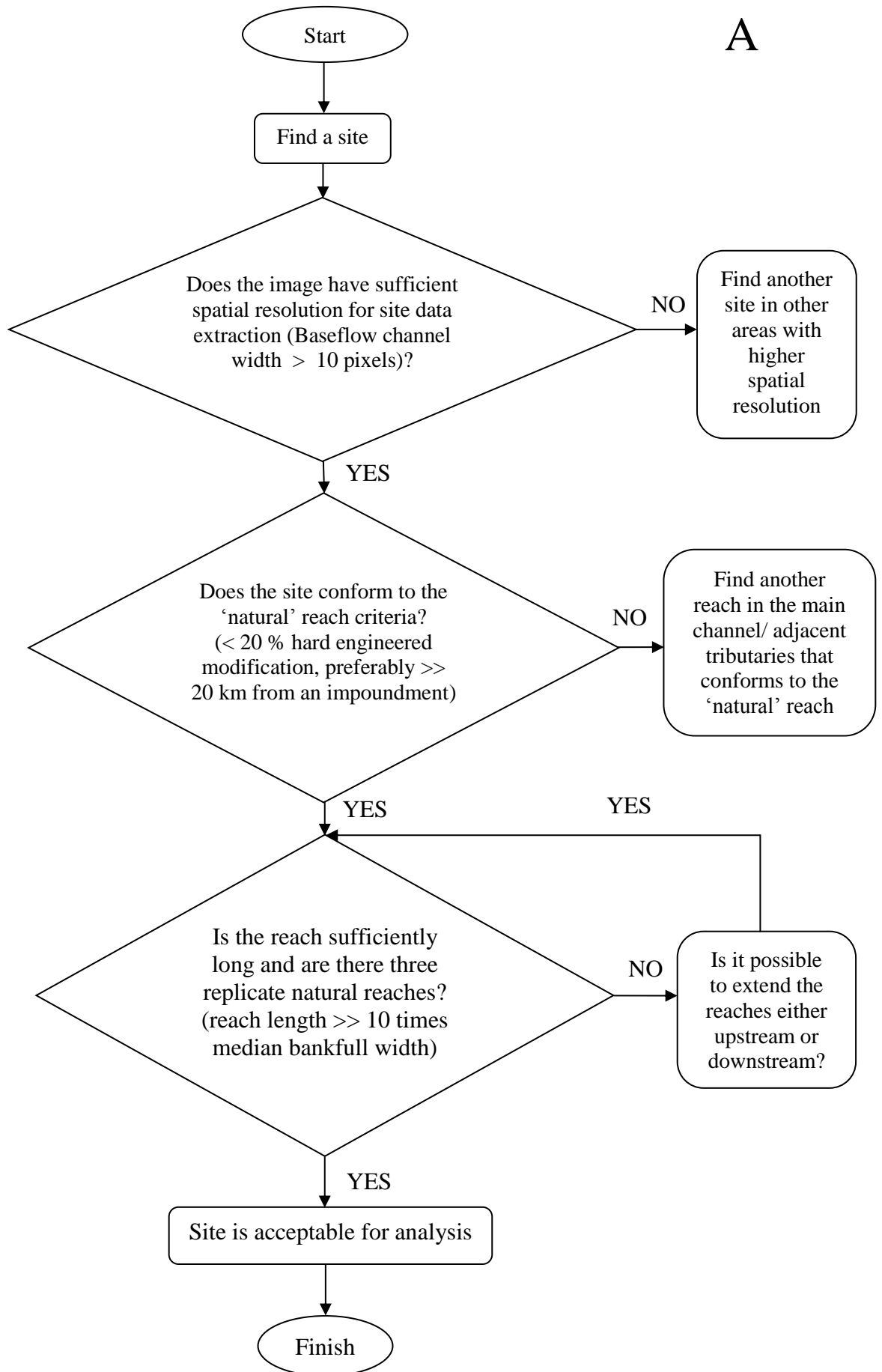


Figure 3.3 A (for caption see page 74)

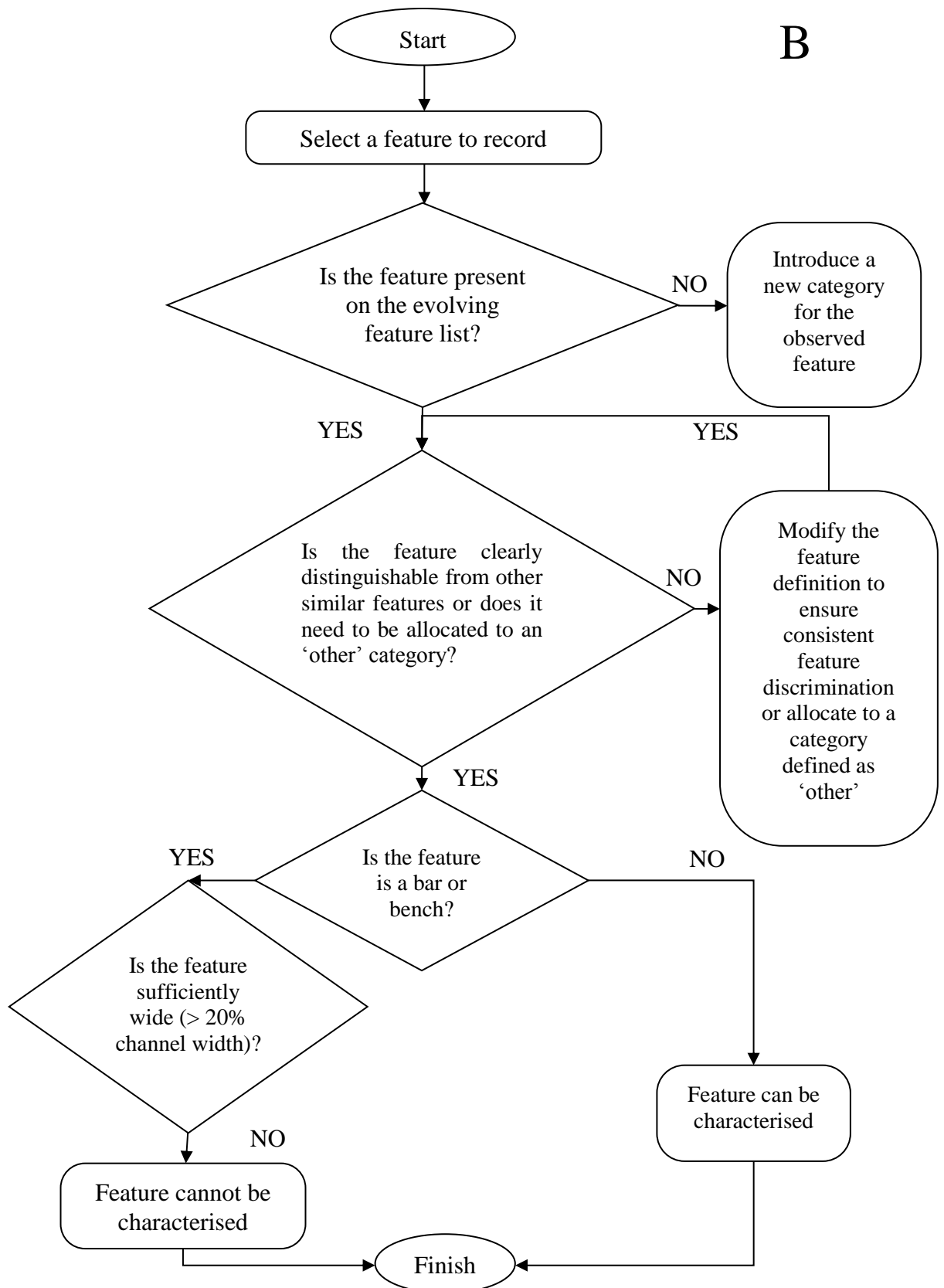


Figure 3.3 A. Decision tree used to identify sites and reaches for analysis B. Decision tree used to refine the recorded feature set and to record individual features

3.3.2 Defining relevant geomorphological, vegetation, and channel geometry features to support consistent data extraction

Geomorphologists recognise many different geomorphological features and often devise different terms to describe similar features. In addition, the vegetation, landform and geometric features that can be extracted from aerial imagery may not correspond with those that can be identified on the ground. Furthermore, if features are to be identified from 2-D images, they may require a different definition than that which would be used for ground identification. Therefore, it is important that the features extracted from Google Earth are named and defined in a consistent way, even if this means grouping features that could be separated on the ground, or defining features in a broader way to ensure consistency. Figure 3.3 describes the decision tree used to record features.

Google Earth provides multi-temporal images for most sites. The recent images available for each site were studied, in order to select one that was of good resolution, was a spring, summer or early autumn image to reveal the vegetation characteristics, and showed the river under baseflow conditions to allow bed and bar features to be recognised. This image was then used for data extraction, with reference to other images of the same site where there was uncertainty about feature recognition.

The terminology and definitions developed for application to Google Earth data are presented in two tables: Table 3.1 defines geomorphological and vegetation features and Table 3.2 defines the measured river channel dimensions. These tables show the most detailed list of variables that was felt to be identifiable from aerial imagery.

The intention was to collect a detailed data set that could subsequently be used to create a suitable set for underpinning a river classification. Thus the rationale was that information could always be amalgamated at a later stage, but it would not be desirable to have to return to the sampled sites at a later stage and to add new variables that had not been included in the initial data extraction.

Table 3.1 Definitions of geomorphological and vegetation features of rivers and floodplain that were extracted from Google Earth images (yellow arrow/circle in images indicates the geomorphic features, flow direction is consistently from left to right or top to bottom of each image)




CHANNEL FEATURES		
Channel Bed Features		
Feature Name	Descriptions	
Pool		Topographic depression in the river bed, providing deep areas of water and tranquil flows
Riffle		Relatively shallow area of the river bed with rapid flow (generally subcritical or near critical).
Boulder		Large irregular rocks exposed clearly through the water surface at normal flows
Cascade		>50 % of water surface is broken (supercritical flow) across a river bed comprising disorganized boulders

Table 3.1 (ctd.)




<p>Step, waterfall</p>		<p>Flow falls near vertically over bedrock/boulder steps (<1 m high) or waterfalls (>> 1 m high). These features were grouped because it is impossible to judge feature height from a plan image.</p>
<p>Exposed bedrock</p>		<p>Elongated, fairly flat exposure of rock that forms a semi-continuous surface close to the water surface</p>
<p>Bars and benches</p>		
<p>Bar (or bench) types</p>	<p>Descriptions</p>	
<p>Mid-channel bar</p>	<p>Mid-channel depositional feature that is not attached to the banks at normal flow and occupies a minimum of 20 % channel width</p>	
<p>Mid-channel longitudinal</p>		<p>Mid-channel depositional feature whose main axis is oriented parallel to the river banks</p>

Table 3.1 (ctd.)




Mid-channel transverse			Mid-channel depositional feature whose main axis is oriented perpendicular to the river banks
Mid-channel complex			(Usually large) mid-channel depositional feature with complex shape and surface features.
Other mid-channel bars		None of the aforementioned mid-channel bars	
Marginal Bar		Depositional features attached to the river bank and extending into the channel for at least 20% of the bankfull width	
Point bar (Arc-shaped, bank attached bar formed	Plain point bar		Simple point bar

Table 3.1 (ctd.)




	<p>With scrolls</p>		<p>Point bar with ridges running parallel to the river bank superimposed on its surface</p>
	<p>With chutes</p>		<p>Point bar with a channel parallel to the river bank cut along all or the downstream part of its surface, dissecting and in some cases separating the point bar from the bank.</p>
<p>Counterpoint bar</p>		<p>Bank-attached depositional feature located on the upstream limb of a, usually tightly curved, convex river bank</p>	

Table 3.1 (ctd.)




<p>Point-to-counterpoint bar</p>		<p>Inclined marginal depositional feature that extends continuously along a convex and concave river bank or vice-versa</p>
<p>Lateral bar</p>		<p>Bank-attached bar that runs along the base of one river bank in relatively straight or low sinuosity reaches</p>
<p>Diagonal bar</p>		<p>Bank-attached elongated bar that runs diagonally across the river channel</p>

Table 3.1 (ctd.)




<p>Tributary bar</p>		<p>Bank-attached depositional feature located at a channel confluence</p>
<p>Other channel margin bars</p>	<p>None of the aforementioned marginal bars</p>	
<p>Bench</p>		<p>Intermediate depositional feature formed along the river bank that is usually vegetated and has a clear break of slope at bank and channel edges (marked by shadows)</p>
<p>Point bench</p>		<p>Intermediate depositional feature formed along the river bank face on the inside of a river bend that is usually vegetated and has a clear break of slope at bank and channel edges (marked by shadows).</p>

Table 3.1 (ctd.)




Wood and Vegetation		
Emergent macrophytes at channel margin		Clumps of emergent aquatic plants exposed above the water surface close to the channel margins
Emergent macrophytes across channel		Clumps of emergent aquatic plants exposed above the water surface across the central part of the channel, sometimes extending to the banks
Lateral wood accumulation		Accumulation of large wood pieces or a single large tree at the channel margin (often inducing development of a bank-attached bar)
Mid-channel wood accumulation		Mid-channel accumulation of large wood pieces or a single large tree, often inducing sediment deposition and the creation of a mid-channel bar
Vegetation cover on channel features		
Vegetation development	Descriptions	
Unvegetated		No significant vegetation cover

Table 3.1 (ctd.)






<p>Sparse vegetation development</p>		<p>< 30 % coverage of poorly-developed, low vegetation patches</p>
<p>Intermediate vegetation development</p>		<p>< 80% vegetation cover usually including some large vegetation patches and some shrubs</p>
<p>Mature vegetation development</p>		<p>> 80% cover, usually of well developed, mainly closed canopy, vegetation including shrubs and trees (for mid-channel bars, this level of vegetation cover would be equivalent to an island)</p>
<p>RIPARIAN AND FLOODPLAIN FEATURES</p>		
<p>Water-filled features</p>		
<p>Feature name</p>	<p>Descriptions</p>	
<p>Side channel</p>		<p>Smaller-scale secondary channel attached at both ends to main channel</p>
<p>Swamp/wetland</p>		<p>Wet vegetated depression with little open water</p>

Table 3.1 (ctd.)



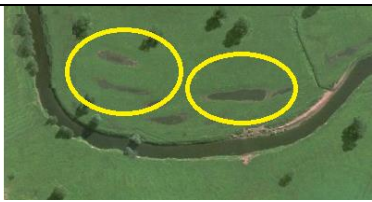

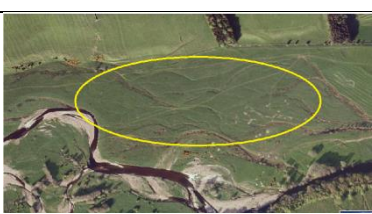

Pond / Lake types	Oxbow		Disconnected, water-filled, single meander (remaining after meander neck/ chute cut-off)
	Meander		Water-filled, disconnected section of meandering channel comprising more than one meander bend
	Linear		Disconnected, linear/elongated dry scour / channel water-filled feature
	Other	None of the aforementioned	
Moist-dry Features			
Feature name		Descriptions	
Moist-dry pond / lake type	Oxbow		Dried-up abandoned single meander (often remaining after, meander neck/ chute cut-off)
	Meander		Dried-up abandoned section of meandering channel comprising more than one meander loop
	Linear		Linear/ elongated dry scour/ channel feature
	Other	None of the aforementioned	

Table 3.1 (ctd.)





Chute		Channel cut by fast moving water draining off the floodplain or bar surfaces into the channel, usually through head-cutting
Ridges and Swales		Linear, usually curved, parallel ridges separated by linear lows or swales. These are vegetated remnants of scroll bars (snow covered in this illustration)
Number of branches		A count of larger-scale secondary channels attached at both ends to main channel
Riparian Vegetation		
Vegetation Structure	Vegetation along margins within 50 % bankfull width of the main channel (This limit was placed to focus on vegetation that may be interacting with the channel and is less likely to be heavily modified by human activity than vegetation set back from the channel margins)	
Bare		Mainly bare earth/rock

Table 3.1 (ctd.)

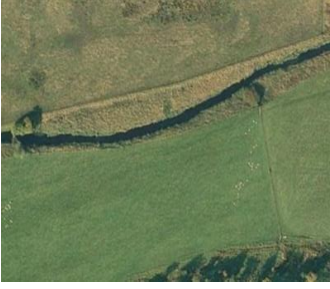




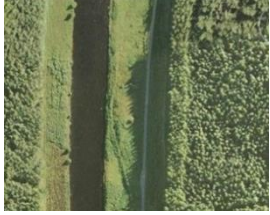
Uniform		<p>Mainly one structural type of vegetation (one from low (e.g. grass), intermediate (e.g. grasses/herbs))—identified by colour, texture, shadow</p>
Simple		<p>Two or three vegetation structural types (from low (e.g. grass), intermediate (e.g. grasses/herbs), and shrubs)</p>
Complex		<p>All four vegetation structural types (low (e.g. grass), intermediate (e.g. grasses/herbs), shrubs, trees)</p>
Tree Distribution	<p>Tree distribution along bank tops within 50% bankfull width of the main channel. (This limit was placed to focus on vegetation that may be interacting with the channel and is less likely to be heavily modified by human activity than vegetation set back from the channel margins)</p>	
None	<p>No trees</p>	
Isolated		

Table 3.1 (ctd.)









<p>Regularly Spaced</p>		
<p>Occasional clumps</p>		
<p>Semi-continuous</p>		
<p>Continuous</p>	 <p>images from Environment Agency (2003)</p>	

Table 3.2 Definitions of channel dimensions that were extracted from Google Earth

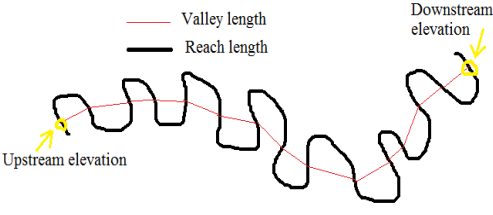


Dimension name	Description	Image (where necessary)
Upstream elevation (m)	Elevation of the lower bank top at the upstream end of the reach	
Downstream elevation (m)	Elevation of the lower bank top at the downstream end of the reach	
Valley length (m)	Sum of straight line lengths between channel bend inflection points – (points where curvature disappears or where curvature changes direction from minus to plus, or plus to minus – i.e. inflection points)	 <p>The diagram shows a meandering channel with a black line representing the channel path. A red line connects the inflection points of the channel, representing the valley length. A black line segment between two inflection points represents the reach length. Yellow arrows point to the upstream and downstream ends of the channel, labeled 'Upstream elevation' and 'Downstream elevation' respectively. A legend indicates that the red line is 'Valley length' and the black line is 'Reach length'.</p>
Bankfull reach length (m)	Mid-line length of bankfull channel (i.e. channel width to continuous terrestrial vegetation cover – exposed bars are part of channel width)	
Baseflow reach length (m)	Mid-line length of baseflow channel (i.e. channel width at baseflow – exposed bars are excluded)	
Maximum bankfull channel width (m)	Maximum width of the bankfull channel within the reach (e.g. 342 m)	 <p>An aerial satellite image of a river bend. A yellow line is drawn across the widest part of the channel, with the text '342 m' overlaid. A small Google Earth interface element is visible in the top left corner of the image.</p>
Minimum bankfull channel width (m)	Minimum width of the bankfull channel within the reach (e.g. 342 m)	

Table 3.2 (ctd.)

Minimum baseflow channel width (m)	Minimum width of the baseflow channel within the reach	
Bankfull sinuosity	Bankfull channel length / Valley length	
Baseflow sinuosity	Baseflow channel length / Valley length	
Bankfull gradient (o/oo)	(Upstream elevation – Downstream elevation)/ Bankfull channel length	
Baseflow gradient (o/oo)	(Upstream elevation – Downstream elevation)/ Baseflow channel length	
Valley gradient (o/oo)	(Upstream elevation – Downstream elevation)/ Valley length	

3.3.3 Data extraction and preparation

This section explains some of the rules that were developed to ensure (a) consistency in feature identification and (b) data extraction from Google Earth images. Following extraction, it was also necessary to (c) standardize and (d) aggregate variables so that they were representative of similar units, fell within a similar abundance / magnitude range, and did not over-emphasise very rare features that might distort any classification that was developed.

a) Setting thresholds

Because natural features are complex and gradually transform from one type to another, many features had the potential to be defined as one of two or more types. Therefore, it was crucial to set thresholds so that features could be consistently identified when they fell into the transition zone between several types. This issue applied to both geomorphological features and vegetation structure / abundance categories. For example, how continuous is the tree distribution and how complex is the vegetation structure along channel margins? These problems are investigated below:

Separating transitional features: Lateral bars versus point bars

Theoretically, it seems simple to separate lateral and point bars, but this is not always the case (see Figure 3.4). Therefore, lateral bars were defined to have a maximum angle of curvature of 20 degrees.



Figure 3.4 An example of lateral bar

Separating transitional features: Point bars with chutes versus chutes in the floodplain

Frequently, there is no clear boundary on an image that firmly separates river and floodplain. Some features have exactly the same physical appearance but may function differently and have different names when they occur within the active river channel or on the floodplain. Therefore, the limit / edge of the ‘permanent’ vegetation was used as the separation zone between the active channel and floodplain, although even this criterion was sometimes difficult to apply (see Figure 3.5).

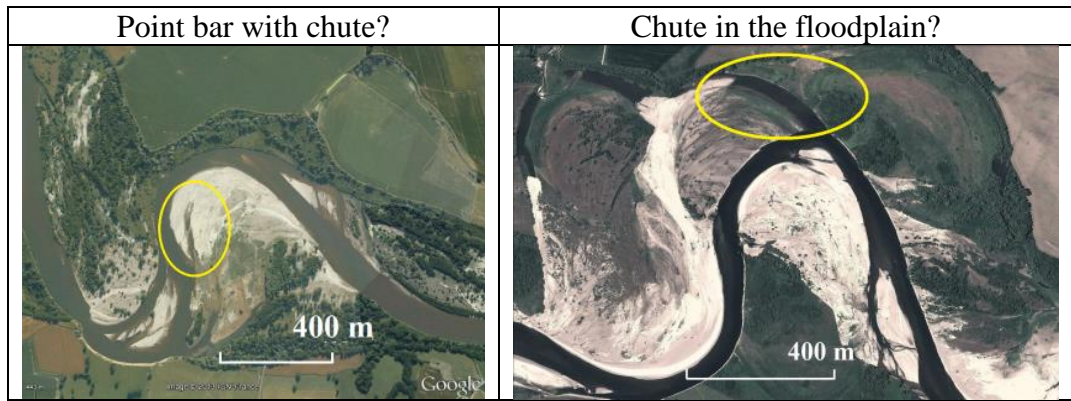


Figure 3.5 A. Instream chute feature B. Floodplain chute feature

Separating transitional features: Benches versus bars

Bars and benches are easily detectable in sunlit images when the sun-angle is appropriate. Benches have a step-shaped cross profile and so clear shadows highlight the elevation difference between bank top and bench top and also between bench edge and water surface, if the flow is low at the time the image was collected (see Figure 3.6). However, where illumination is not ideal, the shadow criterion cannot be used. Under the latter circumstances, the feature was identified as a bar. Therefore, benches are undoubtedly under-represented in the collected data, but when they are identified, this is done with confidence.

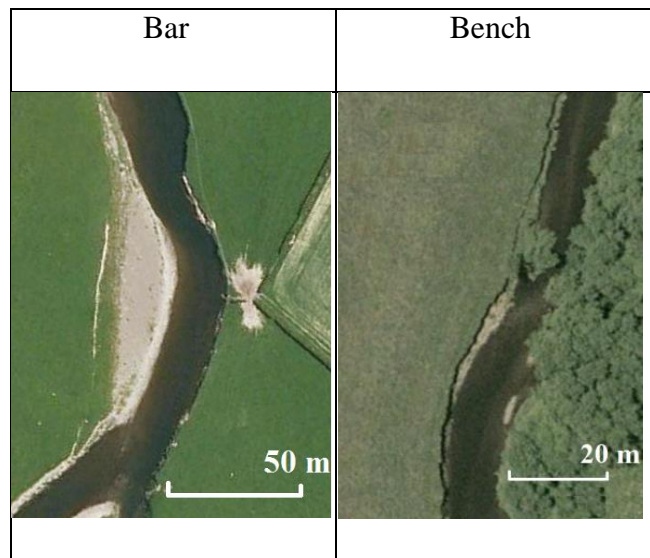


Figure 3.6 A. Bar and B. Bench

Vegetation development: Vegetation on Bars

The development and abundance of vegetation on bars is assigned to one of four classes (unvegetated, sparse, intermediate, and mature). The correct identification of

these classes is important as an indicator of bar age and stability, and was based on two criteria – the presence of gaps in the vegetation, exposing the bare sediment and the degree to which the vegetation included mature trees and shrubs as opposed to simply a low grass-herb layer. Where there was doubt, the bars were assigned to the less-stable class (Figure 3.7).

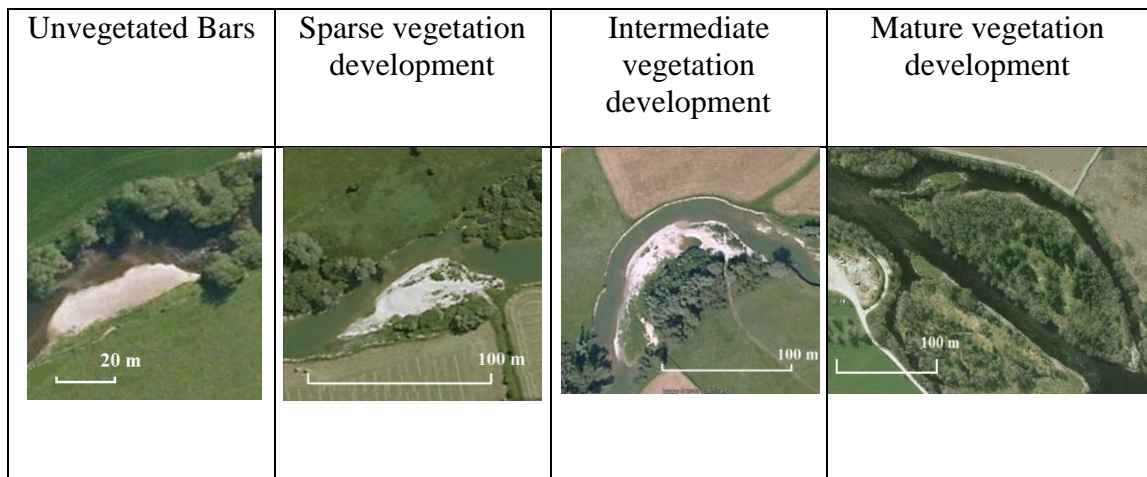


Figure 3.7 Vegetation development

Vegetation development: Floodplain Vegetation

As with bar vegetation, floodplain vegetation structure varies according to the patchiness of the vegetation and the homogeneity of the vegetation structure (mature trees, shrubs, grasses and herbs). Floodplain vegetation structure was assigned to four classes according to the complexity of the mix of different vegetation structural types: bare, short grasses and herbs, tall grasses and herbs, shrubs, mature trees. Thus complexity increases with increasing variability in vegetation height as the taller (shrubs, trees) types of vegetation appear (Figure 3.8). This distinction is detectable by the mix of colours and textures / shapes of vegetation in the imagery.

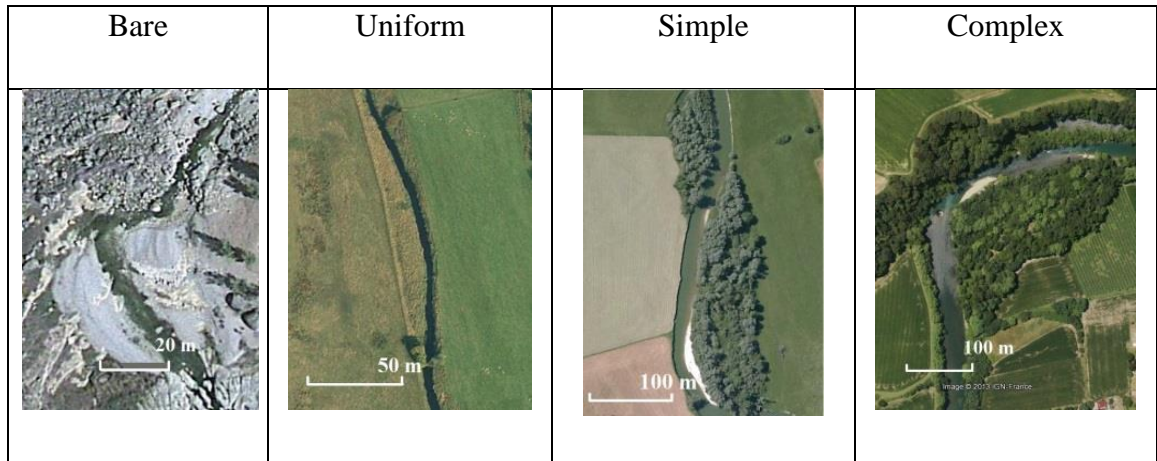


Figure 3.8 Classes of Riparian Vegetation Complexity

Vegetation development: Bank top tree distribution

Because the distribution of trees along the river channel margin is an important indicator of bank stability as well as being a crucial ecological component of the river (large wood, shade, root habitats etc.), this aspect is recorded separately from the above vegetation complexity assessment. Six classes of tree continuity are identified on each bank and it was crucial to keep the example images in Figure 3.9 available, to ensure consistency when assessing tree distributions for the sampled river reaches.

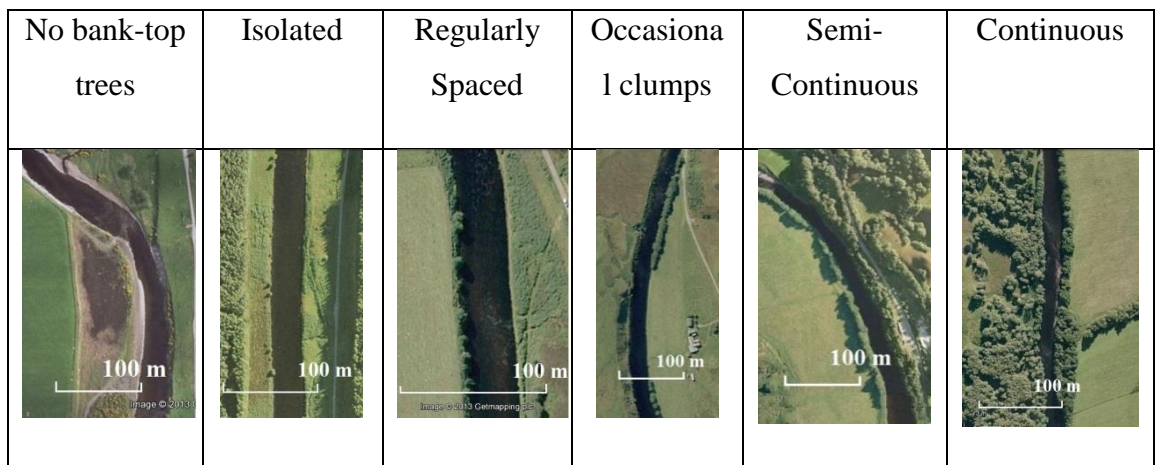


Figure 3.9 Bank-top Riparian Tree Distribution

b) Quantifying variables

Each sampled reach was scanned for the presence of each of the geomorphological and vegetation features listed in Table 3.1, supported by the decision

tree described in Figure 3.3B. The frequency of each type of feature was recorded, regardless of their individual size. For example, a reach might be recorded as having 11 unvegetated point bars and 9 sparsely-vegetated mid-channel longitudinal bars. The only exception to the frequency count method was riparian vegetation, where vegetation structure and tree distribution types were extracted for every 1 to 2 meander loops or river bends for each of the left and right banks.

In contrast to the vegetation and geomorphological features, channel dimensions were much more straightforward to measure. The tool 'path' ruler tab within Google Earth was used to quantify reach length and sinuosity, and elevation was extracted directly for appropriate points to underpin slope estimates. Whilst most channel dimensions could be directly and completely measured using these tools (e.g. reach length, slope, sinuosity), measures of channel width were derived by sampling using the 'path' ruler tab. Careful and consistent judgment was required to locate the boundary between the channel and floodplain as the limit / edge of the 'permanent' vegetation. This indication of bankfull width was especially challenging for single-thread rivers that were close to the transition to multi-thread. However, baseflow widths were readily identified from the water edges shown on images representative of the low flow conditions. For each reach, sections that appeared to show maximum or minimum values of each of minimum baseflow, maximum baseflow, minimum bankfull and maximum bankfull conditions were identified and in each case at least 10 measurements were taken within these sections of the reach to identify the smallest or largest values.

c) Standardizing variables

A particular problem associated with extracting geomorphological features from aerial images is that many features may be obscured by the land cover, particularly by mature vegetation cover. This means that the frequency with which particular features may be recorded will often be lower than their actual occurrence. Even if all features are recorded accurately, their frequency (particularly for channel features) is affected by the dimensions of the river reach, including its length (the longer the length the greater the expected number of any particular feature) and also width (the wider the river, the smaller the expected number of any particular feature within a particular length of reach). Within the collected data set, reaches ranged from 1 to 37 km in length and 10 to 400 m in bankfull width. Therefore, the recorded geomorphic and vegetation variables required some standardisation for the scale of the reach before the properties of the reaches could be compared with confidence.

The geomorphological and vegetation frequency measurements were standardised to allow for the size of each sampled reach by multiplying each frequency by the ratio of bankfull channel width to bankfull reach length. However, the riparian vegetation abundance measurements were combined through a weighted mean which used weightings from 0 to 3 for vegetation structure and 0 to 5 for tree distribution to give an integrated, comparable assessment for each sampled reach.

d) Aggregating and rejecting variables

The data extraction method was applied to 221 reaches of river distributed across 75 sites. Once the data set was assembled, it was possible to investigate how frequently different features were observed. Since the intention was to analyse the data to produce a classification of different morphological types of river, it was important to develop a data set for analysis that (i) did not contain features that were so rare that they simply represented anomalies (from a river type perspective), (ii) did contain variables that were truly informative in relation to river-floodplain form and dynamics, and (iii) contained a small enough set of variables for the meaning of any classification to be clear and interpretable. To achieve these aims, the data set was inspected to exclude very rare variables from analysis and to aggregate other variables to provide representative and robust variables for analysis.

In practice, no variables were so rare and obscure that they could not be aggregated with other variables to produce something that was robust and could contribute to river classification. However, aggregation was particularly useful where geomorphologically-related features were not easily distinguished from one another on aerial imagery (e.g. waterfalls and steps). The aggregate variables that were used in subsequent statistical analyses are listed in Table 3.3.

Table 3.3 Aggregate Variables derived from the Raw Variables extracted from Aerial Imagery

Calculation Formula	Aggregate Feature Name
Channel Dimensions	
Average of minimum baseflow width and maximum baseflow width	Baseflow Median Width
Average of minimum bankfull width and maximum bankfull width	Bankfull Median Width
Ratio of Baseflow Median Width to Bankfull Median Width	Baseflow_Bankfull Median Width
Ratio of Baseflow Channel Slope to Bankfull Channel Slope	Baseflow_Bankfull Channel Slope
Ratio of Baseflow Sinuosity to Bankfull Sinuosity	Baseflow_Bankfull Sinuosity
Channel Bed Features	
Number Waterfalls + Number Steps	Steps
Channel Bar and Bench features	
Number Unvegetated Marginal Bars + Number Sparsely Vegetated Marginal Bars	Total Active Marginal Bars
Number Intermediately Vegetated Marginal Bars + Number Maturely Vegetated Marginal Bars	Total Stabilising Marginal Bars
Number Unvegetated Mid-Channel Bars + Number Sparsely Mid-Channel Bars	Total Active Mid-Channel Bars
Number Intermediately Vegetated Mid-Channel Bars + Number Maturely Vegetated Mid-channel Bars	Total Stabilising Mid-Channel Bars
Number Unvegetated Benches + Number Sparsely Vegetated Benches	Total Active Benches
Number Intermediately Vegetated Benches + Number Maturely Vegetated Benches	Total Stabilizing Benches
Channel Margin Transitional and Floodplain Features	
Number Water-filled depressions (oxbow + meander + linear + other)	Total Water-filled Depressions
Number Water-filled side-channels + Number of branches	Total Connected Side Channels
Number Moist / dry ponds (oxbow +meander + linear + other)	Total Dry Depressions
Number (water-filled + moist / dry) oxbows	Total Oxbows
Number Floodplain scrolls + Number Floodplain chutes	Ridges and Swales
Number Intermediate and Maturely Vegetated Point and Counterpoint Bars (Point + Point with Scrolls + Point with Chutes + Counterpoint + Point-to-Counterpoint)	Total Stabilising Arcuate Bars
Number Intermediate and Maturely Vegetated Side Bars (Lateral, Tributary, Other Marginal Bars)	Total Stabilising Non-arcuate Bars
Vegetation	
Inner Bank Vegetation Structure + Outer Bank Vegetation Structure	Riparian Vegetation Complexity
Right Bank Tree Distribution + Left Bank Tree distribution	Riparian Tree Distribution
Marginal Emergent Macrophytes + Mid-Channel Emergent Macrophytes	Emergent Macrophytes
Lateral Wood Accum. + Mid-Channel Wood Accum.	Wood Accumulation

3.3.4 Statistical analysis

All multivariate analysis was conducted using XLSTAT Pro. Two types of multivariate analysis were applied to the 75 river (221 reach) data set. Principal Components Analysis (PCA) was used to investigate the nature of any environmental gradients present in the data set, whereas Agglomerative Hierarchical Cluster Analysis (AHC) was used to group reaches into clusters with similar characteristics. Kruskal-Wallis tests were used to assess the statistical significance of the outcomes of the multivariate analyses.

a) Principal Component Analysis (PCA)

Principal Components Analysis (PCA) reduces data sets comprising observations on a large number of variables, which are often strongly inter-correlated, to a series of independent components that represent multivariate gradients present within the data. Fundamentally, it projects observations from m-dimensional space with m-variables to n-dimensional spaces (where $n \leq m$) in order to preserve potential of information from original dimensions (Jolliffe, 2002). The first few principal components (PCs) 'explain' the largest proportions of the variance in the data set and each PC can be interpreted in terms of the original variables with the highest positive or negative 'loadings' on the PC.

In the present analysis, the original and aggregate variables were split into subgroups representing particular sets of 'traits' of the analysed reaches. Because the majority of the variables were not normally distributed and were only semi-continuous, PCA was conducted on a Spearman's rank correlation matrix among the variables. Following the analysis, those variables with eigenvalues > 1 were inspected to identify their geomorphological meaning, because PCs with eigenvalues > 1 account for more of the variance in the data set than any original variable (Cattell, 1996). The contribution of each the original variables to a PC is indicated by their 'loading' on the PC. The value of loadings ranges between +1 (positive relationship) and -1 (negative relationship), thus variables with high positive and negative loadings can be used to interpret the meaning of the environmental gradient described by the PC. In the present analysis, variables with loadings > 0.7 or < -0.7 were used to interpret the meaning of the PC, supported by those variables with loadings between 0.6 to 0.7 or -0.7 to -0.6.

Table 3.4 lists the six groups of variables subjected to Principal Components Analysis.

**Table 3.4 Groups of Raw (Table 3.1 and Aggregate Variables (Table 3.3))
subjected to Principal Components Analysis**

Group	Variable (units)
River dimensions	Baseflow Median Width (m) Baseflow Sinuosity Baseflow Channel Slope (per mil) Bankfull Median Width (m) Bankfull Sinuosity Bankfull Channel Slope (per mil) Valley Gradient (per mil)
Dimension ratios	Baseflow_Bankfull Median Width Baseflow_Bankfull Sinuosity Baseflow_Bankfull Channel Slope
Channel bed features	Pool Riffle Cascade Waterfall / Step Boulder Exposed bedrock
Channel bar and bench features	Total Active Marginal Bars Total Stabilising Marginal Bars Total Active Mid-Channel Bars Total Stabilising Mid-channel Bars Total Active Benches Total Stabilising Benches
Channel-margin-transitional and floodplain features	Swamp-Wetland Total Water-filled Depressions Total Connected Side Channels Total Dry Depressions Total Ridges and Swales Total Oxbow Total Stabilising Arcuate Bars Total Stabilising Non-Arcuate Bars
Vegetation	Riparian Vegetation Complexity Riparian Tree Distribution Wood Emergent Macrophytes

b) Agglomerative Hierarchical Clustering Analysis (AHCA) for grouping

Hierarchical Cluster Analysis (HCA) groups objects (in this case reaches) according to their similarity (the values of a set of variables recorded for each object). The “Agglomerative” clustering technique employed in this research uses a “bottom up” approach where similar objects are grouped and then these are grouped again so that progressively larger groups are formed in a hierarchical fashion (Everitt, et al., 2001).

The clustering proceeds using a measure of dissimilarity based upon an appropriate distance metric (a measure distance between pairs of observations), and a linkage criterion (a technique to specify the rules by which the distance measure is used to construct the clusters).

In this research, Euclidian distance was employed as the measure of dissimilarity:

$$\|a - b\|_2 = \sqrt{\sum_i (a_i - b_i)^2} \quad (3.1)$$

The Ward's linkage method was used, so that within group inertia increases as little as possible to retain cluster homogeneity (Ward, 1963).

Agglomerative Hierarchical Clustering (AHC) was applied to the reach scores on the PCs generated from the 6 PCAs listed in Table 3.4 which had eigenvalues > 1.

Following AHC, the cluster dendrogram and agglomeration schedule plots were inspected to identify the number of clusters that best described the data set. The aim was to select a small number of clusters that represented a high level of within-cluster similarity. These clusters provided an initial classification of the analysed reaches.

c) **Kruskal-Wallis tests**

The Kruskal-Wallis test is a non-parametric statistical test that compares groups of samples to assess whether they are drawn from the same population. In essence it is a non-parametric analysis of variance and is applied to ranked data.

In this research, Kruskal-Wallis tests were used to assess whether the classes generated by the AHC were statistically significantly different from one another. Kruskal-Wallis tests were applied to the scores on each of the PCs included in the AHC analysis, grouped according to the selected classification.

Where the Kruskal-Wallis test generated a statistically-significant result ($p < 0.05$), it was followed by multiple comparisons between the classes using Dunn's procedure with Bonferroni correction in order to identify which classes were statistically significantly different from one another. In this way, it was possible to identify which geomorphological properties distinguished each of the classes and also to describe the characteristics of each class.

If any one of the classes had not been found to be statistically-significantly different from the others in relation to at least one of the PCs, this would have led to a re-evaluation of the classification. The non-significant class would have been merged with another using the AHC agglomeration plot as a guide and then the statistical significance of the new classes would have been investigated using Kruskal-Wallis tests until a final, statistically-significant classification was devised. In the present research, such a re-evaluation of the classes was not necessary.

3.4 Results

The results are presented in four sections. The first three sections present the results of the PCAs, AHC and Kruskal-Wallis tests. The final section presents the classification.

3.4.1 Principal Components Analysis (PCA)

a) River Dimensions

The PCA on the river dimensions variables produced two PCs with eigenvalues greater than 1, which explain 84% of the variance in the data set (Table 3.5). PC1 describes a gradient of decreasing sinuosity and increasing valley and channel gradient, whereas PC2 describes a gradient of increasing channel low flow and bankfull width.

Table 3.5 River Dimensions PCA: Eigenvalues, Variance Explained and Loadings (loadings greater than 0.7 are emboldened)

	PC1	PC2	PC3
Eigenvalue	4.180	1.726	0.876
Variability (%)	59.716	24.663	12.518
Cumulative %	59.716	84.379	96.897
Loadings			
Baseflow Median Width	-0.558	0.730	0.208
Baseflow Sinuosity	-0.749	-0.424	0.499
Baseflow Channel Slope	0.959	-0.092	0.259
Bankfull Median Width	0.047	0.874	0.401
Bankfull Sinuosity	-0.773	-0.461	0.427
Bankfull Channel Slope	0.959	-0.089	0.262
Valley Gradient	0.932	-0.145	0.324

b) Dimension Ratios

Only three ratio variables were included in this PCA and it generated a single PC with an eigenvalue greater than 1, which explains 87% of the variance in the data (Table 3.6). PC1 describes a gradient of increasing sinuosity of the baseflow channel relative to the bankfull channel, which is associated with the baseflow channel filling a decreasing proportion of the bankfull channel (i.e. wide exposure of marginal bars at low flow), and an increasing divergence between the baseflow channel slope and the bankfull channel slope.

Table 3.6 Dimension Ratios PCA: Eigenvalues, Variance Explained and Loadings (loadings greater than 0.7 are emboldened)

	PC1	PC2
Eigenvalue	2.616	0.333
Variability (%)	87.192	11.087
Cumulative %	87.192	98.279
Loadings		
Baseflow_Bankfull Median Width	-0.876	0.481
Baseflow_Bankfull Sinuosity	0.971	0.171
Baseflow_Bankfull Channel Slope	-0.951	-0.269

c) Channel Bed Features

The PCA identified two PCs with eigenvalues greater than 1, which explain 61% of the variance in the data set (Table 3.7). Riffles show a strong (>0.7) positive loading on PC1, which is complemented by a positive loading on pools and thus a gradient of increasing riffle-pool features. Boulders show a negative loading that exceeds 0.6 on this PC, which is supported by a weaker negative loading on exposed bedrock. Therefore, this PC shows an interpretable geomorphological gradient from boulder and bedrock dominated sites to those with riffles and pools. None of the loadings exceed 0.7 on PC2 but all variables have relatively high positive loadings making its geomorphological meaning difficult to interpret, so it was excluded from the AHC analysis.

Table 3.7 Channel Bed PCA: Eigenvalues, Variance Explained and Loadings (loadings greater than 0.7 are emboldened and those between 0.6 and 0.7 underlined)

	PC1	PC2	PC3
Eigenvalue	2.044	1.589	0.938
Variability (%)	34.070	26.482	15.639
Cumulative %	34.070	60.552	76.191
<u>Loadings</u>			
Pool	<u>0.686</u>	0.525	-0.348
Riffle	0.760	0.505	-0.157
Cascade	0.408	0.306	0.697
Waterfall and Steps	-0.357	0.578	0.370
Boulders	<u>-0.617</u>	<u>0.640</u>	0.043
Exposed bedrock	-0.569	0.471	-0.409

d) Channel Bar and Bench Features

The PCA identified three PCs with eigenvalues greater than 1, which explained 71% of the variance in the data set (Table 3.8). PC1 described a gradient of increasing active mid channel bars and both active and stabilising marginal bars, whereas PC2 described a gradient of increasing benches. Only one variable had a loading greater than 0.7 on PC3 (stabilising mid-channel bars) and the eigenvalue only fractionally exceed 1, so this PC was excluded from the AHC, to avoid over-emphasising a single variable.

Table 3.8 Channel Bar and Bench PCA: Eigenvalues, Variance Explained and Loadings (loadings greater than 0.7 are emboldened and those between 0.6 and 0.7 underlined)

	PC1	PC2	PC3	PC4
Eigenvalue	1.976	1.209	1.069	0.794
Variability (%)	32.937	20.142	17.814	13.231
Cumulative %	32.937	53.079	70.893	84.124
<u>Loadings</u>				
Total Active Marginal Bars	0.841	-0.035	-0.346	-0.004
Total Stabilising Marginal Bars	<u>0.673</u>	0.222	0.281	0.177
Total Active Mid-channel Bars	0.850	0.015	-0.161	0.004
Total Stabilising Mid-channel Bars	0.197	0.376	0.835	-0.093
Total Active Benches	-0.068	0.732	-0.298	<u>-0.600</u>
Total Stabilising Benches	-0.227	<u>0.693</u>	-0.242	<u>0.627</u>

e) **Channel-margin-transitional and Floodplain Features**

The PCA identified three PCs with eigenvalues greater than 1, which explained 63% of the variance in the data set (Table 3.9). However, there was only one variable with a loading exceeding 0.6 on PC3, so the PC was excluded from the AHC. Water filled, moist and dry depressions including oxbows showed a strong positive association with PC1, whereas PC2 described an increasing presence of stabilising (vegetated) bars being incorporated into the floodplain.

Table 3.9 Channel-margin-transitional and Floodplain PCA: Eigenvalues, Variance Explained and Loadings (loadings greater than 0.7 are emboldened and those between 0.6 and 0.7 underlined)

	PC1	PC2	PC3	PC4
Eigenvalue	2.442	1.411	1.187	0.993
Variability (%)	30.522	17.636	14.834	12.416
Cumulative %	30.522	48.158	62.992	75.408
Loadings				
Swamp-Wetland	0.323	-0.411	-0.185	0.774
Total Water-filled Depressions	0.786	-0.100	-0.095	0.267
Total Connected Side Channels	0.489	0.343	<u>0.619</u>	0.128
Total Dry Depressions	0.735	-0.073	-0.322	-0.353
Total Ridges and Swales	0.562	0.398	0.492	0.031
Total Oxbows	0.788	-0.120	-0.291	-0.339
Total Stabilising Arcuate bars	-0.062	<u>0.652</u>	-0.431	0.239
Total Stabilising Non-arcuate bars	0.013	0.715	-0.380	0.092

f) **Vegetation**

The PCA identified two PCs with eigenvalues greater than 1, which explained 75% of the variance in the data set (Table 3.10). PC1 describes an increasing gradient of vegetation complexity and tree cover, whereas PC2 shows an increasing cover of emergent macrophytes.

Table 3.10 Vegetation PCA: Eigenvalues, Variance Explained and Loadings (loadings greater than 0.7 are emboldened and those between 0.6 and 0.7 underlined)

	PC1	PC2	PC3
Eigenvalue	1.922	1.091	0.794
Variability (%)	48.042	27.282	19.849
Cumulative %	48.042	75.324	95.173
Loadings			
Riparian Vegetation Complexity	0.931	-0.030	-0.187
Riparian Tree Distribution	0.926	-0.045	-0.212
Wood	0.380	<u>0.668</u>	<u>0.640</u>
Emergent Macrophytes	-0.230	0.802	-0.552

g) Summary

Overall the PCAs generated a total of 10 PCs that had eigenvalues greater than 1, and described geomorphologically-informative gradients in the data set. These are listed and described in Table 3.11 and provide the input data from the HCA presented in section 3.2.

Table 3.11 The 10 PCs selected from the 6 PCAs to describe geomorphologically-interpretable gradients in the 75 river data set

Variable Group	PC	Name
1. River dimensions	PC1.1	Slope(+)Sinuosity(-)
	PC1.2	Width(+)
2. Dimension ratios	PC2.1	Baseflow/Bankfull(Sinuosity(+))Slope(-)Width(-)
3. Channel bed features	PC3.1	Riffle-Pool(+)Boulder-Bedrock(-)
4. Channel bar and bench features	PC4.1	Marginal&Mid-channelBars(+)
	PC4.2	Benches(+)
5. Channel-margin-transitional and floodplain features	PC5.1	FloodplainDepressions&Ponds(+)
	PC5.2	VegetatedSideBars(+)
6. Vegetation	PC6.1	RiparianComplexity&TreeCover(+)
	PC6.2	EmergentMacrophytes(+)

In order to gain an overall perspective of how the 221 analysed reaches were discriminated by these PCs, a final aggregate PCA was conducted on the 221 reach scores on all of the ten PC-based variables listed in Table 3.12. Aggregate PC1 describes a gradient of increasing marginal and mid-channel bars (Marginal&Mid-channelBars(+)), which are also being incorporated into the floodplain as stable side bars (VegetatedSideBars(+)) along a gradient of channels where the baseflow channel is

increasingly narrower, more sinuous and of lower slope relative to the bankfull channel (Baseflow/Bankfull(Sinuosity(+))Slope(-)Width(-)). PC2 shows a gradient of increasing riparian vegetation complexity and tree cover (RiparianComplexity&TreeCover(+)). PC3 has no loadings greater than 0.7, but the highest loading (0.651) indicates a gradient of decreasing boulders and increasing riffle-pools (Riffle-Pool(+))Boulder-Bedrock(-)), which suggests some discrimination of bed material calibre.

Table 3.12 Integrated PCA of the scores on the PCs listed in Table 3.11: Eigenvalues, Variance Explained and Loadings (loadings greater than 0.7 are emboldened and those between 0.6 and 0.7 underlined)

	PC1	PC2	PC3
Eigenvalue	3.063	1.991	1.284
Variability (%)	30.631	19.913	12.842
Cumulative %	30.631	50.545	63.387
Loadings	F1	F2	F3
PC1.1 Slope(+))Sinuosity(-)	0.594	0.192	-0.363
PC1.2 Width(+)	<u>0.627</u>	-0.238	0.411
PC2.1 Baseflow/BankfullSinuosity(+))Slope(-)Width(-)	0.731	-0.342	-0.295
PC3.1 Riffle-Pool(+))Boulder-Bedrock(-)	-0.073	-0.287	<u>0.651</u>
PC4.1 Marginal&Mid-channelBars(+)	0.892	0.203	-0.164
PC4.2 Benches(+)	0.194	<u>0.629</u>	0.259
PC5.1 FloodplainDepressions&Ponds(+)	-0.262	<u>-0.614</u>	0.181
PC5.2 VegetatedSideBars(+)	0.750	-0.129	0.052
PC6.1 RiparianComplexity&TreeCover(+)	0.341	0.740	0.287
PC6.2 EmergentMacrophytes(+)	-0.446	-0.565	-0.511

3.4.2 Agglomerative Hierarchical Cluster Analysis (AHC)

Agglomerative Hierarchical Cluster Analysis (AHC) based on Euclidian distance and Ward's agglomeration algorithm was applied to the scores of the 221 river reaches on the 10 PCs listed in Table 3.11. The analysis generated the dendrogram shown in Figure 3.10.

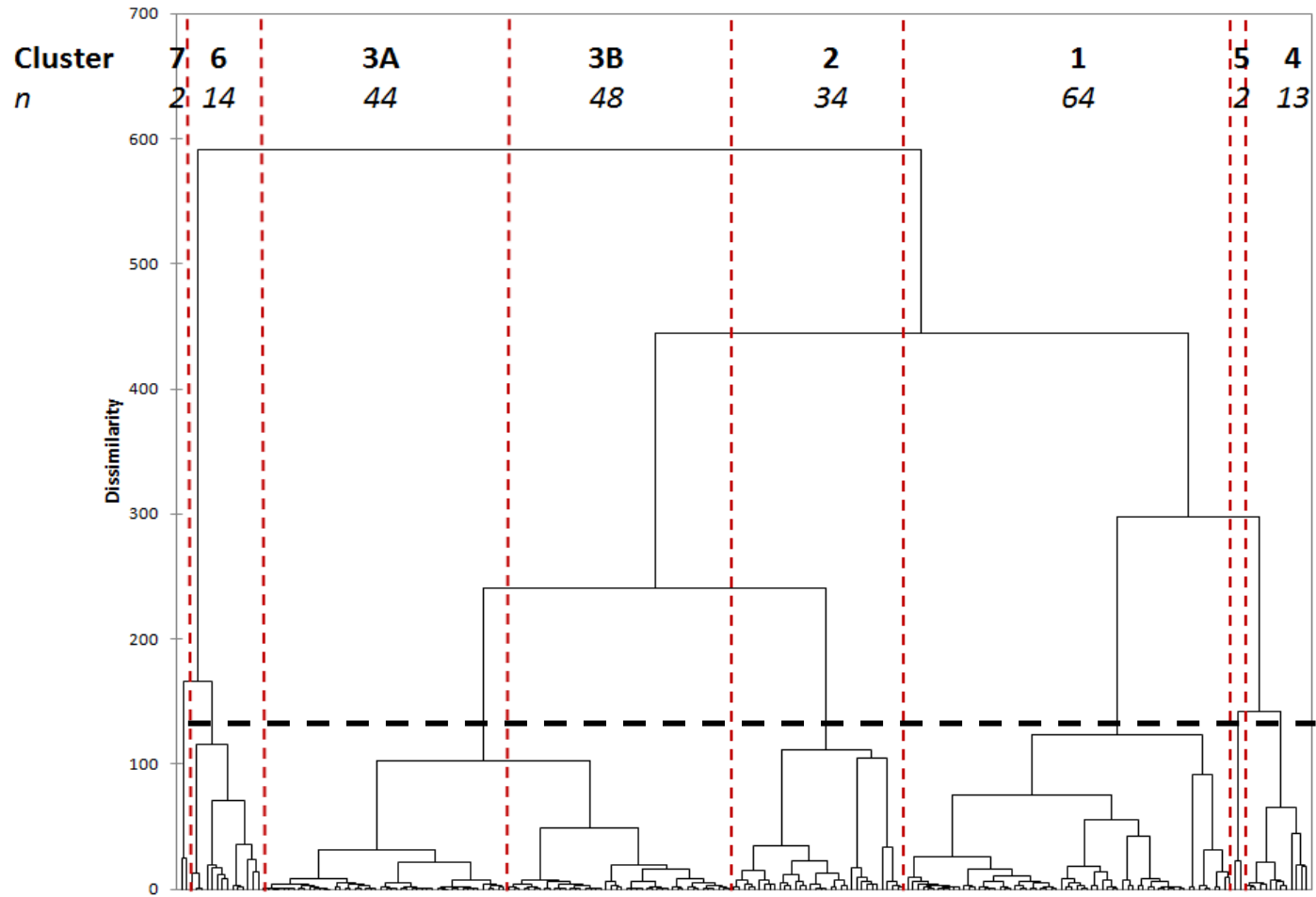


Figure 3.10 AHC Dendrogram based on the scores of 221 river reaches on 10 geomorphologically-informative PCs (the emboldened numbers labelling each cluster correspond to those in the text and the number of reaches (*n*) in each cluster is indicated in italics).

After consideration of several levels of clustering, the black dashed line Figure 3.10 illustrates the level that appeared to produce a simple and interpretable classification with relatively even-sized tight clusters. The clusters contained 64 (Cluster 1), 34 (Cluster 2), 92 (Cluster 3), 13 (Cluster 4), 2 (Cluster 5), 14 (Cluster 6), and 2 (Cluster 7) reaches. Clusters 5 and 7, which only contained two reaches, represented outliers from the remainder of the data set. These were two reaches of the river Siret (Romania) in cluster 5 and one reach of the river Loreintal (Austria) and Hinterhein (Switzerland) in cluster 7. Other reaches from these rivers contributed to clusters other than 5 and 7. The largest cluster (Cluster 3) was split into two (clusters 3A and 3B) because of its large size and the existence of two distinct subgroups in the dendrogram (Figure 3.10). Therefore, the data were subdivided into six main groups (1, 2, 3A, 3B, 4, 6) with two small outlier groups (5, 7) prior to exploring the degree to which the six main groups represented statistically-significant properties in relation to their scores on the contributing PCs.

Kruskal-Wallis tests were applied to the PC scores on the 10 PCs listed in Table 3.11, grouped according to the six main AHC clusters (Table 3.13). All Kruskal-Wallis tests had 5 degrees of freedom and were highly significant ($p < 0.0001$). All clusters that were significantly different from one another ($p < 0.01$ as a result of multiple pairwise comparisons assessed using Dunn's procedure followed by Bonferroni correction) are listed in Table 3.13, with the clusters ordered according to the magnitude of their median score on the PC.

A further check on the degree to which the clusters illustrated different channel properties involved coding each site according to its cluster membership with respect to some of the PCs. Since PC1.1 and PC1.2 represent broad gradients in channel morphology and size, respectively, a scatter plot was produced of reach scores on each of these two PCs coded according to cluster membership (Figure 3.11). The scatter plot shows the clear separation of group 6 from the other groups with respect to slope (steeper) and sinuosity (lower) and groups 1 and 3A show an intermediate position with respect to PC1.1. The plot also illustrates a trend of increasing channel width from groups 2 and 3B through 1, 3A and 6 to group 4. Reach scores on each of PC1.1 and PC1.2 are plotted against scores on all of the remaining eight PCs (Figure 3.12 to Figure 3.15). These graphs support the significant differences identified by Kruskal-Wallis tests (Table 3.13).

Table 3.13 Results of Kruskal-Wallis tests applied to the PC scores on the 10 PCs listed in Table 3.11, grouped according to AHC clusters 1, 2, 3A, 3B, 4, 6

Principal Component	Kruskal-Wallis K value (p<0.0001 in all cases)	Significant differences between groups (p<0.01) following multiple pairwise comparisons (Dunn's procedure with Bonferroni correction)
PC1.1 Slope(+)Sinuosity(-)	81.8	6 > 1, 3A > 2, 3B, 4
PC1.2 Width(+)	95.0	4 > 3A, 1, 6, 2, 3B 3A, 1 > 2, 3B
PC2.1 Baseflow/Bankfull Sinuosity(+)Slope(-)Width(-)	121.2	1 > 2, 3A, 3B 6 > 3A, 3B 4, 2, 3A > 3B
PC3.1 Riffle-Pool(+)Boulder-Bedrock(-)	58.2	3A > 1, 3B, 4, 6 2, 1, 3B > 6
PC4.1 Marginal&Mid-channelBars(+)	134.1	6, 1, 4 > 3A, 2, 3B 3A > 3B
PC4.2 Benches(+)	55.3	4, 2, 1 > 3A, 3B, 6
PC5.1 FloodplainDepressions&Ponds(+)	67.5	2, 4 > 3A, 3B, 1, 6
PC5.2 VegetatedSideBars(+)	105.7	4, 1 > 3A, 3B, 2
PC6.1 RiparianComplexity&TreeCover(+)	54.9	3B, 1, 6, 4, 3A > 2
PC6.2 EmergentMacrophytes(+)	56.7	6, 2 > 3B, 3A, 1, 4

Scatter plots were also produced for reach scores on the aggregate PCs coded by cluster membership. These illustrate good separation of clusters 2, 3A, 3B, 4 and 6 with respect to the first two aggregate PCs, but with some overlap between cluster 1 and clusters 4 and 6 (Figure 3.16). However, aggregate PC3 discriminates well between clusters 1, 4 and 6.

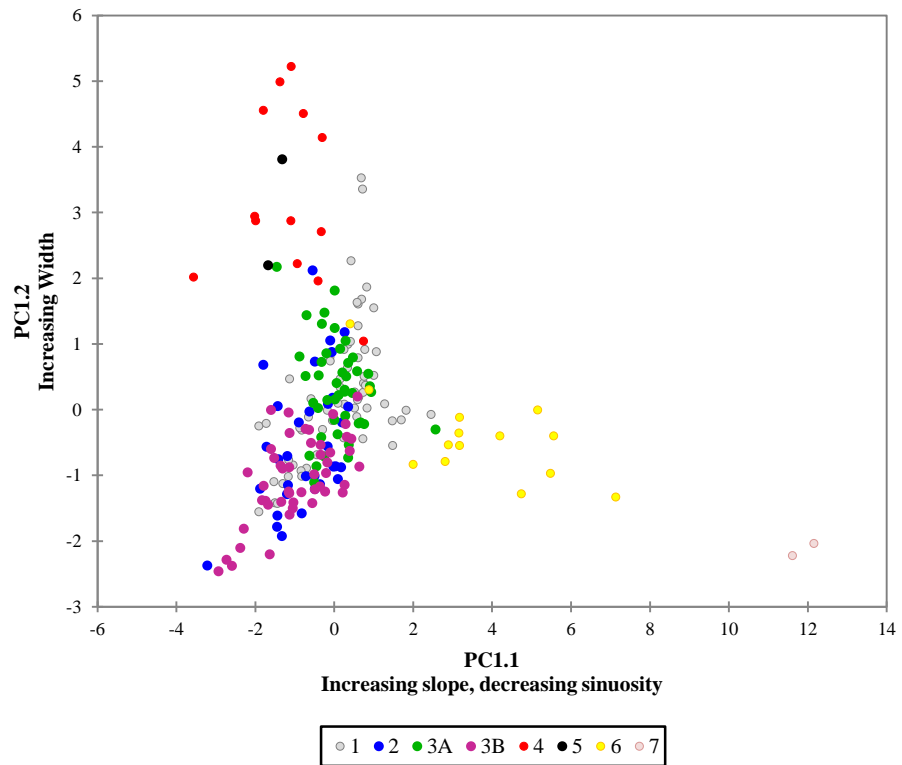


Figure 3.11 Scatter plot illustrating the scores of reaches within the eight clusters on PC1.1 and PC1.2.

Table 3.13 synthesises information on the six main clusters. The colouring of the table cells indicates those clusters that have significantly higher (pink) or lower (blue) scores on each of the PCs (Kruskal-Wallis tests, Table 3.14). The columns are arranged with cluster 4 on the left (a cluster of relatively wide rivers) and then the remaining groups are arranged in order of decreasing slope. This ordering is supported by both the upper and lower quartile values of channel bankfull width and slope and also by the significant differences identified by Kruskal-Wallis tests.

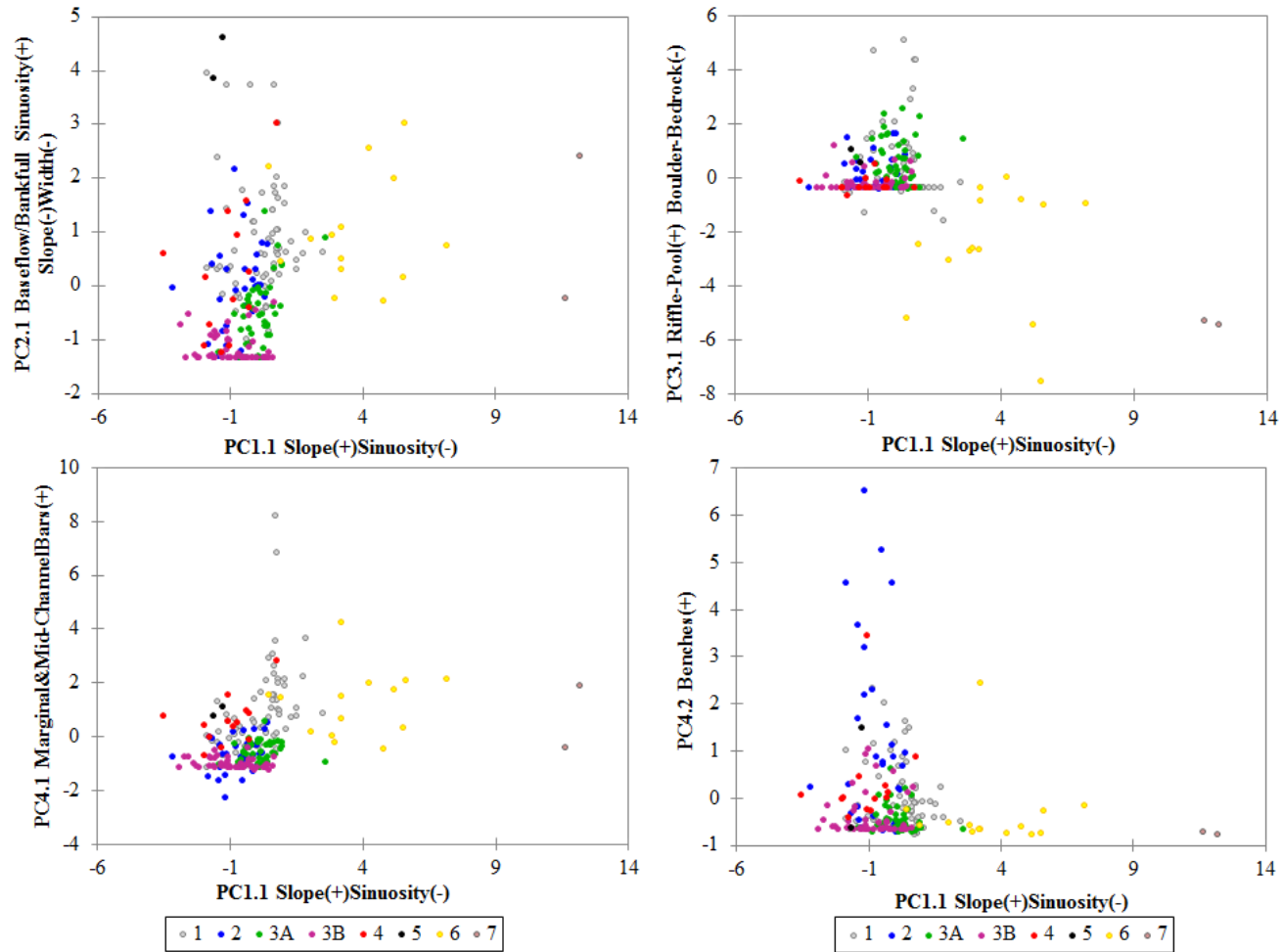


Figure 3.12 Scatter plots of reach scores on PC1.1 against PC2.1 (top left), PC3.1 (top right), PC4.1 (bottom left) and PC4.2 (bottom right) coded by cluster membership

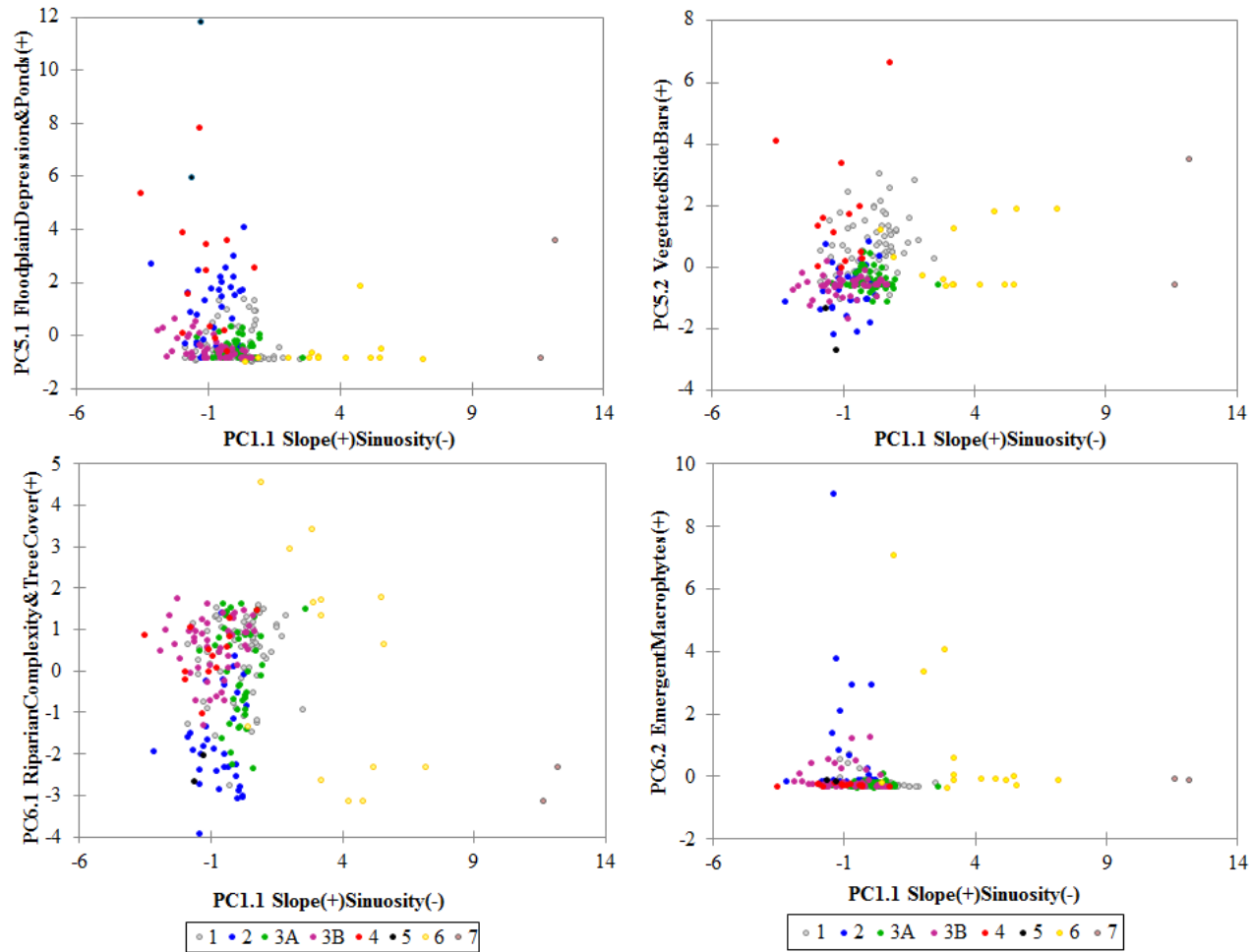


Figure 3.13 Scatter plots of reach scores on PC1.1 against PC5.1 (top left), PC5.2 (top right), PC6.1 (bottom left) and PC6.2 (bottom right) coded by cluster membership

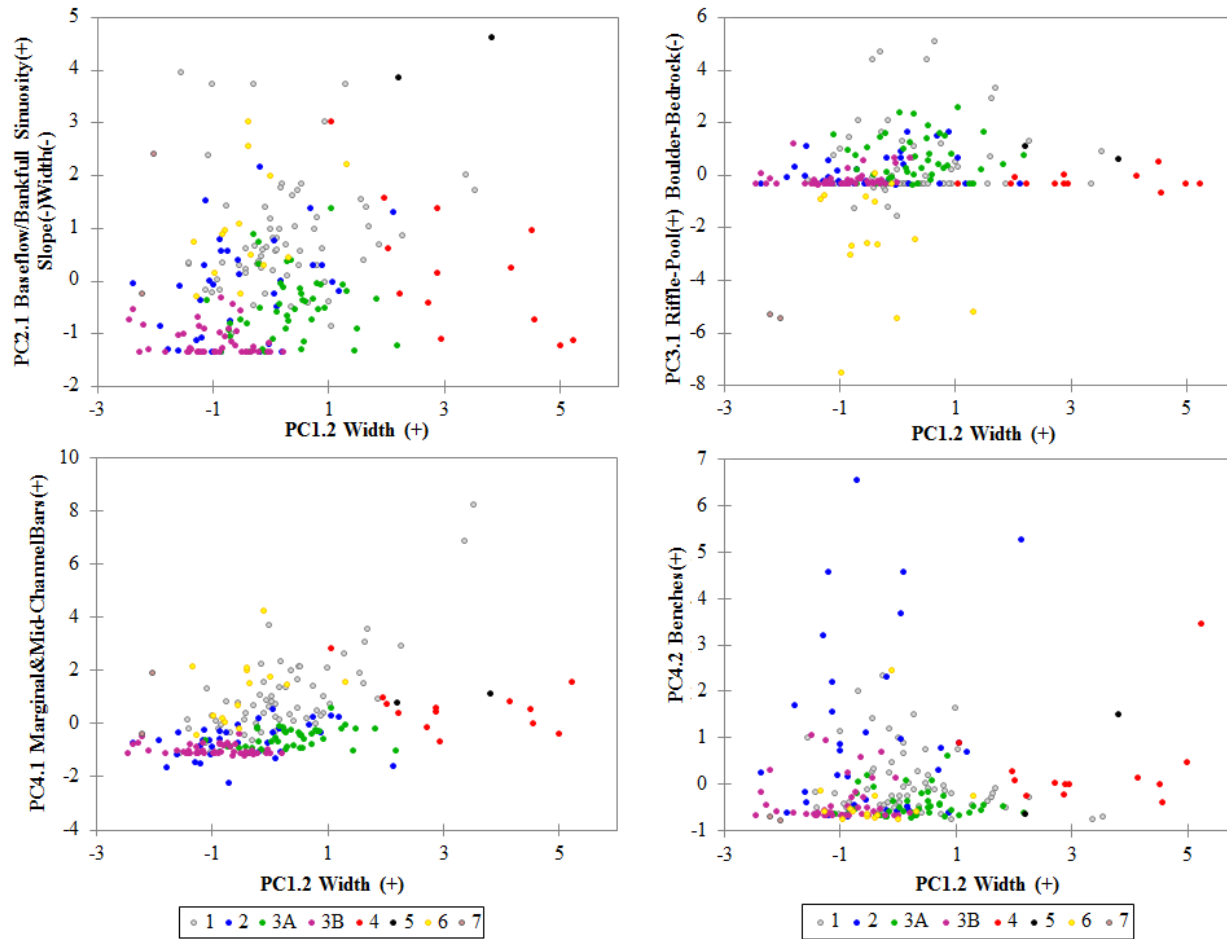


Figure 3.14 Scatter plots of reach scores on PC1.2 against PC2.1 (top left), PC3.1 (top right), PC4.1 (bottom left) and PC4.2 (bottom right) coded by cluster membership

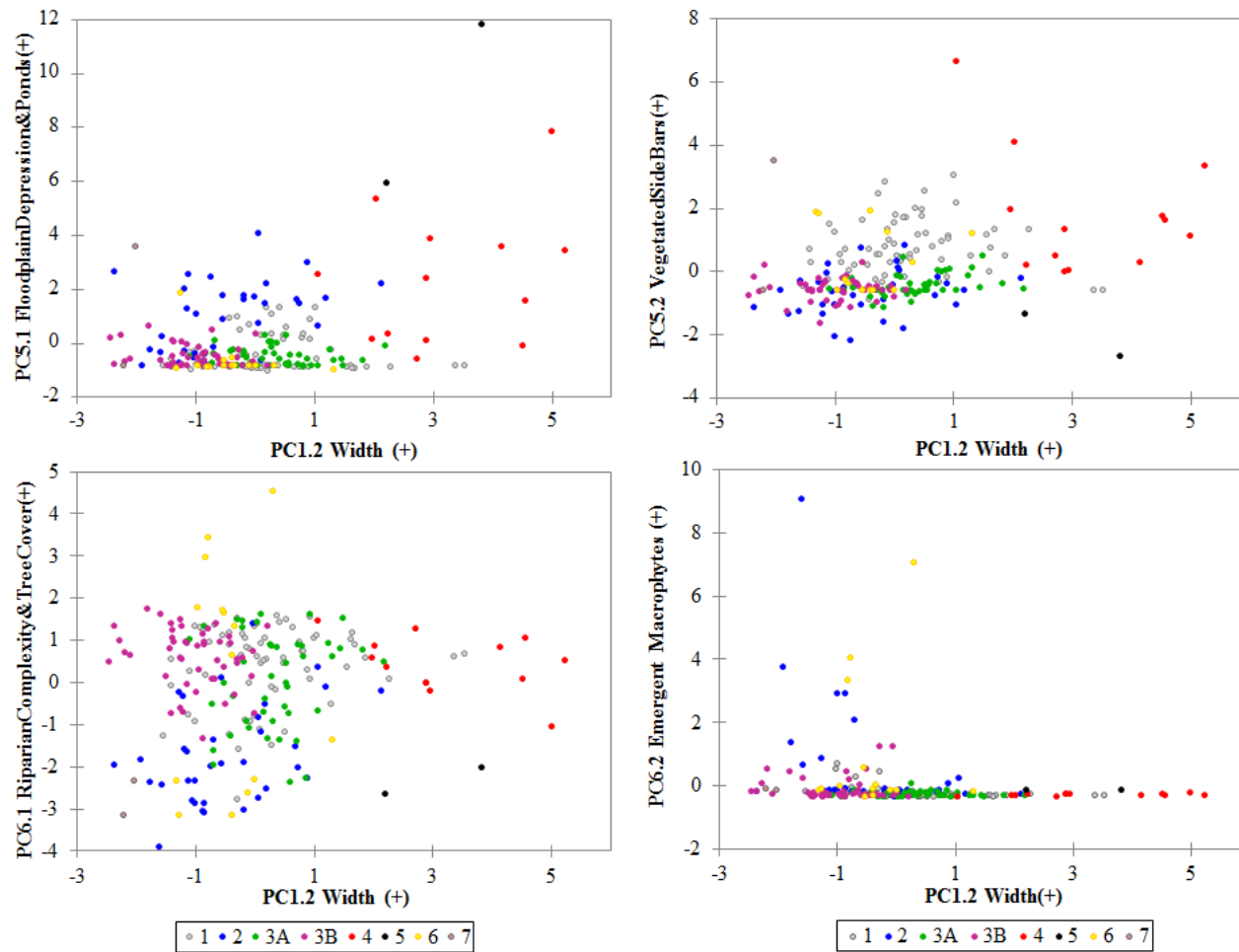


Figure 3.15 Scatter plots of reach scores on PC1.2 against PC5.1 (top left), PC5.2 (top right), PC6.1 (bottom left) and PC6.2 (bottom right) coded by cluster membership

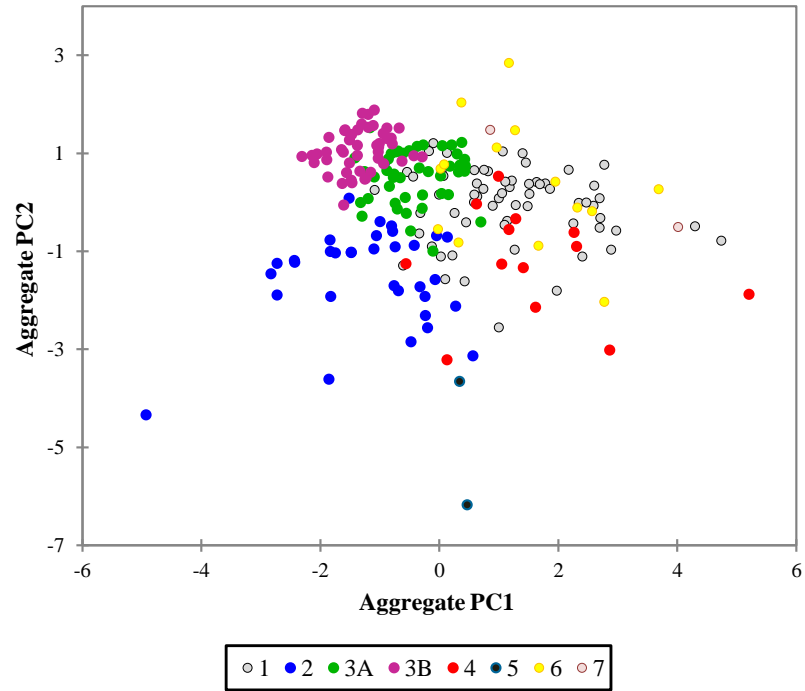


Figure 3.16 Reach scores on aggregate PCs 1 and 2 coded according to cluster membership

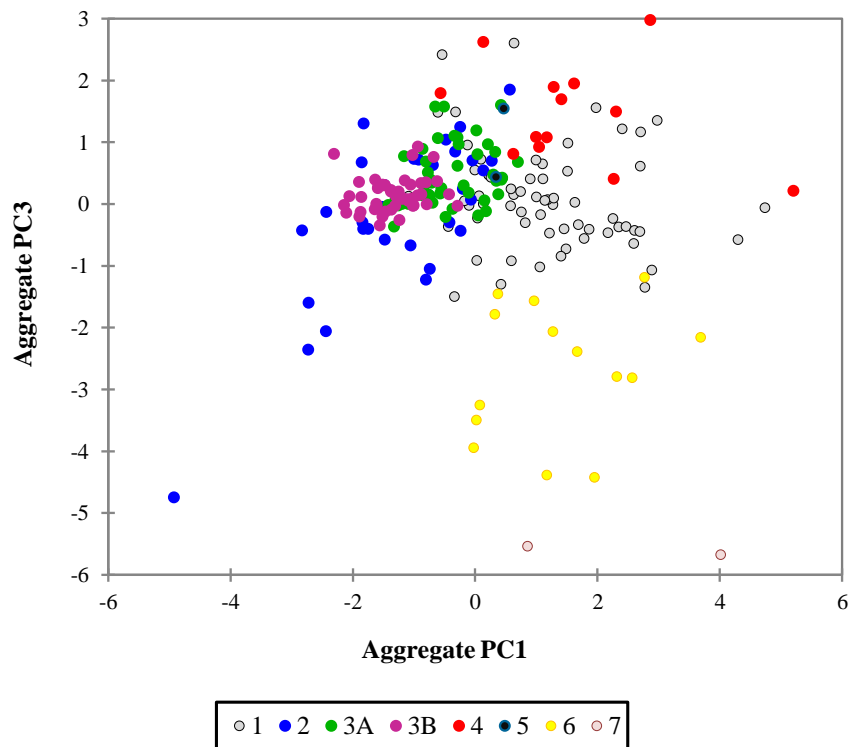


Figure 3.17 Reach scores on aggregate PCs 1 and 3 coded according to cluster membership

Table 3.14 Upper and lower quartile values of channel bankfull width, slope and sinuosity of river reaches within each cluster and the degree to which each cluster shows significantly higher (pink shading) or lower (blue shading) than other clusters with respect to each of the 10 PCs.

Cluster	4	6	1	3A	2	3B
Bankfull Channel Width in m (lower and upper quartile)	131.0 - 186.6	30.0 - 63.0	36.1 - 82.2	25.6 - 60.1	14.7 - 57.8	12.8 - 30.5
Bankfull Channel Slope in o/oo (lower and upper quartile)	0.2 - 1.5	35.4 - 68.2	2.0 - 8.0	1.6 - 5.6	0.4 - 2.3	0.5 - 3.0
Bankfull Channel Sinuosity (lower and upper quartile)	1.10 - 1.39	1.04 - 1.16	1.09 - 1.38	1.10 - 1.24	1.20 - 1.53	1.31 - 1.60
PC1.1 Slope(+)/Sinuosity(-)						
PC1.2 Width(+)						
PC2.1 Baseflow/Bankfull Sinuosity(+)/Slope(-) Width(-)						
PC3.1 Riffle-Pool(+)/Boulder-Bedrock(-)						
PC4.1 Marginal&Mid-channelBars(+)						
PC4.2 Benches(+)						
PC5.1 FloodplainDepressions&Ponds(+)						
PC5.2 VegetatedSideBars(+)						
PC6.1 RiparianComplexity&TreeCover(+)						
PC6.2 EmergentMacrophytes(+)						

3.5 Discussion

3.5.1 Interpreting the River Classification

Before assessing the degree to which Google Earth has proved to be a useful data source for characterising rivers, it is important to consider the classification that has been produced and whether it makes sense. In this way, an initial assessment can be made of potential problems with using information extracted from Google Earth as well as the strengths of this data source in yielding a useful classification.

Cluster 4 is clearly distinguished from the remaining clusters by the large width of the rivers in this cluster. River reaches in the remaining clusters are all considerably narrower than those in cluster 4 and show clear differences in their characteristics along a gradient of decreasing width and slope and increasing sinuosity in the following order: cluster 6, cluster 1, cluster 3A, cluster 2 and cluster 3B. Based on the information in Table 3.14 Upper and lower quartile values of channel bankfull width, slope and sinuosity of river reaches within each cluster and the degree to which each cluster shows significantly higher (pink shading) or lower (blue shading) than other clusters with respect to each of the 10 PCs. Table 3.14, the nature of the physical characteristics of reaches in each of the clusters along this gradient can be summarised as follows:

Cluster 4: A distinct group of wide river reaches that have a relatively low gradient and high sinuosity. These reaches display a significant range of bars and benches of varying type and vegetation cover and of floodplain landforms.

Cluster 6: Relatively steep, low sinuosity reaches of intermediate width. These reaches display a significant range of lateral and mid-channel bars and many of them also have exposed bedrock features.

Cluster 1: Reaches of intermediate slope, relatively low sinuosity and intermediate and width. These reaches show a significant contrast in the sinuosity, width and slope of their bankfull and baseflow channels, and as a result, they display a wide range of bars, particularly active bars, and benches of varying type.

Cluster 3A: Reaches of intermediate slope, sinuosity and width with relatively few in-channel or marginal features, although riffle-pools are more frequent in this cluster than in any of the other clusters.

Cluster 2: Reaches of relatively low slope, high sinuosity, and low width displaying relatively frequent marginal benches and floodplain depressions and ponds.

Cluster 3B: Reaches of relatively low slope, high sinuosity, and low width, displaying the lowest in channel, marginal and floodplain features of all clusters.

In relation to riparian and aquatic vegetation, only cluster 2 is significantly differentiated from the other clusters by low riparian vegetation complexity and tree cover. This appears to reflect agricultural pressure up to the channel edge rather than any natural vegetation dynamics. This cluster also shows a relatively high presence of emergent macrophytes, probably reflecting the low shade from riparian vegetation and the low gradients of reaches in this cluster. Low channel gradients have been found to be crucial to the development of significant macrophyte cover in river channels in the UK (Gurnell et al., 2010, 2013).

All of the remaining clusters show higher riparian vegetation complexity and tree cover and lower emergent macrophyte cover than cluster 2, apart from the steep, relatively wide channels of cluster 6. However, on closer inspection of the vegetation properties for cluster 6 reaches, it is apparent that this cluster is actually characterised by large wood accumulations (the second highest loading on PC6.2 after emergent macrophytes), rather than by macrophytes, which are only present in cluster 2 channels (Figure 3.18). Therefore, PC6.2 needs to be interpreted as a large wood (+) and emergent macrophyte (+) gradient, which distinguishes cluster 2 and 6 from the other clusters.

Based on this initial assessment, the classification of the reaches into six main clusters appears to be logical and interpretable, and is illustrated by their relative properties and some example reaches in Figure 3.19.

3.5.2 Google Earth as a Data Source for River Science

Despite the apparent interpretability of the river classification, there are several issues which may have affected the quality of the data extracted from Google Earth:

- (i) Although every attempt was made to identify reaches that were able to adjust freely, some direct human interventions are likely to be difficult to detect from plan images. In particular, bank reinforcement may have been missed, leading to bias in the classification.

- (ii) Bank reinforcement and other in-channel human interventions as well as many channel physical features may have been disguised by overhanging riparian vegetation. This may have resulted in some features being missed or their abundance being underestimated and it is likely that such errors were magnified in the narrowest channels, where trees can overhang a large proportion of the channel width. In particular, the recognition of large wood accumulations has probably been underestimated, since wood is often retained by riparian vegetation.

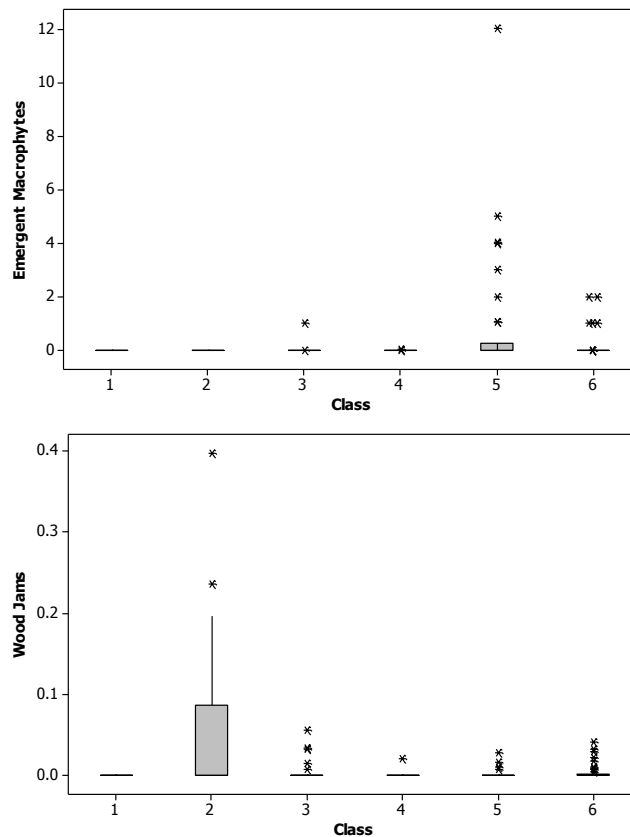


Figure 3.18 Boxplots of emergent macrophyte stand and wood jam frequencies (standardised for reach dimensions) within each reach cluster.

- (iii) The flow conditions at the time of the imagery may also have affected the recording of features. Although every effort was made to identify imagery recorded at baseflow, small changes in flow stage may obscure pools and inundate bars, leading to their underrepresentation in the collected data set.
- (iv) Slope is a key control on river behaviour. This was calculated directly from point heights extracted from Google Earth which may incorporate errors that could significantly affect slope estimates, particularly for reaches of low gradient.

Nevertheless, Google Earth has several advantages as a data source for river research:

- (i) It provides a very low cost source of data that is publicly accessible and easy to use, enabling all users, whatever their skill level, to use the product without difficulty.
- (ii) It provides information from reach to continental spatial scales, and in many locations, provides historical sequences at high spatial resolution.
- (iii) As illustrated by the present application, Google Earth is able to support extraction of a wide range of information from channel dimensions, to landforms and vegetation features. However, the quality of that information is dependent upon the development of clear rules for data extraction, and the consistent application of those rules. The interpretability of the classification that has been achieved, suggests that such a careful approach yields good quality data, despite the possible limitations stated above.

The preliminary classification and accompanying geomorphological interpretation presented in this chapter is further investigated and developed in Chapter 4 by:

- (i) exploring the degree to which further subdivision of the clusters may be appropriate or informative;
- (ii) cross-checking the accuracy of the 'slope' estimates derived from Google Earth, which have an important influence on the classification (Figure 3.19) and are dependent on more than the simple plan measurements involved in the other two key variables (width, sinuosity);
- (iii) considering whether additional information (e.g. discharge, bed material, channel features), which is available for subsets of the reaches, provide support for the classification.







Cluster (Class number)	4 (1)	6 (2)	1 (3)	3A (4)	2 (5)	3B (6)
Relative Width	Very Large	Intermediate	Intermediate	Intermediate	Low	Low
Relative Slope	Very Low	High	Intermediate	Intermediate	Low	Low
Relative Sinuosity	High	Low	Low	Intermediate	High	High
Distinguishing Physical Features	lateral and mid-channel active and vegetated bars and benches, extensive floodplain landforms	lateral and mid-channel bars, exposed bedrock features	lateral and mid-channel active and vegetated bars and benches	few in-channel or marginal features, riffle-pools present	frequent marginal benches, extensive floodplain landforms	the lowest in channel, marginal and floodplain features of all clusters
Distinguishing Vegetation Features		Large wood accumulations			Low riparian tree cover and complexity, Emergent macrophytes	
All images are taken from 2.5 km altitude						
River	Loire, France	Bregenzer, Austria	Eygues, France	S. Tyne, England	Dee, England	La Meurthe, France

Figure 3.19 Summary of the relative properties of the reach clusters and some example river reaches

CHAPTER 4

EXPLORING THE ROBUSTNESS OF THE CLASSIFICATION

4.1 Introduction

Chapter 3 presented methods to extract information on rivers and their floodplains entirely from a new information source, GoogleTM Earth. These methods were used to extract, pre-process and analyse information from 221 reaches of 75 European rivers. The analysis yielded a preliminary classification of this data set into six classes of river reflecting different combinations of channel width, slope and sinuosity and displaying a variety of distinguishing physical and vegetation features (Figure 3.19). These classes were numbered 1 to 6 along a gradient of relative width, slope and sinuosity as follows:

Class 1 (very large width, very low gradient, high sinuosity)

Class 2 (intermediate width, high slope, low sinuosity)

Class 3 (intermediate width, intermediate slope, low sinuosity)

Class 4 (intermediate width, intermediate slope, intermediate sinuosity)

Class 5 (low width, low gradient, high sinuosity)

Class 6 (very low width, very low gradient, very high sinuosity)

This chapter further explores the classification by first examining the properties of the six classes in greater depth (section 4.2) and then considering whether any further subdivisions of the six classes is meaningful (section 4.3). Since slope is so important to the classification and is the only variable that is dependent on data other than aerial images, the accuracy of the elevation and slope estimates extracted from Google Earth are compared with estimates extracted from airborne Lidar data for some of the studied reaches (section 4.4). A final check on the robustness of the classification relates to the short-term temporal dynamics of rivers and thus any bias in the characteristics measured from a particular Google Earth image that may influence the class to which a reach is assigned. Therefore, information for twelve of the original reaches was extracted from Google Earth using images of a different date to those previously analysed. This information was used to investigate whether the PC scores and cluster membership for

each of these reaches remained stable or deviated from their original values (section 4.5). As described in chapters 2 and 3, morphological classification of rivers has traditionally incorporated measures of at least two further controlling variables in addition to slope: discharge (e.g. bankfull discharge or stream power) and bed material calibre (e.g. D_{50}) as the key discriminating variables. Neither of these variables can be quantified from Google Earth. Nevertheless, discharge records and indicators of bed sediment calibre are available for subsets of the studied reaches and so the degree to which the six classes reflect differences in these variables is explored in section 4.6. The results of these various assessments of the river classification from chapter 3 are summarised in section 4.7. A final section (4.8) has been developed in collaboration with the Environment Agency. Here a practical application of the classification is illustrated, whereby a sample of restoration schemes are investigated to assess whether they conform to their expected class based upon apparently naturally-functioning reaches nearby.

4.2 Properties of the six classes of river

4.2.1 Geographical distributions of reaches within the six classes

The geographical distribution of the studied reaches within each of the six classes is presented in Figure 4.1.

Although reaches in each of the classes are quite widely distributed across Europe, there are some gaps as a result of the constraints imposed on the present analysis by the countries for which gauged natural flow regimes had been identified (see section 3.3.1). Nevertheless, there are differences in the spatial patterns between classes. There are only a small number of reaches in class 1 (very large width, very low gradient, high sinuosity) and these show no clear distribution across Europe. Class 2 (intermediate width, high slope, low sinuosity) reaches are confined to areas within or close to the mountain ranges of the Alps and Pyrenees. Class 3 (intermediate width, intermediate slope, low sinuosity) reaches are also located in areas of fairly steep terrain but are distributed more widely than Class 2 reaches, extending from the Alps and Pyrenees to the Vosges mountain range and steep areas of Scotland and Wales. Classes 4 (intermediate width, intermediate slope, intermediate sinuosity) and 5 (low width, low gradient, high sinuosity) show a similar spatial distribution across the British uplands,

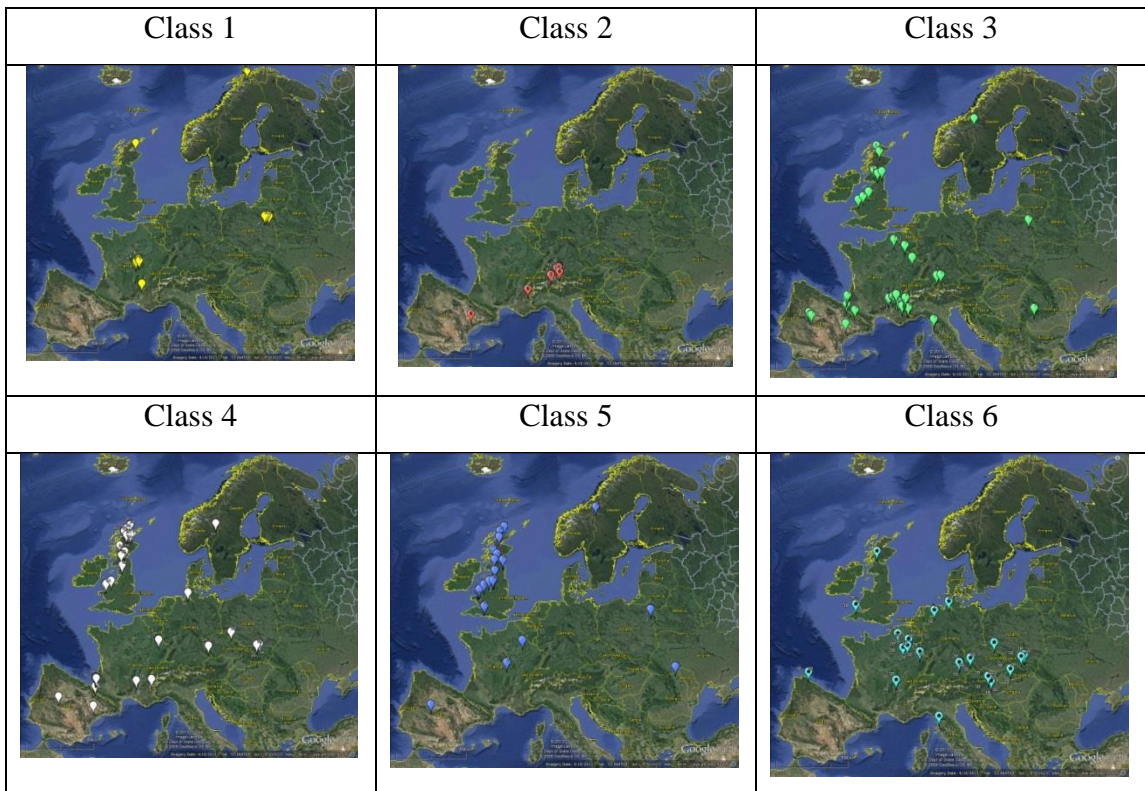
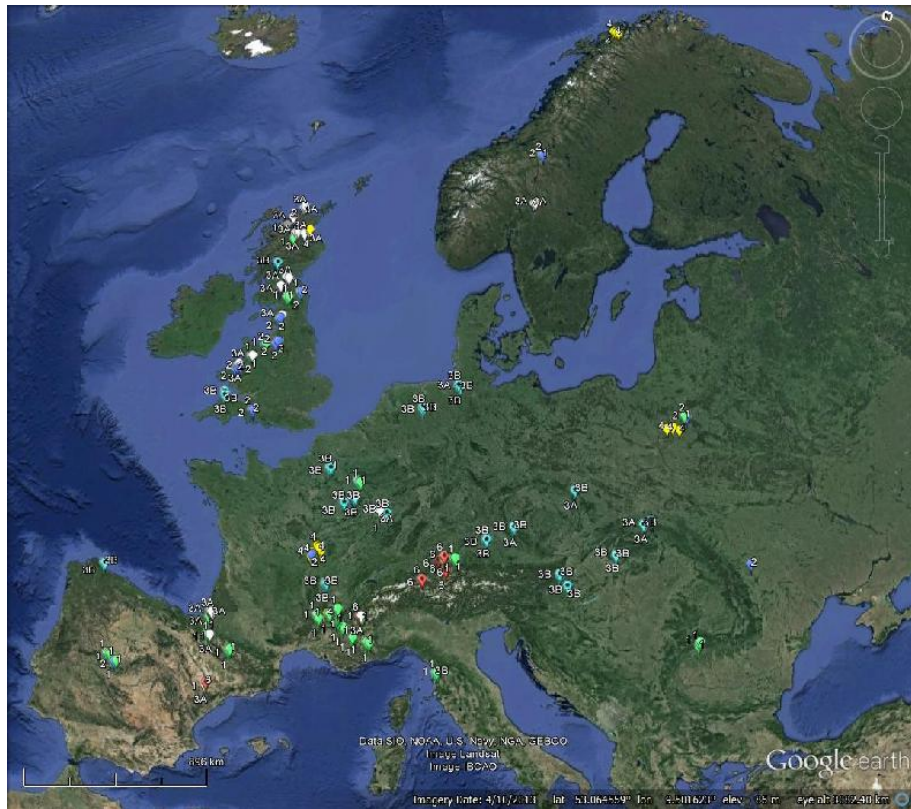


Figure 4.1 Geographical distributions of the studied reaches according to their class membership (top: all classes, below: individual distributions of reaches for each class).

the North European plain, southern France and central Spain. Lastly, reaches in Class 6 (low width, low gradient, high sinuosity) are mainly confined to northern and central mainland Europe.

Overall, the data set provides a reasonable representation of the Alpine, Atlantic and Continental areas of Europe, and some representation of Mediterranean rivers, but the southern Mediterranean, northern Atlantic and eastern Continental areas are not represented.

4.2.2 Frequency distributions of channel and floodplain properties within the six river classes

The river classification was developed using reach scores on PCs that integrated the effects of a number of the original variables that were extracted from Google Earth. This section returns to some of the key variables that were extracted from Google Earth and were listed in Table 3.4 (reproduced below as Table 4.1). It explores the degree to which the river classes can be discriminated and thus interpreted by some of these key variables, so ensuring that the classification reflects actual river and floodplain features and is not distorted in any way by the PCs that were used in the cluster analysis (Chapter 3). Box plots of selected river dimensions, channel bed features, channel bar and bench features, channel-margin-transitional features and vegetation features are illustrated according to the six classes of river in Figure 4.2 to Figure 4.6.

Figure 4.2 illustrates that reaches in class 1 are distinctly wider than the other classes, and that class 6 generally includes narrower channels than the other classes. While the wide channels of class 1 have a lower (baseflow channel) gradient and intermediate (baseflow channel) sinuosity than the other classes, there is a general decrease in baseflow channel slope and an increase in baseflow channel sinuosity across reaches in classes 2 to 5.

The boxplots in Figure 4.2 confirm the distribution of classes according to their geometric properties as described in section 4.1.

Table 4.1 Groups of Raw and Aggregate Variables describing different properties of the river and its floodplain

Group	Variable (units)
River dimensions	Baseflow Median Width (m) Baseflow Sinuosity Baseflow Channel Slope (per mil) Bankfull Median Width (m) Bankfull Sinuosity Bankfull Channel Slope (per mil) Valley Gradient (per mil)
Dimension ratios	Baseflow_Bankfull Median Width Baseflow_Bankfull Sinuosity Baseflow_Bankfull Channel Slope
Channel bed features	Pool Riffle Cascade Waterfall / Step Boulder Exposed bedrock
Channel bar and bench features	Total Active Marginal Bars Total Stabilising Marginal Bars Total Active Mid-Channel Bars Total Stabilising Mid-channel Bars Total Active Benches Total Stabilising Benches
Channel-margin-transitional and floodplain features	Swamp-Wetland Total Water-filled Depressions Total Connected Side Channels Total Dry Depressions Total Ridges & Swales Total Oxbow Total Stabilising Arcuate Bars Total Stabilising Non-Arcuate Bars
Vegetation	Riparian Vegetation Complexity Riparian Tree Distribution Wood Emergent Macrophytes

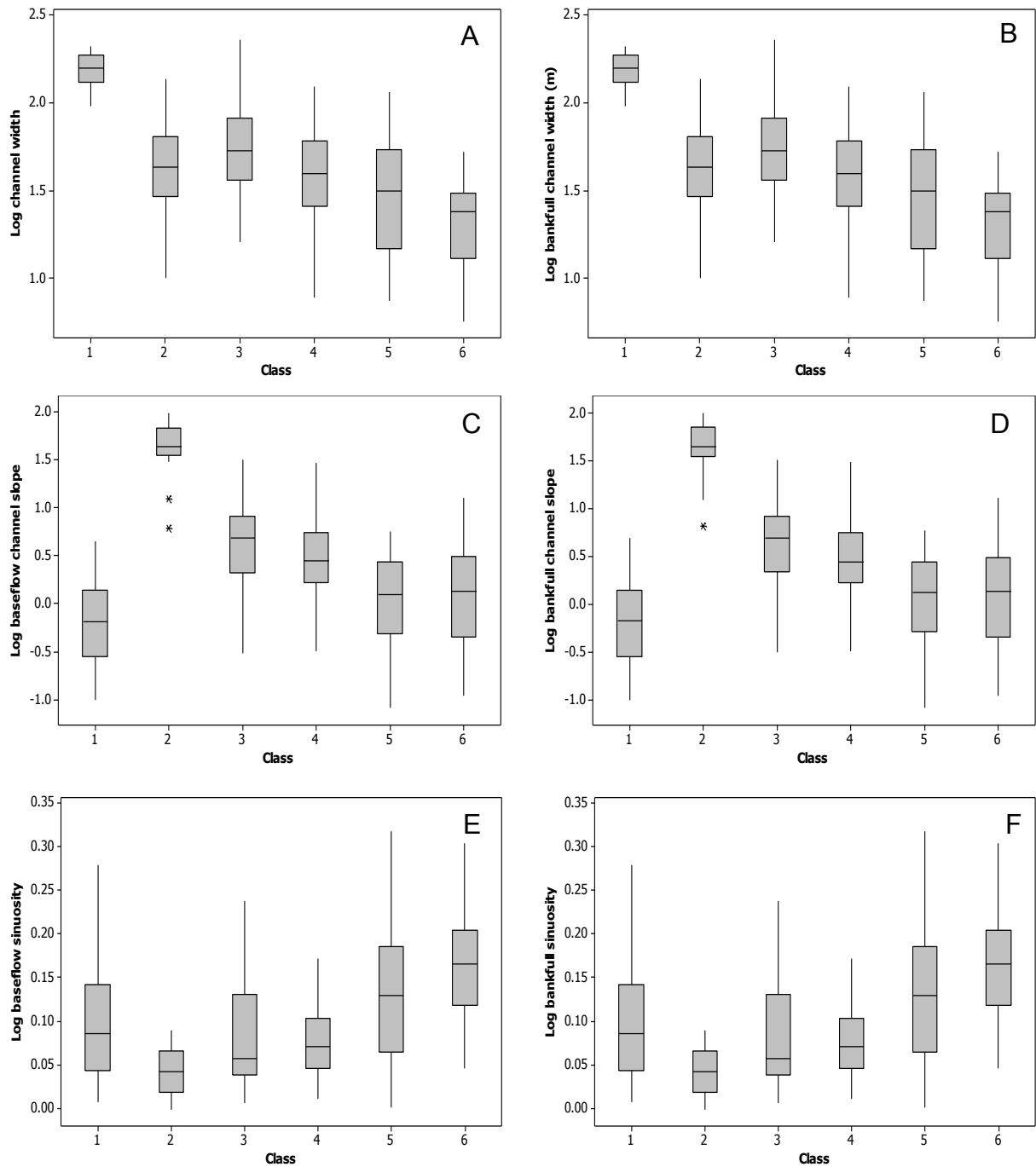


Figure 4.2 Boxplots illustrating differences in three river dimension variables across the six classes of river reach: **A and B: log₁₀ baseflow channel width and log₁₀ bankfull channel width; C and D: log₁₀ baseflow channel slope and log₁₀ bankfull channel slope; E and F: log₁₀ baseflow channel sinuosity and log₁₀ bankfull channel sinuosity**

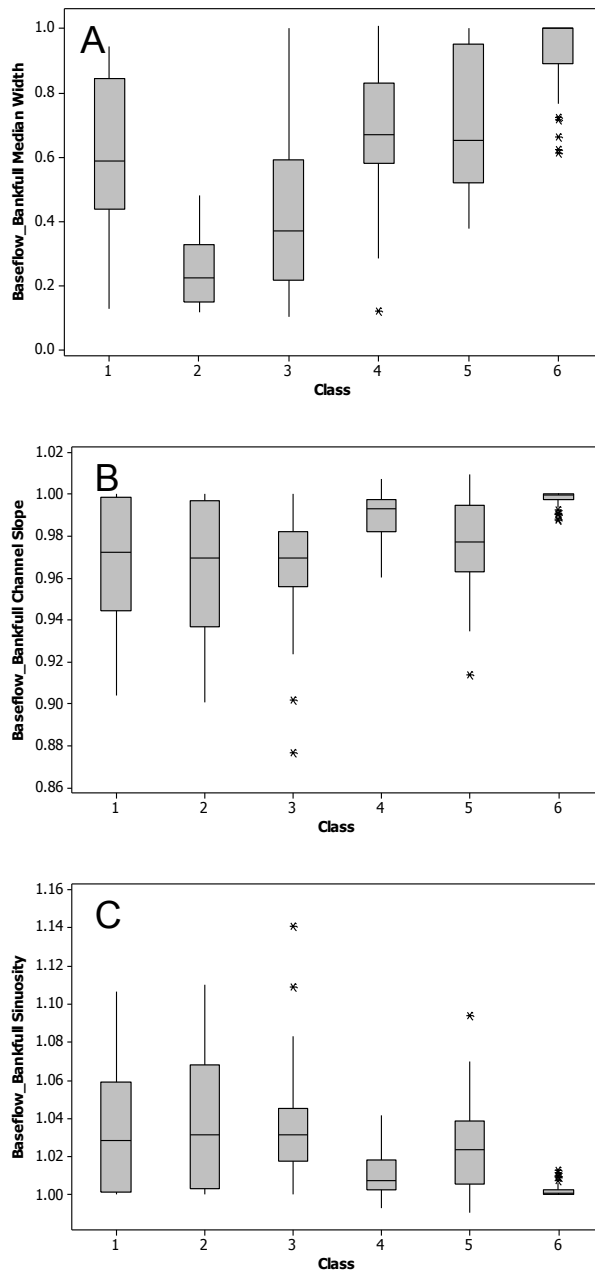


Figure 4.3 Boxplots of channel dimension ratios **A: Baseflow:Bankfull Width; B: Baseflow:Bankfull Slope; C: Baseflow:Bankfull Sinuosity**

The boxplots in Figure 4.3 display three baseflow:bankfull ratios across the classes. The closer the three ratios (baseflow:bankfull width, baseflow:bankfull channel slope, baseflow:bankfull sinuosity) are to 1 the less side bars are exposed at low flow. The ratio of baseflow to bankfull width (Figure 4.3A) clearly illustrates a trend from high to low bar exposure across classes 2 to 6, whereas the other two ratios show a lot

of within-class variance and thus a rather subdued trend across classes 2 to 6. Class 1 is intermediate in its characteristics in comparison with classes 2 to 6.

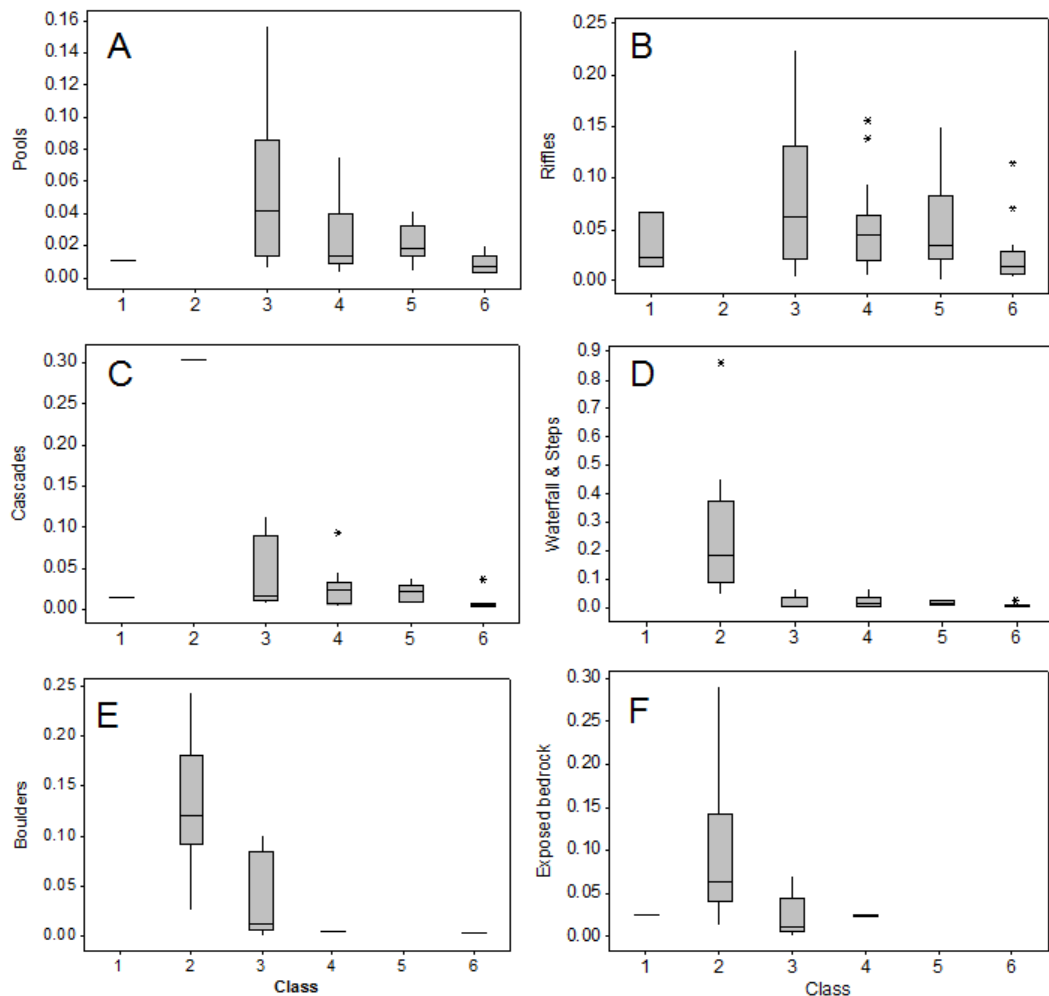


Figure 4.4 Boxplots illustrating differences in the frequency of six channel bed features, standardised for channel width and reach length, across the six classes of river reach: **A. pools; B. riffles; C. cascades; D. waterfalls plus steps; E. exposed boulders; F. bedrock exposures.**

There are strong contrasts in the frequency of particular bed features between reaches within the six classes (Figure 4.4). Apart from riffles, the large channels in class 1 show negligible bed features. Class 2 reaches are distinguished by a higher standardised frequency of exposed bedrock, boulders and water falls and steps than the other classes, indicating extremely coarse bed material and some bed rock sections, and also no pools or riffles. Reaches in Class 3 have a higher frequency of exposed bedrock, boulders and cascades than all other classes apart from class 2, and this class also shows the highest frequency of riffles and pools. These features indicate relatively coarse bed

material and features typical of relatively steep, channels. Classes 4, 5 and 6 all show the presence of pools and riffles with negligible frequencies of other bed features. These are indicative of finer bed material than all other classes apart from the large channels in class 1.

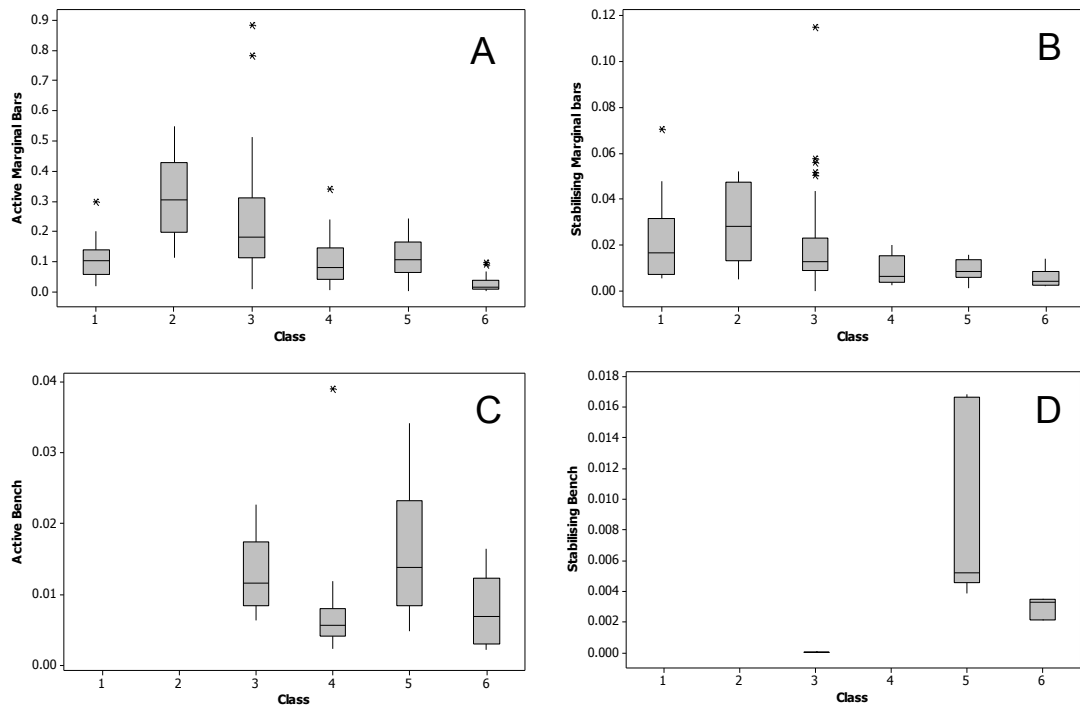


Figure 4.5 Boxplots illustrating differences in the frequency of channel marginal bar and bench features, standardised for channel width and reach length, across the six classes of river reach: active (A) and stabilising (B) marginal bars; active (C) and stabilising (D) marginal benches.

Active and stabilising channel marginal bar and bench features also show differences in frequency across the six classes (Figure 4.5). Class 1 is characterised by low to intermediate frequencies of marginal bars but no benches. There is a gradual decrease in the frequency of active and stabilising marginal bars from class 2 through to class 5, but classes 3 to 6 all display active benches and classes 5 and 6 are distinguished by the presence of stabilising benches.

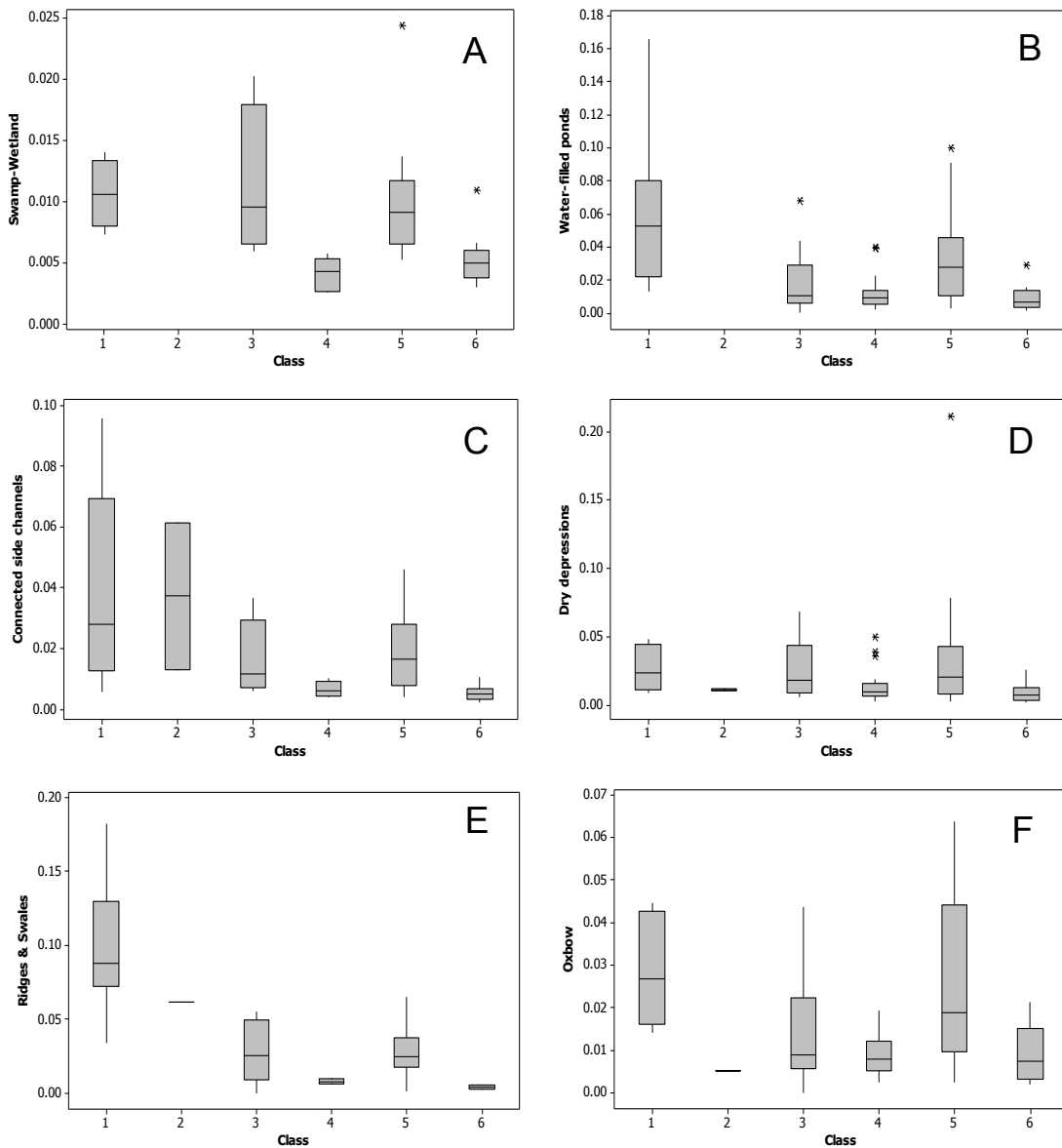


Figure 4.6 Boxplots illustrating differences in the frequency of channel-margin-transitional and floodplain features across the six classes of river reach: **A.** swamp-wetlands; **B.** water-filled depressions; **C.** connected side channels; **D.** dry depressions; **E.** ridges and swales; **F.** oxbows.

Channel margin-transitional features (Figure 4.6) do not show such a clear distinction between classes as the geometric, bed and bar-bench features illustrated in Figures 4.2 to 4.4. Nevertheless, the large rivers of class 1 display relatively high frequencies of all six features shown in Figure 4.6. In contrast, class 2 reaches only display connected side channels; class 3 and 5 reaches show the presence of most of the features but class 3 has a particularly high frequency of swamp-wetland features,

whereas class 5 shows a relatively high frequency of oxbows. Classes 4 and 6 show modest frequencies of all features apart from ridges and swales.

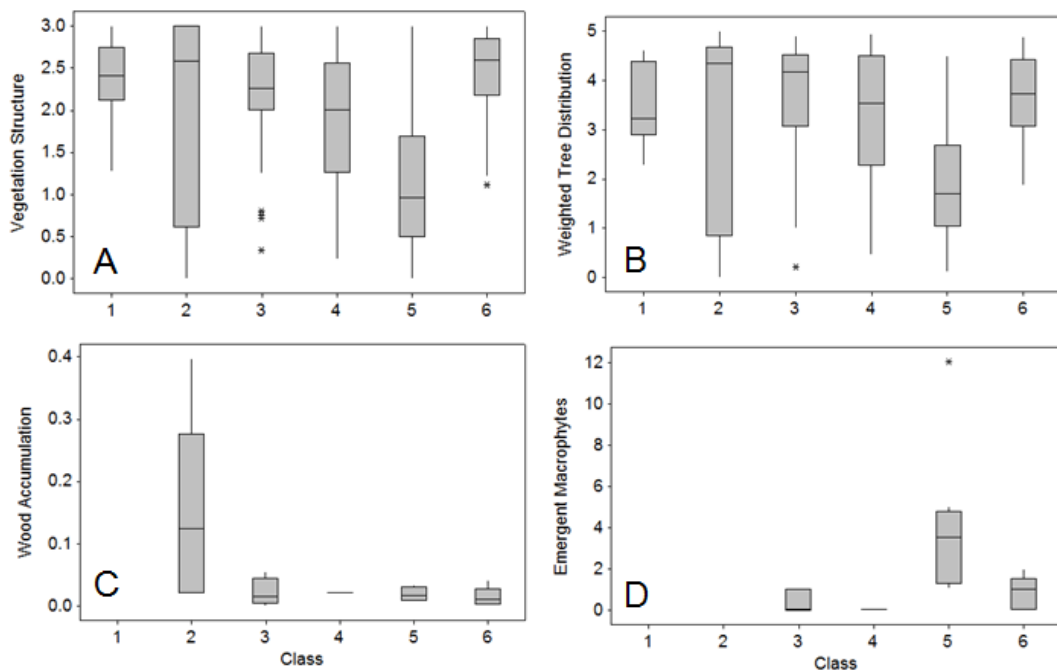


Figure 4.7 Boxplots illustrating differences in vegetation features across the six classes of reach: **A.** (Riparian) vegetation structure; **B.** Tree distribution along the bank tops; **C.** wood accumulations; **D.** (abundance of) emergent macrophytes.

There is little variation in riparian vegetation characteristics, wood accumulations and emergent aquatic macrophyte abundance across the six classes (Figure 4.7). However, class 5 is distinguished by less developed riparian vegetation, lower marginal tree abundance and a higher abundance of emergent aquatic macrophytes than the other classes, and class 2 displays the highest frequency of large wood accumulations.

The above observations on the relative standardised frequencies of particular dimensional, channel bed, channel bar and bench, channel margin-transitional, and vegetation features confirms the interpretations already made in chapter 3 based on the PC scores, and thus confirm that the classification is not an artefact of the Principal Components Analyses.

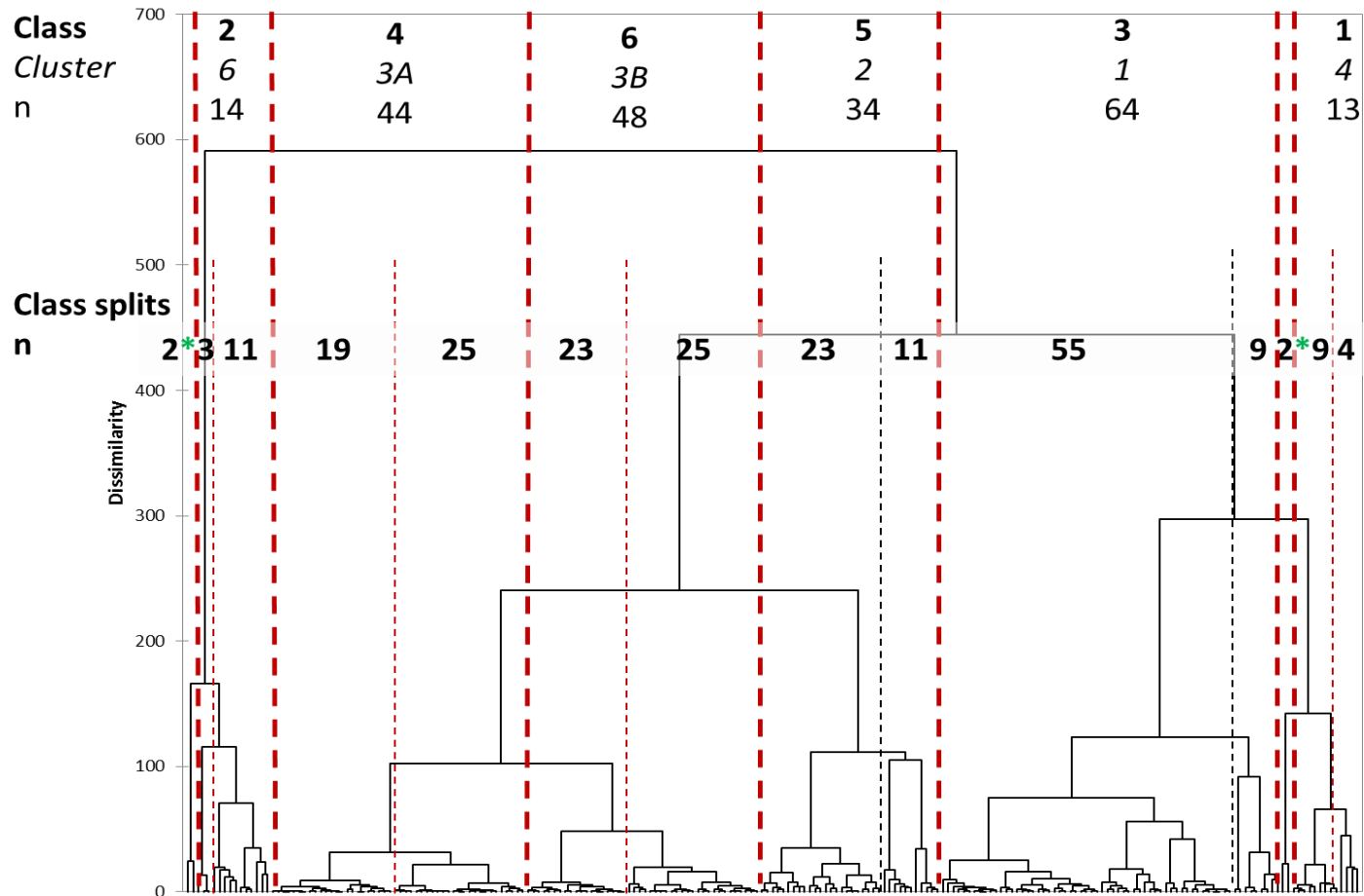
4.3 Is subdivision of the 6 classes informative

From section 4.2, it is apparent that there are notable differences in the presence and abundance of many of the original geomorphic features extracted from Google Earth across the six river classes. It is now necessary to consider whether these six classes adequately describe the river characteristics that are present or whether further subdivision of the classes would be informative. In this section, the first subdivision or split of each class in the cluster dendrogram is investigated to explore whether there are any important and statistically significant differences that might justify extending the classification to a larger number of classes.

The original 6 classes / clusters and their first splits, with the number of reaches contained in each split, are presented in Figure 4.8. Classes 4, 5, and 6 split at lower dissimilarity level than the other classes, and the splits lead to relatively even sized clusters. Meanwhile, cluster 1, 2 and 3 split at a higher dissimilarity and the number of river reaches in each split are uneven. The dissimilarity level on dendrogram nodes indicates the homogeneity within the cluster, the higher the value, the less homogeneous are the clusters. This is the first indication that it may be more appropriate to split some of the clusters than others.

However, to judge whether any split is scientifically informative, it is necessary to test whether any of the splits or sub-classes show river reaches with significantly different characteristics. Therefore, the Mann-Whitney U test was used to assess whether the split classes could be differentiated on the basis of their reach scores on the 10 PCs that underpin the cluster analysis (Table 4.2). Where the table shows pink cells, this indicates that that a sub-class or split shows significantly higher ($P < 0.05$) scores on the particular PC than the other subclass.

To aid interpretation of Table 4.2, relevant data extracted from Table 3.14 are reproduced in Table 4.3. This table illustrates how the original six classes of river reach can be distinguished from one another in relation to each of the 10 PCs that underpinned the cluster analysis.



* Two outlier reaches are excluded

Figure 4.8 Cluster dendrogram showing the original six classes / clusters with the number of reaches (n) contained in each (divided by thick red lines) and the first splits of each cluster (divided by the narrow red lines) with the number of reaches (n) contained in each split

Table 4.3 Statistically significant differences (Kruskal-Wallis tests) in reach scores within the 6 classes of river on each of the 10 PCs that underpin the classification. The shaded cells indicate classes that show significantly higher (pink) or lower (blue) reach scores than the other classes on each individual PC.

Class	PC1.1 Slope(+)/Sinuosity(-)	PC1.2 Width(+)	PC2.1 Baseflow/Bankfull Sinuosity(+)/Slope(-) Width(-)	PC3.1 Riffle-Pool(+) Boulder-Bedrock(-)	PC4.1 Marginal&Mid- channelBars(+)	PC4.2 Benches(+)	PC5.1 Floodplain Depressions &Ponds(+)	PC5.2 Vegetated SideBars(+)	PC6.1 RiparianComplexity &TreeCover(+)	PC6.2 Emergent Macrophytes(+)
1	Blue	Pink			Pink	Pink	Pink	Pink	Pink	Blue
2	Pink			Blue	Pink	Blue	Blue		Pink	Pink
3			Pink		Pink	Pink	Blue	Pink	Pink	Blue
4				Pink		Blue	Blue	Blue	Pink	Blue
5	Blue	Blue				Pink	Pink	Blue	Blue	Pink
6	Blue	Blue	Blue		Blue	Blue	Blue	Blue	Pink	Blue

Class 1: was described in chapter 3 as ‘a distinct group of wide river reaches that have a relatively low gradient and high sinuosity. These reaches display a significant range of bars and benches of varying type and vegetation cover and of floodplain landforms’. There were only 13 reaches in this class, but there appears to be a sub-group of 4 reaches which show greater frequencies of floodplain features (depressions, ponds) and stabilising channel margin features (vegetated side bars and benches). This suggests that at least two distinct sub-classes are present within class 1. However, any firm subdivision into two new classes is not sufficiently reliable without investigation of a larger sample of reaches.

Class 2: was described in chapter 3 as ‘relatively steep, low sinuosity reaches of intermediate width. These reaches display a significant range of lateral and mid-channel bars and many of them also have exposed bedrock features’. Class 2 contains a relatively small number of reaches (14) but the subdivision distinguishes one subgroup which is steeper and less sinuous and one subgroup that shows more complex riparian and aquatic vegetation. These were all properties that distinguished class 2 from the other classes in the original classification, so the subdivision indicates some subtle within-class variations in these properties. A larger sample size might support division of this class into two classes, particularly as the sub-classes join at quite a high level of dissimilarity.

Class 3: was described in chapter 3 as ‘reaches of intermediate slope, relatively low sinuosity and intermediate and width. These reaches show a significant contrast in the sinuosity, width and slope of their bankfull and baseflow channels, and as a result, they display a wide range of bars, particularly active bars, and benches of varying type’. This class is comprising 64 reaches but the split only reveals differences in two properties that did not distinguish class 3 from the other classes in the original classification (channel width and riffle-pool-boulder-bedrock features). Therefore, subdivision could provide two transitional classes between class 2 and classes 4 to 6, based on bed features and channel width, but there is no strong reason to split class 3, since it would not produce particularly distinct river types.

Class 4: was described in chapter 3 as ‘reaches of intermediate slope, sinuosity and width with relatively few in-channel or marginal features, although riffle-pools are more frequent in this cluster than in any of the other clusters’. In this relatively large

class of reaches (44), the subdivision reveals a group of reaches with relatively more macrophytes, benches, floodplain depressions and ponds, and a group with relatively more complex riparian vegetation. The former subdivision may indicate an intermediate class between classes 4 and 5 (class 5 reaches are characterised by a high presence of benches, floodplain depressions and ponds whereas class 4 reaches are characterised by a low presence of these features), but there is no evidence for this in the dendrogram (Figure 4.8), where the greatest similarity is with class 6. Furthermore, the potential subdivision may simply reflect the partial coverage of the distinguishing marginal-floodplain features by the more complex riparian vegetation structure in the second split category. Therefore, it is difficult to justify any subdivision of class 4.

Class 5: was described in chapter 3 as ‘reaches of relatively low slope, high sinuosity, and low width, displaying relatively frequent marginal benches and floodplain depressions and ponds’. Class 5 is comprising 34 reaches which split into one subgroup with greater slope, lower sinuosity, greater contrast in baseflow to bankfull sinuosity, more bars and floodplain depressions and ponds, and a second subgroup with more benches. These differences could well describe distinguishably different river types forming transitions between classes 4 and 6 if the split were supported by larger samples of reaches, particularly given the high value of dissimilarity at which the split classes join. However, without a larger sample of reaches, any such split is difficult to justify.

Class 6: was described in chapter 3 as ‘reaches of relatively low slope, high sinuosity, and low width, displaying the lowest in channel, marginal and floodplain features of all clusters’. The class subdivides into two quite large subclasses (23 and 25 reaches) and the split reflects a higher slope and width and lower sinuosity in one subgroup of reaches and higher occurrence of floodplain depressions and ponds in the other. Once more, this could be interpreted as an important transitional distinction within this class, although the two subclasses join at quite a low level of dissimilarity.

Overall, there is little strong evidence to support the extension of the classification to more than the six original classes without a larger sample of reaches to support such an extension. The strongest case for a subdivision relates to Class 1, which is very different from the other classes and, despite the small sample size, appears to have some geomorphologically distinct types within it. Elsewhere, the splits generally reveal transitional sub-classes that could be usefully distinguished if a more detailed

classification were needed. The most compelling evidence for subdivisions are associated with classes 1, 4, 5 and 6.

4.4 Assessment of the accuracy of elevation data extracted from Google Earth

Reach slope is an important factor in the classification, since this is one of the geometric properties that underpins PC1.1 and helps to separate classes 1, 5, and 6 from classes 3 and 4 and from class 2. The estimates of slope used in the classification analysis were derived from spot elevation values extracted from Google Earth images, so it is important to assess their accuracy.

Google Earth has the ability to view the Earth three-dimensionally by using interpolated data collected from NASA's Shuttle Radar Topographic Mission (SRTM). This section attempts to use airborne Lidar data to assess the precision of the upstream and downstream elevation values and thus the derived slope estimates for 25 of the studied reaches where both data types are available. In ArcGIS version 10, placemarks for each reach that had been extracted from Google Earth were converted from KML format to a shapefile and were then projected into the same coordinate system as the Lidar data. This allowed the floodplain elevation around the projected upstream and downstream points to be extracted for comparison with the estimates from Google Earth. Table 4.4 lists the two sets of elevation values for 36 points. The resolution of information from the two data sets is different (nearest m for Google Earth, nearest cm for Lidar), but this difference is maintained in the comparison to present the genuine difference that would arise if either data set were used. Percent error was estimated using the following equation:

$$\text{mean \% error} = 100 \times (|\text{Lidar elevation} - \text{Google Earth elevation}|) / (\text{Google Earth elevation})$$

Only a 6.73% average error was found across the 36 points, which plot close to the 1:1 line on the graph shown in Figure 4.9. This gives great confidence in the precision of the Google Earth estimates of point elevation. However, Lidar data were only available for reaches with a limited elevation range (0 to 140 m.a.s.l.). Such low elevations are only found for reaches in classes 1, 4, 5 and 6 (Figure 4.10). It is highly possible that in the higher elevation reaches of class 3 and particularly class 2, elevations are less accurate because of void filling within narrow valleys in the SRTM

data set. Therefore, the outcomes of this analysis are very supportive of using Google Earth elevation estimates to derive river channel and floodplain gradients, but further checks are needed for higher elevation and more confined river reaches.

Table 4.4 Values of elevation for the same points extracted from Google Earth (nearest m) and Lidar data (nearest cm)

Reach no.	Name of Rivers	Replicate reach	(U)pstream/ (D)ownstream	Google Earth			LiDAR		Absolute Error	Percent Error
				Latitude	Longitude	Elevation (m)	BNG	Elevation (m)		
1	Frome	1	U	50.69	-2.26	19	SY8187	17.30	1.70	8.95
2		2	U	50.68	-2.20	10	SY8586	9.67	0.33	3.26
3		3	U	50.68	-2.15	7	SY8986	4.13	2.87	41.00
		3	D	50.68	-2.11	1	SY9286	0.75	0.25	25.00
4	Dee	1	U	53.01	-2.91	14	SJ3845	14.35	0.35	2.50
5		2	U	53.02	-2.87	13	SJ4147	11.59	1.41	10.85
6		3	U	53.05	-2.86	10	SJ4250	9.73	0.27	2.70
		3	D	53.07	-2.88	10	SJ4153	8.74	1.26	12.60
7	Caersws	2	D	52.00	-3.98	121	SO0391	121.76	0.76	0.63
8		4	D	51.95	-4.13	113	SO0890	110.77	2.23	1.97
9	Lune	1	U	54.29	-2.58	75	SD6288	73.10	1.9	2.53
10		1	D	54.20	-2.60	52	SD6178	41.50	10.5	20.19
		2	U	54.20	-2.60	32	SD6074	31.80	0.20	0.63
		2	D	54.12	-2.64	24	SD5869	22.34	1.66	6.92
		11	3	U	54.11	-2.66	21	SD5768	20.69	0.31
3			D	54.09	-2.70	15	SD5465	14.68	0.32	2.13
12	Coquet	1	U	55.33	-2.07	133	NT9503	127.00	6.00	4.51
13		2	U	55.31	-2.05	116	NT9601	113.00	3.00	2.59
		2	D	55.30	-2.01	95	NT9900	92.00	3.00	3.16
14		3	U	55.31	-1.99	89	NU0001	88.86	0.14	0.16
		3	D	55.31	-1.93	79	NU0401	77.50	1.50	1.90

Table 4.4 (ctd.)

Reach no.	Name of Rivers	Replicate reach	(U)pstream/ (D)ownstream	Google Earth			LiDAR		Absolute Error	Percent Error
				Latitude	Longitude	Elevation (m)	BNG	Elevation (m)		
15	Bollin	1	U	53.32	-2.18	82	SJ8879	78.45	3.55	4.33
16		2	U	53.32	-2.19	77	SJ8780	73.14	3.86	5.01
17		3	U	53.32	-2.20	75	SJ8780	70.71	4.29	5.72
18	Tywi	1	U	51.99	-3.81	63	SN7533	61.40	1.60	2.54
		1	D	51.96	-3.88	46	SN7130	45.10	0.90	1.96
19		2	U	51.92	-3.92	38	SN6825	35.80	2.20	5.79
		2	D	51.89	-3.98	26	SN6322	26.70	0.70	2.69
20		3	U	51.87	-4.05	20	SN5821	20.38	0.38	1.90
		3	D	51.87	-4.14	14	SN5221	14.90	0.90	6.43
21	Twrch	2	D	52.04	-3.96	97	SN6435	95.00	2.00	2.06
22		3	U	51.99	-4.00	93	SN6234	92.30	0.70	0.75
		3	D	51.95	-4.13	75	SN5329	60.00	15.00	20.00
23	Dane	1	U	53.18	-2.24	77	SJ8464	69.87	7.13	9.26
24		2	U	53.19	-2.28	58	SJ8165	55.13	2.87	4.95
25		3	U	53.20	-2.31	54	SJ7936	46.80	7.2.0	13.33
N		36					Average		2.59	6.73

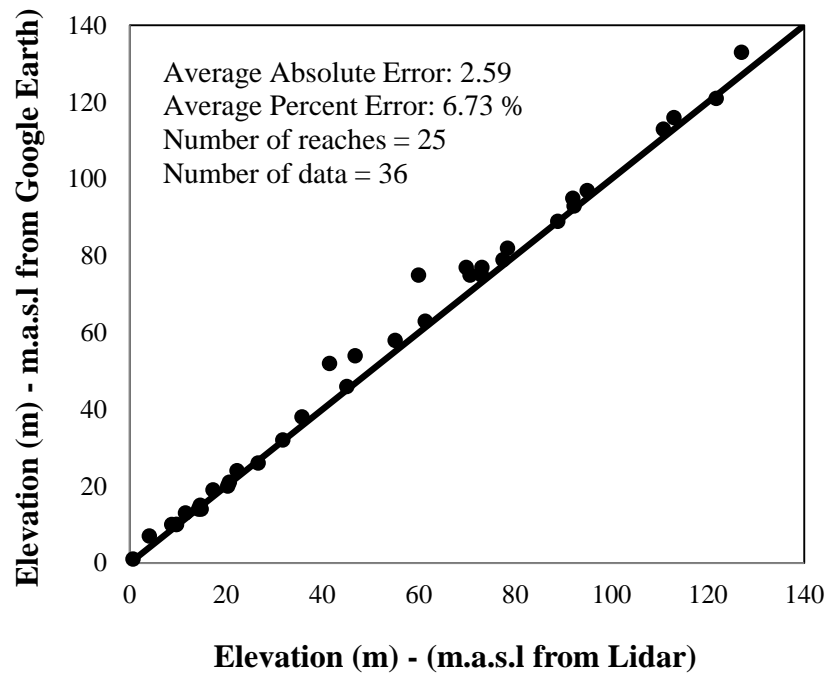


Figure 4.9 Scatter plot comparing elevation estimates in m.a.s.l. extracted from Google Earth (vertical axes) and Lidar (horizontal axes) data for 25 reaches and 36 points

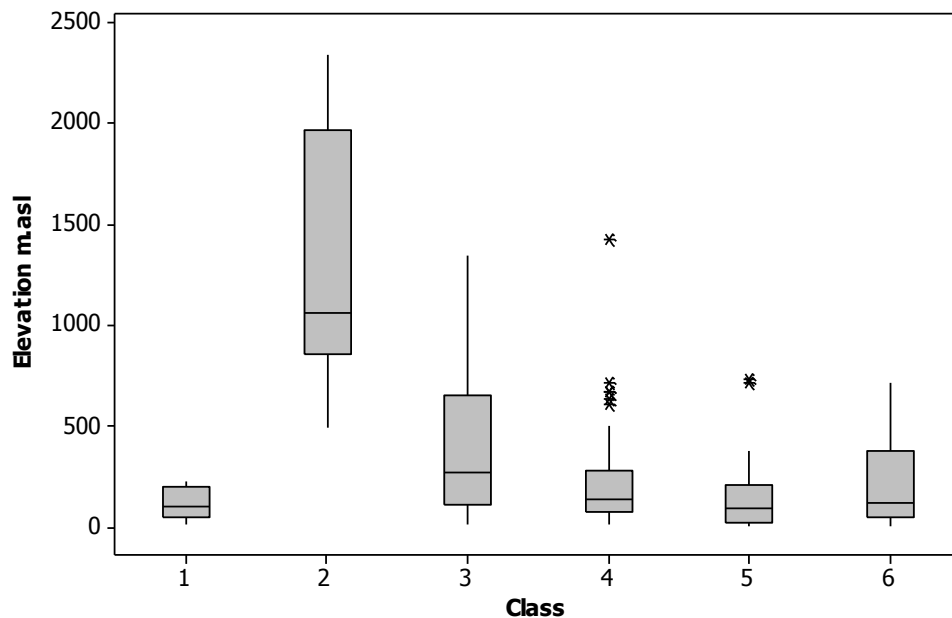


Figure 4.10 Box and whisker plots illustrating the elevation (m.a.s.l.) recorded within the six river classes for all reaches whose elevation was extracted from Google Earth.

4.5 Influence of the image selected on river reach classification

In order to assess the degree to which the choice of Google Earth image may have affected the class to which each river reach was assigned, a second image was analysed for 12 of the reaches that had been included in the original classification (Table 4.5). This took advantage of the ‘historical imagery’ that was available through Google Earth. Two reaches were selected in each of the six classes and images were selected to maximise the potential contrast with those that had been selected previously for the classification. This was achieved by selecting images that were either displaced by several years from the original image and / or were representative of a different season of the year.

Table 4.5 Details of the 12 reaches for which a second image was analysed from a different year and/or different season

Class	Country	River name	Reach*	Original image date	New image date
1	France	Allier	3	1/1/2008	1/1/2002
1	France	Roubion	3	14/5/2012	30/11/2007
2	Austria	Lareintal	2	6/9/2011	31/12/2007
2	Austria	Frutz	2	21/7/2003	1/1/2000
3	Wales	Caersws	2	1/1/2009	1/1/2006
3	Italy	Cecina	1	15/10/2006	21/6/2002
4	England	Irthing	1	27/4/2006	1/1/2002
4	Slovakia	Biela	2	12/7/2009	1/1/2004
5	France	Le Saulx	2	1/1/2008	1/1/2004
5	Wales	Dee	2	10/10/2010	27/4/2005
6	Germany	Isen	2	1/1/2009	30/6/2002
6	Hungary	Raba	1	21/3/2012	21/11/2007

*The reach number refers to whether it is an upstream (1), middle (2) or downstream (3) reach at site analysed on the named river.

Table 4.6 summarises the standardised values of the variables extracted for each of the images listed in Table 4.5. In order to assess changes in the reaches as a result of using different images for the analysis, shifts in the plotting position of each reach with respect to the first two PCs of the integrated PCA (Table 3.12) were explored. The PC scores for the second image of each of the 12 selected reaches were computed manually using matrix multiplication of standardised values (mean, standard deviation, eigenvectors) from the original PCAs (of 221 reaches). Thus, the 12 new reaches are placed within the spaces defined by the original PCAs of 221 reaches. This procedure is illustrated in Figure 4.11, which describes the flow of the computation used to achieve the 10 sets of new PC scores. The same procedure allows the final two aggregate PC scores to be calculated, which locate the 12 new reaches within the scatterplot of Figure 3.14.

Figure 4.12 illustrates the old and new plotting positions for the 12 sites in comparison with the original 221 reaches within the space defined by PC1 and PC2 of the aggregate PCA (which incorporated the 10 component PCs). The arrows on Figure 4.12 indicate the shift in each of the 12 reaches from their original position. In general, the length of the arrows reduces from class 1 to 6. Class 1, which contains the largest rivers, shows the greatest changes in plotting position, although the reaches still remain within the correct area of the graph. Classes 2 and 3 also show quite prominent changes in their PC scores but they remain located within the relevant area of the plot. Reaches within classes 4 to 6 show very small changes in their plotting position. Overall the new reach scores seem to fall within the area of the plot defined by other reaches in the same class suggesting that the classification is robust to changes in the date of the images that are analysed.

Table 4.6 Summary information on standardised variables extracted from the images listed in Table 4.5

Descriptions				Dimensions							Dimension ratio			Flow features					
Class	Reach no.	River Name	Country	Baseflow Median Width (m)	Baseflow Sinuosity	Baseflow Channel Slope (per mil)	Bankfull Median Width (m)	Bankfull Sinuosity	Bankfull Channel Slope (per mil)	Valley Gradient (per mil)	Baseflow_Bankfull Median Width	Baseflow_Bankfull Sinuosity	Baseflow_Bankfull Channel Slope	Pools	Riffles	Cascade	Waterfall & Steps	Boulders	Exposed bedrock
1	3	Allier	France	87.18	1.31	0.79	376.79	1.16	0.89	1.04	0.23	1.12	0.89	0	0	0	0	0	0
2	2	Lareintal	Austria	4.20	1.11	98.38	11.84	1.07	101.67	108.77	0.35	1.03	0.97	0	0	0.09	0	0.14	0
3	2	Caersws	England	19.98	1.29	2.16	39.12	1.25	2.25	2.80	0.51	1.04	0.96	0.16	0.20	0	0	0	0
4	1	Irthing	England	18.19	1.47	5.38	22.65	1.44	5.49	7.91	0.80	1.02	0.98	0	0.04	0.01	0.01	0.04	0
5	2	Le Saulx	France	25.00	1.66	0.74	27.49	1.66	0.74	1.23	0.91	1.00	1.00	0.04	0	0	0	0	0
6	2	Isen	Germany	10.79	1.37	4.70	10.79	1.37	4.70	6.43	1.00	1.00	1.00	0	0.02	0	0	0	0
1	3	Roubion	France	15.12	1.11	4.61	80.60	1.03	4.95	5.12	0.19	1.07	0.93	0	0	0	0	0	0
2	2	Frutz	Austria	10.50	1.18	68.63	40.05	1.15	70.33	80.90	0.26	1.02	0.98	0	0	0	0.17	0.15	0
3	1	Cecina	Italy	17.46	1.18	1.23	70.49	1.11	1.32	1.46	0.25	1.07	0.93	0	0	0	0	0	0
4	2	Biela	Slovakia	14.08	1.14	10.50	28.64	1.14	10.56	12.01	0.49	1.01	0.99	0	0.06	0	0.02	0.02	0
5	2	Dee	Wales	32.64	1.70	0.42	34.29	1.69	0.43	0.72	0.95	1.01	0.99	0	0	0	0	0	0
6	1	Raba	Hungary	29.39	2.00	0.40	29.37	2.00	0.40	0.81	1.00	1.00	1.00	0	0	0	0	0	0

Table 4.6 (ctd.)

Descriptions				Vegetation				Floodplain Features								Bars and Benches					
Class	Reach no.	River Name	Country	Vegetation Structure	Weighted Tree Distribution	Total Wood Jams	Emergent Macrophytes	Total Swamp-Wetland	Total Water-fille ponds	Total connected side channels	Total Dry depressions	Total Ridges & Swales	Total Oxbow	Total Stabilising arcuate bars	Total Stabilising Marginal bars (non-arcuate shape)	Total Active Marginal Bars	Total Stabilising Marginal Bars	Total Active Mid-Channel Bars	Total Stabilising mid-channel bar	Total Active Bench	Total Stabilising Bench
1	3	Allier	France	2.20	3.80	0	0	0	0	0	0	0	0	0.04	0	0.41	0.04	0.04	0	0	0
2	2	Lareintal	Austria	0	0	0	0	0	0	0.04	0	0	0	0	0	0.08	0	0.08	0	0	0
3	2	Caersws	England	1.29	1.80	0	0	0	0	0	0	0	0	0.02	0	0.21	0.02	0.01	0.03	0	0
4	1	Irthing	England	2.00	4.45	0.02	0	0	0	0	0	0	0	0	0	0.01	0	0	0	0	0
5	2	Le Saulx	France	2.38	3.41	0	0	0	0.01	0.01	0.03	0	0.02	0.02	0.01	0.10	0.03	0.02	0.01	0	0
6	2	Isen	Germany	1.78	3.27	0	0	0	0	0	0	0	0	0	0	0	0	0	0	0	0
1	3	Roubion	France	2.90	4.67	0	0	0	0	0.03	0	0	0	0	0	0.34	0	0.09	0	0	0
2	2	Frutz	Austria	2.80	4.75	0.08	0	0	0	0	0	0	0	0	0	0.25	0	0	0	0	0
3	1	Cecina	Italy	2.83	4.56	0	0	0	0	0	0	0	0	0	0	0.28	0	0.05	0	0	0
4	2	Biela	Slovakia	2.55	4.45	0	0	0	0	0.01	0.02	0	0	0	0	0.20	0	0.01	0	0	0
5	2	Dee	Wales	0.17	1.33	0	0	0	0	0	0.02	0	0.02	0	0	0.04	0	0	0	0.07	0
6	1	Raba	Hungary	2.89	4.93	0	0	0	0	0	0	0	0	0.01	0	0	0.01	0	0.01	0	0

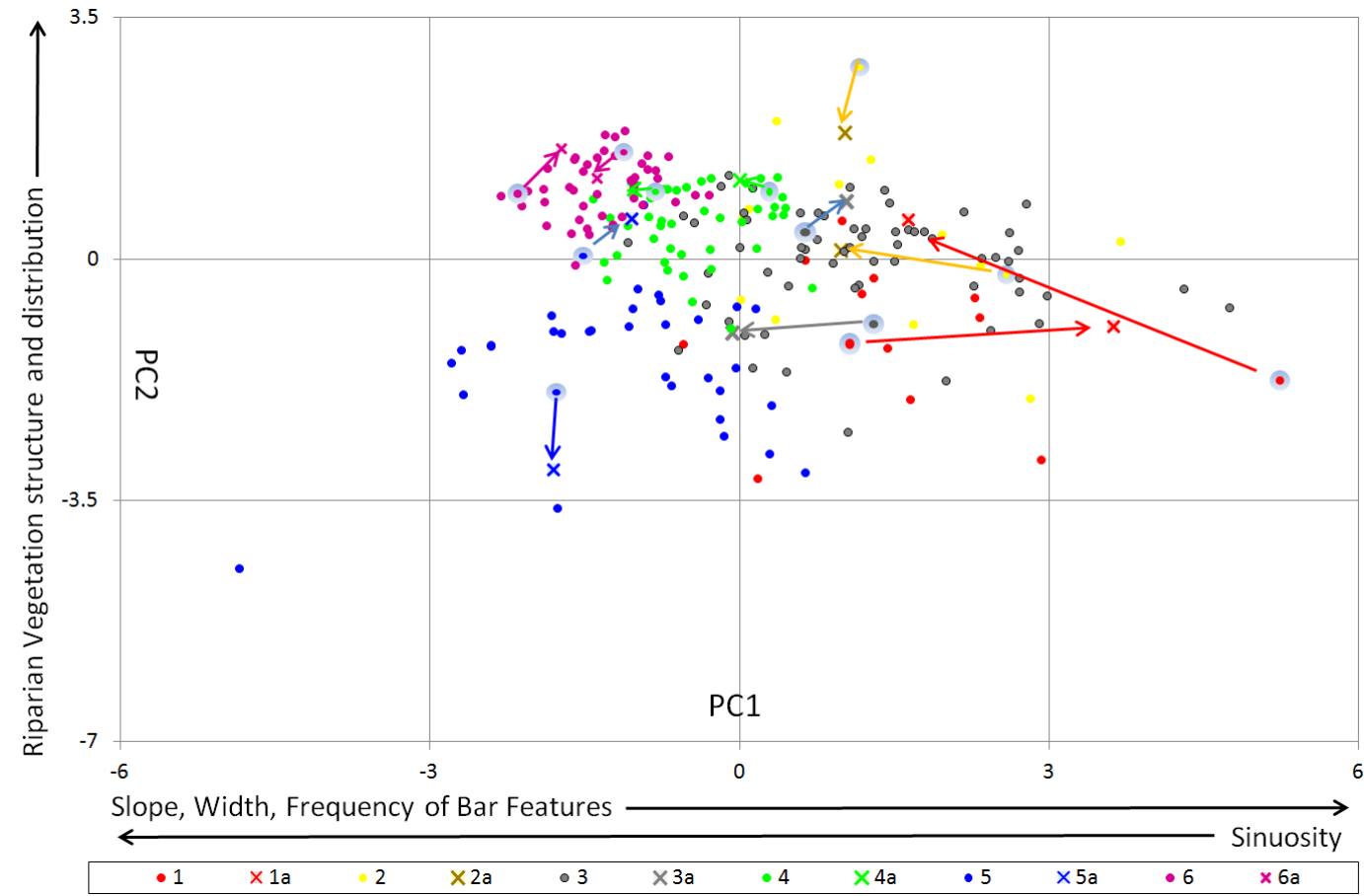


Figure 4.12 Changes in plotting position (from O to X) of 12 reaches for which two images were analysed in relation to the first two PCs of the aggregate PCA and in comparison to the 221 rivers originally analysed.

4.6 Impact of including additional variables from other data sources

Geometric variables extracted from Google Earth images have underpinned an interpretable and apparently robust classification of European rivers. However, key variables that would normally form fundamental components of such a classification are not available from Google Earth, in particular information on the river's discharge and bed material. Therefore this section explores the degree to which available discharge and sediment information for some of the analysed rivers supports the classification based on Google Earth images.

4.6.1 River flow data

River flow data were available for 55 of the 75 river reaches previously analysed. The rivers and gauging stations are listed in Table 4.6, along with the length of record and proximity of the gauging stations to the studied reaches. The length of the data series was restricted by that available from a previous European project (see page 72), particularly for countries other than the UK. However, a minimum 30 year record was analysed, which in many non-UK cases was constrained by data availability to be 1961-1990. Whilst not ideal in terms of the end date, these data at least represented a substantial length of record, which was consistent across many of the rivers considered. Since the lowest temporal resolution of the available data was daily flows, all analyses used daily data. The maximum daily flow in each year was extracted and the 2, 5, and 10-year flood events were computed using the automated Gumbel approach (Ponce, 1989).

Boxplots of the computed 2, 5 and 10 year flows show no clear trends linking discharge to river class (Figure 4.13), although the largest rivers show the largest discharges. However, when total stream power is calculated ($\Omega = \rho g Q S$ where Ω is total stream power ($\text{W}\cdot\text{m}^{-1}$), ρ is water density ($1000 \text{ kg}\cdot\text{m}^{-3}$), g is gravitational acceleration ($9.8 \text{ m}\cdot\text{s}^{-2}$), S is channel gradient ($\text{m}\cdot\text{m}^{-1}$) and Q is discharge ($\text{m}^3\cdot\text{s}^{-1}$)), clear associations with river class are apparent (Figure 4.14). Unit stream power ($\omega = \frac{\rho g Q S}{B}$, where B is bankfull width) for the same three floods is displayed in Figure 4.15, and shows a similar although less clear trend when compared with Figure 4.14.

Table 4.7 Gauging station names, codes, locations, record lengths and computed 2, 5, 10 year floods (annual series based on daily flows) for 55 rivers

River	Country	Source*	Gauging station name	Code	Gauging station location	Length of record	Years**	Q ₂ (m ³ /s)	Q ₅ (m ³ /s)	Q ₁₀ (m ³ /s)
Abhainn	Scotland	NRFA	Carron at Sgodachall	CEH 3002	4.5 km downstream reach 3	30	1974-2003	105	148	177
L'Aisne	France	Eau-France	L'Aisne à Mouron	H6201010	on reach 1	30	1961-1990	144	197	232
Allier	France	Eau-France	L'Allier à Moulins	K3450810	500 m upstream reach 1	30	1968-1997	721	1008	1197
Annan	Scotland	NRFA	Annan at Woodfoot	CEH 78006	on reach 1	28	1984-2012	82	107	124
Aragon	Spain	Hidrográficos – Spain	Rio Aragon en Jaca	9018	on reach	30	1961-1990	144	242	307
L'Ardeche	France	Eau-France	L'Ardeche à St Martin	V5064010	on reach 3	30	1961-1991, 1986**	957	1476	1820
Asse	France	Eau-France	L'Asse à Beynes	X1424010	35 km downstream reach 3	30	1961-1991, 1978**	41	66	83
Beaume	France	Eau-France	La Beaume à Rosieres	V5035020	3 km upstream on reach 1	14	1999-2012	165	307	401
Bergantes	Spain	Hidrográficos – Spain	Rio bergantes en Zorita	9031	on reach 2	19	1961-1970 & 1991-2009	117	354	511
Bollin	England	CEH	Bollin at Wimslow	CEH690012	on reach 3	30	1976-2005	8	10	12

Table 4.7 (ctd.)

River	Country	Source*	Gauging station name	Code	Gauging station location	Length of record	Years**	Q ₂ (m ³ /s)	Q ₅ (m ³ /s)	Q ₁₀ (m ³ /s)
Bregenzer	Austria	REFORM	Bregenzerbach	AU 8001024	on reach 1	30	1961-1990	21	27	31
Caersws	Wales	NRFA	Severn at Dolwen	CEH54080	3.5 km upstream reach 1	19	1977-1983 & 2001- 2012	48	68	81
Coquet	England	NRFA	Coquet at Rothbury	CEH 22009	2km downstream reach 3	30	1974-2003	73	111	136
Dane	England	NRFA	Dane at Hulme Walfield	CEH 68006	300 m upstream	20	1961-1976 & 1981- 1984	24	39	50
Dee	Wales/Engl and	REFORM	Dee at Manley Hull	CEH67015	13.5 km upstream reach 2	30	1961-1990	187	265	316
Divorka Olice	Czech Republic	REFORM	Divorka Orlice	CR0240	18 km downstream reach 1	30	1961-1990	26	38	47
Durance	France	Eau- France	La Durance à l'Argentiere	X0130010	2.5 km upstream reach 1	30	1961-1978 & 1984- 1995	112	153	180
Endrick	Scotland	NRFA	Endrick Water at Gaidrew	CEH 85002	on reach 2	30	1963-1992	66	80	89
Eygues	France	Eau- France	L'Aygues à Saint-May	V5324919	3.5 km downstream reach 3, after tributary	30	1964-1993	53	87	109
Feshie	Scotland	NRFA	Feshie at Feshiebridge	CEH 8013	on reach 3	20	1992-2012, 2000**	62	81	94

Table 4.7 (ctd.)

River	Country	Source*	Gauging station name	Code	Gauging station location	Length of record	Years**	Q ₂ (m ³ /s)	Q ₅ (m ³ /s)	Q ₁₀ (m ³ /s)
Findhorn	Scotland	REFORM	Findhorn at Shenachie	CEH7001	on reach 2	30	1961-1990	118	169	203
Frome	England	REFORM	Frome at East Stoke	CEH44001	on reach 2	30	1965-1994	20	23	25
Frutz	Austria	REFORM	Frutz	AU 8001015	on reach 2	30	1961-1990	17	22	26
Hinterrhein	Switzerland	REFORM	Hinterrhein	CH2224	5km downstream reach 3	30	1961-1990	30	45	56
Irthing	England	NRFA	Irthing at Greenholme	CEH76008	7.5 km downstream reach 3	30	1968-1997	81	126	155
Isabena	Spain	Hidrográficos – Spain	Isabena en Capella	9047	7.5 km downstream reach 3	30	1961-1991, 1970**	65	141	191
Isen	Germany	REFORM	Isen	G_BY 18381500	on reach 2	30	1961-1990	10	14	17
Kinnel Water	Scotland	CEH	Kinnel Water at Redhall	CEH78004	on reach 1	30	1961-1990	28	37	43
L'Aube	France	Eau-France	L'Aube à Arcis	H1501010	2.5 km downstream reach 3	30	1961-1990	162	236	285
L'Oise	France	Eau-France	L'Oise à Sempigny	H7401010	1.5 km downstream reach 3	30	1961-1990	116	165	198
La Meurthe	France	Eau-France	La Meurthe à Laneuveville	A6921010	1.5 km downstream reach 3	27	1986-2012	285	393	464

Table 4.7 (ctd.)

River	Country	Source*	Gauging station name	Code	Gauging station location	Length of record	Years**	Q₂ (m³/s)	Q₅ (m³/s)	Q₁₀ (m³/s)
Le Gave d'Oloron	France	Eau-France	Le Gave D'Oloron à Escos	Q7412910	1.5 km downstream reach 3	30	1961-1990	734	1007	1187
Saulx	France	Eau-France	Le Saulx à Vitry	H5172010	1 km downstream reach 3	30	1961-1990	138	186	218
Le Var	France	Eau-France	La Var à Malaussene	Y6432010	on reach 3	30	1961-1990	262	397	486
Loire	France	Eau-France	La Loire à Gilly-sur-Loire	K1440010	7.5 km upstream reach 1	30	1969-1999, 1988**	906	1237	1237
Lune	England	REFORM	Lune at Killington New Bridge	gdf72005	upstream reach 1	30	1970-1999	131	201	248
Meig	Scotland	NRFA	Meig at Glenmeannie	CEH4005	on reach 1	27	1986-2012	64	90	108
Mitternacher Oh	Germany	REFORM	Mitternacher Oh	G_BY17425000	2.5 km upstream reach 1	30	1961-1990	17	24	29
Moselle	France	REFORM	La Moselle à Epinal	A4250640	35-40 km upstream reach 1	30	1961-1990	311	418	489
Nairn	Scotland	NRFA	Nairn at Balnafoich	CEH 7008	7 km downstream reach 3	20	1993-2012	41	63	77
Naver	Scotland	NRFA	Naver at Apigill	CEH 96002	on reach 3	30	1977-2006	119	168	200
Oste	Germany	REFORM	Oste	G_NS5983110	on reach 2	30	1961-1990	35	52	63

Table 4.7 (ctd.)

River	Country	Source*	Gauging station name	Code	Gauging station location	Length of record	Years**	Q ₂ (m ³ /s)	Q ₅ (m ³ /s)	Q ₁₀ (m ³ /s)
Roubion	France	Eau-France	Le Roubion à Soyans	V4414010	8.5 km upstream reach 1	30	1965-1995, 1994**	23	34	42
St Medard	France	Eau-France	La Coise à St. Medard	K0673310	on reach 2	30	1961-1991, 1979**	17	35	47
Saison	France	Eau-France	le Saison Mauleon	Q7322510	6km upstream reach 2	30	1967-1996	233	337	405
San Tirso	Spain	REFORM	Eo at San Tirso de Abres	1427	on reach 1	30	1961-1990	149	227	279
South Tyne	England	NRFA	South Tyne at Alston	Ceh23009	100 m upstream reach 2	29	1970-2008 (1979,1984-1991)**	50	72	86
Spey	Scotland	NRFA	Spey at Boot o Brig	CEH8006	on reach 2	30	1961-1990	346	525	643
Subersach	Austria	REFORM	Subersach	AU8001028	on reach 1	30	1961-1990	20	27	32
Tietar	Spain	Hidrográficos – Spain	Rio Tietar en Arenas de San Pedro	3161	on reach 3	30	1968-1997	145	257	332
Tormes	Spain	Hidrográficos – Spain	Tormes at Hoyos del Espino	2006	12 km upstream reach 1	30	1961-1990	18	30	37
Torridge	England	REFORM	Torridge at Torrington	CEH50002	on reach 3	30	1963-1992	162	216	253
Tweed	Scotland	REFORM	Tweed at Boleside	CEH21006	20 km downstream on	30	1961-1990	253	365	439

Table 4.7 (ctd.)

River	Country	Source*	Gauging station name	Code	Gauging station location	Length of record	Years**	Q ₂ (m ³ /s)	Q ₅ (m ³ /s)	Q ₁₀ (m ³ /s)
					reach 3					
Twrch	Wales	REFORM	Twrch at Ddol las	CEH 60012	on reach 1	28	(1971-1981, 1990-2006)	6	9	11
Tywi	Wales	NRFA	Tywi at Dolau Hiroin	CEH 60007	2.5 km upstream reach 1	30	1969-1998	90	137	168

* (1) NRFA : National River Flow Archive, (2) CEH: Central for Ecology and Hydrology; (3) REFORM: Restoring rivers for Effective Catchment Management (4) Eau-france : www.hydro.eaufrance.fr/selection.php (5) Hidrográficos - Spain: hercules.cedex.es/anuariofos/afo/estaf-datos_anual.asp

** missing year

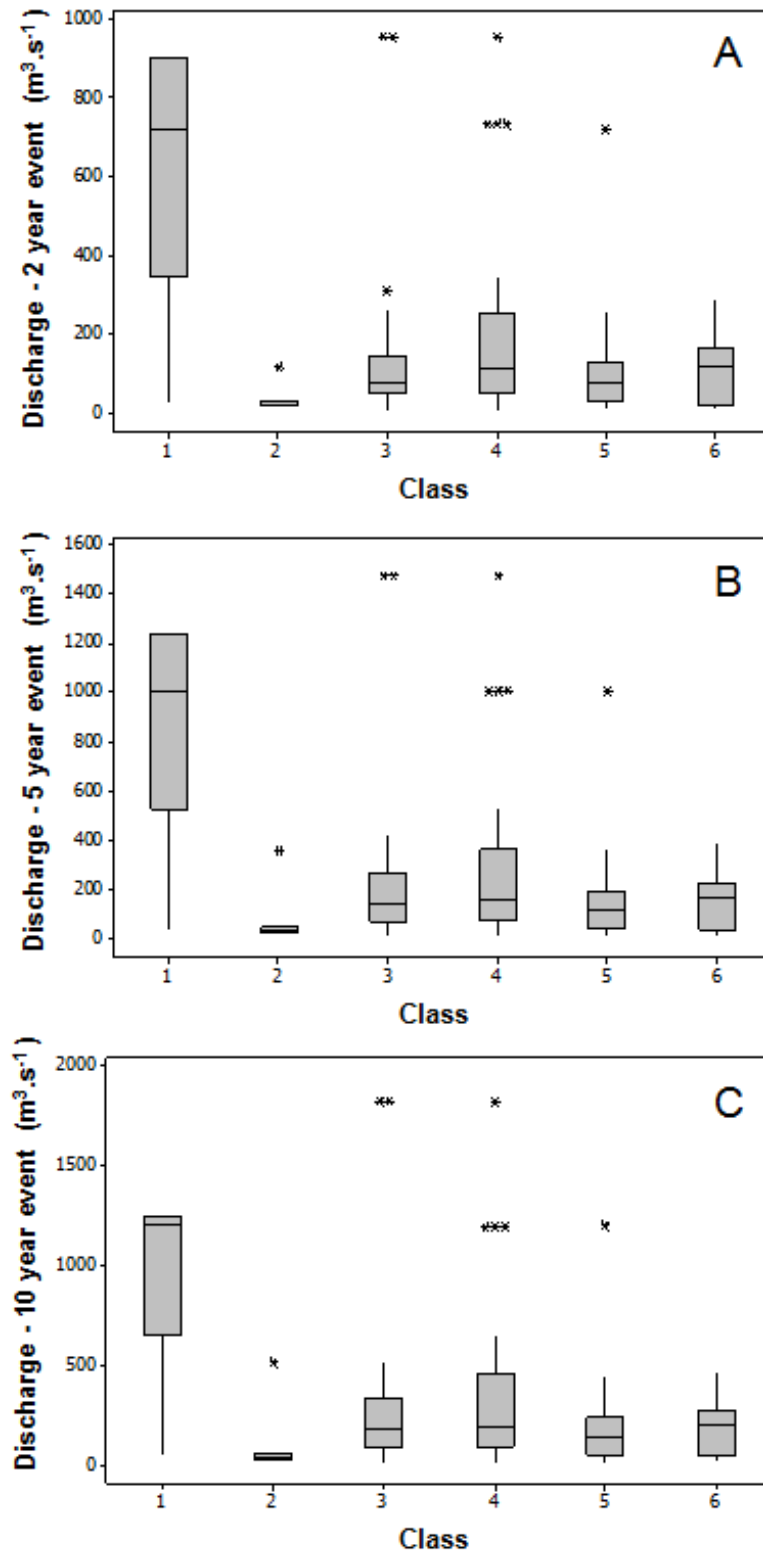


Figure 4.13 Boxplots illustrating variation in discharges of different flood recurrence interval (daily flow data, annual maximum series) according to river class. (A) 2 year flood, (B) 5 year flood, (C) 10 year return period.

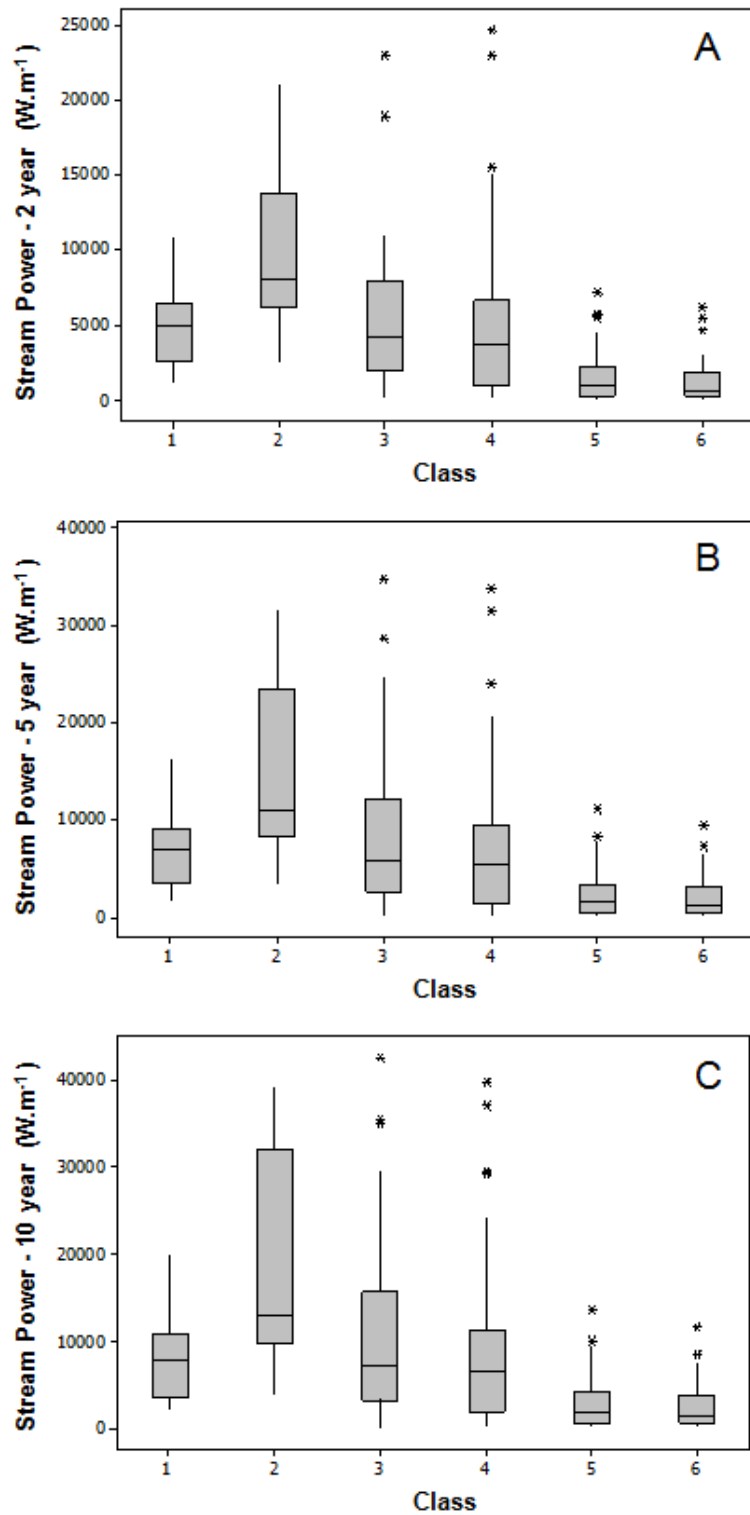


Figure 4.14 Boxplots illustrating variations in stream power for discharges of different flood recurrence interval (daily flow data, annual maximum series) according to river class. (A) 2 year flood, (B) 5 year flood, (C) 10 year return period.

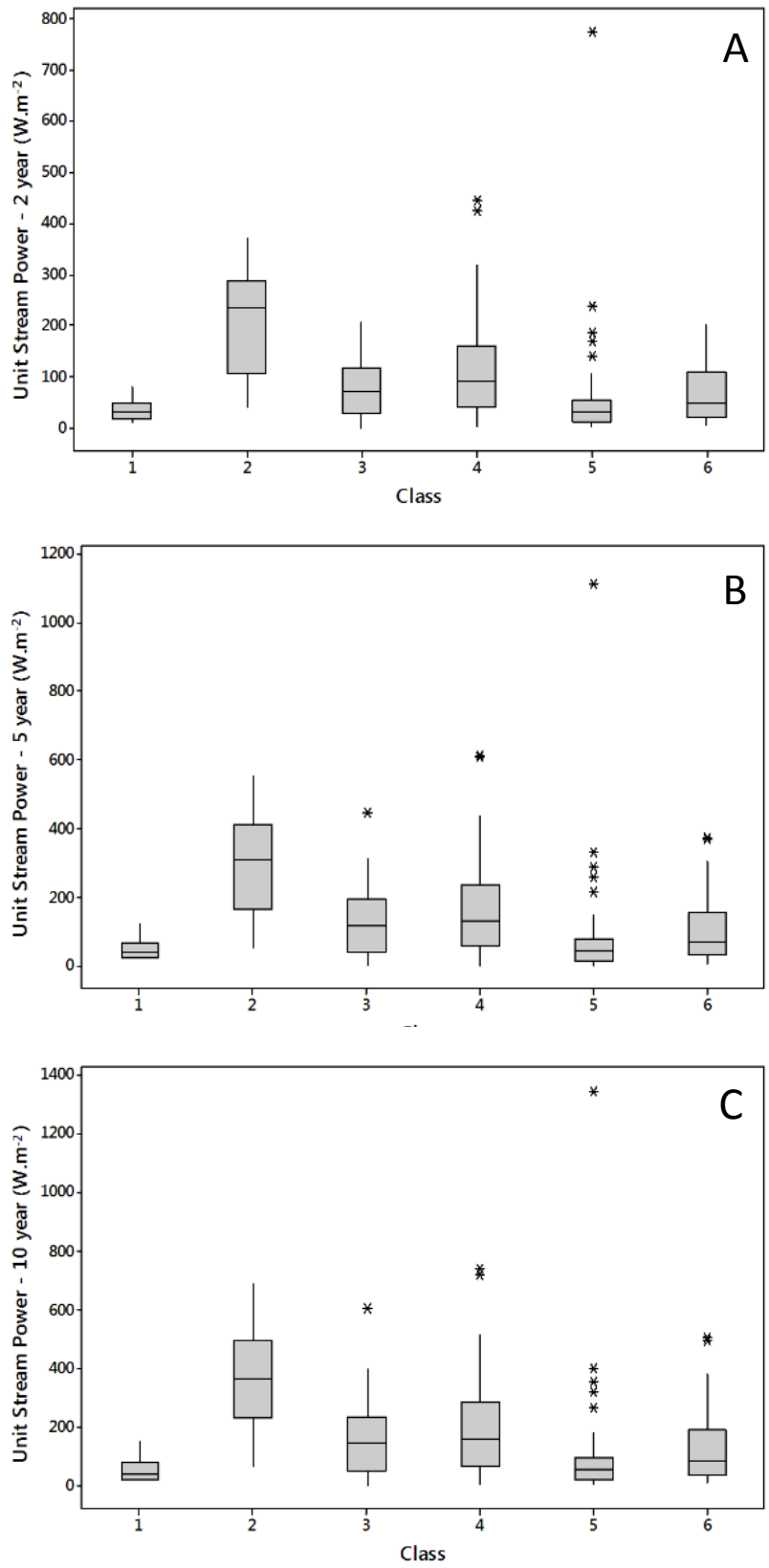


Figure 4.15 Boxplots illustrating variations in unit stream power for discharges of different flood recurrence interval (daily flow data, annual maximum series) according to river class. (A) 2 year flood, (B) 5 year flood, (C) 10 year return period.

Stream power is a more relevant variable for a geomorphological analysis than discharge, since it represents the rate of energy dissipation against the bed and banks of a river or stream per unit downstream length, and is fundamentally a function of discharge and slope. Stream power is highest for the steep class 2 rivers and lowest for classes 5 and 6, with intermediate values for classes 1, 3 and 4. This pattern is what would be expected for the river classes, particularly the general decline in stream power for classes 2 to 6 as sinuosity increases and channels appear to become more stable (Table 4.3).

4.6.2 Sediment data

Purpose-specific measurements of the calibre of bed material were only available for a few rivers from published sources. However, a surrogate for bed material calibre was extracted from River Habitat Survey (RHS) data for 58 reaches of British river in the data set. The River Habitat Survey (Environment Agency, 2003) is a field survey that is used for assessing the character and habitat quality of British rivers. Within each 500m length of river that is surveyed, 10 ‘spot-checks’ are recorded at 50 m intervals that include observations of the dominant bed sediment material. The observations are visual assessments and are usually observed from the river bank, but they provide 10 observations from which a simple estimate of bed material calibre can be made.

Before the RHS data could be used, it was necessary to assess the proximity of RHS sites to any of the 75 river sites that were used for the classification. Information relevant to RHS site locations were converted from the British National Grid to World Geodetic System 1984 so that they could be projected onto Google Earth images. RHS sites that were within or very close to any of the 75 river sites were identified. RHS surveys were found located close to 19 river sites and 58 reaches in Great Britain (Table 4.8).

Depending on the availability of surveys, each reach may have 10 or more spot-checks from which information on bed material may be extracted. Each spot check identifies the dominant bed material size according to 12 possible categories (RHS, 2003: AR = artificial; BE = bedrock; BO = boulder; CO = cobble; GP = gravel-pebble (sometimes G = gravel; P = pebble are distinguished); SA = sand; SI = silt; CL = clay; PE = peat; NV = not visible). Of these classes, BO, CO, G, GP, P, SA, SI and CL relate to the calibre of the bed material. Therefore, following Boitsidis and Gurnell (2004),

observations falling into these classes were combined to give an estimate of the D_{50} in phi units:

$$D_{50} (\text{phi}) = \frac{(-8*BO)+(-7*CO)+(-4*P)+(-3.5*GP)+(-2*G)+(1.5*SA)+(6*SI)+(9*CL)}{(BO+CO+P+GP+G+SA+SI+CL)}$$

Where BO, CO, etc. refer to the number of spot checks falling into each sediment calibre class.

Table 4.8 58 river reaches for which at least one RHS survey was available (RHS Ids are provided for all surveys that were analysed)

River name	Reach no.	River Habitat Survey ID									
Annan	1	15565	15564	15566	15567						
Annan	2	15568	15569	15570	15571						
Annan	3	15572	15573	15574	13812	30564	13813				
Bollin	1	16577	6409								
Bollin	2	16578									
Bollin	3	16579									
Caersws	1	16742	721								
Caersws	2	16795									
Caersws	3	6682									
Caersws	4	682									
Coquet	1	13968									
Coquet	2	13968									
Coquet	3	13968									
Dane	1	441									
Dane	2	9011									
Dane	3	3440									
Endrick Water	1	30542	30542	31459							
Endrick Water	2	31459	30542								
Endrick Water	3	30542	30542								
Feshie	1	2355									
Feshie	2	2355									
Feshie	3	2355									
Findhorn	1	15609	15610	9053	9054						
Findhorn	2	15622	15623	15624	15625						
Findhorn	3	9071	15632	9070	15633						
Frome	1	25246	25247	25248	25249	25250	25251	25252	25253		
Frome	2	25254	25255	25256	1473	25258	25259	25260	25261	25262	25263
Frome	3	25265	10694	25267	25268						
Irthing	1	6046									
Irthing	2	3049	33361								
Irthing	3	48									
Kinnel Water	1	13820									
Kinnel Water	2	13820									
Kinnel Water	3	13818	13819	13817	13815						

Table 4.8 (ctd.)

River name	Reach no.	River Habitat Survey ID									
Lune	1	9013	21108	21024							
Lune	2	9013	21108	21024							
Lune	3	9013	21108	21024							
Meig	1	N/A									
Meig	2	N/A									
Meig	3	N/A									
Nairn	1	2262									
Nairn	2	21410	21408								
Nairn	3	21403	21402	21404	21405	21406					
South Tyne	1	34357									
South Tyne	2	34357									
South Tyne	3	34429	6062								
Spey	1	23399	23398	2238	23397	23396	23395	23394	23393	23392	23390
Spey	2	23379	23378	23377	23376	23375	23374				
Spey	3	23373	9098	9097	2159						
Towy	1	24153									
Towy	2	973	15523	21289	15522	15521					
Towy	3	15534	20661	15533	20695	20696	15531	6972	15530	15529	
Tweed	1	10250									
Tweed	2	10250	30800								
Tweed	3	30804	10253	30806	10254	30807					
Twrch	1	882	20677								
Twrch	2	20705	6882	20716							
Twrch	3	21307	35036	20701	35037	20713					

A second analysis was undertaken to include exposed bedrock (BE) by allocating a very large sediment size to this category (-10 phi). Although this does not strictly represent mobile bed material, it allows exposed bedrock reaches to be integrated in the analysis through application of the following formula:

$$D_{50B}(\text{phi}) = \frac{(-10*BE)+(-8*BO)+(-7*CO)+(-4*P)+(-3.5*GP)+(2*G)+(1.5*SA)+(6*SI)+(9*CL)}{(BE+BO+CO+P+GP+G+SA+SI+CL)}$$

Table 4.9 presents the number of spot checks falling into each of the calibre classes included in the estimation of D₅₀ (phi) and D_{50B} (phi) for each reach, the estimated D₅₀ and D_{50B} values (in phi and mm).

Table 4.9 Spot-check observations of channel substrate calibre, with associated sample sizes and estimates of D₅₀ (in phi and mm units) for 58 reaches of British rivers (substrate calibre classes: BE = bedrock; BO = boulder; CO = cobble; P = pebble; GP = gravel-pebble; G = gravel; SA = sand; SI = silt; CL = clay)

River name	Reach no.	Class	BE	BO	CO	P	GP	G	SA	SI	CL	Total spot checks	Analysed spot checks (excl. BE)	D ₅₀ (phi)	D ₅₀ (mm)	D _{50B} (phi)	D _{50B} (mm)
Annan	1	4	0	0	24	7	0	1	0	0	0	40	32	-6.19	72.88	-6.19	72.88
Annan	2	4	0	4	16	14	2	1	0	0	0	40	37	-5.65	50.17	-5.65	50.17
Annan	3	4	0	0	12	23	3	1	1	0	0	40	40	-4.68	25.55	-4.68	25.55
Bollin	1	5	0	0	4	2	7	1	1	2	0	20	17	-2.88	7.37	-2.88	7.37
Bollin	2	5	0	0	0	2	1	1	0	0	0	10	4	-3.38	10.37	-3.38	10.37
Bollin	3	5	0	0	0	1	2	3	1	0	0	10	7	-2.21	4.64	-2.21	4.64
Caersws	1	3	0	0	3	0	10	0	0	1	0	20	14	-3.57	11.89	-3.57	11.89
Caersws	2	3	0	0	2	4	3	1	0	0	0	10	10	-4.25	19.03	-4.25	19.03
Caersws	3	5	0	0	0	0	10	0	0	0	0	10	10	-3.50	11.31	-3.50	11.31
Caersws	4	4	0	0	0	0	8	0	0	0	0	10	8	-3.50	11.31	-3.50	11.31
Coquet	1	5	0	0	1	0	9	0	0	0	0	10	10	-3.85	14.42	-3.85	14.42
Coquet	2	5	0	0	1	0	9	0	0	0	0	10	10	-3.85	14.42	-3.85	14.42
Coquet	3	3	0	0	1	0	9	0	0	0	0	10	10	-3.85	14.42	-3.85	14.42
Dane	1	6	2	0	0	0	3	0	0	3	0	10	6	1.25	0.42	-1.56	2.95
Dane	2	5	0	0	0	0	10	0	0	0	0	10	10	-3.50	11.31	-3.50	11.31
Dane	3	6	0	0	0	0	1	0	5	1	0	10	7	1.43	0.37	1.43	0.37
Endrick Water	1	6	3	2	5	2	0	6	0	10	0	30	25	-0.44	1.36	-1.46	2.76
Endrick Water	2	4	3	2	5	1	0	3	0	5	0	20	16	-1.94	3.83	-3.21	9.26
Endrick Water	3	5	0	0	0	2	0	6	0	10	0	20	18	2.22	0.21	2.22	0.21

Table 4.9 (ctd.)

River name	Reach no.	Class	BE	BO	CO	P	GP	G	SA	SI	CL	Total spot checks	Analysed spot checks (excl. BE)	D ₅₀ (phi)	D ₅₀ (mm)	D _{50B} (phi)	D _{50B} (mm)
Feshie	1	3	2	3	2	0	3	0	0	0	0	10	8	-6.06	66.83	-6.85	115.36
Feshie	2	3	2	3	2	0	3	0	0	0	0	10	8	-6.06	66.83	-6.85	115.36
Feshie	3	3	2	3	2	0	3	0	0	0	0	10	8	-6.06	66.83	-6.85	115.36
Findhorn	1	4	0	4	34	0	1	0	0	0	0	40	39	-7.01	129.14	-7.01	129.14
Findhorn	2	4	0	1	28	4	0	0	0	0	0	40	33	-6.67	101.59	-6.67	101.59
Findhorn	3	4	13	3	10	0	0	0	0	0	0	40	13	-7.23	150.20	-8.62	392.18
Frome	1	5	0	0	0	0	9	19	2	0	0	40	30	-2.22	4.65	-2.22	4.65
Frome	2	5	0	0	0	1	20	0	0	0	0	40	21	-3.52	11.50	-3.52	11.50
Frome	3	5	0	0	0	0	19	3	0	0	0	40	22	-3.30	9.82	-3.30	9.82
Irthing	1	4	0	0	0	0	0	0	0	10	0	10	10	6.00	0.02	6.00	0.02
Irthing	2	3	0	1	8	3	3	1	1	0	0	20	17	-5.12	34.72	-5.12	34.72
Irthing	3	3	0	0	8	0	0	0	0	0	0	10	8	-7.00	128.00	-7.00	128.00
Kinnel Water	1	4	0	0	0	0	0	0	10	0	0	10	10	1.50	0.35	1.50	0.35
Kinnel Water	2	3	0	0	0	0	0	0	10	0	0	10	10	1.50	0.35	1.50	0.35
Kinnel Water	3	5	0	0	9	0	2	0	20	0	0	40	31	-1.29	2.45	-1.29	2.45
Lune	1	4	0	0	10	0	20	0	0	0	0	30	30	-4.67	25.40	-4.67	25.40
Lune	2	5	0	0	10	0	20	0	0	0	0	30	30	-4.67	25.40	-4.67	25.40
Lune	3	5	0	0	10	0	20	0	0	0	0	30	30	-4.67	25.40	-4.67	25.40
Nairn	1	5	0	0	0	0	6	0	4	0	0	10	10	-1.50	2.83	-1.50	2.83
Nairn	2	5	1	1	0	0	0	6	3	0	0	20	10	-1.55	2.93	-2.32	4.99
Nairn	3	5	1	6	1	0	0	3	27	0	0	50	37	-0.55	1.47	-0.80	1.74

Table 4.9 (ctd.)

River name	Reach no.	Class	BE	BO	CO	P	GP	G	SA	SI	CL	Total spot checks	Analysed spot checks (excl. BE)	D ₅₀ (phi)	D ₅₀ (mm)	D _{50B} (phi)	D _{50B} (mm)
South Tyne	1	4	0	1	8	0	0	0	0	0	0	10	9	-7.11	138.25	-7.11	138.25
South Tyne	2	4	0	1	8	0	0	0	0	0	0	10	9	-7.11	138.25	-7.11	138.25
South Tyne	3	4	0	1	19	0	0	0	0	0	0	20	20	-7.05	132.51	-7.05	132.51
Spey	1	4	3	29	44	0	0	0	2	2	0	100	77	-6.82	112.84	-6.94	122.57
Spey	2	4	0	12	29	1	0	0	4	0	0	60	46	-6.46	87.82	-6.46	87.82
Spey	3	1	0	0	30	6	0	0	0	0	0	40	36	-6.50	90.51	-6.50	90.51
Towy	1	5	1	0	0	0	4	0	0	0	0	10	4	-3.50	11.31	-4.80	27.86
Towy	2	5	0	0	3	10	13	3	0	1	0	40	30	-3.55	11.71	-3.55	11.71
Towy	3	5	0	0	0	2	13	0	0	3	4	40	22	0.02	0.98	0.02	0.98
Tweed	1	5	0	0	3	0	7	0	0	0	0	10	10	-4.55	23.43	-4.55	23.43
Tweed	2	4	0	0	7	0	8	0	0	0	0	20	15	-5.13	35.10	-5.13	35.10
Tweed	3	4	0	1	22	0	6	1	0	0	0	50	30	-6.17	71.84	-6.17	71.84
Twrch	1	4	0	3	16	0	1	0	0	0	0	20	20	-6.98	125.80	-6.98	125.80
Twrch	2	3	0	0	15	4	11	0	0	0	0	30	30	-5.32	39.85	-5.32	39.85
Twrch	3	4	10	2	23	8	3	0	0	0	0	50	36	-6.10	68.46	-6.95	123.27

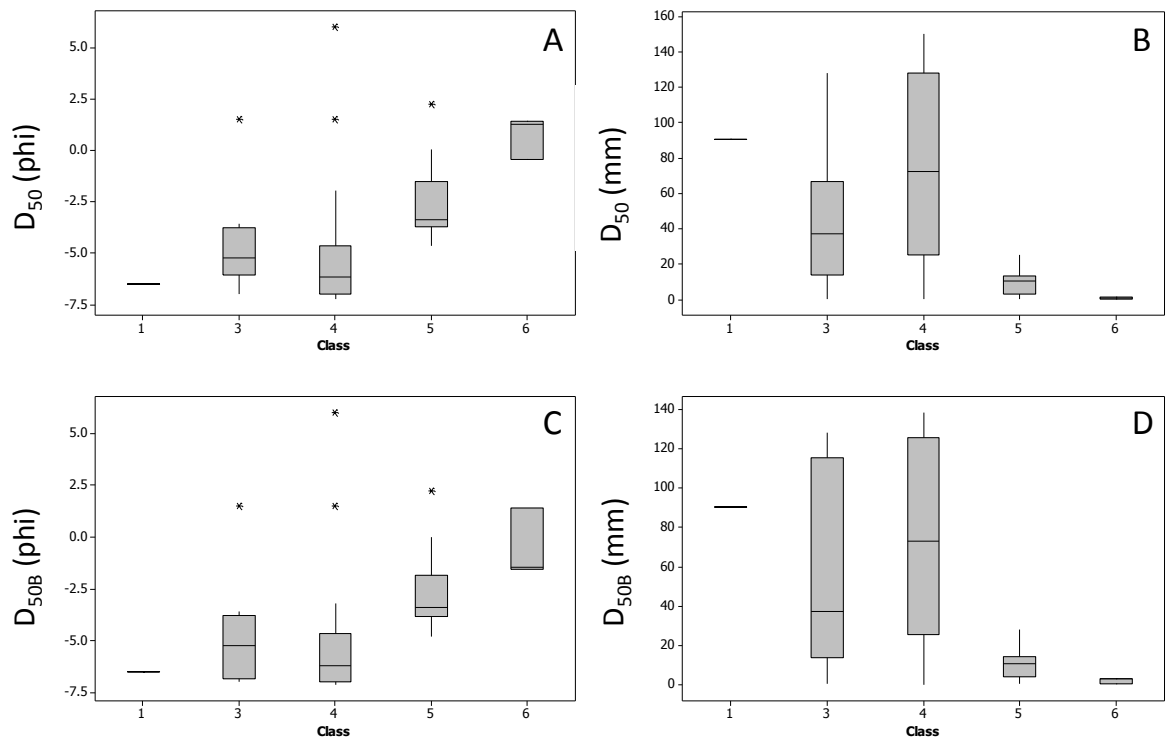


Figure 4.16 Boxplots illustrating bed sediment calibre estimates for British rivers in five of the six river classes. Upper graphs show D_{50} ; lower graphs D_{50B} (includes bedrock data and excludes Findhorn reach 3); left graphs are in phi units; right graphs are in mm.

Figure 4.16 Boxplots illustrating bed sediment calibre estimates for British rivers in five of the six river classes. Upper graphs show D_{50} ; lower graphs D_{50B} (includes bedrock data and excludes Findhorn reach 3); left graphs are in phi units; right graphs are in mm. Figure 4.16 illustrates the distribution of estimated bed material calibre across 5 of the six river classes (1, 3 to 6), which has been derived from RHS data for British rivers according to the above formulae for D_{50} and D_{50B} . Only one reach was drawn from class 1. Findhorn reach 3 is excluded from the lower graphs that incorporate bed rock exposure because of its extremely high calibre estimate, reflecting 50% of spot checks recorded as BE. This reach, which was allocated to class 4, is included in the upper graphs. Inclusion of bedrock as very coarse sediment (lower two graphs) strengthens a pattern of decreasing bed material calibre from class 3 to class 6 that is evident in the upper two graphs. However, Findhorn reach 3 is included in the upper graphs and shows the largest D_{50} values even when the bedrock weighting is excluded (-7.23 phi, 150 mm). This explains the deviation of class 4 from the sediment fining gradient across the five classes. In conclusion, the indicators of bed material calibre estimated from RHS spot check data all show an expected gradient of sediment fining

across the five classes represented by this British data set, and show provide further proof of the robustness of the classification.

4.7 Summary

This chapter has investigated several aspects of the river classification developed in chapter 3 with the following conclusions.

The geographical distribution of rivers in each of the classes, was found to show evidence of both elevation and latitude influencing the river types present in different regions of Europe (section 4.1).

Since the classification was based on a cluster analysis of principal component scores derived from several different thematic PCAs, section 4.2 investigated the degree to which the classification showed discrimination among the original variables that were derived from Google Earth images. The six river classes were found to reflect gradients in river dimensions (channel width, slope, sinuosity), and dimension ratios (particularly baseflow channel width : bankfull channel width). They were also well discriminated by channel bed, marginal bar and bench, transitional and floodplain geomorphological features. However, vegetation showed weak discrimination among the six classes, although wood accumulations were more associated with class 2 and emergent macrophytes were more associated with classes 5 and 6 than the other classes. It is unclear whether vegetation management is the cause of this relatively weak discrimination and also whether well-developed riparian vegetation may have induced under-representation of some marginal and floodplain features.

The potential for a more complex classification was explored by considering whether there were any statistically significant differences in the characteristics of the first split subgroups of each of the six classes according to the cluster dendrogram (section 4.3). In general, the analyses showed that although distinctive sub-groups were present, they mainly represented transitional classes, which could be informative if a more complex classification was needed. The only class that appeared to show very marked internal contrasts that could lead to additional classes of similar significance to the original classes was class 1. This class was represented by only a small sample of relatively large (wide) rivers, and a larger sample of such rivers is needed before such a subdivision could be made reliably.

Having explored the six river classes using only the data set derived from Google Earth (sections 4.1 to 4.3), additional data sets were used to further test the validity of the classification. The elevation data extracted from Google Earth, although of coarser resolution, was found to be very similar to data extracted from airborne Lidar (section 4.4). Nevertheless, further tests are needed for higher altitude, confined sites, which were not represented by the available Lidar data.

Analysis of a second image from a different year and/or season for 12 reaches showed some changes in the assessed reach characteristics, with the largest changes for class 1 reaches (section 4.5). However, all of the reaches remained within the appropriate area of the PC1-PC2 plot for the integrated PCA (Figure 4.12), suggesting that their class membership had not changed.

Finally, discharge and bed material calibre data sets were introduced to test whether the six classes reflected expected variations in stream power and average bed sediment size (section 4.6). Distinct changes in stream power were observed between classes, with class 2 showing the highest values, classes 5 and 6 showing the lowest values and classes 1, 3 and 4 showing intermediate values. Given the geomorphological characteristics of each of the classes, these differences in stream power are as expected. Bed sediment data was more difficult to obtain but two indices of bed sediment calibre were estimated from RHS spot check observations for 19 British river sites and 58 reaches. No data was available for class 2 and only one reach was drawn from class 1. Nevertheless, a clear gradient of sediment fining was revealed in all of the indicators from class 1 through to class 6 and particularly across classes 3 to 6, further confirming the robustness of the classification.

Overall, the analyses presented in this chapter have shown the classification to be remarkably robust as well as making geomorphological sense. This illustrates that Google Earth is a useful tool for the analysis of river dimensions and geomorphological features, although it is essential that clear rules are developed, such as those presented in chapter 3, prior to extracting information. It also appears that further analysis of a larger data set could be very profitable to ensure that large rivers are represented in greater detail and that subclasses of the other 5 classes can be recognised and their geomorphological characteristics accurately described.

Throughout this chapter, integrated PC scores were used to explore the allocation of new river reaches to river classes. While this is an effective method for exploring the

likely classification of new reaches, further research is needed to develop a robust way of directly allocating new reaches to a river class. Such research is not trivial, requiring several months of further analysis to identify robust class boundaries, most probably through a maximum likelihood analysis of both PC scores and a selection of the most informative original variables to develop something equivalent to a decision tree. Therefore, owing to time constraints, it was not possible to develop such an allocation methodology within the present research programme. However, this issue is discussed in chapter 6 as an important area for future research.

One group of geomorphological features that have contributed strongly to class differentiation are the different bar types. Bar theory has featured widely in the literature as a means of classifying different river types. Therefore, chapter 5 builds on the classification by exploring the degree to which the six river classes can be related to theory in relation to their bar features.

Section 4.8 follows as an addendum to this chapter. It represents an analysis undertaken in collaboration with the SMART Associate Partner to this research project, the UK Environment Agency, and it applies the river classification methodology to restored and apparently naturally-functioning (control) reaches on four English rivers to assess whether the restoration has resulted in an appropriate channel classification being achieved.

4.8 Application of the Classification to Restored River reaches in England

This section investigates the degree to which restoration of a sample of river reaches within England conforms to the channel class occupied by nearby and apparently naturally-functioning reaches.

The River Restoration Centre website (www.therrc.co.uk) was consulted to identify a sample of river reaches in England where morphological restoration had been attempted and where nearby, apparently naturally-functioning reaches were present, that conformed to the definitions for reach selection provided in Chapter 3). Four suitable restored reaches were selected (Table 4.10) where re-meandering or reconnection to old channel sections had been implemented. To be selected, every restored reach was required to have three replicate ‘control’ reaches located on the same river either upstream and downstream the from restored reach.

Table 4.10 Summary information on the four restored reaches selected for analysis
(source: www.therrc.co.uk)

Reach No	Project Name	River	Year completed	Reach length (m)	Morphological-oriented aspirations	Google Image date
1	Western Rother at Shopham Loop River	Arun	2004	850	Reconnect an old bend	06/06/13
2	River Skerne Restoration Project	Tees	1997	500	Re-meander a straightened river	05/02/08
3	River Cole Restoration Project – Colehill	Thames	1996	500	Create a new meandering channel	30/05/09
4	Little Ouse at Thetford	Great Ouse	1994	900	Reconnect an old meander	01/01/05

Table 4.11 Summary of information extracted from Google Earth images for the 4 restored and 12 control reaches.

Descriptions					Dimensions							Dimension ratio			Bed flow features					
Project Name	Restored/Natural	Restoration completed in/ (U) pstream and (D)ownstream restored site	Google Earth Image taken	Country	Baseflow Median Width (m)	Baseflow Sinuosity	Baseflow Channel Slope (per mil)	Bankfull Median Width (m)	Bankfull Sinuosity	Bankfull Channel Slope (per mil)	Valley Gradient (per mil)	Baseflow_Bankfull Median Width	Baseflow_Bankfull Sinuosity	Baseflow_Bankfull Channel Slope	Pools	Riffles	Cascade	Waterfall & Steps	Boulders	Exposed Bedrock
Western Rother	Restored	2004	06/06/2013	England	8.41	1.29	1.14	11.05	1.29	1.14	1.47	0.76	1.00	1.00	0	0.01	0	0	0	0
	Control	U	01/01/2005	England	12.96	1.10	1.33	17.84	1.10	1.33	1.46	0.73	1.00	1.00	0	0	0	0	0	0
	Control	U	02/01/2005	England	12.24	1.24	0.97	12.58	1.24	0.97	1.20	0.97	1.00	1.00	0	0	0	0	0	0
	Control	D	03/01/2005	England	11.56	1.13	0.69	14.92	1.13	0.69	0.78	0.78	1.00	1.00	0	0	0	0	0	0
Skerne	Restored	1997	05/02/2008	England	10.53	1.23	1.79	10.53	1.23	1.79	2.21	1	1	1	0	0	0	0	0	0
	Control	U	05/02/2008	England	8	1.13	1.73	8.00	1.13	1.73	1.96	1	1.00	1.00	0	0	0	0	0	0
	Control	U	05/02/2008	England	9.145	1.13	1.90	9.15	1.13	1.90	2.15	1	1	1	0	0	0	0	0	0
	Control	D	05/02/2008	England	11.06	1.23	0.97	11.06	1.23	0.97	1.19	1	1.00	1.00	0.01	0	0	0	0	0
Cole	Restored	1996	30/05/2009	England	5.56	1.18	1.81	5.56	1.18	1.81	2.14	1	1	1	0	0.01	0	0	0	0
	Control	U	31/05/2009	England	8.66	1.19	1.26	8.66	1.19	1.26	1.50	1	1	1	0	0.01	0	0	0	0
	Control	D	01/06/2009	England	5.07	1.24	0.84	5.07	1.24	0.84	1.04	1	1	1	0	0	0	0	0	0
	Control	D	02/06/2009	England	5.77	1.55	1.18	5.77	1.55	1.18	1.83	1	1	1	0	0	0	0	0	0
Little Ouse	Restored	1994	01/01/2005	England	7.09	1.20	1.27	7.09	1.20	1.27	1.52	1	1	1	0	0	0	0	0	0
	Control	U	02/01/2005	England	5.045	1.10	0.53	5.05	1.10	0.53	0.59	1	1	1	0	0	0	0	0	0
	Control	U	03/01/2005	England	9.85	1.14	0.87	9.85	1.14	0.87	0.99	1	1	1	0	0	0	0	0	0
	Control	D	04/01/2005	England	12.63	1.05	0.68	12.63	1.05	0.68	0.72	1	1	1	0	0	0	0	0	0

Table 4.11 (ctd.)

Descriptions					Vegetation				Floodplain Feature								Bars and Benches						
Project Name	Restored/Natural	Restoration completed in/ (U) pstream and (D)ownstream restored site	Google Earth Image taken	Country	Vegetation Structure	Weighted Tree Distribution	Total Wood Jams	Emergent Macrophytes	Total Swamp-Wetland	Total Water-filled ponds	Total connected side channels	Total Dry depressions	Total Ridges & Swales	Total Oxbow	Total Stabilising arcuate bars	Total Stabilising Marginal bars (non-arcuate shape)	Total Active Marginal Bars	Total Stabilising Marginal Bars	Total Active Mid-Channel Bars	Total Stabilising mid-channel bar	Total Active Bench	Total Stabilising Bench	
Western Rother	Restored	2004	06/06/2013	England	1.17	1	0	0	0	0.025	0	0.013	0	0	0	0	0	0	0	0	0	0	
	Control	U	01/01/2005	England	2.21	2.93	0	0	0.006	0	0	0.006	0	0	0	0	0	0	0	0	0	0	
	Control	U	02/01/2005	England	2.06	2.94	0	0	0.004	0	0	0.004	0.008	0	0	0	0	0	0	0	0	0	0
	Control	D	03/01/2005	England	1.63	1.87	0	0	0	0	0	0.016	0	0	0	0	0	0	0	0	0	0	0
Skerne	Restored	1997	05/02/2008	England	2.17	2.83	0	0	0	0	0	0	0	0	0	0	0	0	0	0	0	0	
	Control	U	05/02/2008	England	1.75	1.25	0	2.14	0	0	0	0	0	0	0	0	0	0	0	0	0	0	0
	Control	U	05/02/2008	England	2.13	2.31	0	2.03	0	0	0	0.003	0	0	0	0	0	0	0	0	0	0	0
	Control	D	05/02/2008	England	2.77	2.57	0	6.07	0	0	0	0	0	0	0	0	0	0	0	0	0	0	0
Cole	Restored	1996	30/05/2009	England	1	0	0	0	0	0	0	0	0	0	0	0	0	0	0	0	0	0	
	Control	U	31/05/2009	England	2.5	3.25	0.007	2.03	0	0	0	0	0	0	0	0	0	0	0	0	0	0	0
	Control	D	01/06/2009	England	2	2.5	0	5.02	0	0	0	0	0	0	0	0	0	0	0	0	0	0	0
	Control	D	02/06/2009	England	2	2.5	0	3	0	0	0	0	0	0	0	0	0	0	0	0	0	0	0
Little Ouse	Restored	1994	01/01/2005	England	1.63	1.5	0	0.12	0	0	0	0	0	0	0	0	0	0	0	0	0	0	
	Control	U	02/01/2005	England	1.83	1.17	0	5.04	0	0	0	0.008	0	0	0	0	0	0	0	0	0	0	0
	Control	U	03/01/2005	England	1.92	1.83	0	5.04	0	0.004	0	0.004	0	0	0	0	0	0	0	0	0	0	0
	Control	D	04/01/2005	England	2.63	3.8	0	11.06	0	0	0	0	0	0	0	0	0	0	0	0	0	0	0

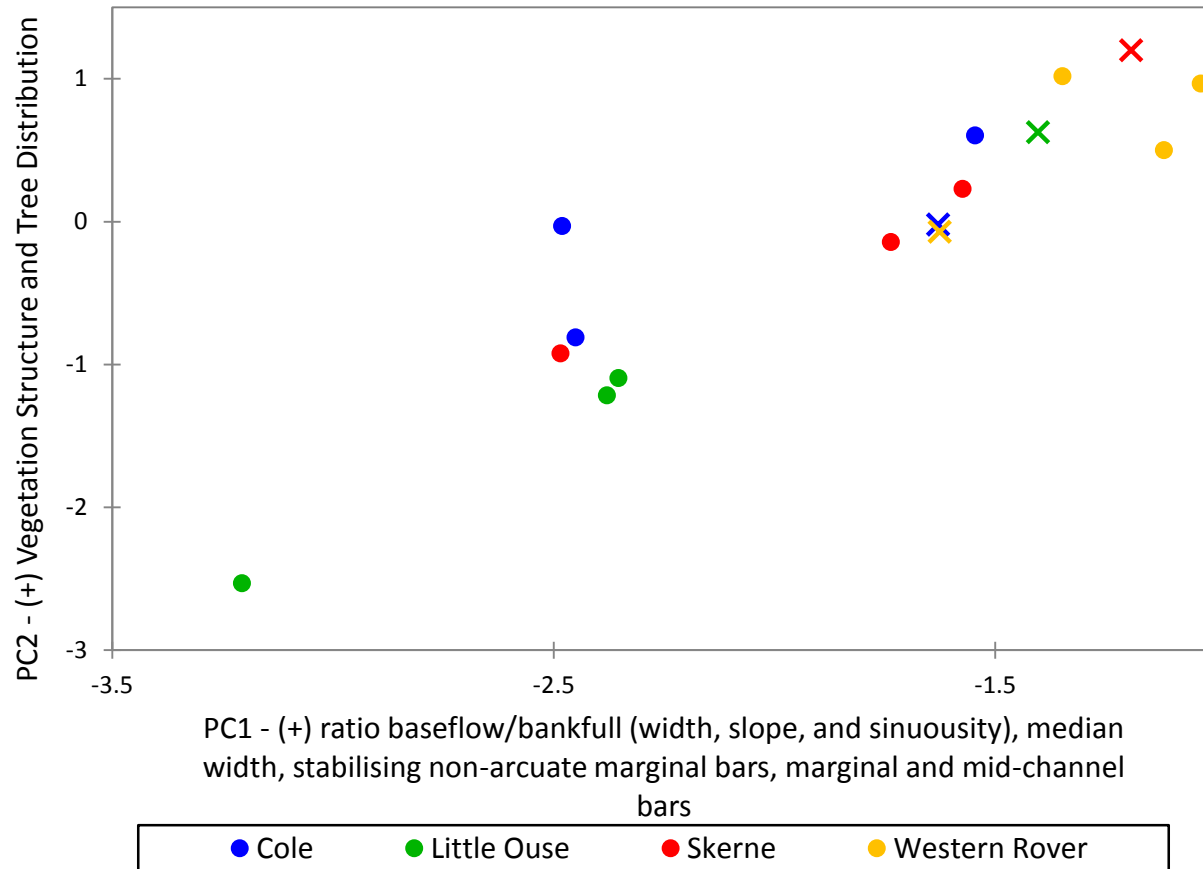


Figure 4.17 PC scores of restored (X symbols) and control (O symbol) reaches in relation to PC1 and PC2 of the integrated PCA (note that the lengths of the axes are much shorter than in the graph representing the original 221 reaches: PC1 was previously plotted in the range -6 to +6 and PC2 in the range -7 to + 3.5).

Information was extracted from the Google Earth images listed in Table 4.10 for the four restored and 12 control reaches. The extracted information (Table 4.11) was used to apply the method described in section 4.5 (see Figure 4.11) that evaluates scores for the 10 contributing PCs and the integrated PCA that was performed on the original 21 reach data set. In this way, the scores for all 16 reaches could be entered on the PC1 – PC2 integrated graph so that the plotting position of the restored reaches could be compared with nearby control reaches (Figure 4.16).

Despite the shorter numerical range in the axes plotted in Figure 4.17 in comparison with those used for the plot of the original 221 reach sample (PC1 was previously plotted in the range -6 to +6 and PC2 in the range -7 to + 3.5), there are large differences in some of the plotting positions:

The Western Rother scheme seems to be most successful restoration project of the four that were evaluated, with the plotting position of the restored and all of the control/near-natural functioning reaches located in close proximity. In this case the reconnection of an old bend has created a channel with similar properties to nearby control reaches. However, a similar restoration on the Little Ouse has been less successful, and in all three remaining restorations, some if not all of the control reaches plot in a very different location to the restored reach on Figure 4.17.

Only one of the control reaches on the Skerne plots in a different location from the control reach, suggesting that this restoration conforms to the character of some nearby reaches. The restored section of the Cole plots near to one nearby control reach but all of the control reaches for the Little Ouse plot in totally different locations from the restored reach.

Overall, three of the restored reaches show similar properties to at least one of the control reaches, suggesting that they incorporate similar characteristics. However, these results must be interpreted with caution for three reasons:

- (i) The control reaches may not be truly naturally-functioning reaches.
- (ii) The restored reaches may not have fully recovered from restoration activities
- (iii) All of the restored reaches were less than 1 km in length and so were strictly too short for reliable information extraction from Google Earth. The vertical resolution of the elevation data was too poor for reliable slope

estimates to be extracted and yet slope has a heavy influence on the estimated scores on integrated PC1. Furthermore, restoring a reach by creating a diversion or new meandering side-channel, as in the case of the River Cole, could lead to reaches of different width, which further degrade the channel geometrical accuracies that influence the PC1 score.

CHAPTER 5

EMBEDDING THEORETICAL MORPHODYNAMICS 'BAR THEORY' INTO THE CLASSIFICATION OF SINGLE-THREAD RIVERS

5.1 Introduction

Bars are common in-channel depositional features that play an important role in river morphodynamics. Bars serve as short- or long-term sediment stores within river channels, and so have a notable impact on channel morphology. Any management interventions that affect the size or frequency of bars in a river channel, such as sediment dredging, inevitably affect the flux of sediment through the river channel with consequences for bar and channel morphology and stability. In addition, vegetation that establishes on bars also influences in-channel sediment retention, bar accretion and sediment flux, with continuous feedback effects on channel ecology and morphology. In these ways, unvegetated and vegetated bars form crucial elements of the river channel and its dynamics, and so understanding of their natural location, morphology and mobility provides an important contribution to river condition assessment, where bars can be used as indicators of contemporary processes and historical alterations (Hooke and Yorke, 2011).

The presence of bars in single-thread reaches, and the way in which they establish within straight to meandering channels has attracted a great deal of research attention. Research interest reflects the fact that as major in-channel sediment stores, bars 'manage' the river system. Their dynamics is a key process within 2D (planform) morphological change (Tubino et al., 1999, Zolezzi et al., 2012a), 'fundamentally define(ing) the style and morphology of unconfined alluvial rivers' (Church and Rice, 2009). In addition, bars have importance for a number of specific issues of management application. Bars are closely linked to bank erosion, and they have important implications for navigation, flood risk, and the maintenance of built structures.

To date, research on bars has followed complementary approaches, with mechanistic-based theoretical models and laboratory experiments probably contributing the largest share of scientific contributions.

Bar theories have been used as physically-based predictors of alluvial channel pattern (Parker, 1976). Alternating and central bars have been shown to characterise meandering, wandering and braided streams (e.g. Zolezzi, et al., 2012a), often exhibiting striking regularity in their morphological pattern. Such marked regularity of their forms have led many researchers since the 1960s to view the development of bars and meandering as possibly due to instabilities inherent in the physical system composed by an incompressible fluid flow over an erodible bed made of sediments that can be selectively eroded, transported and deposited. On this line of thinking, linear and nonlinear instability theories based on the basic principles of fluvial hydraulics and sediment transport relations have been proposed. Most of these theories refer to rather idealized river configurations, like that of an indefinitely long straight channel with fixed banks and erodible bed, and of simplifying assumptions, like those of constant discharge, channel width and homogeneous sediment size. Besides computational constraints typical of the time when most of the theories have been developed, this tendency to simplification is motivated by the fundamental aim of these ‘bar’ theories to capture the main physical processes beneath such surprising regularity of forms that is sometimes detected even in relatively natural, complex river systems.

Several families of ‘bar’ and ‘bend’ theories have been developed, e.g Callander (1969), Ikeda et al. (1981), Blondeaux and Seminara (1985), Colombini et al. (1987), through different analyses of the 2-D Saint-Venant – Exner mathematical system. ‘Bar’ theories investigate altimetric instabilities of the channel bed mathematically in order to predict the conditions under which bars should form, as well as their main geometrical and kinematic properties, such as amplitude, length, and migration speed. In contrast, ‘bend’ theories investigate instabilities of the idealized, straight channel planform to predict the geometric and kinematic properties of meander bends. Both bar and bend theories can be linear (Blondeaux and Seminara, 1985) or non-linear (Colombini et al., 1987, Seminara and Tubino, 1992). Outcomes from linear theories can now be considered quite established and have received robust validation especially from flume experiments. The ‘theory of free bars’, like that of Colombini et al (1987), has shown how the development and growth of alternate bars in straight alluvial channels relates irrefutably to an in-built (‘free’) instability of the erodible bed triggered by its interaction with turbulent flow, which subsequently leads to the development of riverbed perturbations that scale with the average channel width and migrate downstream. Free alternate bar stability has long been associated with bend stability but

the work of Blondeaux and Seminara (1985) has illustrated that bend instability is actually related to a planform instability mechanism rather than a bedform instability mechanism, which is analogous to the mechanism governing the formation of free alternate bars. Bars developing in curved channels or, more generally, in channels with either spatial variations of channel curvature (Blondeaux and Seminara, 1985), channel width (Repetto et al., 2002) or of both (Zolezzi et al., 2012a) are often referred to as ‘forced’ bars, in contrast with the ‘free’ ones that develop in straight, equiwidth channels. The two types of bars have been shown to interact in natural streams (Tubino and Seminara, 1990, Repetto and Tubino, 1999), eventually producing more complex topographic patterns and morpho-dynamics that more closely correspond to observations.

The above experimental and theoretical findings indicate that a key control parameter on free bar morphodynamics is the channel width-to-depth ratio at ‘bar-forming’ conditions, β , for which two fundamental threshold values can be theoretically derived that correspond to distinct modes of functioning of the system or ‘morphodynamic regimes’ (Blondeaux and Seminara, 1985, Struiksmas and Crosato, 1989, Johannesson and Parker, 1989). These thresholds are: (a) the free bar-formative threshold, $\beta_{critical}$, below which free bars cannot develop, and (b) the resonant threshold, $\beta_{resonant}$, which theoretically separates two well distinct regimes of morphodynamic behaviour, whereby 2D morphodynamic ‘information’ can only propagate upstream if $\beta > \beta_{resonant}$ (Zolezzi and Seminara, 2001). Both thresholds mainly depend on the Shields stress θ , a dimensionless sediment mobility parameter, and on the ratio between the average bed roughness and flow depth, d_s ‘ (Blondeaux and Seminara, 1985).

Figure 5.1 illustrates these concepts in more detail in relation to the key outcomes of the free bar theory in the $(\beta-\lambda)$ parameter space, where λ is the wavenumber of the free bars, i.e. related to the reciprocal of the bar wavelength ($\lambda = \pi W / L$, with W average channel width). The two curves correspond to neutral stability (no growth/decay in time) and neutral migration of the free bars. The neutral curve for bar stability always displays a minimum aspect ratio value ($\beta_{critical}$) below which the flat bed configuration is invariably stable regardless of bar wavelength. Moreover, the intersection between the two neutral curves defines the second threshold $\beta_{resonant}$ below which all unstable bar wavelengths invariably migrate downstream, i.e. no upstream propagation of information (in the form of small amplitude 2D river bed waves) can theoretically occur (Zolezzi and Seminara, 2001). Qualitatively, the aspect ratio β can

be viewed as the ‘2D analogue’ of the Froude number (Fr) in 1D flows, and the threshold $\beta_{resonant}$ the analogue of the unit Froude value, which separates subcritical ($Fr < 1$) from supercritical ($Fr > 1$), with subcritical conditions being the only ones allowing 1D hydrodynamic information to propagate upstream. Wider and shallower channels, i.e. with bar-forming aspect ratio β above the resonance barrier, $\beta_{resonant}$, can be characterized by upstream morphodynamic influence. This finding complements the original experiment of Struiksma et al. (1985), where they recognized a downstream influence on two straight channels connected by a bend. Zolezzi et al (2005) subsequently repeated similar experiments and experimentally confirmed the idea of two directionalities of influence (morphodynamic regimes): an upstream influence, occurring when β falls above the threshold value of $\beta_{resonant}$, which is more likely to occur on ‘wide’ and ‘shallow’ channels; and a downstream influence when β falls below $\beta_{resonant}$, which is more likely to occur on channels that are ‘narrow’ and ‘deep’.

Overall, the two threshold values $\beta_{resonant}$ and $\beta_{critical}$ define three different regions in the aspect ratio parameter space within which three well-defined and distinct morphodynamic regimes are theoretically predicted, thus forming a possible, theoretically-based, classification scheme for single-thread river reaches. The three regions have been renamed as in Figure 5.1 with the aim of providing a more intuitive matching between their names and their theoretical implications. The ‘sub-critical’ region ($\beta < \beta_{critical}$) can be viewed as a ‘morphologically stable’ region, because free bars are not expected to form. The ‘super-critical and sub-resonant’ region ($\beta_{critical} < \beta < \beta_{resonant}$) can be viewed as a ‘morphologically unstable’ region, because free bars tend to grow. The ‘super-resonant’ region can be considered ‘morphologically complex’ because it is the only region where 2D morphodynamic information can theoretically propagate both upstream and downstream, in addition to free bars being unstable (Zolezzi et al., 2009). The above concepts are developed and illustrated in more detail in section 5.2.

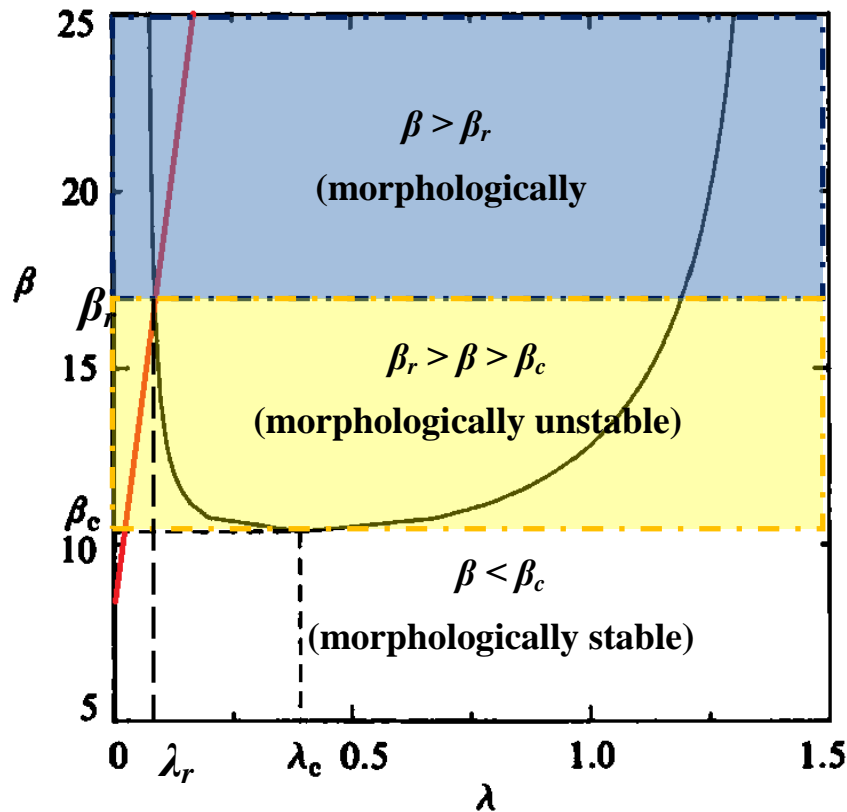


Figure 5.1 Theoretical regimes according the positioning of β , width-to-depth ratio to the threshold of β_c , aspect ratio critical and β_r , aspect ratio resonant

Whilst many studies have been undertaken theoretically, experimentally, and numerically, only a few field studies have been conducted to verify this ‘free bar theory’. Furthermore, much of this work is process-based and focussed on the establishment of sedimentary structures (Bluck, 1971). Lewin (1978) followed the initial development of bars on actual straight to meandering river planforms. Subsequently, Welford (1994) positively tested Tubino’s (1991) alternate bar theory under unsteady flow conditions in a straightened channel, concluding that the general principles could be applied. Hooke and Yorke (2011) tested ‘bar’ theory to some extent, under the condition that these ‘free’ bars are unattached (midchannel) bars. In the River Dane, on which their analysis centred, they dismissed the presence of alternate bars and any sign of mobile bars, but concluded that all bars are ‘fixed’ and appeared ‘forced’ and so more closely fitted ‘bend’ theory, which is consistent with the meandering planform of the River Dane. Crosato and Mosselman (2009) developed an analogous physics-based channel pattern predictor to the one originally proposed by Parker (1976) and Fredsoe (1978), though based on the theories of fixed ‘forced’ bars rather than of migrating ‘free’ bars as in the case of Fredsoe’s and Parker’s previous work. The new predictor of Crosato and Mosselman (2009) yielded more consistent outcomes with

observed channel patterns of the natural streams they examined in comparison to the ‘free bars’ -based predictors. Overall, geomorphological observations on the temporal dynamics of bars are relatively infrequent because of constraints imposed by the space and time scales required for their proper observations. Only in recent years are these constraints becoming relaxed as a result of the development of new monitoring technologies (Rodrigues et al., 2012, Adami et al., 2014). On the other hand, Zolezzi et al. (2009) also attempted to explore the possible existence of both sub- and super-resonant morphodynamic regimes in real gravel-bed rivers, using field data from natural single-thread rivers. They suggested that the tendency of single-thread rivers to behave in a superresonant or subresonant fashion is dependent on autogenic and environmental factors, with super-resonant behaviour being more likely for steeper reaches with coarser bed sediment.

Though theoretical developments have further incorporated some of the complexities typical of natural channels, such as channel width variation (Repetto, et al. 2002, Zen et al., 2014), hydrograph characteristics (Tubino, 1991), and sediment sorting (Lanzoni and Tubino, 1999), existing differences between natural settings and theoretical assumptions could cause inconsistencies that could not be predicted by the theoretical bar models.

The analysis presented in this chapter aims to explore the possible correspondence between the theoretically derived, classification for real, single-thread river reaches and the geomorphic classification developed and tested in the previous chapters. This is achieved by assessing whether there are any associations between the classes of single thread rivers developed in Chapter 3, and the classification based on the bar theory rather than aiming to provide field evidence of the specific behaviour of the theoretical (bar-theory based) morphodynamic regime river classification. Mathematical and statistical methods used in this analysis are described in section 5.2, then results obtained concerning the relation between the theoretical classification and the one leading to the six river classes of Chapter 3 are presented in section 5.3. Additional sensitivity checking of variables that employ different flood event and sediment predictors are considered in section 5.4. The chapter ends with a brief discussion of the results (section 5.5).

5.2 Methods

The geometric, geomorphic and vegetation measurements extracted from Google Earth imagery have been fully described (chapter 3) and evaluated (chapter 4). Therefore, the methods described in this chapter focus upon evaluating the theoretical parameter, β and its threshold values for resonant, β_r , and free bar formation phenomenon, β_c .

This requires understanding of the formulation of the problem of free bar theory (section 5.2.1), the chosen predictors (5.2.2), the linear solution of the problem (5.2.3), the input variables / parameters (5.2.4), and consequently assumptions used to simplify the complexities (section 5.2.5).

5.2.1 Problem formulation

As a first step in the method description, it is useful to recall the main features of the free bar theory. The theory investigates the stability of a uniform flow over a flat erodible bed made of homogeneous sediment occurring in a straight, rectangular channel under steady flow conditions. Firstly, the St Venant equations of quasi-steady shallow water flow in a straight channel with a slowly varying erodible bed are applied. The river bed is assumed to be composed of the same particle size (D_{50}) as the particles transported by the water flow. Governing equations are obtained by imposing mass conservation and momentum equations for x and y direction, followed by Exner's sediment mass conservation equation. In a dimensional form, they read:

Water mass conservation:

$$\frac{\partial D^* U^*}{\partial x^*} + \frac{\partial D^* V^*}{\partial y^*} = 0 \quad (5.1)$$

Momentum conservation in the x and y direction:

$$U^* \frac{\partial U^*}{\partial x^*} + V^* \frac{\partial U^*}{\partial y^*} + gH^* \frac{\partial H^*}{\partial x^*} + \frac{\tau_{fx}^*}{\rho D^*} = 0 \quad (5.2)$$

$$U^* \frac{\partial V^*}{\partial x^*} + V^* \frac{\partial V^*}{\partial y^*} + gH^* \frac{\partial H^*}{\partial y^*} + \frac{\tau_{fy}^*}{\rho D^*} = 0 \quad (5.3)$$

Sediment mass conservation

$$(1 - \lambda_p) \frac{\partial(H^* - D^*)}{\partial t^*} + \frac{\partial q_x^*}{\partial x^*} + \frac{\partial q_y^*}{\partial y^*} = 0 \quad (5.4)$$

In equations (5.1 to 5.4) a star (*) is used to denote dimensional quantities, as is common in theoretical models that are then solved within a dimensionless framework to ensure more generality and comparability of results. Namely, in (5.1 to 5.4) $H^*(x, y, t)$ [m] denotes the free water surface elevation; $D^*(x, y, t)$ [m] is normal water depth, $U^*(x, y, t)$ [m/s] and $V^*(x, y, t)$ [m/s] represent uniform velocity components in the x and y directions, respectively, $\tau_{fx}^*(x, y, t)$ [kg/ms²]; $\tau_{fy}^*(x, y, t)$ [kg/ms²] represents bed shear stress in the x and y directions, respectively; and $q_x^*(x, y, t)$ and $q_y^*(x, y, t)$ [m²/s] represent sediment discharge per unit width in the x and y directions, where $g = 9.81$ m/s² and λ_p is bed porosity.

These variables can be made non-dimensional as follows:

$$(U^*, V^*) = U_0^*(U, V), \quad (H^*, D^*) = D_0^*(F_0^2 H, D), \quad (5.5a, b)$$

$$(x^*, y^*) = B^*(x, y), \quad (\tau_{fx}^*, \tau_{fy}^*) = \rho U_0^{*2}(\tau_{fx}, \tau_{fy}), \quad (5.6a, b)$$

$$(q_x^*, q_y^*) = \sqrt{\Delta g d_{50}^{*3}}(q_x, q_y), \quad t^* = \frac{B^*}{U_0^*} t, \quad (5.7a, b)$$

Equations (5.1 to 5.4) contain 8 unknowns ($H, D, U, V, q_x, q_y, \tau_{fx}, \tau_{fy}$), and so the system is not fully determined. To achieve ‘closure’, expressions relating to shear stress (τ), and sediment flow rate (q_s) to flow characteristics (q) are formulated. These closure relationships evaluate the friction and sediment discharge terms, and relate shear stresses (τ) and the sediment flow rate (q_s) to flow characteristics (q), respectively. Therefore, following a well-established procedure (Parker, 1976; Blondeaux and Seminara, 1985), the shear stress is expressed in terms of a friction coefficient C_f , where the bed configuration is assumed to be planar, so that Einstein’s (1950) drag coefficient (d_s) can be employed within the Chezy coefficient C :

$$(\tau_s, \tau_n) = C_f (U, V) |\widehat{U}|; \quad C_f = C^{-\frac{1}{2}} = 6 + 2.5 \ln \left(\frac{D}{2.5 d_s} \right) \quad (5.8)$$

In (5.8), $|\widehat{U}|$ denotes the modulus of the depth-averaged velocity vector $\widehat{U} = (U, V)$. Setting the roughness parameter equal to $(2.5 d_s)$ after (Engelund and Hansen, 1972) and the non-dimensional sediment diameter equal to $d_s = D_{50}^*/D_0^*$, where D

represents water depth and D_{50} is average grain size, the function for unit sediment discharge, q_s becomes crucially dependent on the reach-averaged Shields sediment mobility parameter θ :

$$q_s = \frac{\sqrt{g\Delta D_{50}}}{1 - \lambda_p} \Phi(\theta) \quad (5.9)$$

Under the assumption that transported sediment is mainly bed load, the local angle of sediment transport is usually related to an average angle of particle trajectories (δ), and expresses q_s in non-dimensional form as:

$$q_s = (q_{sx}, q_{sy}) = (\cos \delta, \sin \delta)\Phi \quad (5.10)$$

Engelund (1981) formulates the small value of δ as:

$$\sin \delta = \frac{q_y}{\sqrt{q_x^2 + q_y^2}} - \frac{r}{\beta\theta^2} \frac{\partial}{\partial y} (F_0^2 H - D); \cos \delta \leq 1 \quad (5.11)$$

Where θ denotes the Shields parameter, and r the so-called ‘Ikeda’s parameter’. The key dimensionless input data for the analysis are the reach-averaged, bar-forming values of the channel half-width to depth ratio β , the Shields sediment mobility parameter θ and the relative roughness (ratio between D_{50} and depth) d_s . They are defined as follows:

$$\beta = 0.5 \frac{W}{D}; \theta = \frac{\tau_0}{(\rho_s - \rho)gd_{50}}; d_s = \frac{D_{50}}{D}. \quad (5.12a,b,c)$$

Using the above closure relations for the unit sediment load and near-bed shear stress vectors, the unknowns of the governing dimensionless mathematical system are now four: (U, V, H, D).

5.2.2 Sediment load predictors

This section illustrates how the potential sediment load predictors ($\Phi(\theta)$) for our analysis, are estimated. These are particularly relevant because the thresholds β_c and β_r are known to quantitatively depend on the choice of the sediment load predictor. Three approaches were considered. The first was that of Engelund and Hansen (1972), which is a predictor for the total load (bedload + suspended load) based on the stream power concept and was mainly developed for sand river beds. For this reason it has mainly been used for the finer-grained streams in the data set. The second predictor is based on

Parker's (1990) equation, which was developed with the concept of equal mobility for mainly gravel river beds. Using this equation, as bed material is assumed to be a single representative diameter, D_{50} , local bed material movement would be initiated when the bed shear stress exceeds the critical value at a particular location or area of the bed. Third, the approach of Meyer-Peter and Müller (1948) was considered. This accounts for bedload transport largely with a single critical threshold ($\theta_{cr} = 0.047$). These three sediment transport predictors and their limits of application are presented in Table 5.1. For the present analysis, Parker's approach was employed for gravel sediment ($D_{50} > 6.3\text{mm}$), and Engelund and Hansen's approach was employed for sand bed reaches. However, since the method used for estimating sediment load is likely to have a significant influence on the results of the present analyses, the sensitivity of the results to this choice is explored in section 5.4.

Table 5.1 Sediment transport formula implemented on the mathematical analysis

	Formula	Limits
Engelund and Hansen (1972)	$\Phi = 0.05 \theta^{2.5} C^2$	$D_{50} < 6.3 \text{ mm}$
Parker (1990)	$W_i = \xi^{14.2}; \xi < 1$ $W_i = e^{[14.2(\xi-1)-9.28(\xi-1)^2]}; 1 \leq \xi \leq 1.59$ $W_i = 5474 \left(1 - \frac{0.853}{\xi}\right)^{4.5}; \xi > 1.59$ With $\Phi = W_i 0.00218 \theta^{1.5}$ and $\xi = \frac{\theta}{0.0386}$	$D_{50} > 6.3 \text{ mm}$
Meyer-Peter and Müller (1948)	$\Phi = 8(\theta - \theta_{cr})^{1.5}; \theta_{cr} = 0.047$	$D_{50} > 0.4 \text{ mm}$

5.2.3 Linear solution

It is important to understand how unperturbed uniform flow loses its stability due to periodic perturbation. To achieve this, a classical stability analysis is performed, aimed at investigating under which conditions sufficiently small, sinusoidal and alternate perturbations of the bed topography and of the flow field tend to grow because of an inherent instability of the system. For this purpose, the dimensionless unknowns

are expanded in power series of the ‘small’ (theoretically infinitesimal) amplitude parameter A as follows, and neglecting nonlinear terms (i.e. those in A^2, A^3 etc.)

$$(U, V, D, H) = (1, 0, 1, H_0) + A(U_1, V_1, D_1, H_1) \quad (5.13)$$

with C_0 and Φ_0 as the friction coefficient and bed-load function of the undisturbed uniform flow, respectively.

The structure of the governing equations suggests the following space-temporal structure of the linear perturbations (U_1, V_1, D_1, H_1) :

$$(U_1, V_1, D_1, H_1) = e^{\Omega t} (S(y)u_1, C(y)v_1, S(y)d_1, S(y)h_1) E(x, t) + c.c \quad (5.14)$$

Where c.c is a conjugate of complex numbers, and we define

$$S(y) = \sin\left(\frac{\pi y}{2}\right), C(y) = \cos\left(\frac{\pi y}{2}\right), E = e^{i(\lambda x - \omega t)} \quad (5.15a,b,c)$$

With λ , ω , and Ω denoting wave number, angular frequency and growth rate of the perturbation, respectively. Growth rate is a complex number, which has two values as it consists of $\Omega = \Omega_r + i\Omega_i$; and λ is bar wavenumber, defined as:

$$\lambda = \frac{\pi W_0}{L} \quad (5.16)$$

By substituting (5.15) into (5.10) and in (5.1 to 5.4), the governing differential system is transformed into an algebraic system for the complex unknowns (u_1, v_1, h_1, d_1) . Such resulting algebraic systems require a solvability condition to be satisfied, for the solution to be different from the null vector. This solvability condition provides the relation that gives the dependence of the complex growth rate Ω on dependence of the input parameters (β, θ, d_s) and on bar wavenumber l , which is the key outcome of the stability analysis, because it allows to determine under which conditions (linear) free bars grow ($\Omega_r > 0$) or decay in time ($\Omega_r < 0$) and migrate downstream ($\Omega_i < 0$) or upstream ($\Omega_i > 0$).

$$A(t) = e^{\Omega_r t} \Rightarrow \frac{dA}{dt} = \Omega_r A \quad (5.17)$$

Using the constant value of θ_{l0} and $d_{s,l0}$, bar amplification can be predicted and it becomes higher as the value of β increases (portrayed in Figure 5.2A). This graph in (λ, Ω) plane later is extracted at varying β intersections at $\Omega_i, \Omega_r = 0$ to produce the

marginal or neutral amplification/migration curves in the (λ, β) plane (e.g., Figure 5.1 or 5.2B).

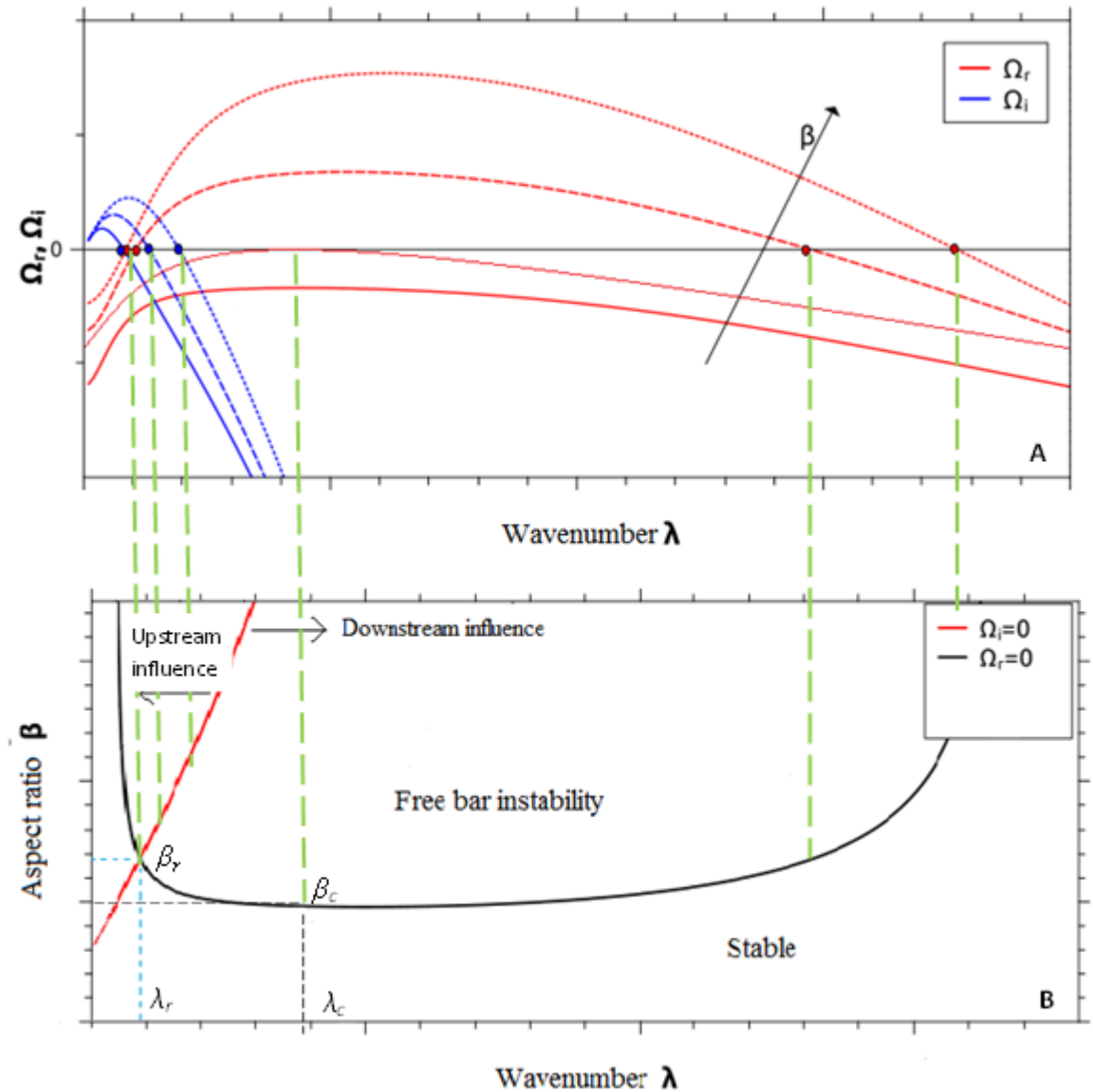


Figure 5.2 A. Amplification of Ω_r and Ω_i versus wavenumber λ , for a fixed θ and ds and varying β and B. Marginal curve of bar amplification is produced at the crossing of Ω_r and $\Omega_i = 0$

The intersection of $\Omega_r = 0$ and $\Omega_i = 0$ is the resonance condition, where $\lambda = \lambda_r$ and $\beta = \beta_r$. Figure 5.2B displays this marginal curve where the area above $\Omega_r = 0$ represents free bar formation and the area below only corresponds to steady bars forced by localized persistent geometrical constraints (e.g. Struiksma et al., 1985). Above the curve defined by $\Omega_i = 0$, the curve $\Omega_r = 0$ separates an area where there is upstream amplification of bars from an area of the plot that defines downstream amplification. Thus Figure 5.2B defines three possible classes of bar amplification: stable ($\beta < \beta_{critical}$: 'morphodynamic stability'), unstable with only downstream information propagation

(($\beta_{critical} < \beta < \beta_{resonant}$: ‘morphodynamic instability’), unstable with both downstream and upstream information propagation (($\beta > \beta_{resonant}$: ‘morphodynamic complexity’).

5.2.4 Input data

The analyses presented in chapters 3 and 4 yielded a classification of single thread rivers corresponding to broad differences in river width, gradient and sinuosity, that could be expected to correspond to gradients in the above theoretical parameters. Because no bed sediment size data were available for many of the reaches analysed in previous chapters, only 5 of the original 6 channel classes could be analysed using the above theory (see Table 5.2):

Class 1 (very large width, very low gradient, high sinuosity)

Class 3 (intermediate width, intermediate gradient, low sinuosity)

Class 4 (intermediate width, intermediate gradient, intermediate sinuosity)

Class 5 (low width, low gradient, high sinuosity)

Class 6 (very low width, very low gradient, very high sinuosity)

The main dimensional parameters required to investigate the theoretical morphodynamics regimes are those needed to compute the reach-averaged, bar forming values of (β, θ, d_s). The following dimensional parameters were employed for each selected replicate reach:

- (i) Width (W) refers to bankfull width, obtained from Google Earth (see chapter 3) – 221 observations
- (ii) Slope (S) refers to bankfull channel slope, obtained from Google Earth (see chapter 3) – 221 observations
- (iii) Median bed sediment size (D50), estimated mainly using spot check observations from River Habitat Surveys (only available for British rivers, see chapter 4) – 64 observations






(Class number)	(1)	(3)	(4)	(5)	(6)
Relative Width	Very Large	Intermediate	Intermediate	Low	Low
Relative Slope	Very Low	Intermediate	Intermediate	Low	Low
Relative Sinuosity	High	Low	Intermediate	High	High
Distinguishing Physical Features	lateral and mid-channel active and vegetated bars and benches, extensive floodplain landforms	lateral and mid-channel active and vegetated bars and benches	few in-channel or marginal features, riffle-pools present	frequent marginal benches, extensive floodplain landforms	the lowest in-channel, marginal and floodplain geomorphic features of all clusters
Distinguishing Vegetation Features				low riparian tree cover and complexity, emergent macrophytes	
Example rivers for each class (all images are taken from 2.5 km altitude)					
River	Loire, France	Feshie, Scotland	S. Tyne, England	Dee, England	Torridge, England

Table 5.2 Summary properties of the 5 river classes investigated in this chapter.

(iv) Discharge (Q) refers to bankfull discharge, and is estimated from daily discharge time series from gauging stations within or close to the studied river reaches. Flows for two, five and ten year return periods (Q_2 , Q_5 , and Q_{10}) were estimated from the annual maximum series extracted from daily discharge data using the Gumbel probability distribution (see chapter 4) – 164 observations. The analysis would have been more suitable for the present application if instantaneous peak flow data had been available, and it raises concerns regarding the flow frequency to be used as a surrogate for bar-forming, fully sediment-transporting discharge. In the end, Q_{10} was selected, but the sensitivity of the analysis to this choice is assessed in section 5.4.1.

To increase the number of reaches in Class 1 (very large width, very low gradient, high sinuosity), two Italian rivers (Orco and Sesia) are incorporated into the analysis. These provide data for 6 new reaches (3 replicate reaches on each river). For these rivers, bankfull discharge is estimated using nearby gauging station flood event records in a different way than the other analysed reaches, while median bed sediment size was based on a visual assessment of the beds of the two rivers.

The data set compiled for analysis is summarized in Table 5.1. It consists of 64 reaches, mainly located in Great Britain (England, Scotland and Wales), but with some in France and Italy, for which all necessary input data was available. Table 5.3 summarises the distribution of these 64 reaches across the five classes of single thread river channel.

Table 5.3 Reaches, observed / estimated values of D_{50} , width, slope, sinuosity, Q_2 , Q_5 , Q_{10} and derived estimates of the three parameters (β , θ , d_s) required in the analyses presented in this chapter.

Reach no.	River Name	Country	Class	D_{50} (mm)	Q_2 (m ³ /s)	Q_5 (m ³ /s)	Q_{10} (m ³ /s)	Width (m)	Slope (o/oo)	Sinuosity	β_{10}	θ_{10}	ds_{10}
1.1	Caersws	Wales	3	11.89	48	68	81	36.99	2.06	1.12	17.74	0.11	0.01
1.2	Caersws	Wales	3	19.03	48	68	81	52.08	2.24	1.23	30.10	0.06	0.02
1.3	Caersws	Wales	5	11.31	48	68	81	62.83	1.30	1.37	36.52	0.06	0.01
1.4	Caersws	Wales	4	11.31	48	68	81	35.43	0.43	1.14	10.29	0.04	0.01
3.1	Allier	France	1	6.20	721	1008	1197	99.82	0.66	1.23	12.71	0.25	0.00
3.2	Allier	France	5	6.20	721	1008	1197	114.53	0.58	1.16	15.30	0.21	0.00
3.3	Allier	France	1	6.20	721	1008	1197	153.48	0.92	1.26	28.46	0.24	0.00
8.1	Dane	England	6	0.42	24	39	50	14.68	2.96	1.73	7.74	4.05	0.00
8.2	Dane	England	5	11.31	24	39	50	19.88	0.78	1.53	6.41	0.06	0.01
8.3	Dane	England	6	0.37	24	39	50	15.36	1.99	1.53	7.41	3.37	0.00
19.1	Frome	England	5	4.65	20	23	25	17.21	1.54	1.41	10.50	0.16	0.01
19.2	Frome	England	5	11.31	20	23	25	16.44	0.43	1.60	6.00	0.03	0.01
19.3	Frome	England	5	9.82	20	23	25	14.31	1.10	1.63	6.45	0.07	0.01
20.1	Findhorn	Scotland	4	129.14	118	169	203	45.69	6.27	1.09	15.03	0.04	0.08
20.2	Findhorn	Scotland	4	101.59	118	169	203	75.39	3.23	1.22	28.50	0.03	0.08
20.3	Findhorn	Scotland	4	150.20	118	169	203	50.18	5.47	1.21	16.41	0.03	0.10
43.1	Tywi	Wales	5	11.31	90	137	168	62.16	2.53	1.14	28.26	0.15	0.01
43.2	Tywi	Wales	5	11.71	90	137	168	53.32	1.37	1.55	18.23	0.10	0.01
43.3	Tywi	Wales	5	0.98	90	137	168	57.75	0.46	1.59	18.12	0.45	0.00
45.1	Endrick Water nr. Drymen	Scotland	6	1.36	66	80	89	12.80	3.92	1.41	4.24	2.64	0.00
45.2	Endrick Water nr.	Scotland	4	3.83	66	80	89	25.09	1.67	1.37	9.22	0.36	0.00

Table 5.3 (ctd.)

Reach no.	River Name	Country	Class	D ₅₀ (mm)	Q ₂ (m ³ /s)	Q ₅ (m ³ /s)	Q ₁₀ (m ³ /s)	Width (m)	Slope (o/oo)	Sinuosity	β ₁₀	θ ₁₀	ds ₁₀
	Drymen												
45.3	Endrick Water nr. Drymen	Scotland	5	0.21	66	80	89	50.43	0.16	2.08	17.36	0.69	0.00
46.1	Tweed	Scotland	5	23.43	253	365	439	7.42	2.31	1.24	0.31	0.72	0.00
46.2	Tweed	Scotland	4	35.10	253	365	439	20.31	3.48	1.14	2.37	0.26	0.01
46.3	Tweed	Scotland	4	71.84	253	365	439	34.96	1.69	1.09	4.42	0.06	0.02
47.1	Spey	Scotland	4	112.84	346	525	643	50.79	2.76	1.33	7.17	0.05	0.03
47.2	Spey	Scotland	4	87.82	346	525	643	94.83	2.84	1.11	20.55	0.05	0.04
47.3	Spey	Scotland	1	90.51	346	525	643	136.06	3.18	1.22	37.70	0.04	0.05
48.1	Feshie	Scotland	3	66.83	62	81	94	55.12	8.32	1.09	37.72	0.06	0.09
48.2	Feshie	Scotland	3	66.83	62	81	94	108.56	7.24	1.05	105.28	0.03	0.13
48.3	Feshie	Scotland	3	66.83	62	81	94	53.35	11.71	1.15	39.51	0.07	0.10
49.1	Bollin	England	5	7.37	8	10	12	11.56	2.70	1.48	9.75	0.13	0.01
49.2	Bollin	England	5	10.37	8	10	12	11.08	1.92	1.37	7.89	0.08	0.01
49.3	Bollin	England	5	4.64	8	10	12	11.29	0.60	1.61	6.12	0.07	0.01
60.1	Twrch	Wales	4	125.80	6	9	11	16.05	6.12	1.19	14.93	0.02	0.23
60.2	Twrch	Wales	3	39.85	6	9	11	35.24	4.05	1.23	55.72	0.02	0.13
60.3	Twrch	Wales	4	68.46	6	9	11	31.59	1.47	1.10	32.30	0.01	0.14
62.1	Irthing	England	4	0.02	81	126	155	24.56	5.67	1.44	13.10	161.05	0.00
62.2	Irthing	England	3	34.72	81	126	155	23.43	3.67	1.36	5.99	0.13	0.02
62.3	Irthing	England	3	128.00	81	126	155	25.22	2.41	1.44	5.07	0.03	0.05
63.1	Kinnel	England	4	0.35	28	37	43	60.50	0.32	1.48	44.30	0.38	0.00
63.2	Kinnel	England	3	0.35	28	37	43	35.79	1.00	1.55	26.78	1.16	0.00
63.3	Kinnel	England	5	2.45	28	37	43	30.83	5.54	1.00	30.63	0.69	0.00
64.1	Lune	England	4	25.40	131	201	248	55.31	1.69	1.24	15.04	0.07	0.01

Table 5.3 (ctd.)

Reach no.	River Name	Country	Class	D ₅₀ (mm)	Q ₂ (m ³ /s)	Q ₅ (m ³ /s)	Q ₁₀ (m ³ /s)	Width (m)	Slope (o/oo)	Sinuosity	β ₁₀	θ ₁₀	ds ₁₀
64.2	Lune	England	5	25.40	131	201	248	57.86	1.44	1.13	15.41	0.06	0.01
64.3	Lune	England	5	25.40	131	201	248	42.73	5.60	1.16	14.22	0.20	0.02
65.1	Coquet	England	5	14.42	73	111	136	55.77	3.08	1.42	27.91	0.13	0.01
65.2	Coquet	England	5	14.42	73	111	136	32.30	1.41	1.52	9.03	0.11	0.01
65.3	Coquet	England	3	14.42	73	111	136	70.05	0.98	1.25	28.50	0.05	0.01
66.1	Nairn	Scotland	5	2.83	41	63	77	11.61	5.40	1.28	4.12	1.63	0.00
66.2	Nairn	Scotland	5	2.93	41	63	77	12.09	4.20	1.22	4.06	1.29	0.00
66.3	Nairn	Scotland	5	1.47	41	63	77	13.56	1.97	1.24	4.08	1.35	0.00
67.1	Annan	England	4	72.88	82	107	124	48.12	4.01	1.12	20.72	0.04	0.06
67.2	Annan	England	4	50.17	82	107	124	32.58	2.41	1.11	9.96	0.05	0.03
67.3	Annan	England	4	25.55	82	107	124	24.87	1.24	1.27	5.60	0.07	0.01
70.1	South Tyne	England	4	138.25	50	72	86	38.81	7.23	1.03	19.56	0.03	0.14
70.2	South Tyne	England	4	138.25	50	72	86	25.29	9.57	1.15	10.73	0.05	0.12
70.3	South Tyne	England	4	132.51	50	72	86	40.70	7.58	1.04	21.53	0.03	0.14
77.1	Orco	Italy	1	60	53.99	560.21	895.31	189.23	8.02	1.03	72.57	0.11	0.05
77.2	Orco	Italy	1	30	53.99	560.21	895.31	245.62	5.15	1.12	104.92	0.12	0.03
77.3	Orco	Italy	1	16	53.99	560.21	895.31	145.06	2.77	1.14	40.01	0.19	0.01
78.1	Sesia	Italy	1	30	1538.77	2020.91	2340.07	181.52	5.14	1.05	36.36	0.26	0.01
78.2	Sesia	Italy	1	15	1538.77	2020.91	2340.07	184.47	4.51	1.05	38.38	0.44	0.01
78.3	Sesia	Italy	1	8	1558.99	2056.31	2385.52	182.23	3.13	1.04	35.16	0.61	0.00

Table 5.4 The number of reaches analysed from each of classes 1, 3, 4, 5 and 6

Class	1	3	4	5	6
N	9	10	20	22	3

5.2.5 Assumptions

In the analysis, the following assumptions were set for the application of the free bar theory to the developed single-thread rivers data set:

- (i) Steady, uniform flow and regular rectangular channels with non-erodible banks are assumed for all of the chosen reaches to calculate the input parameters β , θ , d_s needed to run the model. Therefore, the reach-averaged channel depth has been approximated using the Chezy friction formula (1776), C (see equation 5.18 and 5.19) as a unique value for every replicate reach.

$$C_d = \frac{1}{\left(6 + 2.5 \ln \left(\frac{h}{2.5 d_{50}} \right)\right)^2} \quad (5.18)$$

$$C^2 = \frac{g}{C_d} \quad (5.19)$$

- (ii) The sinuosity of each reach is also assumed to be within the range of straight to weakly meandering. Therefore, the maximum threshold for channel sinuosity adopted was 1.5 (e.g. Leopold et al., 1964, for further discussion see chapter 2). This assumption is applicable to the present analysis since the sinuosity at bankfull within the reaches selected for analysis is less than this threshold.
- (iii) Following Colombini et al. (1987) and Crosato and Mosselman (2009) a bar mode type = 1 (i.e. marginal bars, see Figure 5.3) is also selected, reflecting the fact that most of the channels analysed for the classification in chapter 3 show or are dominated by marginal bars (bank-attached features).

The above assumptions are appropriate to an analysis of the data set presented in chapter 3, since the data set consists almost entirely of single-thread rivers with very few transitional/wandering reaches included. From the above assumptions, the parameters that are needed to test the bar theory are defined and are computed as constant values for each replicate reach. Once all the assumptions are met, the next step would be to estimate the two key parameters, β_r and β_c .

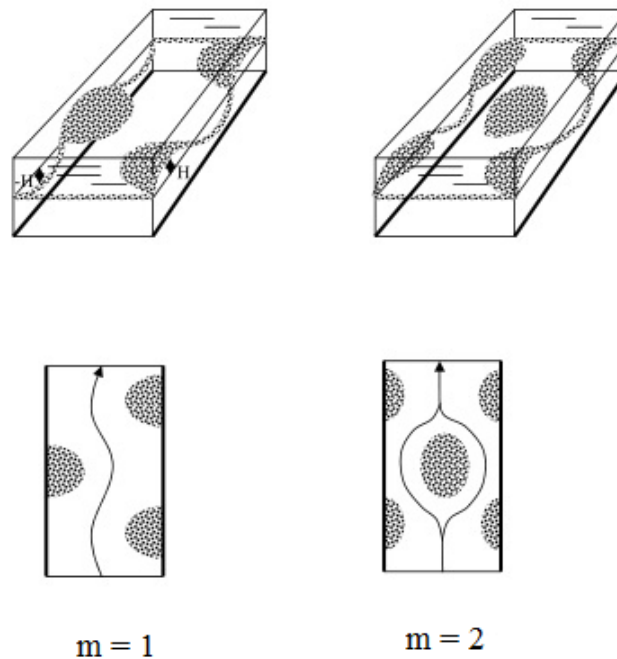


Figure 5.3 Illustrative patterns of flow and bed deformation associated with the presence of bars (from Crosato, 2008)

5.3 Implications of morphodynamic “Bar” Theory for single-thread rivers

This section presents results and relevant interpretations of bar theory when applied to the selected single-thread rivers. The adopted approach has been to assess the variability of theoretical parameters across the five, geomorphologically-derived classes, as well as the complementary information of the variability of the selected geomorphic and vegetational features across the three theoretical morphodynamic regimes. First an overview of the examined reaches is presented in relation to the main parameters of the reaches (section 5.3.1). Second, features identified from Google Earth are investigated in relation to the three morphodynamic regimes: (1) superresonant (2) subresonant with free bars (3) subresonant with no free migrating bars (section 5.3.2).

5.3.1 Behaviour of the values of theoretical parameters across the five classes of river reach

Boxplots are used to illustrate the distribution of six properties that are central to the bar theory across the five classes of river reach investigated (Figure 5.4). The boxplots appear to display some notable trends across the river classes. Width shows a clear, expected, declining trend across the five classes 1, 3, 4, 5 and 6 (Figure 5.4A), whereas depth (which is estimated from discharge, width, slope and sediment size

excludes Tweed reach 1) shows only a slight decrease (Figure 5.4B). Sinuosity shows an increasing trend (Figure 5.4C), whereas slope shows little variation between classes (Figure 5.4D). Lastly the D_{50} (Figure 5.4E) shows an increasingly coarse gravel bed from class 1 through 3 to 4, with the remaining 2 classes showing notable finer bed sediment. Overall, clear trends appear for width, width-to-depth ratio, and sinuosity from class 1 through to 6, while less clear trends are shown for slope, sediment size, and depth.

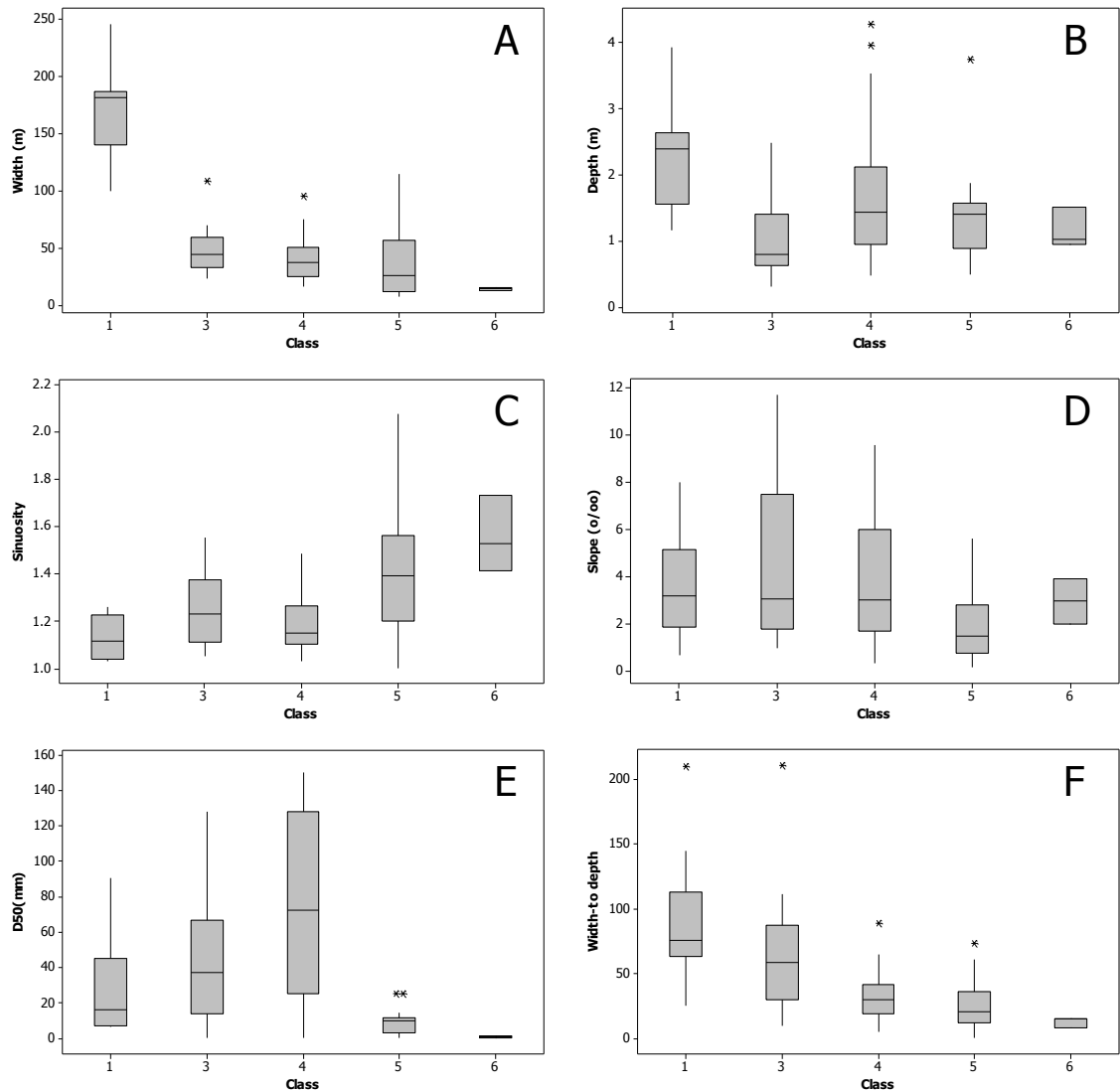


Figure 5.4 Boxplots illustrating channel dimension and sediment properties of reaches across five classes of single-thread river

Following Zolezzi et al. (2009), the general theoretical morphodynamic regimes of the selected reaches can be visualized through scatter plots (Figure 5.5). In Figure 5.5 the data are represented using different coloured symbols to highlight the bed material classes and sediment transport predictors that were used (Figure 5.5A and B), and

whether superresonant or subresonant behaviour is indicated (Figure 5.5C), where the tendency of reaches to super-resonant behaviour occurs at higher values of β and lower values of θ , and the tendency to subresonant behaviour occurs at increasing values of θ and lower values of β . The results are in qualitative agreement with the findings of Zolezzi et al. (2009) who used the gravel-bed rivers data sets of Hey and Thorne (1986) and

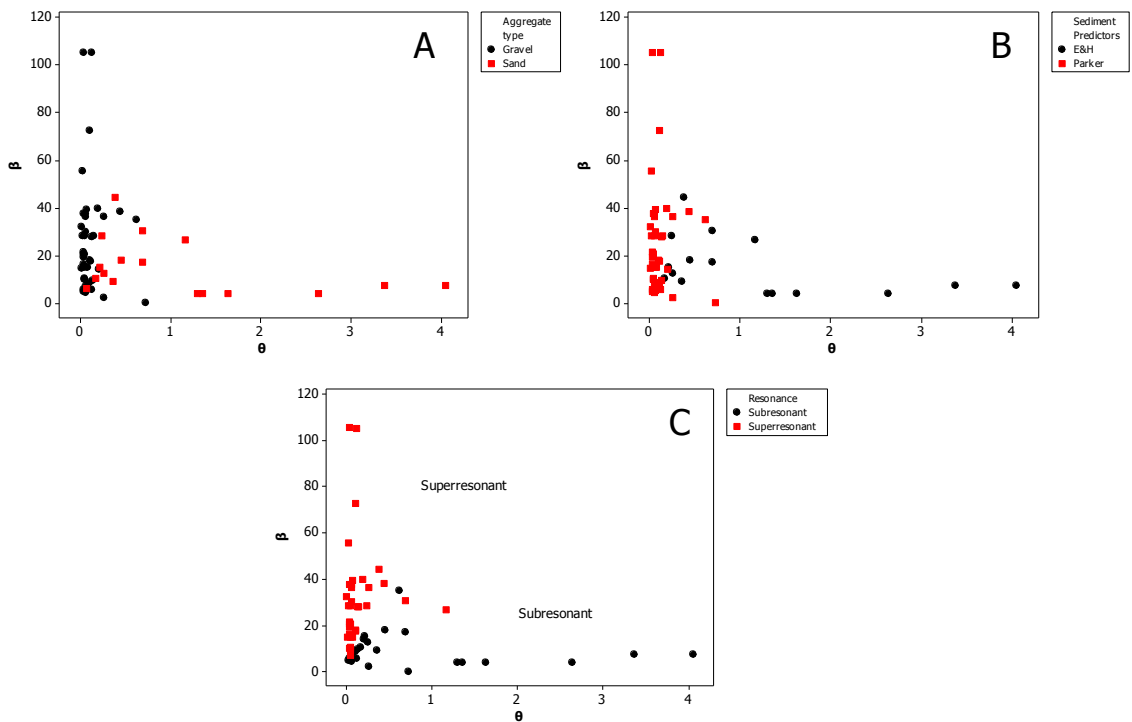


Figure 5.5 Scatterplots of β to θ with different symbols identifying: A. Aggregate type (black = gravel, red = sand); B. Sediment predictors (red = Engelund and Hansen, black = Parker); C. Super-resonant and subresonant behaviour (red = super-resonant, black = subresonant).

Figure 5.6 uses boxplots to illustrate how the values of the three parameters of the bar theory vary across the five river classes. The width-to-depth ratio (β , Figure 5.6A) shows a decreasing trend across classes 1, 3, 4, 5 and 6, reflecting the trend in channel width (Figure 5.4A). In contrast, β_c and β_r (Figure 5.6B and C) show a decreasing trend through classes 1, 3, 4 followed by intermediate values in classes 5 and 6 – an inverse pattern to that shown by D_{50} (Figure 5.4E).

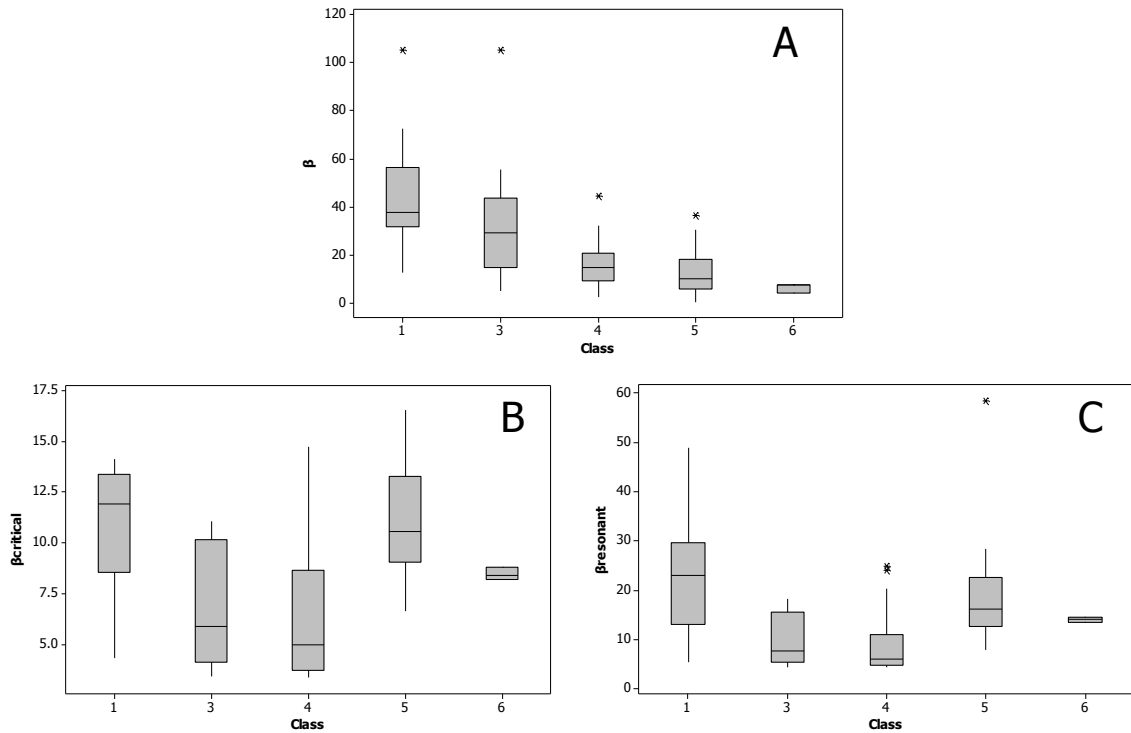


Figure 5.6 Boxplots illustrating variations in the values of the computed aspect ratios across the five classes of river reaches: **A:** aspect ratio, **B:** β critical, and **C:** β resonant.

Finally, Figure 5.7 displays boxplots illustrating the behaviour of differences in these thresholds across the river classes. The difference $\beta - \beta_r$ (Figure 5.7B) indicates the tendency of the reaches to behave in a superresonant and sub-resonant way, which might be described as the ‘morphodynamic complexity’ of the system. The difference $\beta - \beta_c$ (Figure 5.7A) demonstrates the tendency of the reaches to form freely migrating bars, or ‘morphodynamic instability’. Both properties display a decreasing trend across classes 1, 3, 4, 5 and 6, implying a decrease in both morphodynamic complexity and instability in the transition towards the most stable classes. Overall, classes 1, 3 and 4 tend to display a complex regime, whereas class 5 tends to display an unstable regime and class 6 a stable regime.

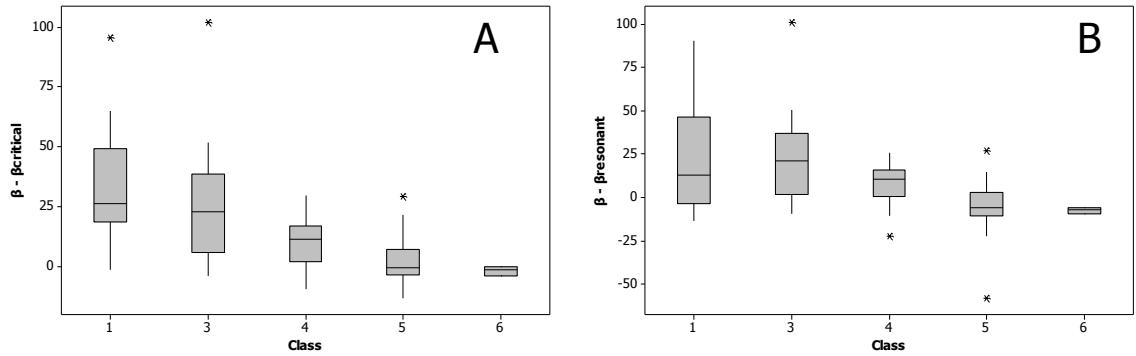


Figure 5.7 A and B: Contrasts in A. the difference between the aspect ratio (β) and $\beta_{critical}$ and B. the difference between the aspect ratio (β) and $\beta_{resonant}$, across river classes 1, 3, 4, 5 and 6.

5.3.2 Geomorphic and vegetation features observed within reaches associated with the three theoretical regimes

In this section, we test whether there are statistically significant differences in the channel features measured from Google Earth among the three theoretical morphodynamic regimes. From the assumptions stated in section 5.2.1, every replicate reach is considered as a separate system that possesses its own value for β_r and β_c . For each reach, the width-to-depth ratio, β , is an important indicator in relation to these two threshold values, since it positions each reach within one of the three theoretical morphodynamic regimes (Table 5.5): morphodynamic complexity (superresonant condition), morphodynamic instability (sub-resonant with free bars), morphodynamic stability (sub-resonant with no free bars).

Table 5.5 Abbreviations used to refer to the three morphodynamic regimes

	Morphodynamic complexity (complex)	Morphodynamic instability (unstable)	Morphodynamic stability (stable)
Regimes	$\beta > \beta_r$	$\beta_r < \beta < \beta_c$	$\beta < \beta_c$

The behaviour of geomorphic and vegetation variables extracted from Google Earth according to these theoretical morphodynamic regimes, was investigated statistically in relation to the three morphodynamic regimes listed in Table 5.5 (complex, unstable, stable). Because of unequal variances in many of the measured

variables across the three theoretical morphodynamic regime groups, non-parametric Kruskal-Wallis tests were applied to assess whether there was any statistically significant difference in each feature among the groups ($k=3$). Where a significant difference was indicated ($p<0.05$), multiple comparisons between groups were conducted using Dunn's procedure with Bonferroni's correction for $k(k-1)/2$ possible comparisons, to identify which groups were significantly different from one another ($p<0.05$). These analyses were conducted using XLStat 2014.1.

Table 5.6 summarises the results of the above analyses, with the analysed variables presented in the order (1) channel bed features; (2) bar and bench features; (3) floodplain features; (4) vegetation features. All Kruskal-Wallis tests had two degrees of freedom. Pools, riffles, active and stabilizing marginal bars and active mid channel bars all show higher values in the superresonant group (complex) than in the subresonant with no bar group (stable), and both active and stabilizing bars also show higher values in the subresonant with free bars group (unstable) than in the subresonant with no bar group (stable). In addition water filled-ponds display higher values in the super resonant (complex) and subresonant (unstable) group, followed by oxbow and stabilizing non-arcuate bars on the floodplain-channel margin that also show higher values in the subresonant (unstable) than in the subresonant with no bar group (stable). Yet, the opposite is true for emergent macrophytes which show higher values in the subresonant with no bar group (stable) than in the super-resonant group (complex). Above all, it seems that there are no significant difference between 'complex' regime and 'unstable' regime among these in-channel features.

The 'bar theory' analysis consisted of hydraulic and morphological parameters, which are 'in-channel' indicators, and so it is not surprising that channel bed and bar features correspond to groupings based on these parameters, with more features, suggesting greater morphodynamic complexity, on reaches displaying a superresonant (complex) regime. Water filled floodplain ponds are often indicative of high lateral dynamics (old channel positions), which are often associated with high bar dynamics, and so their association with reaches displaying a superresonant regime is also coherent. In contrast, reaches that display sub-resonant behaviour with no free bars (stable) are associated with high emergent macrophyte cover, implying that this type of vegetation promotes or can colonise and grow thanks to morphodynamic stability.

Table 5.6 Results of Kruskal-Wallis (comparison of k samples) test applied to the geomorphic and vegetational units grouped according to the three regimes in Table 5.2

Group	Variable	K-observed (K-critical = 5.991)	Probability (embold- ened if p < 0.05)	Significant differences (p<0.05) in variable among the 3 regimes (multiple pairwise comparisons using Dunn's procedure with Bonferroni correction)
Channel bed features	Pools	7.207	0.027	Complex > Stable
	Riffles	11.601	0.003	Complex > Stable, Unstable
	Cascade	2.393	0.302	-
	Waterfall & steps	1.060	0.589	-
	Boulders	2.163	0.339	-
	Exposed bedrock	0.778	0.678	-
Channel bar and bench features	Active marginal bars	16.373	0.000	Complex, Unstable > Stable
	Stabilising marginal bars	11.198	0.004	Complex, Unstable > Stable
	Active mid- channel bars	8.088	0.018	Complex > Stable
	Stabilising mid- channel bars	3.668	0.160	-
	Active bench	2.060	0.357	-
	Stabilising bench	2.278	0.320	-
Channel margin transitional and floodplain features	Swamp-wetland	0.045	0.978	-
	Water-filled ponds	14.338	0.001	Complex, Unstable > Stable
	Connected side channels	5.872	0.053	-
	Dry depressions	3.977	0.137	-
	Ridges & swales	1.617	0.446	-
	Oxbow	6.492	0.039	Unstable > Stable
	Stabilising arcuate bars	6.479	0.039	-
	Stabilising non- arcuate bars	7.287	0.026	Unstable > Stable
Vegetation	Vegetation structure	3.827	0.148	-
	Weighted tree distribution	4.885	0.087	-
	Wood accumulation	5.055	0.080	-
	Emergent macrophytes	24.671	< 0.0001	Stable > Complex, Unstable

5.4 Sensitivity of outcomes to input variables

Two main choices may be expected to have a sizeable effect on the theoretical results: (i) the return interval chosen to select the constant discharge value that should correspond to ‘bar-forming’, fully sediment transporting conditions over the whole cross-section, and (ii) the sediment load predictor. This section explores the sensitivity of the obtained results to different choices of these two input parameters: the river discharge event frequency that was used as a surrogate for bankfull discharge (section 5.4.1) and the sediment load predictors (refer to Table 5.1) that were employed (section 5.4.2).

5.4.1 Choice of bar forming discharge value

In this section, the impact of using daily flows of different return period (Q_2 , Q_5 , Q_{10}) to estimate β_r and β_c across the river classes 1, 3, 4, 5 and 6 are evaluated.

Figure 5.8 displays boxplots of estimates of both β_c (graphs A, B, C) and β_r (graphs D, E, F) for each of Q_2 (A, D), Q_5 (B, E) and Q_{10} (C, F) across classes 1, 3, 4, 5, 6. Similar trends across the classes are displayed for all three discharges, but estimates based on Q_5 and Q_{10} display higher median values than those based on Q_2 . These two parameters are indicators of direct outputs of the bar theory and indicate their sensitivity to the chosen discharge return period.

Figure 5.9 displays boxplots of $\beta - \beta_r$ (graphs A, B, C) and $\beta - \beta_c$ (graphs D, E, F) for each of Q_2 (A, D), Q_5 (B, E) and Q_{10} (C, F) across classes 1, 3, 4, 5, 6. The analysis shows that the trends of $\beta - \beta_r$ and $\beta - \beta_c$ would change slightly if Q_2 were used instead of Q_5 or Q_{10} . Conversely, the trends for Q_5 and Q_{10} are similar (note the differences in the vertical axis scales on the graphs).

Movements of bed sediments can be predicted from river discharge and Shields stress, θ (a ratio of depth to sediment grain size), and since the depth is dependent on river discharge, this makes Shields range dependent on river discharge as well. The Meyer-Peter Müller threshold, $\theta_{cr} = 0.047$, was employed to assess the threshold of computed θ (θ_2 , θ_5 , θ_{10}) based on three discharges of different return period (Q_2 , Q_5 , and Q_{10}). Boxplots of the Shields range are presented Figure 5.11, suggesting that many estimates based on Q_2 fall below the threshold theoretical assumption. On the contrary, estimates based on Q_{10} passes exceed the threshold values in the largest number of cases (Q_{10} : 49 reaches, Q_5 : 45 reaches, Q_2 : 36 reaches). This reflects a physical problem

between the flow and the sediment transport. The low value of discharge (Q_2) indicates that the flow is not strong enough to lift sediment from the bed or to eventually induce bar forming activity within the channel. Since there is no sediment transport activity, theoretical bar activity cannot be assessed well. In brief, Q_{10} is the most suitable choice for estimating θ because this value can provoke ‘more bar formation’ in most reaches.

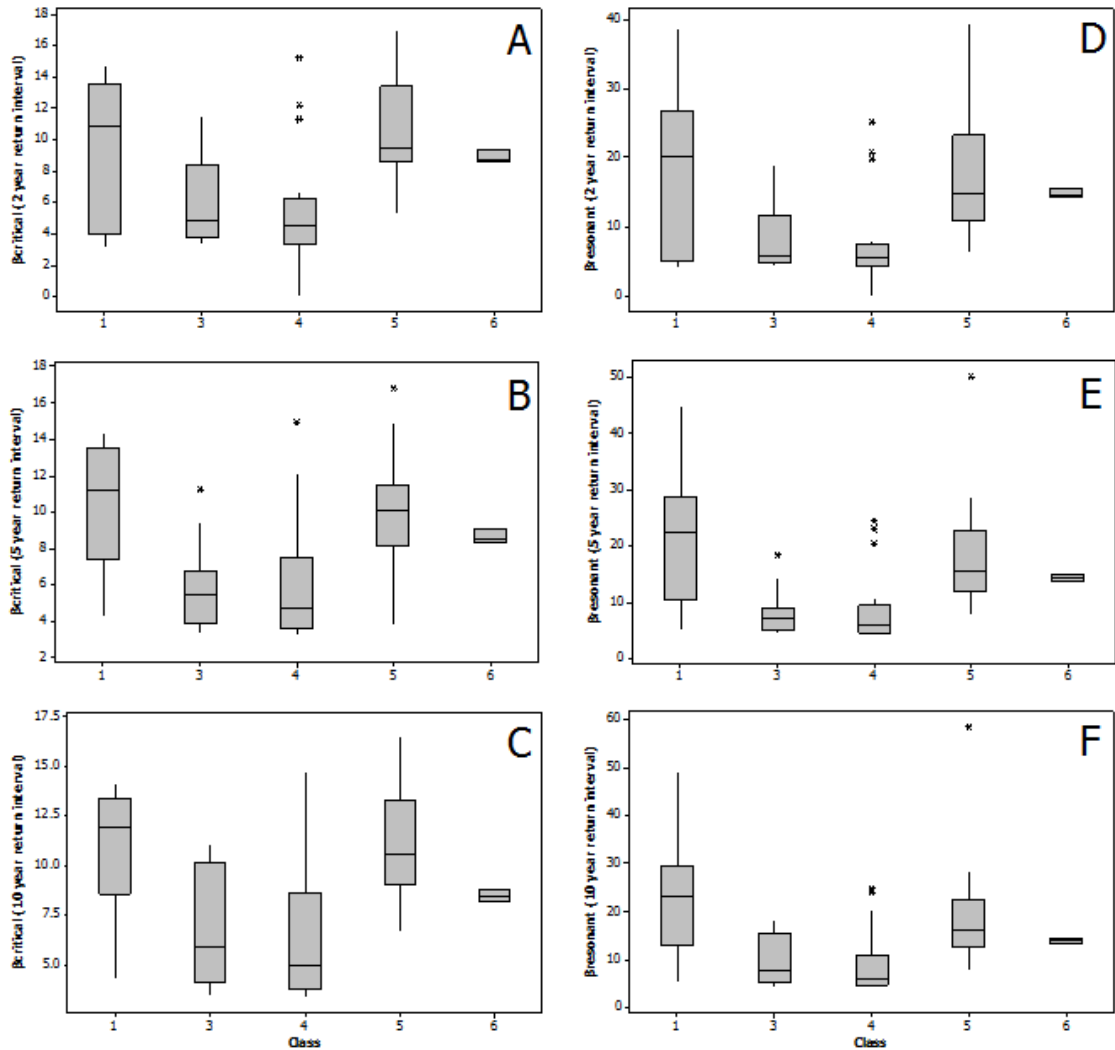


Figure 5.8 Boxplots illustrating values of computed $\beta_{critical}$ (left) and $\beta_{resonant}$ (right) across the 5 investigated classes of river reach when computed using a daily discharge of: A. and D. (Q_2) – the 2 year return period event; B. and E. (Q_5) – the 5 year return period event; C. and F. (Q_{10}) – the 10 year return period event.

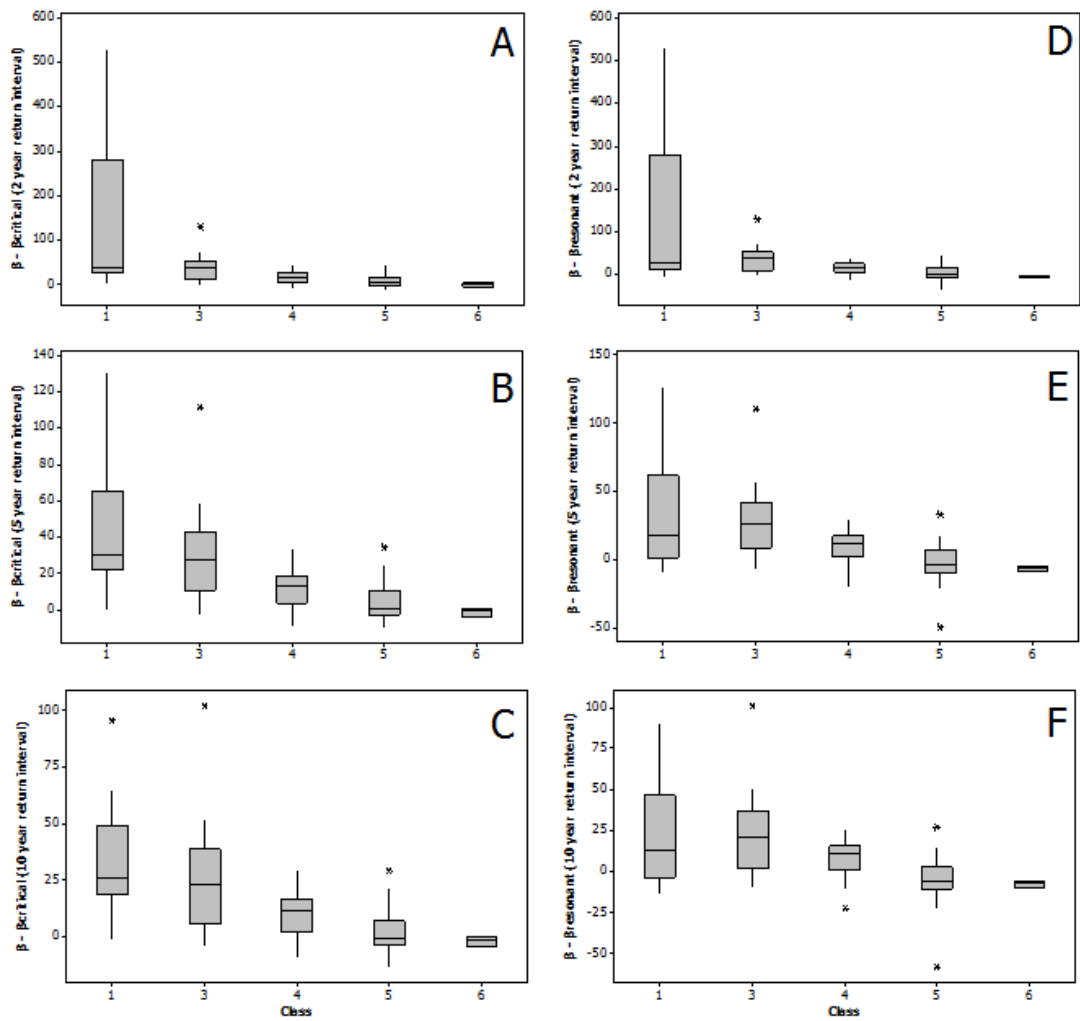


Figure 5.9 Boxplots illustrating variation in the values of computed β -critical (left) β -presonant (right) across the 5 classes of river reaches when computed using discharge of A, D 2-year interval B, E 5-year interval and C, F 10-year interval

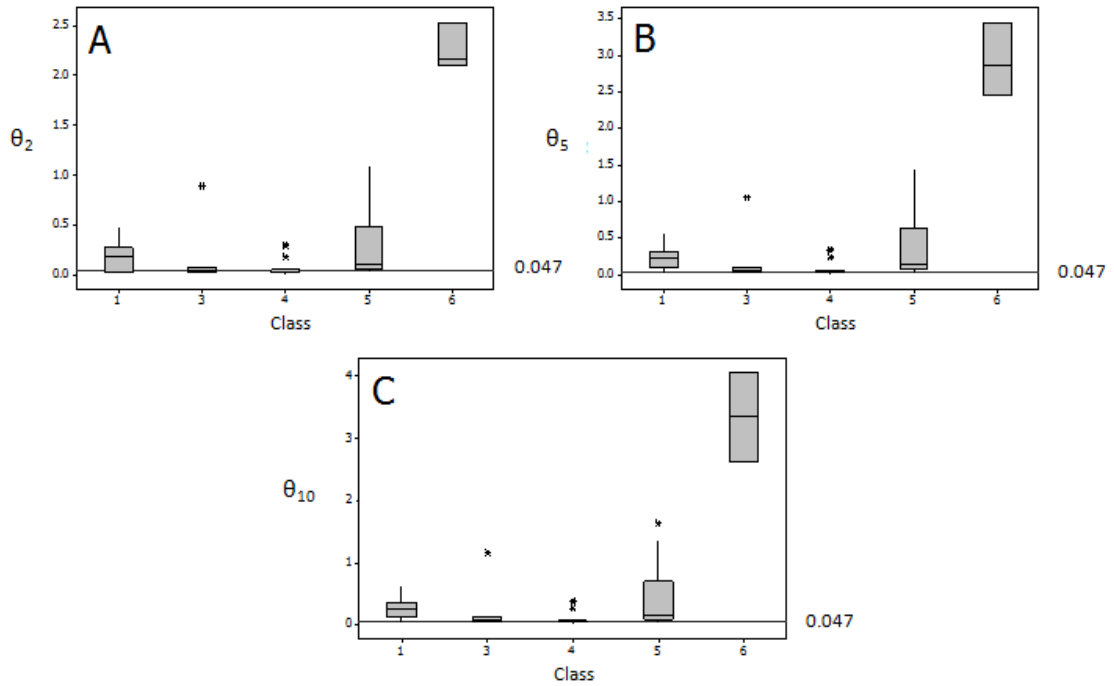


Figure 5.10 Boxplots illustrating variation in the values of Shields range across the 5 classes of river reaches when computed using a daily discharge of: **A. 2-year recurrence interval; B. 5-year recurrence interval; and C. 10-year recurrence interval**

5.4.2 Sediment predictors

Out of 64 selected reaches, bedload predictors for 38 reaches were computed using Meyer-Peter Müller, 57 using Parker’s equation and only 41 reaches were computed using Engelund and Hansen. Due to the numbers of reaches for which it was not appropriate to calculate each of the three predictors (Figure 5.7), a combination of Parker (for gravel bed only, $D_{50} > 6.3$ mm) and Engelund and Hansen (for sand only $D_{50} < 6.3$ mm) was selected to be the most suitable way of calculating the sediment predictors for the whole analysis because this allowed theoretical classes to be estimated for 63 reaches (see the bold numbers in Table 5.7). Therefore, this section aims to assess the sensitivity of these two predictors with respect to the more widely used Meyer-Peter Müller equation.

The graphs in Figure 5.11 A, B and C show the difference in the resonance condition $((\beta - \beta_r) / \beta_r)$, stability $((\beta - \beta_c) / \beta_r)$ and the distance between them $(\beta_r - \beta_c) / \beta_r$, respectively, when based on the Parker (black dots) and Engelund and Hansen equations (red dots), in comparison with the Meyer-Peter Müller equation, plotted with respect to the x-axis. The accuracy of the values can be evaluated by their distance from the dashed (1:1) lines. In Figure 5.11A and B, both Parker and Engelund and Hansen

equations provide values close to the Meyer-Peter Müller equation for smaller values of resonance and stability. However, there are some sizeable outliers when Meyer-Peter Müller-based values exceed 3. The chosen predictor within that range was the Parker equation, and Figure 5.11A and B show that this equation generates estimates that are closest to those from the Meyer-Peter Müller equation. Furthermore, although there are outliers in Figure 5.11C related to the Engelund and Hansen's formula, most of the estimates based on Parker's equation fall quite close to the dashed line. It can also be concluded that, regardless of the sediment transport equation that is employed, the theoretical parameters would not vary significantly in terms of the morphodynamic regime identified for each reach (36 complex, 6 unstable, 21 stable). In practice, Parker's formula was employed as the bedload estimator for 46 out of the 63 reaches.

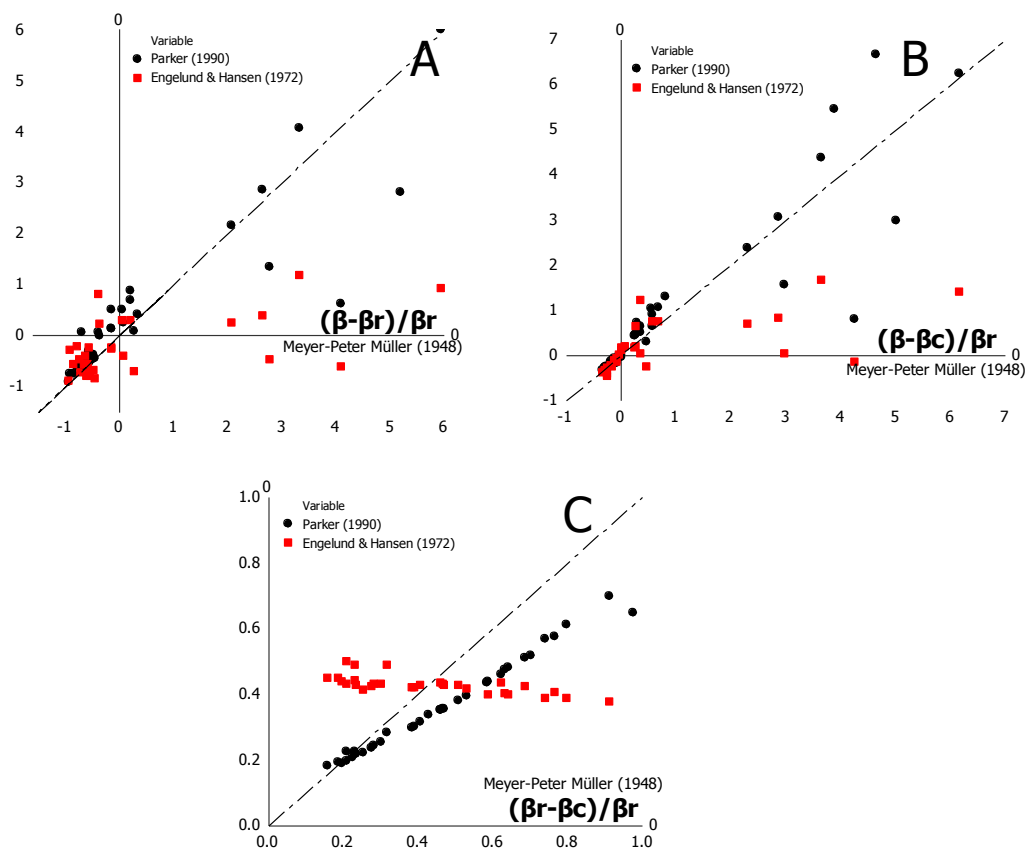


Figure 5.11 Sensitivity of the morphodynamic regimes to the choice of different bed load predictors: A. $(\beta - \beta_r) / \beta_r$ B. $(\beta - \beta_c) / \beta_r$ C. $(\beta_r - \beta_c) / \beta_r$. The x-axis is Meyer-Peter Müller, and y-axis in black = Parker (1990) for gravel; red= Engelund and Hansen (1972) for sand.

Table 5.7 Output of β_{cr} and β_r (computed using fixed values of θ_{10} and ds_{10}) in different sediment predictors (*MPM=Meyer-Peter Muller, EH=Engelund and Hansen)

Reach no.	River Name	Country	Class	D_{50} (mm)	θ	ds	B	Figure 5.11: X-axis		Figure 5.11: Y-axis			
								Meyer- Peter Müller		Parker		Engelund and Hansen	
								β_{cr}	β_r	β_{cr}	β_r	β_{cr}	β_r
1.1	Caersws	Wales	3	11.89	0.11	0.01	17.74	12.52	21.04	10.56	15.43	12.96	22.71
1.2	Caersws	Wales	3	19.03	0.06	0.02	30.10	7.58	9.82	7.34	9.46	13.29	23.87
1.3	Caersws	Wales	5	11.31	0.06	0.01	36.52	7.94	10.01	7.52	9.39	14.78	26.02
1.4	Caersws	Wales	4	11.31	0.04	0.01	10.29	*	*	6.54	7.70	*	*
3.1	Allier	France	1	6.20	0.25	0.00	12.71	17.44	48.46	15.55	30.07	14.15	23.62
3.2	Allier	France	5	6.20	0.21	0.00	15.30	17.56	42.45	15.44	27.55	14.72	24.58
3.3	Allier	France	1	6.20	0.24	0.00	28.46	16.65	45.14	14.77	28.14	13.62	22.90
8.1	Dane	England	6	0.42	4.05	0.00	7.74	*	*	*	*	8.19	13.51
8.2	Dane	England	5	11.31	0.06	0.01	6.41	9.99	12.87	9.34	11.84		
8.3	Dane	England	6	0.37	3.37	0.00	7.41	*	*	*	*	8.81	14.46
19.1	Frome	England	5	4.65	0.16	0.01	10.50	14.77	31.27	12.70	21.03	13.10	22.51
19.2	Frome	England	5	11.31	0.03	0.01	6.00	*	*	6.63	7.83	*	*
19.3	Frome	England	5	9.82	0.07	0.01	6.45	11.10	15.31	9.75	12.80	14.93	25.94
20.1	Findhorn	Scotland	4	129.14	0.04	0.08	15.03	*	*	3.74	4.74	10.70	20.87
20.2	Findhorn	Scotland	4	101.59	0.03	0.08	28.50	*	*	4.29	5.37	*	*
20.3	Findhorn	Scotland	4	150.20	0.03	0.10	16.41	*	*	3.70	4.70	*	*
43.1	Tywi	Wales	5	11.31	0.15	0.01	28.26	13.33	26.98	11.36	18.38	12.18	21.29
43.2	Tywi	Wales	5	11.71	0.10	0.01	18.23	13.14	21.26	11.10	15.85	13.96	24.19
43.3	Tywi	Wales	5	0.98	0.45	0.00	18.12	18.17	88.78	16.87	43.71	13.80	22.68
45.1	Endrick Water nr.	Scotland	6	1.36	2.64	0.00	4.24	*	*	*	*	8.38	13.97

Table 5.7 (ctd.)

Reach no.	River Name	Country	Class	D ₅₀ (mm)	θ	ds	B	Figure 5.11: X-axis		Figure 5.11: Y-axis			
								Meyer- Peter Müller		Parker		Engelund and Hansen	
								β _{cr}	β _r	β _{cr}	β _r	β _{cr}	β _r
	Drymen												
45.2	Endrick Water nr. Drymen	Scotland	4	3.83	0.36	0.00	9.22	15.49	65.58	14.13	33.60	11.94	20.21
45.3	Endrick Water nr. Drymen	Scotland	5	0.21	0.69	0.00	17.36	19.67	219.19	18.69	62.68	14.57	23.47
46.1	Tweed	Scotland	5	23.43	0.72	0.00	0.31	*	*	13.72	58.54	10.53	17.72
46.2	Tweed	Scotland	4	35.10	0.26	0.01	2.37	13.73	43.39	12.17	24.94	11.00	19.12
46.3	Tweed	Scotland	4	71.84	0.06	0.02	4.42	6.62	8.23	6.34	7.84	14.13	25.17
47.1	Spey	Scotland	4	112.84	0.05	0.03	7.17	4.64	5.69	5.18	6.42	12.86	23.51
47.2	Spey	Scotland	4	87.82	0.05	0.04	20.55	*	*	4.63	5.71	12.88	23.78
47.3	Spey	Scotland	1	90.51	0.04	0.05	37.70	*	*	4.31	5.34	*	*
48.1	Feshie	Scotland	3	66.83	0.06	0.09	37.72	4.19	5.45	4.14	5.37	9.95	19.48
48.2	Feshie	Scotland	3	66.83	0.03	0.13	105.28	*	*	3.39	4.36	*	*
48.3	Feshie	Scotland	3	66.83	0.07	0.10	39.51	6.24	9.12	5.53	7.75	9.12	17.92
49.1	Bollin	England	5	7.37	0.13	0.01	9.75	12.74	23.99	10.78	16.78	12.16	21.38
49.2	Bollin	England	5	10.37	0.08	0.01	7.89	10.44	14.93	9.05	12.18	13.46	23.80
49.3	Bollin	England	5	4.64	0.07	0.01	6.12	11.78	15.75	10.50	13.50	16.58	28.31
60.1	Twrch	Wales	4	125.80	0.02	0.23	14.93	*	*	3.36	4.43	*	*
60.2	Twrch	Wales	3	39.85	0.02	0.13	55.72	*	*	3.96	5.06	*	*
60.3	Twrch	Wales	4	68.46	0.01	0.14	32.30	*	*	5.15	6.56	*	*
62.1	Irthing	England	4	0.02	161.05	0.00	13.10	*	*	*	*	*	*
62.2	Irthing	England	3	34.72	0.13	0.02	5.99	11.85	21.95	9.99	15.45	11.53	20.53
62.3	Irthing	England	3	128.00	0.03	0.05	5.07	*	*	4.63	5.73	*	*

Table 5.7 (ctd.)

Reach no.	River Name	Country	Class	D ₅₀ (mm)	θ	ds	B	Figure 5.11: X-axis		Figure 5.11: Y-axis			
								Meyer- Peter Müller		Parker		Engelund and Hansen	
								β _{cr}	β _r	β _{cr}	β _r	β _{cr}	β _r
63.1	Kinnel	England	4	0.35	0.38	0.00	44.30	19.06	73.21	17.52	40.70	14.72	24.10
63.2	Kinnel	England	3	0.35	1.16	0.00	26.78	*	*	14.85	128.91	11.05	18.18
63.3	Kinnel	England	5	2.45	0.69	0.00	30.63	*	*	12.18	56.33	9.29	15.98
64.1	Lune	England	4	25.40	0.07	0.01	15.04	10.16	14.12	8.94	11.84	13.84	24.40
64.2	Lune	England	5	25.40	0.06	0.01	15.41	8.88	11.59	8.33	10.69	*	*
64.3	Lune	England	5	25.40	0.20	0.02	14.22	12.31	32.44	10.66	19.85	10.30	18.33
65.1	Coquet	England	5	14.42	0.13	0.01	27.91	12.38	23.18	10.46	16.25	11.89	21.01
65.2	Coquet	England	5	14.42	0.11	0.01	9.03	13.20	21.62	11.15	16.02	13.87	24.03
65.3	Coquet	England	3	14.42	0.05	0.01	28.50	5.44	4.61	6.19	7.45	*	*
66.1	Nairn	Scotland	5	2.83	1.63	0.00	4.12	*	*	*	*	8.51	14.38
66.2	Nairn	Scotland	5	2.93	1.29	0.00	4.06	*	*	12.40	*	9.05	15.28
66.3	Nairn	Scotland	5	1.47	1.35	0.00	4.08	*	*	13.57	*	9.96	16.55
67.1	Annan	England	4	72.88	0.04	0.06	20.72	*	*	4.06	5.07	*	*
67.2	Annan	England	4	50.17	0.05	0.03	9.96	1.65	1.96	4.94	6.07	13.30	24.27
67.3	Annan	England	4	25.55	0.07	0.01	5.60	9.25	12.07	8.63	11.05	14.80	25.93
70.1	South Tyne	England	4	138.25	0.03	0.14	19.56	*	*	3.38	4.35	*	*
70.2	South Tyne	England	4	138.25	0.05	0.12	10.73	2.26	2.85	3.51	4.54	9.58	19.24
70.3	South Tyne	England	4	132.51	0.03	0.14	21.53	*	*	3.34	4.30	*	*
77.1	Orco	Italy	1	60	0.11	0.05	72.57	9.38	16.31	7.84	11.85	*	*
77.2	Orco	Italy	1	30	0.12	0.03	104.92	10.98	20.30	9.23	14.30	*	*
77.3	Orco	Italy	1	16	0.19	0.01	40.01	13.76	33.03	11.93	21.19	*	*
78.1	Sesia	Italy	1	30	0.26	0.01	36.36	12.90	42.94	11.41	23.83	*	*

Table 5.7 (ctd.)

Reach no.	River Name	Country	Class	D ₅₀ (mm)	θ	ds	B	Figure 5.11: X-axis		Figure 5.11: Y-axis			
								Meyer- Peter Müller		Parker		Engelund and Hansen	
								β _{cr}	β _r	β _{cr}	β _r	β _{cr}	β _r
78.2	Sesia	Italy	1	15	0.44	0.01	38.38	3.44	127.91	12.37	35.36	*	*
78.3	Sesia	Italy	1	8	0.61	0.00	35.16	*	*	13.19	48.87	*	*

5.5 Discussion and Conclusions

This chapter has investigated the correspondence between a theoretical classification of channels based on ‘bar theory’ (three morphodynamic regimes) and a classification based on measurements and observations of channel dimensions, geomorphological and vegetation features (the 6 class channel classification presented in Chapters 3 and 4). Distinct correspondences have been found between the two classifications, which is surprising given the strongly contrasting fluid mechanics based and observation based approaches that were used to define each classification.

The observation-based classification presented in chapter 3 has generated classes of reach which show distinct gradients in both the difference between the aspect ratio, β and $\beta_{critical}$, and also the difference between the aspect ratio β and $\beta_{resonant}$ across river classes 1, 3, 4, 5, and 6 (Figure 5.7). Furthermore, when the presence-abundance of vegetation-geomorphic units within reaches falling into the three morphodynamic regimes are investigated, statistically significant differences are found in pools; riffles; active and stabilizing marginal, mid-channel and arcuate bars; oxbows; water-filled ponds; and macrophytes across the three regime types (Table 5.6).

These results provide further evidence of the robustness of the classification presented in chapter 3 and tested in chapter 4. They also provide a logical interpretation of the single-thread river complexities across the theoretical morphodynamic regimes. In particular, the ‘morphologically complex’ regime corresponds to high frequencies of both in-channel and floodplain features, whereas the ‘morphologically stable’ regime has few such features but is characterized by the high presence of emergent macrophytes. There is also an apparent transition between these two regimes through the ‘morphologically unstable’ regime, which shows some similarities in its features with each of the other two regimes.

The results also provide a further illustration of the utility of data extracted from Google Earth (chapter 3), complemented by additional data sources (chapter 4), for reliably exploring the properties of rivers to support the estimation of theoretical parameters. Several clear trends are present in the geometrical properties of reaches in the five river classes (Figure 5.4), which contribute to the estimation of β , β_r and β_c (Figure 5.6) and result in clear decreasing trends in the main indicators of the theoretical morphodynamic regimes, $\beta-\beta_r$ and $\beta-\beta_c$, across the Google Earth based river classes (Figure 5.7). The linkage between the classification system and “bar” theory results are

clearly shown in Figure 5.12 where scatterplots clearly separate the three morphodynamics regimes.

Overall, the analysis presented in this chapter suggests that the inherent, theoretical tendency of system behaviour as predicted by the bar theory, may leave a signature even in complex natural river systems across a wide range of environmental settings that are quite distinct from the assumptions underlying the theory.

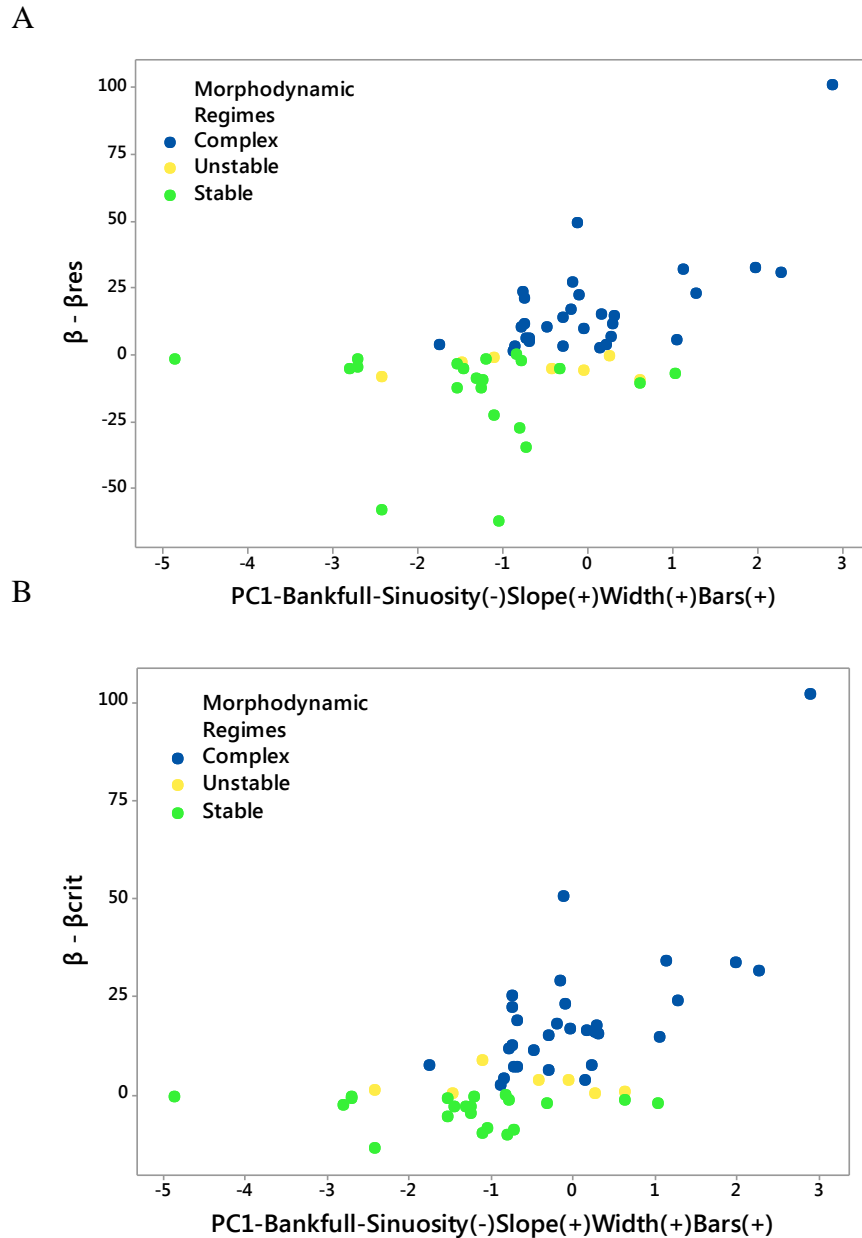


Figure 5.12 Reach scores on aggregate “Google Earth” PC1 plotted against “bar theory” parameters: **A.** the difference between the aspect ratio (β) and β_{resonant} ; **B.** the difference between the aspect ratio (β) and β_{critical} , according to morphodynamics regimes

CHAPTER 6

DISCUSSION

6.1 Introduction

The research reported in this thesis is concerned with the characteristics of European single thread rivers including their geometric, geomorphic and vegetation properties. Following a review of the literature (chapter 2), three research questions were posed and subsequently addressed in chapters 3, 4 and 5:

- (i) Can a geomorphologically-interpretable classification of single-thread sinuous to meandering European rivers be compiled using data extracted from aerial imagery (Chapter 3)?
- (ii) To what extent does the classification remain robust, when tested using data sets from other information sources (Chapter 4)?
- (iii) To what extent does the classification based on information extracted from aerial imagery correspond to a classification of single-thread rivers based on theory (Chapter 5)?

This chapter briefly summarises and discusses the outcomes and possible future trajectories of the research. The results from chapters 3, 4 and 5 are summarised in section 6.2 and then discussed in the context of previous research and potential management applications in section 6.3. Section 6.4 considers some limitations of the research, which leads into suggestions on how the research could be developed in the future (section 6.5).

6.2 Research results

This section summarises the results obtained in relation to each of the three research questions, bringing together the outcomes of chapters 3, 4 and 5.

6.2.1 Can a geomorphologically-interpretable classification of single-thread sinuous to meandering European rivers be compiled using data extracted from aerial imagery (Chapter 3)?

This research question is addressed in Chapter 3, which developed *a preliminary classification of single thread European rivers using data extracted from GoogleTM Earth*. Using knowledge from the literature review (Chapter 2) of the types of geomorphological features that might be encountered, a list of geometric (e.g. width, sinuosity and slope), in-channel and floodplain geomorphic and vegetation features identifiable from aerial imagery was assembled. Rules were then developed for identifying each feature in a consistent way. Using these rules, a large data set was assembled. In order to maintain consistency in identifying features from aerial imagery, some features had to be defined in ways that deviated slightly from the literature. In addition, when data extraction was complete, some rare features were combined to provide a useable sample of features of each type. The final data set extracted from Google Earth comprised 221 river reaches (approximately 3 replicate reaches from each of 75 different European rivers) for which information was extracted for 50 variables, with some separated into sub-categories according to their vegetation cover. These were then reduced to 25 aggregate variables representing channel dimensions, bed features, bar and bench features, channel margin transitional and floodplain features, and vegetation.

The data set was then used to support a classification of European single-thread rivers by subjecting it to a combination of ordination and classification techniques. First ordination was used to reduce the dimensions of the data set to a set of broad, geomorphologically-meaningful gradients or trends in the data set. Principal Components Analysis was selected for ordination method because it is a linear ordination technique (it assumes underlying linear trends and associations in the data). Linear ordination is usually appropriate for physical and environmental data sets. Since some of the variables were not continuous, the PCA was estimated using a rank correlation matrix rather than the usual product moment correlation matrix. PCA was applied to five subgroups of the aggregate variables (channel dimensions; bed features; bar and bench features; channel margin transitional and floodplain features: vegetation) from which 10 strong (i.e. high eigenvalues and % variance explained) and interpretable

(i.e. high loadings on a few meaningful variables) principal components (PCs) were extracted.

Following the ordinations, the reaches were classified based upon their scores on each of the 10 PCs using cluster analysis. Hierarchical agglomerative clustering was used because it progressively joins reaches to build clusters (classes) of similar characteristics. Ward's linkage method was used because of its wide and successful application to physical data and its potential to generate relatively evenly-sized clusters, with Euclidean distance selected as the measure of dissimilarity.

Based upon the agglomeration schedule plot, six clusters were identified as providing a compromise between a simple but at the same time potentially informative classification. The classes were compared statistically to establish whether or not there were statistically-significant differences between them. This was achieved using the Kruskal-Wallis test with multiple pairwise comparisons between classes assessed using Dunn's procedure with Bonferonni correction. Kruskal-Wallis tests were applied to the reach scores on each of the 10 PCs in turn to assess the degree to which the reach classes differed significantly from one another. All classes showed a statistically significant difference from all other classes in relation to their scores on at least one of the 10PCs.

The classification of the reaches into six classes is summarised in Figure 6.1 and the classes were named as follows:

Class 1 (very large width, very low gradient, high sinuosity)

Class 2 (intermediate width, high slope, low sinuosity)

Class 3 (intermediate width, intermediate slope, low sinuosity)

Class 4 (intermediate width, intermediate slope, intermediate sinuosity)

Class 5 (low width, low gradient, high sinuosity)

Class 6 (very low width, very low gradient, very high sinuosity)

This preliminary classification is plausible and geomorphologically sensible, with large rivers occupying a single class (class 1), and the remaining classes showing a clear gradient in channel width, slope and sinuosity and a set of reasonably distinct geomorphic and vegetation features. However, the classification required further testing to establish its robustness, and, since it is based entirely on one rather unconventional

data source, it needed validating using other, more traditional, data sets. These further investigations are reported in Chapter 4.







Class number	1	2	3	4	5	6
Relative Width	Very Large	Intermediate	Intermediate	Intermediate	Low	Low
Relative Slope	Very Low	High	Intermediate	Intermediate	Low	Low
Relative Sinuosity	High	Low	Low	Intermediate	High	High
Distinguishing Physical Features	lateral and mid-channel active and vegetated bars and benches, extensive floodplain landforms	lateral and mid-channel bars, exposed bedrock features	lateral and mid-channel active and vegetated bars and benches	few in-channel or marginal features, riffle-pools present	frequent marginal benches, extensive floodplain landforms	the lowest in channel, marginal and floodplain features of all clusters
Distinguishing Vegetation Features		Large wood accumulations			Low riparian tree cover and complexity, Emergent macrophytes	
All images are taken from 2.5 km altitude						
River	Loire, France	Bregenzer, Austria	Eygues, France	S. Tyne, England	Dee, England	La Meurthe, France

Figure 6.1 Summary of the relative properties of the river classes and some example river reaches

6.2.2 To what extent does the classification remain robust, when tested using data sets from other information sources (Chapter 4)?

Following an evaluation of the geographical distribution of the analysed reaches, Chapter 4 explored the robustness of the classification presented in chapter 3, in the following ways:

- (i) The association between the six classes and some of the original extracted and aggregated variables was explored using boxplots. This illustrated geomorphologically interpretable trends in channel dimensions and geomorphic features across the six classes, with some classes also distinguished by properties of their vegetation.
- (ii) The first split of each class within the cluster dendrogram was investigated to assess whether subdivision of any class could be justified. In each case the Mann-Whitney U test was used to assess whether the split revealed sub classes that had statistically significantly different scores on each of the 10 contributing PCs. In many cases the splits resulted in small sample sizes within the subgroups, and also the split classes reflected an expected within-class gradient that did not distinguish strongly different subclasses. Nevertheless, there appeared to be two distinct subgroups within Class 1, indicating that a larger sample of large rivers could lead to a useful subdivision of that class. A larger sample might also justify splitting class 2 since the subclasses join at a high level of dissimilarity.
- (iii) The accuracy of elevation estimates derived from Google Earth was assessed because these heavily influence channel and floodplain gradient estimates which contribute strongly to the classification. Where airborne LiDAR surveys were available, elevation estimates from both data sources were compared, yielding an average 6.73% error. The outcome of this analysis provides considerable confidence in the quality of the data extracted from Google Earth. However, since all the data were for British sites, further testing for more mountainous situations is recommended.
- (iv) There are often several images available for any location on Google Earth, so the influence of image selection on the classification of a reach was explored. Data was extracted from 12 new images, representing different years and

seasons, for reaches that had been incorporated in the original analysis. The data for each new image was extracted in the same way as the original data set and its scores on the 10 PCs were calculated so that each could be positioned on the aggregate PCA PC1-PC2 plot representing all 10 contributing PCs. All reaches remained in the same area of the plot as the river class to which the assessment based on the original image had been allocated. However, there were changes in plotting position, with Class 1 showing the greatest change, classes 2 and 3 also showing quite prominent changes, and reaches within classes 4 to 6 show very little movement in their plotting position.

- (v) Correspondence of Google-Earth derived classes to two controlling variables: discharge and bed material. Discharge and bed material are two traditionally-used strong discriminators of river channel type. Therefore, data were assembled to check whether the derived classes mapped onto distinct discharge and sediment characteristics.

55 of the sampled 75 rivers were positioned near flow gauging stations for which data were available for analysis. This provided a sample of 163 reaches for which flow frequency analysis could be conducted. Estimates of Q_2 , Q_5 and Q_{10} were extracted from daily flow records, based on the annual maximum series. These were then converted into estimates of stream power (in $W.m^{-1}$). Class 2 reaches showed the highest values of stream power followed by classes 1, 3, and 4, and then by classes 5 and 6. This illustrates that the large river class (class 1) shows intermediate values of stream power, and the remaining medium to smaller-sized rivers show a decline in stream power from Class 2 through to classes 5 and 6. This pattern is what would be expected, given the geomorphic characteristics of classes 2 to 6.

Consistent bed material size data was difficult to obtain for the 75 studied rivers. However, River Habitat Surveys are widely conducted within the UK and yield 10 qualitative estimates of bed material size as part of the survey's spot check component. Therefore, British rivers were used to investigate variations in bed material calibre across the river classes. Reaches of 19 out of the 22 British rivers in the data set were positioned close to RHS survey sites providing a total of 58 reaches for which the median bed material size (D_{50}) could be estimated. A clear gradient of sediment fining was identified from classes 4 through class 5

to class 6. This conforms to what would be expected based on the geomorphic features characterising the classes.

6.2.3 To what extent does the classification based on information extracted from aerial imagery correspond to a classification of single-thread rivers based on theory (Chapter 5)?

Chapter 5 investigated a sample of reaches within each of the six river classes to assess correspondence between the six classes and the theoretical thresholds, $\beta_{resonant}$ and $\beta_{critical}$ that define three morphodynamic regimes relative to the river's aspect ratio, β :

- (i) 'morphologically complex' $\beta > \beta_r$,
- (ii) 'morphologically unstable' $\beta_r > \beta > \beta_c$, and
- (iii) 'morphologically stable' $\beta < \beta_c$

Reaches representing the six classes of the classification presented in chapter 3 and based on channel dimensions, geomorphic and vegetation features were found to show distinct gradients in both the difference between β and $\beta_{resonant}$ and the difference between β and $\beta_{critical}$. Moreover, when the reaches were allocated to the three theory-based morphodynamic regimes, statistically-significant differences were found in several of the geomorphic and vegetation features, including pools; riffles; active and stabilizing marginal, mid-channel and arcuate bars; oxbows; other water-filled ponds; and macrophytes. Specifically, the 'morphologically complex' regime corresponded to a high frequency of both in-channel and floodplain features, whereas the 'morphologically stable' regime had fewer features, but was strongly characterized by the high presence of emergent macrophytes. The apparent transition between the two regimes through the 'morphologically unstable' regime was also clearly shown by some similarities in its features with each of the other two regimes.

Overall, the research in this chapter illustrates distinct correspondences between the two classifications, which is surprising given the strongly contrasting fluid mechanics based and observation based approaches that were used to define each classification. This analysis provides further proof of robustness of the classification presented in chapter 3 and tested in chapter 4. Analysis presented in chapter 5 suggests that the inherent, theoretical tendency of system behaviour as predicted by the bar

theory, may leave a signature even in complex natural river systems across a wide range of environmental settings that are quite distinct from the assumptions of the underlying theory.

6.3 Discussion of the Research Outcomes

In this section, the outcomes of the research, which were summarised in section 6.2, are discussed in the light of previous research and in relation to their usefulness. Section 6.3.1 discusses the scientific advances inherent in the Google Earth based classification developed and tested in chapters 3 and 4, both as a classification method or approach and also in relation to how the classification compares with other widely used classifications. Section 6.3.2 discusses the links that were found between the Google Earth based classification and a three-category classification based on bar theory. Finally, section 6.3.3 considers the usefulness of the Google Earth based classification and how it might be applied in management.

6.3.1 Scientific Advances in Relation to Previous River Classification Research

(i) Approach to classification

In chapter 2, it was noted that numerous river channel planform classifications have been proposed, but they are generally based on one of two broad types of approach: (i) qualitative analyses (e.g. Schumm, 1985; Mosley, 1987; Church, 2006) or (ii) the estimation of empirically-based thresholds between river styles (e.g. Leopold and Wolman, 1957; Carson, 1984; Edgar, 1984; Ferguson, 1987; Van den Berg, 1995; Church 2002). In practice, classifications tend to incorporate some elements of both approaches, but with a greater emphasis on one rather than another.

The approach developed in the present research is different from both of these approaches, although it is informed by them. The methodology is quantitative rather than qualitative, differentiating it from approach (i). It is bottom-up and empirically based, as in approach (ii), but it uses measures of form to support classification of rivers. Furthermore, by using a single, spatial data source (aerial imagery) from which

‘form’ properties are extracted, it incorporates vegetation as well as geomorphic features into the classification.

As pointed out by Rosgen (1994, p171):

‘the morphology of the present day channel is governed by the laws of physics through observable stream channel features and related fluvial processes. Stream pattern morphology is directly influenced by eight major variables including channel width, depth, velocity, discharge, channel slope, roughness of channel materials, sediment load, and sediment size (Leopold et al., 1964). A change in any one of these variables sets up a series of channel adjustments which lead to a change in the others, resulting in channel pattern alteration. Because stream morphology is the product of this integrative process, the variables that are measurable should be used as stream classification criteria’.

This link between form and process underpins the classification approach adopted in this thesis and thus, at first sight, might appear to be similar to that of Rosgen (1994). However, on closer inspection, Rosgen’s method largely falls into the qualitative type of classification. It is hierarchical and top-down in nature, at the first stage dividing river types according to their longitudinal gradient, cross sectional form and planform to discriminate eight river types of which six are single thread, and then adding bed material calibre and a further slope-based subdivision at a second stage to define a total of 94 types. Although quantitative data are presented, they appear to be used to inform class-splitting once it has been applied, with stream gradient being particularly heavily used. Although form and features are stressed in the description of the Rosgen method, these appear to be interpreted rather than contributing quantitatively to defining the classes.

Therefore, the approach developed here appears to be unique among geomorphological river classifications in using form to quantitatively inform classification in a bottom-up direction, by identifying naturally-occurring form-based groupings in a large data set. As such, the present approach allows the features of river reaches to indicate their class in a way that conforms to the idea of ‘getting to know your river’ that is inherent in the reach-scale components of the ‘River Styles Framework’ proposed by Brierley and Fryirs (2005).

Furthermore, the only previous classification to formally incorporate vegetation is that of Eaton et al. (2010), following the recognition by Millar (2000) that bank reinforcement by riparian vegetation may influence the threshold between single thread and braided channel patterns. Not only may vegetation ‘significantly affect channel mobility in a similar way to engineering structures, hard rock and strong clay layers’ (Kleinhans and Van den Berg, 2011, p733) and thus affect planform development, but it also indirectly affects any classification based on aerial imagery because its presence can both disguise (overhang) as well as discriminate geomorphic features. Thus, the incorporation of vegetation, albeit in a relatively simple way, is a second unique component of the present research.

(ii) Classification outcomes and links to processes (bullets B and D)

The six categories of channel identified in the present analysis can be compared with classes of single thread channel identified in previously-developed qualitative classifications, since both are characterised by properties such as sinuosity and channel geomorphic features, and can be further supported by information on bed material calibre. Three qualitative classifications are selected for comparison: Church (2006); Rosgen (1994) and the floodplain classification of Nanson and Croke (1992), since the latter incorporates floodplain as well as channel features. Because river class 1 in the present classification relates to large rivers, which appear to have the potential to split into at least two very different sub-types if a larger sample of river were available, the following comparisons will be confined to classes / types 2 to 6 of the present classification.

Church (2006) built on Schumm’s (1985) qualitative classification of alluvial channel forms to distinguish 17 channel types of which 10 are single thread types (Figure 6.2). These include six types of straight channel, with (types 1, 2, 5) or without (type 14) exposed bedforms and with mobile alternating bars (types 6, 9). These graded into a further four types of sinuous channel: slightly sinuous channels of different stability (type 3, 15) and more sinuous, truly meandering channels of different stability (types 10, 16).

Church’s development of Schumm’s (1985) classification, illustrates some of the types of in-channel features associated with each channel type as well as the calibre of the bed material. These properties provide a basis for identifying similarities with the

six classes identified in the present research. Church's types 1, 2, 3 and 5 have similar sinuosity and bed forms to class 2 of the present classification, Church's class 6 appears similar to the present class 3 since both are relatively high gradient types characterised by a low sinuosity and distinct lateral and mid channel bars. Church's class 9, with its intermediate gradient, low sinuosity and few in-channel features appears similar to the present class 4. Church's class 10 with its intermediate gradient, intermediate sinuosity and few in-channel features appears similar to the present class 5. Lastly, Church's classes 15 and 16, with their low gradient and intermediate to high sinuosity appear similar to the present class 6. The only single-thread type remaining in Church's classification, which is not obviously represented in the present classification, is type 14. This type has a low sinuosity but is in other ways similar to Church's classes 15 and 16, and so can be interpreted as a low sinuosity version of the present class 6. Based on the analysis of the bed material calibre of a subset of UK rivers, these similarities are also supported by the limited evidence on bed material calibre for each class: the present class 6 has the finest bed material (D_{50} : sand and finer), class 5 also has relatively fine bed material (D_{50} : sand to granules), whereas classes 3 and 4 display varied bed material size with D_{50} ranging from pebbles to cobbles. These correspond to the suggested calibre for the equivalent classes identified in Church's classification.

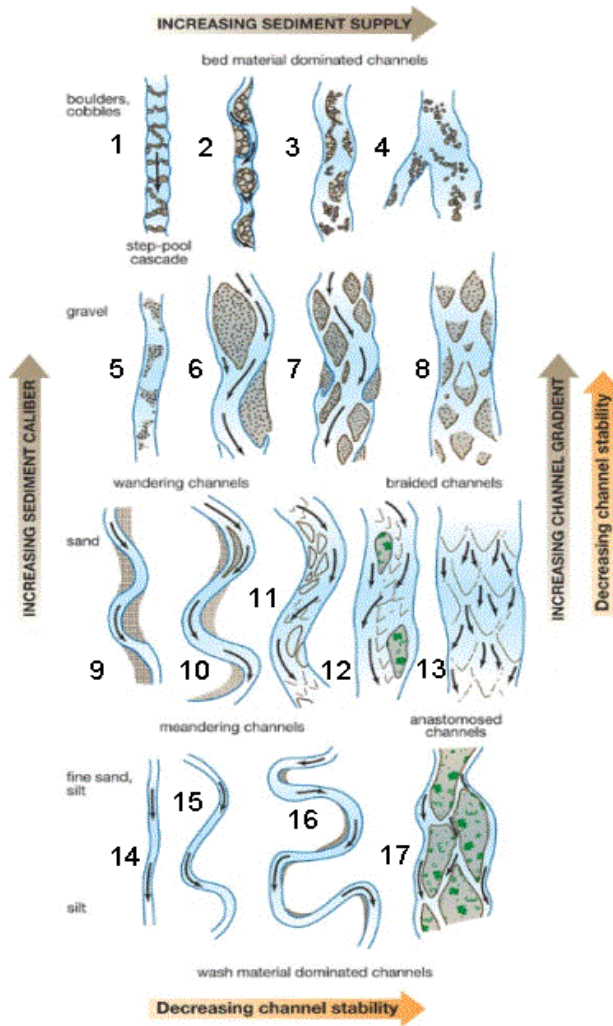


Figure 6.2 Classification of channel patterns (from Church, 2006)

Dominant Bed Material	A	B	C	D	DA	E	F	G
1 BEDROCK								
2 BOULDER								
3 COBBLE								
4 GRAVEL								
5 SAND								
6 SILT/CLAY								
ENTR.H.	<1.4	1.4-2.2	>2.2	N/A	>2.2	>2.2	<1.4	<1.4
SIN.	<1.2	>1.2	>1.4	<1.1	1.1-1.6	>1.5	>1.4	>1.2
W/D	<12	>12	>12	>40	<40	<12	>12	<12
SLOPE	.04-.099	.02-.039	<.02	<.02	<.005	<.02	<.02	.02-.039

Figure 6.3 Illustrations of classes of river channel based upon (i) their slope – sinuosity - cross profile - entrenchment (ratio of floodplain width to channel width), horizontally across the diagram, and (ii) their bed material calibre, vertically down the diagram.

Figure 6.3 provides a pictorial representation of some of Rosgen's river types. His classification allows for an extraordinarily wide range of combinations of slope, sinuosity, entrenchment and bed material calibre, many of which, as discussed below, are unlikely to occur in nature. Furthermore, his classification gives a poor representation of the bed and bank features that may be observed, which are fundamental to the present classification, and which Rosgen suggests are also incorporated in his classification. Therefore, comparison between the two classifications is difficult. Rosgen's types A, B, C, E, F and G are all single thread and so an attempt is made, below, to compare them with the present classification.

If we group types A, B, C, E, F and G according to their sinuosity, type A has the lowest sinuosity, types C, E and F have the highest sinuosity, and types B and G have an intermediate sinuosity. Therefore, at least initially, Rosgen's class A can be compared with the present classes 2 and 3, B and G can be compared with the present class 4, and C, E and F can be compared with present classes 5 and 6.

The present class 2 comprises steep channels with low sinuosity, displaying exposed bedrock and bar features, similar to Rosgen's class A channels with coarse bedrock (e.g. A1, A2), whereas the present class 3, has some vegetated bar features indicative of finer bed material and, based on UK evidence supports varied pebble to cobble bed material, similar to Rosgen's class A3 and A4 channels. The present class 4 channels, on UK evidence, are also characterised by pebble to cobble bed material but with a higher sinuosity than class 3 and with features such as vegetated bars and benches, which are indicative of lateral activity, indicating some similarity to Rosgen's B3 and B4, or possibly C3 and C4 channels. The present class 5 channels have high sinuosity, numerous floodplain features, and based on UK evidence, sand to granule (fine gravel) bed material, suggesting similarity with Rosgen's C4, C5, E4, E5 types (the type F entrenchment ratio suggests no significant floodplain and so is not an appropriate equivalent to class 5). The presence of emergent macrophytes is coherent with Rosgen's type E channels. Finally the present type 6 channels have high sinuosity but few in-channel or floodplain features, although they are associated with significant floodplains and the finest bed material, suggesting similarity with Rosgen's C5, C6, E5 and E6 types.

Table 6.1 Floodplain types identified by Nanson and Croke (1992) that are associated with single-thread rivers.

Type	Description	Specific stream power (ω in W/m^2)	Floodplain sediment	Planform	Geomorphic Features
High energy - non-cohesive floodplains					
A1	Confined, coarse-textured	>1000	boulders, gravel	Single thread, straight / irregular	Boulder levees, sand and gravel splays, back channels, scour holes
A2	Confined, vertical accretion	300-1000	gravel, sand	Single thread, straight / irregular	Large levees, deep back channels, scour holes
A3	Unconfined vertical accretion, sandy floodplains	300-600	sandy, interbedded muds	Single thread, wandering	Flat floodplain surface
A4	Cut and fill	~ 300	sand, silt, organic	Straight / irregular	Flat floodplain surface
Medium energy - non-cohesive floodplains					
B3 (with 4 sub-types)	Meandering, lateral migration	10-60	gravel, sand, silt	Meandering	Cut-bank erosion, lateral point bar accretion, counterpoint bar accretion, abandoned channels
	a. non-scrolled floodplain	10-60	gravel, sand, silt	Meandering	Cut-bank erosion, lateral point bar accretion, counterpoint bar accretion, abandoned channels
	b. scrolled floodplain	10-60	sand, minor gravel	Meandering	Cut-bank erosion, lateral point bar accretion, counterpoint bar accretion, abandoned channels, scroll bars
	c. backswamp floodplain	10-60	sand, silt, organic	Meandering	Cut-bank erosion, lateral point bar accretion, counterpoint bar accretion, abandoned channels, scroll bars
	d. counterpoint floodplain	10-60	sand, abundant silt, organic	Confined meandering	Cut-bank erosion, lateral point bar accretion, counterpoint bar accretion, abandoned channels, pronounced counterpoint accretion
Low energy, cohesive floodplains					
C1	Laterally stable, single channel	<10	silt, clay, organic	Straight / Meandering	Fat floodplain, low levees, backswamp

Nanson and Croke (1992) developed a genetic classification of floodplains in which they described the river planform, channel and floodplain geomorphic features, floodplain sediments (note that these are finer than the channel bed material) as well as suggesting an indicative range of specific unit stream power (at bankfull) with which the floodplain types are associated. Table 6.1 summarises these features for the floodplain types associated with single thread rivers.

From the information provided in Table 6.1, a number of similarities can be found with the present classification. The present class 2 channels are similar in their low sinuosity, high slope / energy, and coarse bed / floodplain / floodplain pocket material to Nanson and Croke's class A1, whereas the present class 3 channels are more akin to Nanson and Croke's class A2 in their low sinuosity, lower slope / energy than A2, and bars indicative of vertical accretion. The remaining types 4, 5 and 6, mainly show similarities to Nanson and Croke's class B3. Focussing on Nanson and Croke's subtypes for their class B3 floodplains, the present class 4 and 5 rivers appear to conform most closely, respectively, to subtypes a (unscrolled) and b (scrolled floodplain), reflecting differences in floodplain features. Rivers in the present class 6 appear to most closely conform to subtype c (backswamp floodplains) because they have insufficient floodplain features to fit subtype d (counterpoint floodplains). However, some rivers that fall into class 6 may be equivalent to Nanson and Croke's class C1 as a result of their low gradient, lack of channel or floodplain features, and based on UK evidence, fine bed / bank material.

The above comparisons show considerable coherence between the present classification and three other well-known and widely applied classifications. This is scarcely surprising, since all of these classifications are underpinned by a common set of process gradients, which were first identified by Lane (1955) in what is described as Lane's balance:

$$Q.S \sim Q_s. D_{50}.$$

where Q is water discharge, S is slope, Q_s is bed material load, and D_{50} is the median size of the bed material. Lane's balance implies that alluvial river reaches adjust to changes in four main controlling variables in a complementary way to achieve a dynamic equilibrium channel condition. Equilibrium is established when the amount of sediment transported into a reach is balanced by the amount transported out. Sediment

transport is controlled by the size of the sediment as well as the flow energy available to transport the sediment. If the flow has insufficient energy to transport sufficient sediment of a particular size range, sediment is deposited. This leads to steepening of the channel slope and thus an increase in the flow energy and its ability to transport sediment, and vice versa. As a result, channels tend towards an equilibrium condition combining slope and bed material size through processes of bed aggradation or degradation or lateral erosion and deposition. These processes create sets of geomorphic features within the river channel, some of which contribute to floodplain development and form. In these ways, processes linked through Lane's balance are related to the type or class of channel and floodplain that develops. This implies that we should recognise a continuum of channel styles rather than discrete classes. However, classifications are a useful basis for building channel descriptions that can be easily understood and used in a management context (see section 6.3.3).

The advantage of the present classification in comparison with those with which it is compared above, is that it is based on the presence of geomorphic and vegetation features with the classes being supported by measures of slope, bed/floodplain material and sinuosity, rather than the other way around. Thus river landscape evidence drives the classification, rather than a prescription based on dimensional data to which the river landscape is expected to conform. There are clearly benefits of using both types of approach when attempting to define and understand the river-floodplain type that is present and how it may be functioning.

None of the classifications discussed and compared above go beyond the reach scale, but they can be placed within spatially hierarchical approaches, that attempt to understand and quantify the processes acting at the reach scale (i.e. those incorporated in Lane's balance), by considering factors and processes at larger spatial scales (e.g. Brierley and Fryirs, 2005). This is the type of approach adopted by Gurnell et al. (2014), in which a river typology, floodplain typology and groundwater-surface water typology at the reach scale is combined with a flow regime typology at the river segment scale, and estimates of sediment production, delivery and transfer at landscape unit and river segment scales, to inform managers about river reach condition, character and dynamics.

6.3.2 Links between the Google Earth classification and bar theory.

This section explores whether links between the two types of classification should be expected, how strong and mutually reinforcing they are, and how they can be interpreted in a practical way.

The observed links between the Google Earth classification and the bar theory-based classification could be expected on the basis of the theoretical foundation of the bar theory and of the way bar theories have been used in the past as a rational channel pattern predictor. It is useful to briefly recall the rationale underpinning the bar theories to highlight why such links should be expected.

The outcomes of bar theories have often been used as rational predictors of channel pattern (e.g. Parker, 1976, Fredsoe, 1978). This is motivated by the fact that bar theories account for different types (or “modes”) of bar pattern, from alternate bars (mode 1) to central or mid-channel bars (mode 2), to multiple-row bars (mode 3 or higher). The transition from one bar type to the other is expressed within the theory through a coefficient that is commonly denoted by m (the “bar mode”). Alternate bars are obtained by setting $m=1$, central or mid-channel bars by $m=2$, multiple-row bars by $m=3$ or larger. The theory predicts the bankfull hydraulic conditions for which alternate bars are more unstable than the other ones and *vice versa*. The main underlying idea behind using bar theories as channel pattern predictors is based on establishing an analogy between the riverbed pattern of alternate bars and the planform pattern of single-thread rivers, and between the riverbed pattern of central bars (or higher modes) and the planform pattern of multi-thread rivers. Such an approach is based on conceptual simplifications of the actual complexity and has also shown many limitations in its predictive ability (e.g. Kleinhans and Van den Berg, 2011). It has been improved by Crosato and Mosselman (2009) who also allowed the indicator of bar mode m to be an arbitrary rational number, removing the previous constraint of m having to be an integer number as in previous approaches. Almost invariably, channel pattern predictors based on bar theories have resulted in some threshold value of the channel aspect ratio (denoted using β in Chapter 5) discriminating between single-thread and multi-thread channel patterns, and implying increasing morphological complexity with increasing bankfull aspect ratios.

The three-category based classification of single-thread rivers that was compared in Chapter 5 with the Google Earth-based classification is different from

previous bar theory-based predictors because (i) it concentrates on single-thread streams ($m=1$) and (ii) it jointly employs two aspect ratio thresholds ($\beta_{critical}$ and $\beta_{resonant}$) to define three categories of increasing morphological complexity with increasing aspect ratio β .

To summarize, the established results of previous applications of bar theory based channel pattern predictors yielding increasing morphological complexity for increasing aspect ratio supports the expectation of some links between the two types of classifications presented in this thesis. However, the obtained linkages (Figure 5.7 and Figure 5.12) are not obvious for two reasons. First, the two classifications have been developed from two very different approaches: fluid mechanics-based and geomorphologically-based. Second, the predictive ability of bar theory-based predictors has not previously been tested using a dataset that is comprised only of single-thread rivers, since their use as channel pattern predictors has previously been directed at predicting thresholds between single- and multi-thread channel patterns.

This said, and given the strong methodological foundations of both types of classification, the obtained links between them can be said to be quite robust, and the outcomes of the two classifications do mutually reinforce one another. From the perspective of theoretical, fluid mechanics based morphodynamic modelling the predictive potential of these theories is also better clarified compared with existing work, because very few field verifications have been provided so far for these theories (Welford, 1994; Zolezzi et al, 2012a, b; Adami et al, 2014) and most of them refer to only one or a few case studies, rather than the large dataset used in the present analyses.

6.3.3 The usefulness of the Google Earth classification and its potential application in Management

As discussed in section 6.3.1, unlike many previous classifications, which have tended to use a few properties or dimensions (e.g. bed material calibre, bankfull discharge, slope) to identify the class of a river reach, the present classification couples dimensional properties (e.g. slope, width, sinuosity) with geomorphic and vegetation features that describe what the river and flood plain look like. The present classification method has a number of practical advantages when compared with these previous methods:

- (i) Despite the fact that the approach is different, the classification is coherent with several other commonly used classifications (see section 6.3.1), and thus it maintains some consistency of classification.
- (ii) It uses a single freely-available data source which is available for the entire Earth's surface, albeit with variable resolution. This is an enormous strength, since there are no data barriers to application of the technique, and the data can be assembled quite rapidly. Indeed, once some of the suggestions for further research have been pursued (see sections 6.4 and 6.5), it will be possible to apply the method even more rapidly and over much wider geographic areas.
- (iii) By incorporating geomorphic and vegetation features as well as dimensional data into the classification, the method should be particularly useful in a management context. These features can be considered to be the "building blocks" of river systems (Brierley, 1996), embodying the set of process interactions in operation at a particular location. The approach outlined in this thesis provides managers with a concept of what the river and floodplain should look like given a set of broad dimensions. It, therefore, has the potential to allow comparison of river reaches with similar dimensions to see how feature rich they are, perhaps even defining reference sites that are both feature-rich and also 'typical' for an area. This is the approach that was used in chapter 4 to assess the degree to which 'restored' reaches were displaying the characteristics of more naturally 'functioning' reaches located nearby. It also has the potential to inform river restoration planning by helping managers to determine the types of habitat features that could be sustainably achieved under a given set of design boundary conditions.
- (iv) Although some properties, such as bed material calibre and stream power, cannot be directly extracted from Google Earth, it appears that the classification can be used to infer both of these properties from the attributed class. This provides managers with additional useful information, when field observations of these properties are not initially available.
- (v) Once further research has been conducted to place probabilistic boundaries on the classes, so that a newly surveyed reach can be allocated to a class without using the PCA loadings (see section 6.5.3), it should be possible to emphasise which are the key discriminatory variables and what are the likely ranges of

geomorphic and vegetation features that are associated with each class. To achieve this probably requires several more months of research effort, but at that point it should be possible to assemble a descriptive table rather like that of Nanson and Croke's floodplain classification (Table 6.1), which would give users an even fuller portrait of what rivers look like and how they function within each class.

(vi) Finally, in the context of the practical assessment of the appropriateness or success of restoration interventions (linked to WFD targets) the following applications of the research can be envisaged.

- *Measurement of the morphological success of river restoration actions*

The research in collaboration with the Environment Agency reported in section 4.8 has illustrated that the comparison of PC scores of restored and nearby 'near-natural' reaches (Figure 4.17) is an effective means of assessing the degree to which a restored reach has achieved similar geometric, geomorphic and vegetation properties and thus has achieved characteristics similar to nearby 'reference' reaches. This illustrates one way in which the present research can help to assess the effectiveness of river restoration schemes. This aspect of the research could be further developed.

- *Initial assessment of geomorphic river condition before applying restoration strategies*

The use of PC scores, as described above for assessing the morphological success of restoration, could also be applied to a reach prior to restoration. This could save time and money since information is already available (Google Earth) from which an initial conclusion could be drawn concerning the extent to which the morphological properties and condition of the reach do not match nearby 'reference' reaches (based on PC scatterplots). In this way, the analysis tools developed in this thesis could facilitate the assessment of the geomorphic condition of a reach prior to restoration.

6.4 Limitations of the research

The research presented in this thesis has produced very strong results in terms of an observation-based river classification that has been confirmed by testing and that corresponds to a theoretically-based classification of single thread rivers. It is coherent with previous research while reflecting some new properties that are characteristic of the European landscapes for which it was developed (see section 6.3). Nevertheless, there are limitations that need to be fully described as they may have had an impact on the research outcomes. Furthermore some aspects of these limitations need to be addressed in future research to make the classification more easily applicable by managers (see section 6.5)

6.4.1 Google Earth as a data source

Perhaps the most significant limitations may relate to the use of Google Earth as the central information source. The following limitations of using Google Earth as tool to extract river information were identified:

- (i) The analysis depended upon identifying naturally-functioning rivers, but these are not easily perceptible from an entirely aerial view. Direct human interventions such as bank reinforcements could have been missed and would undoubtedly have affected the features that were recorded.
- (ii) Heavy and overhanging riparian vegetation may have hindered the visualization of important channel features. An entirely aerial view can lead to natural as well as human-induced features to be missed. Geomorphic features such as wood jams, benches and bars can be small enough to be easily obscured by vegetation, and ground vegetation (e.g. aquatic macrophyte coverage) can also be obscured. This may explain the lack of wood features in many of the classes and could contribute to the differences between the low gradient, high sinuosity classes 5 and 6. The former is characterised by low tree cover but has a relatively high range of geomorphic features and also high macrophyte cover, and the latter is characterised by well-developed riparian vegetation and few geomorphic features. Nevertheless, macrophytes and riparian trees tend to occur in inverse proportions in nature, and well developed riparian woodland is often indicative of very stable river environments that would not be expected to show a wide range of distinct geomorphic features.

- (iii) The flow conditions at the time of imagery may have affected the features that were identified and recorded. Although the intention was to use images taken at baseflow conditions, this is difficult to judge from the imagery alone. Fortunately most of Europe is covered by more than one image within Google Earth, so it was possible to select the most suitable image on grounds of clarity as well as apparent flow conditions. Nevertheless, the identification of features such as bars, benches, pools and riffles is affected by the flow stage and may lead to the mis-classification of reaches if the analysed image is at a relatively high flow stage.
- (iv) While the introduction of Google Earth's historical image archive function means that temporal variability and trends in river form and features can be assessed, the patchy and often short temporal coverage of the image database limit opportunities to expand the classification into the realm of river behaviour (c.f. Brierley and Fryirs, 2005).

6.4.2 Thorough testing of the classification

Although every attempt was made to test the classification thoroughly, further testing would be feasible if more information was available:

- (i) Trends in the frequency distribution of channel and floodplain properties and their geographical distribution across the classes. Although box plots revealed clear (increasing/decreasing) trends in most variables across the six river classes, other variables did not show clear differentiation between classes. This raises the question of whether there is no such discrimination of these features between classes or whether the features were not sufficiently well-defined and recorded. This may simply reflect the issues already listed in 6.3.1 concerning the use of Google Earth as an information source, and it suggests that some ground testing of the presence of features might contribute to a better assessment of the classification.
- (ii) Testing the classification using traditional data sets. An attempt was made in Chapter 4 to test the classification using discharge and sediment data. Whilst discharge data was available for the majority of the 75 investigated rivers,

properly constrained estimates of sediment properties were not available for any of the rivers.

Undoubtedly a full set of gauged flow records for the 75 rivers would have provided the most robust basis for testing the classification, but the records that were available were spread across all river classes and were also available for a wide geographical distribution of sites across Europe. Unfortunately, this was not the case for the sediment data. An analysis could only be conducted on some of the British rivers and it had to make use of a subjective data set drawn from RHS surveys. Bed sediment calibre is central to many river classifications, and so this lack of good quality bed material data with a trans-European distribution is a significant limitation in the testing of the classification.

(iii) Improvements that could be made to address the limitations in testing

Given more time, the following improvements could be made to testing and ensuring the robustness of the classification:

1. Incorporating a larger sample of reaches that fall into Classes 1 and 2. One of the outcomes of the classification is that only 13 and 14 reaches out of the 221 analysed fell into classes 1 and 2. In part this reflects the difficulty of finding naturally-functioning reaches that fall into these classes. The large river class (class 1) is particularly challenging, because most large rivers in Europe have been quite heavily modified. Class 2 includes steep mountain rivers. While the sample size here could be quite easily increased, their typical location in steep narrow valleys may result in poorer accuracy in the elevation values extracted from Google Earth, and they may be less likely to be located close to good quality flow gauging stations. Nevertheless, it should be possible to increase the sample size in both classes if this were the specific aim of reach selection.
2. Quantifying bed sediment properties more accurately. Characterisation of any aspect of sediment has proved difficult, but options could include analysis of more British rivers to improve the coverage of the river classes with RHS data, or a focussed field campaign taking direct measurements of bed material calibre on a carefully-selected sample of reaches in each of the classes.

3. Applying the classification to a second independent data set. At present the classification has been devised using a single data set from 75 rivers, and testing has been confined to evaluating whether the classification that is based entirely on data from Google Earth 'makes sense' when it is explored in relation to flow and sediment information that has been more traditionally used to guide such classifications. An additional approach to testing the validity of the classification, would be to extract a second data set from Google Earth and then repeat the analysis to assess whether the outcome is essentially the same as that derived from the first set. During this exercise, it would be particularly beneficial to try to incorporate some sites from the extreme northern Atlantic area, the southern part of the Mediterranean area and the eastern part of the Continental area of Europe. This would extend the geographical range of the data previously analysed and so could test the applicability of the classification beyond the geographical range of the original data set as well as on a set of different rivers within the same geographical range.
4. Operator variance. Another element that needs to be tested is operator variance. At present only one operator has devised the rules for data extraction and has then extracted and analysed data from Google Earth. If others are to use the classification and apply it to different rivers, then it is important to know how the robustness of the guidelines. In developing recommendation 3, a subset of rivers (ca. 30 reaches) with contrasting properties could be analysed by a sample of different operators (ca. 10), to provide a sufficient data set for operator variance to be explored in relation to each of the properties that are quantified. This would allow a sensitivity analysis to be conducted in relation to each property so that those that show high sensitivity could either be removed from the list or the guidelines for their identification / quantification could be improved. For example, it might be necessary to increase the number of channel width measurements extracted from the present 40 to ensure that the four different measures of channel width are quantified more consistently.
5. Reach definition. The sensitivity of the classification to changes in reach length and boundary locations should also be examined. The approach currently uses a minimum reach length that is scaled on channel width. This

is not only pragmatic but also grounded in the principle that the spacing of many in-channel features (e.g. riffles and pools) tends to scale relatively consistently in relation to channel dimensions (Keller and Melhorn, 1978). Nevertheless, recent advances in the use of global boundary hunting algorithms to identify reach boundaries on the basis of their internal properties (e.g. Parker et al., 2012) could potentially be exploited to ensure reaches are composed of truly distinctive assemblages of features and maximise differences between river types.

6.5 Recommendations for future research

This thesis has produced a classification of European rivers that appears to be robust and offers the possibility for further development if more research time were available. The following summarises some of the most promising areas for future research:

6.5.1 Increasing the size and quality of the data set

In section 6.3.2, suggestions were made to improve the quantity and quality of the data available for analysis. This would be an obvious first step in extending the research.

6.5.2 Increasing the complexity of the classification

From a scientific viewpoint a hierarchical classification would be appealing. In chapter 4, first splits of each of the classes were considered, but with the availability of a larger data set, a hierarchical classification could be developed, whereby the 6 classes could be divided into sub-classes and perhaps even further sub-divisions. This might result in a more detailed and satisfactory classification for European regions where only a few of the six classes exist.

6.5.3 Developing the classification into an applicable tool for river managers

Whether or not a more complex classification were to be devised, one obvious research element that could not be pursued because of time constraints, but would be essential if the classification were to be applied operationally, is to develop a simple way of allocating a newly-surveyed reach to a class.

In this thesis, the aggregate PCA PC1-PC2 plot has been used to compare the scores of a newly-surveyed reach with those of reaches allocated to particular classes. From this, the most appropriate class has been inferred. However, an operator-free method is needed to ascertain the most appropriate class for a newly surveyed reach, since the thresholds between classes are in some cases poorly-defined on the aggregate PCA plot.

There is a need to develop a classification methodology that can automatically assign a river to a class based upon clear threshold conditions related to specific river properties. Such an approach requires further detailed investigation of the existing data set. This could be achieved by a combination of expert judgment and the application of statistical tools such as multiple discriminant analysis (a similar method to PCA, but it attempts to model the difference between the classes) coupled with maximum likelihood techniques (which help to estimate the most likely threshold between overlapping frequency distributions). Expert judgement is needed to select the most informative combination of variables and their likely contribution to discriminating particular classes.

6.5.4 Applying the classification in practice

The SMART collaboration with an associate partner, the Environment Agency, led to the idea of assessing restored reaches using the classification. The final section of chapter 4 produced some interesting results on this issue. A small number of restored reaches were investigated by comparing the degree to which the restored reaches were allocated to similar river classes to nearby apparently naturally-functioning reaches. Although, due to time limitations, this was only a small-scale study, it raises issues of how the classification and its geomorphic properties could be used in river assessment and restoration design. Exploring this subject would introduce direct application of the research knowledge to real river cases and problems, and it could provide a link between research and application that might be relevant to meeting the objectives of the EU Water Framework Directive.

6.5.5 Linking the classification to theory

Chapter 5 attempted to find correspondence between ‘bar theory’ and the classification developed in this thesis. The clear correspondence between a theory-based and an observation-based classification were both surprising and exciting. Because of the limited sample size available for this analysis, a promising direction for further

research would be to analyse a larger set of reaches using this approach and then to explore in more detail, using as many data sources as possible including field survey, the fundamental links between the two approaches. In particular, it would be useful to focus in detail on natural bars and the features that develop from them (benches, scrolls etc.) in real rivers and consider how these reflect the properties represented in theory.

6.6 Conclusion

Overall, the research in this thesis has led to the development of a new, robust classification of European single thread rivers that has interesting correspondence to theory. It has also demonstrated how Google Earth can provide invaluable information on river geomorphological characteristics, if it is used with care.

The research has great potential for further development both in relation to its scientific significance and meaning, and also in relation to its practical application. A set of future research objectives have been defined, which can support these endeavours, so that the research can develop further and become something that is useable by river managers.

REFERENCES

- Ackers, P., and Charlton, F. G. (1970a). *Meandering of small streams in alluvium. Rep No. INT 77*. Wallingford, Berkshire, England: Hydraulics Research Station.
- Ackers, P., and Charlton, F. G. (1970b). The slope and resistance of small meandering channels. *Proceedings of the Institution of Civil Engineers*, 47(Supplementary Paper), 7362-S,349-70.
- Adami, L., Bertoldi, W., and Zolezzi, G. (2014). Morphodynamics of alternate bars in the Alpine Rhine River: methods for the applicability of mathematical models using fields observations. Lausanne: River Flow.
- Alabyan, A., and Chalov, R. S. (1998). Types of river channel patterns and their natural controls. *Earth Surface Processes and Landforms, Wiley*, 23, 467-74.
- Allmendinger, N. E., Pizzuto, J. E., Potter, N. J., Johnson, T. E., and Hession, W. C. (2005). The influence of riparian vegetation on stream width, eastern Pennsylvania. *USA GSA Bulletin*, 117(1/2), 229-43.
- American Society of Civil Engineers. (1982). Relationship between morphology of small streams and sediment yield. *Journal of the Hydraulic Division*, 1328-65.
- Amoros, C., Richardot-Coulet, M., and Pautou, G. (1982). Les "ensembles fonctionnels" : des entités écologiques qui traduisent l'évolution de l'hydrosystème en intégrant la géomorphologie et l'anthropisation (exemple du Haut-Rhône français) . *Revue de géographie de Lyon*, 57(1), 49-62.
- Ashmore, P. E. (1991). How do gravel-bed rivers braid? *Canadian Journal of Earth Sciences*, 28(3), 326-41.
- Bagnold, R. A. (1966). An approach to the sediment transport problem from general physics. *US Geological Survey Professional Paper*, 422(I), 37.
- Bagnold, R. A. (1977). Bed load transport by natural rivers. *Water Resources Research*, 13(2), 303-12.

- Beechie, T.J., Sear, D.A., Olden, J.D., Pess, G.R., Buffington, J.M., Moir, H., Roni, P., Pollock, M.M., (2010). Process-based Principles for Restoring River Ecosystems. *BioScience*, 60, 209-222.
- Beeson, C. E., and Doyle, P. F. (1995). Comparison of bank erosion at vegetated and non-vegetated channel bends. *Water Resource Bulletin*(31), 983-90.
- Bisson, P. A., Nielson, J. L., Palmason, R. A., and Grove, L. E. (1982). A system of naming habitat types in small streams, with examples of habitat utilization by salmonids during low stream flow. In N. B. Armantrout, *Acquisition and utilization of aquatic habitat inventory information* (pp. 62-73). Portland, Oregon, USA: Western Division, American Fisheries Society.
- Blondeaux, P., and Seminara, G. (1985). A unified bar-bend theory of river meanders. *Journal of Fluid Mechanics*, 157, 449-70.
- Bluck, B. (1971). Sedimentation in the meandering River Endrick. *Journal of Geology*, 7, 93-138.
- Brice, J. C. (1974). Evolution of Meander Loops. *Geological Society of American Bulletin*, 85, 581-85.
- Brice, J. C. (1975). Air photo interpretation of the form and behavior of alluvial rivers. 10p. st Louis: Washington University.
- Brice, J. C. (1982). Stream channel stability assessment. 42. Federal Highway Administration.
- Brice, J. C. (1984). Planform properties of meandering rivers. In C. M. Elliot, *River Meandering* (pp. 1-15). New Orleans: American Society of Civil Engineers.
- Bridge, J.S. (2003) *Rivers and Floodplains: Forms, Processes and Sedimentary Record*, Blackwell, 491pp.
- Brierley, G. J. (1996). Channel morphology and element assemblages: A constructivist approach to facies modelling. In P. Carling, and M. Dawson, *Advances in Fluvial Dynamics and Stratigraphy* (pp. 263-98). Chichester: Wiley Interscience.

- Brierley, G.J., Fryirs, K.A., (2005). *Geomorphology and River management: Applications of the River Styles Framework*, Blackwell.
- Brookes, A. (1987). The distribution and management of channelized streams in Denmark. *Regulated Rivers: Research and Management*, 1, 3-16.
- Callander, R. A. (1969). Instability and River Channels. *Journal of Fluid Mechanics*, 36(pt 3), 465-80.
- Camporeale, C., Perona, P., Porporato, A., and Ridolfi, L. (2005). On the long-term behaviour of meandering rivers. *Water Resource Research, AGU*, 41, 13.
- Carson, M. A. (1984). The meandering-braided river threshold: a reappraisal. *Journal of Hydrology*, 73, 315-34.
- Cattell, R. B. (1996). The scree test for the number of factors. *Multivariate Behavioral Research*, 1, 245-76.
- Chezy, A. (1776). Formule pour trouver la vitesse constant que doit avoir l'eau dans une rigole ou un canal dont la pente est donnée. In *Dossier 847 (MS 1915) of the manuscript collection of the Evole des Ponts et Chaussées. Reproduced as Appendix 4 Mouret (1921)* (pp. 247-51).
- Chin, A. (2003). The geomorphic significance of step-pools in mountain streams. *Geomorphology*, 55(1-4), 125-37.
- Church, M. (1992). Channel morphology and typology. In P. Calow, and G. E. Petts (Eds.), *The River Handbook* (1st ed., pp. 129-58). Oxford: Blackwell.
- Church, M. (2002). Geomorphic thresholds in riverine landscapes. *Freshwater Biology*, 47, 541-57.
- Church, M. (2006). Bed material transport and the morphology of alluvial river channels. *Annual Review of Earth and Planetary Sciences*, 34, 325-54.
- Church, M. A. (1984). On experimental method in geomorphology. In T. P. Burt, and D. E. Walling (Eds.), *Catchment experiments in fluvial geomorphology* (pp. 563-80). Norwich: Geo Books.
- Church, M., and Jones, D. (1982). Channel bars in gravel-bed rivers. In R. D. Hey, J. Bathurst, and C. R. Thorne (Ed.). Chichester, England: John Wiley and Sons.

- Church, M., and Rice, S. (2009). Form and growth of bars in a wandering gravel-bed rivers. *Earth Surface and Process Landforms*, 34, 1422-32.
- Coleman, J. M. (1969). Brahmaputra River: channel processes and sedimentation. *Sedimentary Geol*, 3(2-3), 129-239.
- Colombini, M., Seminara, G., and Tubino, M. (1987). Finite-amplitude alternate bars. *Journal of Fluid Mechanics*, 181, 212-32.
- Crosato, A. (1987). Simulation model of meandering processes of rivers. Genoa, Italy: Euromech 215 Conference, Univ. of Genoa.
- Crosato, A. (2008). *Analysis and modelling of river meandering*. Amsterdam, The Netherlands: IOS Press.
- Crosato, A., and Mosselman, E. (2009). Simple physics-based predictor for the number of river bars and the transition between meandering and braiding. *Water Resources Research*, 45(3), WO3424. doi:10.1029/2008WR007242
- Davies, N. S., and Gibling, M. R. (2009). *Lower Palaeozoic Alluvial Systems: The Sedimentological Impact of Evolving Vegetation in Terrestrial Environments*. Vienna: EGU General Assembly Conference Abstract 11, 3124.
- Davies, N. S., and Gibling, M. R. (2010). Paleozoic vegetation and the Siluro-Devonian rise of fluvial lateral accretion sets. *Geology*, 38(1), 51-4.
- De Vriend, H. (1981). *Steady flow in shallow channel bends*. PhD Thesis. Delft: Communication on Hydraulics, Dept. of Civil Engineering, Delft University of Technology, The Netherlands.
- Edgar, D. (1984). The role of geomorphic thresholds in determining alluvial channel morphology. 44-54.
- Einstein, H. A. (1950). *The bedload function for sediment transport in open channel flow*. US Dept. Agric. Tech. Bull.
- Engelund, F., and Hansen, E. (1972). *A Monograph on Sediment Transport in Alluvial Streams*. Copenhagen: Danish Technical Press.

- Environment Agency. (2003). *River Habitat Survey in Britain and Ireland, Field Survey Guidance manual: 2003 Version*. Almondsbury, Bristol, UK: Environment Agency.
- Eschner, T. R., Hadley, R. F., and Crowley, K. D. (1983). Hydrologic and morphologic changes in channels of the Platte River Basin in Colorado, Wyoming and Nebraska: a historical perspective. *U.S. Geological Survey*, A1-A39.
- Everitt, B. S., Landau, S., and Leese, M. (2001). *Cluster analysis* (4th ed.). London: Arnold.
- Farr, T. G., Rosen, P. A., Caro, E., Crippen, R., Duren, R., Hensley, S., . . . Alsdorf, D. (2007). The Shuttle Radar Topography Mission. *Reviews of Geophysics*, 45, art no. RG2004.
- Ferguson, R. I. (1973). Regular meander path models. *Water Resources Res*, 9, 1079-86.
- Ferguson, R. I. (1975). Meander irregularity and wavelength estimation. *Journal of Hydrology*, 26, 315-33.
- Ferguson, R. I. (1979). River meanders: regular or random? In N. Wrightley, *Statistical application in spatial sciences* (pp. 229-41). London: Pion.
- Ferguson, R. I. (1981). Channel form and channel changes (Britain). In L. J. (Ed.), *British Rivers* (pp. 90-125). Stirling: George Allen and Ulwin.
- Ferguson, R. I. (1987). Hydraulic and sedimentary controls of channel pattern. In K. Richards, *River Channels: environmental and process* (pp. 129-58). Oxford: Blackwell.
- Ferguson, R. I., Hoey, T. B., Wathen, S. J., Hardwick, R. I., and Sambrook Smith, G. H. (1998). Downstream fining by selective deposition: theory, laboratory, and field observation. In P. C. Klingeman, R. L. Beschta, P. D. Komar, and J. B. Bradley (Eds.), *Gravel-bed rivers in the environment* (pp. 85-114). Highlands Ranch, Colorado, U.S.A.: Water Resources Publications, LLC.
- Fredsøe, J. (1978). Meandering and braiding of rivers. *Journals of Fluid Mechanics*, 84(4), 609-24.

- Friedkin, J. F. (1945). *A laboratory study of the meandering of alluvial rivers*. Vicksburg, Mississippi, U.S.A.: U.S. Army Engineer Waterways Experiment Station.
- Frissel, C. A., Liss, W. J., Warren, C. E., and Hurley, M. D. (1986). A hierarchical framework for stream habitat classification: viewing streams in a watershed context. *Environmental Management*, 10, 199-214.
- Garde, R. J., and Raju, K. G. (1977). *Mechanics of sediment transportation and alluvial stream problems*. New Delhi: Wiley Eastern.
- Gasparini, N. M., Tucker, G. E., and Bras, R. L. (1999). Downstream fining through selective particle sorting in an equilibrium drainage network. *Geology*, 27(12), 1079-82.
- Google. (2013, May 2013). *Google Earth*. Retrieved from Google: http://www.google.co.uk/intl/en_uk/earth/
- Goudie, A. S. (1990). *Geomorphological Techniques*. New York: Routledge.
- Gran, K., and Paola, C. (2001). Riparian vegetation controls on braided stream dynamics. *Water Resources Research*, 37(12), 3275-83.
- Grant, G. E., Swanson, F. J., and Wolman, M. G. (1990). Pattern and origin of stepped-bed morphology in high-gradient streams, Western Cascades, Oregon. *Bulletin of the Geological Society of America*, 102(3), 340-52.
- Grenfell, M., Aalto, R., and Nicholas, A. (2012). Chute channel dynamics in large, sand-bed meandering rivers. *Earth Surface Processes and Landforms*, 37(3), 315-31.
- Gurnell, A.M., Belletti, B., Bizzi, S., Blamauer, B., Braca, G., Buijse, T., Bussettini, M., Camenen, B., Comiti, F., Demarchi, L., García de Jalón, D., González del Tánago, M., Grabowski, R.C., Gunn, I.D.M., Habersack, H., Hendriks, D., Henshaw, A., Klösch, M., Lastoria, B., Latapie, A., Marcinkowski, P., Martínez-Fernández, V., Mosselman, E., Mountford, J.O., Nardi, L., Okruszko, T., O'Hare, M.T., Palma, M., Percopo, C., Rinaldi, M., Surian, N., Weissteiner, C., Ziliani, L. (2014). A hierarchical multi-scale framework and indicators of hydromorphological processes and forms. Deliverable 2.1, a

report in four parts of REFORM (REstoring rivers FOR effective catchment Management), a Collaborative project (large-scale integrating project) funded by the European Commission within the 7th Framework Programme under Grant Agreement 282656.

- Gurnell, A. M., Bertoldi, W., and Corenblit, D. (2012). Changing river channels: The roles of hydrological processes, plants and pioneer fluvial landforms in humid temperate, mixed load, gravel bed rivers. *Earth Science Reviews*, *111*, 129-41.
- Gurnell, A. M., O'Hare, J. M., O'Hare, M. T., Dunbar, M. J., and Scarlett, P. M. (2010). An exploration of the association between assemblages of aquatic plant morphotypes and channel geomorphological properties within British rivers. *Geomorphology*, *116*(1-2), 135-44.
- Gurnell, A. M., O'Hare, M. T., O'Hare, J. M., Scarlett, P., and Liffen, T. R. (2013). The geomorphological context and impact of the linear emergent macrophyte, *Sparganium erectum* L.: A statistical analysis of observations from British rivers. *Earth Surface Processes and Landforms*, *38*(15), 1869-80.
- Gurnell, A. M., Petts, G. E., Hannah, D. M., Smith, B. G., Edwards, P. J., Kollman, J., Tockner, K. (2001). Riparian vegetation and island formation along the gravel-bed Fiume Tagliamento. *Earth Surface Processes and Landforms*, *26*, 31-62.
- Habersack, H.M., (2000). The river-scaling concept (RSC): a basis for ecological assessments. *Hydrobiologia*, *422*, 49-60.
- Halwas, K. L., and Church, M. (2002). Channel units in small, high gradient streams on Vancouver Island, British Columbia. *Geomorphology*, *43*(3-4), 243-56.
- Harvey, D. (1969). *Explanation in geography*. London: Edward Arnold.
- Hey, R. D., and Thorne, C. R. (1986). Stable channels with mobile gravel beds. *Journal of Hydraulic Engineering, ASCE*, *112*(8), 671-89.
- Hickin, E. J. (1984). Vegetation and river channel dynamics. *Canadian Geographer*, *28*(2), 111-26.

- Hickin, E. J., and Nanson, G. C. (1984). Lateral migration rates of river bends. *Journal of Hydraulic Engineering*, 110, 1557-67.
- Hooke, J. M. (1980). Magnitude and distribution of rates of river bank erosion. *Earth Surface Processes and Landforms*, 5, 143-57.
- Hooke, J. M. (1995). River channel adjustment to meander cutoffs on the River Bollin and River Dane, northwest England. *Geomorphology*, 14, 235-53.
- Hooke, J. M. (2004). Cutoffs galore!: occurrence and causes of multiple cutoffs on a meandering river. *Geomorphology*(61), 225-38.
- Hooke, J. M., and Harvey, A. M. (1983). Meander changes in relation to bend morphology and secondary flows (River Dane, Cheshire). *Modern and ancient fluvial systems. Spec. Publs. Int. Ass. of Sediment*, 6, 121-32.
- Hooke, J. M., and Kain, R. P. (1982). *Historical change in the physical environment: a guide to sources and techniques*. London: Butterworth.
- Hooke, J. M., and Yorke, L. (2011). Channel bar dynamics on multi-decadal timescales in an active meandering river. *Earth Surface Processes and Landforms*, 36, 1910-28.
- Howard, A. D., and Hemberger, A. T. (1991). Multivariate characterization of meandering. *Geomorphology*, 4, 161-86.
- Hynes, H. B. (1975). Edgardo Baldi Memorial Lecture. The stream and its valley. *Verh. Internat. Verein. Limnol*, 19, 1-15.
- Ibisate, A., A. Ollero., E. Díaz, (2011). Influence of catchment processes on fluvial geomorphology and river habitats. *Limnetica*, 30(2), 169-182.
- Ikeda, S., Parker, G., and Sawai, K. (1981). Bend theory of river meanders. Part 1. Linear Development. *Journal of Fluid Mechanics*, 112, 363-77.
- Jagers, H. (2003). *Modelling planform changes of braided rivers. PhD thesis*. Twente: University of Twente, the Netherlands.
- Jang, C. L., Shimizu, Y., and Miyazaki, T. (2003). Vegetation effects on channel development in river with erodible banks. In A. Sances-Arcilla, and A. Bateman (Eds.), *River, Coastal and Estuarine Morphodynamics: RCEM*

2003, Barcelona, 1-5 Sept. 2003 ISBN: 90-805649-6-6 (pp. 547-57). Madrid: IAHR.

- Johannesson, H., and Parker, G. (1989). Linear theory of river meanders. In: *River Meandering*, S. Ikeda and G. Parker (eds.) Water Resour. Monogr. Ser., vol. 12, , pp. 181–213, AGU, Washington, D.C.
- Jolliffe, I. T. (2002). *Principal Component Analysis* (2nd ed.). New York: Springer.
- Kalkwijk, J. P., and de Vriend, H. J. (1980). Computation of the flow in shallow river bends. *Journal of Hydraulic Research, IAHR*, 18(4), 327-42.
- Keller, E.A. and Melhorn, W.N, (1978) Rhythmic spacing and origin of pools and riffles. *Geological Society of America Bulletin*, 89, 723-730.
- Kellerhals, R., Church, M., and Bray, D. I. (1976). Classification of river processes. *Journal of the Hydraulics Division American Society of Civil Engineers*, 102, HY7, 813-29.
- Kleinhans, M. G., and Van den Berg, J. H. (2011). River channel and bar patterns explained and predicted y an empirical and a physics-based method. *Earth Surface Processes and Landforms*, 36, 721-38.
- Knighton, A. D., and Nanson, G. C. (1993). Anastomosis and the continuum of channel pattern. *Earth Surface Processes and Landforms*, 18, 613-25.
- Knighton, D. (1998). *Fluvial Forms and Processes: A New Perspective*. London: Oxford University Press.
- Kondolf, G. M. (1995). Geomorphological stream channel classification in aquatic habitat restoration: uses and limitation. *Aquatic Conservation*, 5, 127-41.
- Kurabayashi, H., and Shimizu, Y. (2003). Experiments on braided stream with natural vegetation. In M. I.-8.-6.-6. IAHR (Ed.), *River, Coastal and Estuarine Morphodynamics* (pp. 799-806). Barcelona, 1-5 Sept. 2003: Sánces-Arcilla A. and Bateman.
- Lagasse, P. F., Spitz, W. J., Zevenbergen, L. W., and Zachman, D. W. (2004). Handbook for predicting stream meander migration. In *NHCRP Rep 533* (p. 107). National Highway Research Program.

- Lane, E. W. (1955). Design of Stable Channels. *Transactions, Am. Soc. Civil Eng*, 120, 1234.
- Langbein, W. B., and Leopold, L. B. (1964). Quasi equilibrium states in channel morphology. *American Journal of Science*, 782-94.
- Langbein, W. B., and Leopold, L. B. (1966). River meanders--theory of minimum variance. *United States Geological Survey Professional Paper*, 422H.
- Lanzoni, S., and Tubino, M. (1999). Grain sorting and bar instability. *Journal of Fluid Mechanics*, 383, 149-74.
- Lanzoni, S., Federici, B., and Seminara, G. (2005). On the convective nature of bend instability. In G. Parker, and M. H. Garcia (Eds.), *River, Coastal and Estuarine Morphodynamics: RCEM 2005* (pp. 719-24). London: Taylor and Francis Group. ISBN 0415392705.
- Leopold, L. B., and Wolman, M. G. (1957). River channel patterns-braided, meandering and straight. *United States Geological Survey Professional Paper*, 282B, 39-85.
- Leopold, L. B., and Wolman, M. G. (1960). River meanders. *Bulletin of the Geological Society of America*, 71, 769-94.
- Leopold, L. B., Wolman, M. G., and Miller, J. P. (1964). *Fluvial Processes in Geomorphology*. San Francisco: Freeman.
- Lewin, J. (1978). Floodplain morphology. *Progress in Physical Geography*, 2, 408-37.
- Lewin, J. (1983). Changes in channel pattern and floodplain. In K. J. Gregory, *Background to paleohydrology* (pp. 303-19). Chichester, UK: Wiley.
- Lotspeich, F. B. (1980). Watersheds as the basic ecosystem: this conceptual framework provides a basis for a natural classification system. *Water Resources Bulletin*, 16(4), 581-586.
- Luchi, R., Zolezzi, G., and Tubino, M. (2011). Bend theory of river meanders with spatial width variations. *Journal Fluid Mechanics*, 681, 311-39.
- Makaske, B., Smith, D., Berendsen, H., de Boer, A., van Nielen-Kiezebrink, M., and Locking, T. (2009). Hydraulic and sedimentary processes causing

- anastomosing morphology of the upper Columbia River. *Geomorphology*, *111*, 194-205.
- Martin, Y., Rood, K., Schwab, J. W., and Church, M. (2002). Sediment transfer by shallow landsliding in the Queen Charlotte Islands, British Columbia. *Canadian Journal of Earth Sciences*, *39*(2), 189-205.
- Meitzen, K.M., Doyle, M.W., Thoms, M.C. and Burns, C.E. (2013) Geomorphology within the interdisciplinary science of environmental flows, *Geomorphology*, *200*: 143–54.
- Meyer-Peter, E., and Muller, R. (1948). Formulas for bed-load transport. (pp. 39-64). Stockholm: Proceedings, 2nd Congress, International Association of Hydraulic Research.
- Miall, A.D. (1977). A review of the braided river depositional environment. *Earth Science Reviews*, *13*, 1-62.
- Micheli, E. R., and Larsen, E. W. (2011). River Channel Cutoff Dynamics, Sacramento River, California, USA. *River Research and Applications*, *27*, 328-44.
- Millar, R. G. (2000). Influence of bank vegetation on alluvial channel patterns. *Water Resources Research*, *36*(4), 1109-18.
- Morisawa, M. (1985). *Rivers*. New York: Longman.
- Montgomery, D.R., (1999). Process domains and the river continuum. *Journal of the American Water Resources Association*, *35*, 397-410.
- Montgomery, D.R., Buffington, J.M. (1998). Channel processes, classification and response potential. In: *River ecology and management*. (Eds. Naiman, R.J., Bilby, R.E.), New York: Springer-Verlag Inc., pp 13-42.
- Mosley, M. (1987). The classification and characterisation of rivers. In K. S. Richards (Ed.), *River Channels: environment and Process* (pp. 295-320). Oxford: Blackwell.
- Naiman, R. J., Lonzarich, D. G., Beechie, T. J., and Ralph, S. C. (1992). General principles of classification and the assessment of conservation potential in

- ivers. In P. J. Boon, P. Calow, and G. E. Petts, *River Conservation and Management* (pp. 93-124). Chichester: John Wiley and Sons Ltd.
- Nanson, G. C. (1980). Point bar and floodplain formation of the meandering Beatton River, northeastern British Columbia, Canada. *Sedimentology*, 27(1), 3-29.
- Nanson, G. C. (1981). New evidence of scroll-bar formation on the Beatton river. *Sedimentology*, 28(6), 889-91.
- Nanson, G. C., and Croke, J. C. (1992). A genetic classification of floodplain. *Geomorphology*, 4, 459-86.
- Nanson, G. C., and Hickin, E. J. (1983). Channel migration and incision on the Beatton River. *Journal of Hydraulic Engineering, ASCE*, 109(3), 327-37.
- Nanson, G. C., and Knighton, A. D. (1966). Anabranching rivers: their cause, character and classification. *Earth Surface Processes and Landforms*, 21, 217-39.
- National Rivers Authority. (1992). *River channel typology for river planning and management, Internal report to NRA Thames region, prepared by Geodata Unit*. Southampton: Southampton University.
- Newson, M. D., Clark, M. J., Sear, D. A., and Brookes, A. (1998). The geomorphological basis for classifying rivers. *Aquatic Conservation*, 8, 415-30.
- Osterkamp, W. R. (1998). Processes of fluvial island formation, with examples from plum creek, Colorado and Snake River, Idaho. *Wetlands*, 18(4), 530-45.
- Page, K., and Nanson, G. (1982). Concave-bank benches and associated floodplain formation. *Earth Surface Processes and Landforms*, 7(6), 529-43.
- Pannekoek, A. J., and Van Straaten, L. M. (1984). *Algemene geologie*. Groningen: Wolters-Noordhoff.
- Parker, G. (1976). On the cause and characteristic scales of meandering and braiding in rivers. *Journal of Fluid Mechanics*, 76, 457-80.
- Parker, G. (1990). Surface-based bedload transport relation for gravel rivers. *Journal of Hydraulic Research*, 28, 417-36.

- Parker, G. (1991). Selective sorting and abrasion of river gravel: I Theory. *Journal of Hydraulic Engineering, ASCE*, 117, 131-49.
- Parker, G., and Andrews, E. D. (1985). Sorting of bed load sediment by flow in meander bends. *Water Resources Research, AGU*, 21(9), 1362-73.
- Parker, C., Clifford, N.J. and Thorne, C.R. (2012) Automatic delineation of functional river reach boundaries for river research and applications. *River Research and Applications*, 28, 1708-1725.
- Parker, G., Wilcock, P. R., Paola, C., Dietrich, W. E., and Pitlick, J. (2007). Physical basis for quasi-universal relations describing bankfull hydraulic geometry of single-thread gravel bed rivers. *Journal Geophysical Research: Earth Surface*, 112(4). doi:10.1029/2006JF000549
- Peters, J. (1978). Discharge and sand transport in the braided zone of the Zaire estuary. *Netherlands Journals of Sea Research*, 12(3/4), 273-92.
- Pizzuto, J. E. (1994). Channel adjustments to changing discharges, Powder River, Montana. *Geological Society of American Bulletin*, 106, 1494-501.
- Pizzuto, J. E., and Meckelnburg, T. S. (1989). Evaluation of a linear bank erosion equation. *Water Resources Res*, 25(5), 1005-13.
- Ponce, V. M. (1989). *Engineering Hydrology, Principles and Practices*. Prentice Hall. Retrieved from ponce.sdsu.edu/onlinegumbel.php
- Puhakka, M., Kalliola, R., Rajasilta, M., and Solo, J. (1992). River types, site evolution and successional vegetation patterns in Peruvian Amazonia. *Journal of Biogeography*, 19(6), 651-65.
- Repetto, R., and Tubino, M. (1999), Transition from migrating alternate bars to steady central bars in channels with variable width. In: Proceedings of IAHR-RCEM Symposium, Genova, Italy, 6–10 September, vol. 1, pp. 605–614, Genoa, Italy.
- Repetto, R., Tubino, M., and Paola, C. (2002). Planimetric instability of channel with variable width. *Journal of Fluid Mechanics*, 457, 79-109.

- Requena, P., Weichert, R. B., and Minor, H. E. (2006). Self widening by lateral erosion in gravel bed rivers. In R. M. Ferreira, E. C. Alves, J. G. Leal, and A. H. Cardoso (Eds.), *River Flow 2006, Lisbon, 6-8 Sept* (pp. 1801-9). London: Taylor and Francis.
- Richards, K. S. (1976). Channel width and the riffle-pool sequence. *Bulletin of the Geological Society of America*, 87(6), 883-90.
- Rinaldi, M., Surian, N., Comiti, F., Bussettini, M., (2013). A method for the assessment and analysis of the hydromorphological condition of Italian streams: The Morphological Quality Index (MQI). *Geomorphology*, 180-181, 96-108.
- Rodrigues, S., Claude, N., and Breheret, J. -G. (2012). An opportunity to connect the morphodynamics of alternate bars with their sedimentary products. *Earth Surface Processes and Landforms*, 37(2), 240-248.
- Rosgen, D. L. (1994). A classification of natural rivers. *Catena*, 22, 169-99.
- Rosgen, D. L. (1996). *Applied River Morphology*. Pagosa Springs: Wildland Hydrology.
- Rozovskii, I. (1957). *Flow of the water in bends of open channels*. Kiev, Ukraine: Academy of Science of the Ukrainian SSR, Kiev (in Russian). Translated 1961 by Prushansky, Israel Program for Scientific Translations, S. Monson, Jerusalem, PST Cat. No. 363.
- Rust, B. (1978). A classification of alluvial channel systems. In C. S. Geol., *Fluvial Sedimentology* (Vol. Memoir No. 5, pp. 187-98).
- Schumm, S. (1985). Patterns of alluvial rivers. *Annual Review, Earth and Planetary Sciences*, 13, 5-27.
- Schumm, S. A. (1963). Sinuosity of alluvial river channels. *United States Geological society of America*, 74, 1089-100.
- Schumm, S. A. (1977). *The Fluvial System*. New York: John Wiley and Sons.
- Schumm, S. A. (1981). Evolution and response of the fluvial system, sedimentologic implications. *Sos. Econ. Paleont. Min. Sp. Publ.*, 31, 19-29.

- Schumm, S. A. (2005). *River Variability and Complexity* (1st ed.). Cambridge: Cambridge University Press.
- Schumm, S. A., and Khan, H. R. (1972). Experimental Study of Channel Patterns. *Bulletin of Geological Society of America*, 83, pp. 1755-70.
- Seal, R., Toro-Escobar, C., Cui, Y., Paola, C., Parker, G., Southard, J. B., and Wilcock, P. R. (1998). Downstream fining by selective deposition: theory, laboratory, and field observation. In P. C. Klingeman, R. L. Beschta, P. D. Komar, and J. B. Bradley (Eds.), *Gravel-bed rivers in the environment* (pp. 61-84). Highlands Ranch, Colorado, U.S.A.: Water Resources Publications.
- Seminara, G., and Tubino, M. (1992). Weakly nonlinear theory of regular meanders, *J. Fluid Mech.*, 244, 257–288.
- Seminara, G., Zolezzi, G., Tubino, M., and Zardi, D. (2001). Downstream and upstream influence in river meandering. Part 2. Planimetric development. *Journal of Fluid Mechanics*, 438, 213-30.
- Simons, D. B., and Richardson, E. V. (1966). Resistance to flow in alluvial channels. In *Prof. Paper No. 422-J*. U.S. Geological Survey.
- Simpson, C. J., and Smith, D. G. (2000). Channel change and low energy braiding on the sand-bed Milk River. Southern Alberta - Northern Montana: Conference GeoCanada 2000 - The Millenium Summit. Retrieved from www.cseg.ca/conferences/2000
- Slaymaker, H. O. (1980). Geomorphic field experiments: inventory and prospects. *Z. Geomorphol. NF*, 35, 183-94.
- Smith, C. E. (1998). Modelling high sinuosity meanders in a small flume. *Geomorphology*, 25, 19-30.
- Smith, N. D. (1974). Sedimentology and bar formation in the Upper kicking Horse River, a braided outwash stream. *Journal of Geology*, 82, 205-23.
- Smith, D. G., and Smith, N. D. (1980). Sedimentation in anastomosing river systems: examples from alluvial valleys near Banff, Alberta. *Journal of Sedimentary Petrology*, 50, 157-64.

- Stahl K, Hisdal H, Hannaford J, Tallaksen LM, van Lanen HAJ, Sauquet E, et al. (2010). Streamflow trends in Europe: evidence from a dataset of near-natural catchments. *Hydrol Earth Syst Sci*, 14, 2367–2382.
- Struiksmā, N. and Crosato, A. (1989) Analysis of a 2-D Bed Topography Model for Rivers. In: *River Meandering*, S. Ikeda and G. Parker (eds.), American Geophysical Union, Washington, D. C..
- Struiksmā, N., Olesen, K. W., Flokstra, C., and De Vriend, H. J. (1985). Bed deformation in curved alluvial channels. *Journal of Hydraulic Research, IAHR*, 23(1), 57-79.
- Tal, M., and Paola, C. (2005). Braided morphology and vegetation dynamics in a laboratory channel. *6th International Gravel bed Rivers Workshop*. Lienz, Austria.
- Thorndycraft, V. R., Benito, G., and Gregory, K. J. (2008). Fluvial geomorphology: A perspective on current status and methods. *Geomorphology*, 98, 2-12.
- Thorp, J.H., Thoms, M.C., Delong, M.D., (2006). The riverine ecosystem synthesis: biocomplexity in river networks across space and time. *River Research and Applications*, 22, 123-147.
- Tubino, M. (1991). Growth of Alternate Bars in Unsteady Flow. *Water Resources Research*, 27(1), 37-52.
- Tubino, M., and Seminara, G. (1990). Free forced interactions in developing meanders and suppression of free bars. *Journal of Fluid Mechanics*, 214, 131-159.
- Tubino, M., Repetto, R., and Zolezzi, G. (1999). Free bars in rivers. *Journal of Hydraulic Research*, 37(6), 759-775.
- Van den Berg, J. H. (1995). Prediction of alluvial channel pattern of perennial rivers. *Geomorphology*, 12, 259-79.
- Wang, G., Xia, J., and Wu, B. (2004). Two-dimensional composite mathematical alluvial model for the braided reach of the lower Yellow River. *Water International*, 29(4), 455-66.

- Ward, J. H. (1963). Hierarchical grouping to optimize an objective function. *Journal of the American Statistical Association*, 58, 238-44.
- Ward, P. D., Montgomery, D. R., and Smith, R. (2000). Altered river morphology in South Africa related to the Permian-Triassic extinction. *Science*, 289(5485), 1740-43.
- Welford, M. R. (1994). A field-test of Tubino's (1991) model of alternate bar formation. *Earth Surface Processes and Landforms*, 19(4), 287-97.
- Williams, G. P. (1978). Bankfull discharge in rivers. *Water Resources Research, AGU.* , 14, 1141-54.
- Zen, S., Zolezzi, G., and Tubino, M. (2014). A theoretical analysis of river bars stability under changing channel width. *Advances in Geosciences*, 39, 27-35.
- Zolezzi, G., and Seminara, G. (2001). Downstream and upstream influence in river meandering. Part 1. General theory and application of overdeepening. *Journal of Fluid Mechanics*, 438, 183-211.
- Zolezzi, G., Guala, M., Termini, D., and Seminara, G. (2005). Experimental observation of upstream overdeepening. *Journal of Fluid Mechanics*, 531, 191-219.
- Zolezzi, G., Luchi, R., and Tubino, M. (2009). Coupling the dynamics of channel width and curvature in meandering rivers: a perspective on fluvial patterns. Santa Fe (Argentina): Proc. of RCEM 2009 - VI Symposium in River, Coastal and Estuarine Morphodynamics, 21-25 September.
- Zolezzi, G., Luchi, R., and Tubino, M. (2012a). Modelling morphodynamic processes in meandering rivers with spatial width variations. *Reviews of Geophysics*, 50(4), art. no. RG4005. doi:10.1029/2012RG000392
- Zolezzi, G., Bertoldi, W., and Tubino, M. (2012b), Morphodynamics of bars in gravel-bed rivers: Bridging analytical models and field observations. In: *Gravel-Bed Rivers: Processes, Tools, Environments*, M. Church, P. M. Biron, and A. Roy (eds.), Chapter 6, pp. 69–89, John Wiley, Chichester, U. K.

APPENDIX: FULL DATA SET EXTRACTED FROM GOOGLE EARTH IMAGES

260

Descriptions				Group 1 – Dimensions						Group 2 –Dim. ratio			Group 3 - Flow features					Group 4 - Bars and Benches					Group 5 - Floodplain Features							Group 6 - Vegetation								
Site	Reach no.	River Name	Country	Baseflow Median Width (m)	Baseflow Sinuosity	Baseflow Channel Slope (per mil)	Bankfull Median Width (m)	Bankfull Sinuosity	Bankfull Channel Slope (per mil)	Valley Gradient (per mil)	Baseflow_Bankfull Median Width	Baseflow_Bankfull Sinuosity	Baseflow_Bankfull Channel Slope	Pools	Riffles	Cascade	Waterfall and Steps	Boulders	Exposed Bedrock	Total Active Marginal Bars	Total Stabilising Marginal Bars	Total Active Mid-Channel Bars	Total Stabilising mid-channel bar	Total Active Bench	Total Stabilising Bench	Total Swamp-Wetland	Total Water-fill ponds	Total connected side channels	Total Dry depressions	Total Ridges and Swales	Total Oxbow	Total Stabilising arcuate bars	Total Stabilising Marginal bars (non-arcuate shape)	Vegetation Structure	Weighted Tree Distribution	Total Wood Jams	Emergent Macrophytes	
1	1	Caersws	Wales	16	1	2	37	1	2	2	0.4	1.0	1.0	0.0	0.0	0.0	0.0	0.0	0.0	0.1	0.0	0.0	0.0	0.0	0.0	0.0	0.0	0.0	0.0	0.0	0.0	0.0	0.0	0.0	1.6	1.5	0.0	0.0
1	2	Caersws	Wales	19	1	2	52	1	2	3	0.4	1.1	1.1	0.0	0.0	0.0	0.0	0.0	0.0	0.1	0.0	0.0	0.0	0.0	0.0	0.0	0.0	0.0	0.0	0.0	0.0	0.0	0.0	1.9	1.7	0.0	0.0	
1	3	Caersws	Wales	26	2	1	63	1	1	2	0.4	1.0	0.0	0.0	0.0	0.0	0.0	0.0	0.0	0.2	0.0	0.0	0.0	0.0	0.0	0.0	0.0	0.0	0.0	0.0	0.0	0.0	0.0	0.7	1.3	0.0	0.0	
1	4	Caersws	Wales	22	1	0	35	1	0	0	0.6	1.1	1.1	0.0	0.0	0.0	0.0	0.0	0.0	0.0	0.0	0.0	0.0	0.0	0.0	0.0	0.0	0.0	0.0	0.0	0.0	0.0	1.8	2.7	0.0	0.0		
2	1	Dee	Wales/Engl and	28	1	0	35	1	0	0	0.1	1.1	1.1	0.0	0.0	0.0	0.0	0.0	0.0	0.0	0.0	0.0	0.0	0.0	0.0	0.0	0.0	0.0	0.0	0.0	0.0	0.0	1.3	2.5	0.0	3.0		
2	2	Dee	Wales/Engl and	33	2	0	34	2	0	1	1.0	1.1	1.1	0.0	0.0	0.0	0.0	0.0	0.0	0.0	0.0	0.0	0.0	0.0	0.0	0.0	0.0	0.0	0.0	0.0	0.0	0.0	1.1	1.2	0.0	0.0		
2	3	Dee	Wales/Engl and	25	2	0	27	2	0	0	0.9	1.0	0.0	0.0	0.0	0.0	0.0	0.0	0.0	0.0	0.0	0.0	0.0	0.0	0.0	0.0	0.0	0.0	0.0	0.0	0.0	0.0	1.2	1.7	0.0	0.0		
3	1	Allier	France	81	1	1	10	1	1	1	0.8	1.0	1.0	0.0	0.0	0.0	0.0	0.0	0.0	0.0	0.0	0.0	0.0	0.0	0.0	0.0	0.0	0.0	0.0	0.0	0.0	0.0	2.4	3.2	0.0	0.0		
3	2	Allier	France	61	1	1	5	1	1	1	0.5	1.0	1.0	0.0	0.0	0.0	0.0	0.0	0.0	0.1	0.0	0.0	0.0	0.0	0.0	0.0	0.1	0.0	0.0	0.0	0.0	0.0	0.0	2.1	2.5	0.0	0.0	
3	3	Allier	France	82	1	1	15	1	1	1	0.5	1.0	1.0	0.0	0.0	0.0	0.0	0.0	0.0	0.1	0.0	0.0	0.0	0.0	0.0	0.0	0.0	0.0	0.0	0.0	0.0	0.0	2.3	2.5	0.0	0.0		
4	1	Narrew	Poland	15	1	0	15	1	0	0	1.0	1.1	1.0	0.0	0.0	0.0	0.0	0.0	0.0	0.0	0.0	0.0	0.0	0.0	0.0	0.0	0.0	0.0	0.0	0.0	0.0	0.0	0.0	0.2	0.0	0.0	0.0	
4	2	Narrew	Poland	27	1	0	27	1	0	0	1.0	1.1	1.0	0.0	0.0	0.0	0.0	0.0	0.0	0.0	0.0	0.0	0.0	0.0	0.0	0.0	0.0	0.0	0.0	0.0	0.0	0.0	0.6	0.1	0.0	0.0		
4	3	Narrew	Poland	21	1	0	21	1	0	0	1.0	1.0	0.0	0.0	0.0	0.0	0.0	0.0	0.0	0.0	0.0	0.0	0.0	0.0	0.0	0.0	0.0	0.0	0.0	0.0	0.0	0.0	0.3	0.2	0.0	0.0		
5	1	Tietar	Spain	24	1	2	43	1	2	2	0.5	1.1	1.0	0.0	0.0	0.0	0.0	0.0	0.0	0.0	0.0	0.0	0.0	0.0	0.0	0.0	0.0	0.0	0.0	0.0	0.0	0.0	1.8	3.0	0.0	0.0		
5	2	Tietar	Spain	37	1	1	58	1	1	1	0.6	1.0	1.0	0.0	0.0	0.0	0.0	0.0	0.0	0.0	0.0	0.0	0.0	0.0	0.0	0.0	0.0	0.0	0.0	0.0	0.0	0.0	1.9	3.1	0.0	0.0		

Descriptions				Group 1 – Dimensions						Group 2 – Dim. ratio			Group 3 - Flow features					Group 4 - Bars and Benches					Group 5 - Floodplain Features							Group 6 - Vegetation									
Site	Reach no.	River Name	Country	Baseflow Median Width (m)	Baseflow Sinuosity	Baseflow Channel Slope (per mil)	Bankfull Median Width (m)	Bankfull Sinuosity	Bankfull Channel Slope (per mil)	Valley Gradient (per mil)	Baseflow_Bankfull Median Width	Baseflow_Bankfull Sinuosity	Baseflow_Bankfull Channel Slope	Pools	Riffles	Cascade	Waterfall and Steps	Boulders	Exposed Bedrock	Total Active Marginal Bars	Total Stabilising Marginal Bars	Total Active Mid-Channel Bars	Total Stabilising mid-channel bar	Total Active Bench	Total Stabilising Bench	Total Swamp-Wetland	Total Water-fille ponds	Total connected side channels	Total Dry depressions	Total Ridges and Swales	Total Oxbow	Total Stabilising arcuate bars	Total Stabilising Marginal bars (non-arcuate shape)	Vegetation Structure	Weighted Tree Distribution	Total Wood Jams	Emergent Macrophytes		
5	3	Tietar	Spain	32	1	1	53	1	1	1	0.6	1.0	1.0	0.0	0.0	0.0	0.0	0.0	0.0	0.0	0.1	0.4	0.0	0.1	0.0	0.0	0.0	0.0	0.0	0.0	0.0	0.0	0.0	0.0	0.0	2.8	4.0	0.0	0.0
5	4	Tietar	Spain	23	1	3	23	1	3	3	0.0	0.0	0.0	0.0	0.0	0.0	0.0	0.0	0.0	0.0	0.0	0.0	0.0	0.0	0.0	0.0	0.0	0.0	0.0	0.0	0.0	0.0	0.0	0.0	1.6	1.8	0.0	0.0	
6	1	Knappan	Norway	67	1	1	67	1	1	2	1.0	1.0	1.0	0.0	0.0	0.0	0.0	0.0	0.0	0.0	0.0	0.0	0.0	0.0	0.0	0.0	0.0	0.0	0.0	0.0	0.0	0.0	0.0	2.0	4.9	0.0	0.0		
6	2	Knappan	Norway	96	1	1	96	1	1	2	1.0	1.0	1.0	0.0	0.0	0.0	0.0	0.0	0.0	0.0	0.0	0.0	0.0	0.0	0.0	0.0	0.0	0.0	0.0	0.0	0.0	0.0	0.0	2.0	4.2	0.0	0.0		
7	1	Lafnitz	Austria	16	1	5	24	1	5	6	0.7	1.0	1.0	0.0	0.0	0.0	0.0	0.0	0.0	0.0	0.0	0.0	0.0	0.0	0.0	0.0	0.0	0.0	0.0	0.0	0.0	0.0	0.0	2.9	4.4	0.0	0.0		
7	2	Lafnitz	Austria	13	1	3	15	1	3	4	0.9	1.0	1.0	0.0	0.0	0.0	0.0	0.0	0.0	0.0	0.0	0.0	0.0	0.0	0.0	0.0	0.0	0.0	0.0	0.0	0.0	0.0	0.0	2.3	4.7	0.0	0.0		
7	3	Lafnitz	Austria	13	2	2	16	2	2	3	0.8	1.0	1.0	0.0	0.0	0.0	0.0	0.0	0.0	0.0	0.0	0.0	0.0	0.0	0.0	0.0	0.0	0.0	0.0	0.0	0.0	0.0	0.0	2.8	4.6	0.0	0.0		
8	1	Dane	England	12	2	3	15	2	3	5	0.8	1.0	1.0	0.0	0.0	0.0	0.0	0.0	0.0	0.0	0.0	0.0	0.0	0.0	0.0	0.0	0.0	0.0	0.0	0.0	0.0	0.0	0.0	2.9	3.4	0.0	1.0		
8	2	Dane	England	19	2	1	20	2	1	1	1.0	1.0	1.0	0.0	0.0	0.0	0.0	0.0	0.0	0.0	0.0	0.0	0.0	0.0	0.0	0.0	0.0	0.0	0.0	0.0	0.0	0.0	0.0	1.9	2.9	0.0	1.0		
8	3	Dane	England	14	2	2	15	2	2	3	0.9	1.0	1.0	0.0	0.0	0.0	0.0	0.0	0.0	0.0	0.0	0.0	0.0	0.0	0.0	0.0	0.0	0.0	0.0	0.0	0.0	0.0	0.0	2.1	3.2	0.0	0.0		
9	1	Cecina	Italy	19	1	1	38	1	1	2	0.5	1.0	1.0	0.0	0.0	0.0	0.0	0.0	0.0	0.0	0.0	0.0	0.0	0.0	0.0	0.0	0.0	0.0	0.0	0.0	0.0	0.0	0.0	2.2	4.7	0.0	0.0		
9	2	Cecina	Italy	18	1	2	26	1	2	3	0.7	1.0	1.0	0.0	0.0	0.0	0.0	0.0	0.0	0.0	0.0	0.0	0.0	0.0	0.0	0.0	0.0	0.0	0.0	0.0	0.0	0.0	0.0	2.6	4.6	0.0	0.0		
9	3	Cecina	Italy	18	1	1	25	1	1	2	0.7	1.0	1.0	0.0	0.0	0.0	0.0	0.0	0.0	0.0	0.0	0.0	0.0	0.0	0.0	0.0	0.0	0.0	0.0	0.0	0.0	0.0	0.0	0.0	2.7	2.7	0.0	0.0	
10	1	Naver	Scotland	31	1	3	45	1	3	4	0.7	1.0	1.0	0.0	0.0	0.0	0.0	0.0	0.0	0.0	0.0	0.0	0.0	0.0	0.0	0.0	0.0	0.0	0.0	0.0	0.0	0.0	0.0	1.0	1.9	0.0	0.0		
10	2	Naver	Scotland	26	1	1	39	1	1	1	0.7	1.0	1.0	0.0	0.0	0.0	0.0	0.0	0.0	0.0	0.0	0.0	0.0	0.0	0.0	0.0	0.0	0.0	0.0	0.0	0.0	0.0	0.0	1.3	2.9	0.0	0.0		
10	3	Naver	Scotland	29	1	4	44	1	4	5	0.7	1.0	1.0	0.0	0.0	0.0	0.0	0.0	0.0	0.0	0.0	0.0	0.0	0.0	0.0	0.0	0.0	0.0	0.0	0.0	0.0	0.0	0.0	0.0	1.4	1.7	0.0	0.0	
11	1	Aragon	Spain	35	1	8	61	1	8	9	0.6	1.0	1.0	0.0	0.0	0.0	0.0	0.0	0.0	0.0	0.0	0.0	0.0	0.0	0.0	0.0	0.0	0.0	0.0	0.0	0.0	0.0	0.0	2.6	3.9	0.0	0.0		
11	2	Aragon	Spain	31	1	7	58	1	8	8	0.5	1.0	1.0	0.0	0.0	0.0	0.0	0.0	0.0	0.0	0.0	0.0	0.0	0.0	0.0	0.0	0.0	0.0	0.0	0.0	0.0	0.0	0.0	2.2	4.3	0.0	0.0		
11	3	Aragon	Spain	40	1	6	58	1	6	7	0.7	1.0	1.0	0.0	0.0	0.0	0.0	0.0	0.0	0.0	0.0	0.0	0.0	0.0	0.0	0.0	0.0	0.0	0.0	0.0	0.0	0.0	0.0	2.0	3.3	0.0	0.0		
12	1	San Tirso	Spain	27	2	2	27	2	2	4	1.0	1.0	1.0	0.0	0.0	0.0	0.0	0.0	0.0	0.0	0.0	0.0	0.0	0.0	0.0	0.0	0.0	0.0	0.0	0.0	0.0	0.0	0.0	2.0	4.8	0.0	0.0		

Descriptions				Group 1 – Dimensions							Group 2 – Dim. ratio			Group 3 - Flow features					Group 4 - Bars and Benches					Group 5 - Floodplain Features							Group 6 - Vegetation						
Site	Reach no.	River Name	Country	Baseflow Median Width (m)	Baseflow Sinuosity	Baseflow Channel Slope (per mil)	Bankfull Median Width (m)	Bankfull Sinuosity	Bankfull Channel Slope (per mil)	Valley Gradient (per mil)	Baseflow_Bankfull Median Width	Baseflow_Bankfull Sinuosity	Baseflow_Bankfull Channel Slope	Pools	Riffles	Cascade	Waterfall and Steps	Boulders	Exposed Bedrock	Total Active Marginal Bars	Total Stabilising Marginal Bars	Total Active Mid-Channel Bars	Total Stabilising mid-channel bar	Total Active Bench	Total Stabilising Bench	Total Swamp-Wetland	Total Water-fille ponds	Total connected side channels	Total Dry depressions	Total Ridges and Swales	Total Oxbow	Total Stabilising arcuate bars	Total Stabilising Marginal bars (non-arcuate shape)	Vegetation Structure	Weighted Tree Distribution	Total Wood Jams	Emergent Macrophytes
1	2	San Tirso	Spain	22	2	4	31	2	4	7	0.7	1.1	1.0	0.0	0.0	0.0	0.0	0.0	0.0	0.0	0.0	0.0	0.0	0.0	0.0	0.0	0.0	0.0	0.0	0.0	0.0	0.0	0.0	2.0	4.4	0.0	0.0
2	1	Speller	Germany	37	1	1	37	1	1	1	1.0	1.0	1.0	0.0	0.0	0.0	0.0	0.0	0.0	0.0	0.0	0.0	0.0	0.0	0.0	0.0	0.0	0.0	0.0	0.0	0.0	0.0	0.0	2.0	2.6	0.0	0.0
1	2	Speller	Germany	44	2	0	44	2	0	0	1.0	1.0	1.0	0.0	0.0	0.0	0.0	0.0	0.0	0.0	0.0	0.0	0.0	0.0	0.0	0.0	0.0	1	0	0	0	0	0	3.0	2.1	0.0	0.0
1	3	Speller	Germany	52	2	0	52	2	0	0	1.0	1.0	1.0	0.0	0.0	0.0	0.0	0.0	0.0	0.0	0.0	0.0	0.0	0.0	0.0	0.0	0.0	3	1	0	0	0	0	1.9	1.8	0.0	0.0
1	4	Oste	Germany	12	1	0	12	1	0	0	1.0	1.0	1.0	0.0	0.0	0.0	0.0	0.0	0.0	0.0	0.0	0.0	0.0	0.0	0.0	0.0	0.0	3	0	0	0	0	0	2.0	2.7	0.0	0.0
1	4	Oste	Germany	14	1	1	14	1	1	1	1.0	1.0	1.0	0.0	0.0	0.0	0.0	0.0	0.0	0.0	0.0	0.0	0.0	0.0	0.0	0.0	0.0	1	0	0	0	0	0	2.2	2.1	0.0	0.0
1	4	Oste	Germany	13	1	1	13	1	1	1	1.0	1.0	1.0	0.0	0.0	0.0	0.0	0.0	0.0	0.0	0.0	0.0	0.0	0.0	0.0	0.0	1	0	1	0	0	0	1.7	2.3	0.0	0.0	
1	4	Oste	Germany	13	1	0	13	1	0	0	1.0	1.0	1.0	0.0	0.0	0.0	0.0	0.0	0.0	0.0	0.0	0.0	0.0	0.0	0.0	0.0	0.0	0	0	0	0	0	0	1.8	1.9	0.0	0.0
1	5	Krupinica	Slovakia	10	1	3	10	1	3	4	1.0	1.0	1.0	0.0	0.0	0.0	0.0	0.0	0.0	0.0	0.0	0.0	0.0	0.0	0.0	0.0	0	0	0	0	0	0	2.8	4.0	0.0	0.0	
1	5	Krupinica	Slovakia	11	1	2	11	1	2	3	1.0	1.0	1.0	0.0	0.0	0.0	0.0	0.0	0.0	0.0	0.0	0.0	0.0	0.0	0.0	0.0	0	0	0	0	0	0	2.8	3.7	0.0	0.0	
1	5	Krupinica	Slovakia	14	1	1	14	1	1	1	1.0	1.0	1.0	0.0	0.0	0.0	0.0	0.0	0.0	0.0	0.0	0.0	0.0	0.0	0.0	0.0	0	0	0	0	0	0	2.6	3.3	0.0	0.0	
1	6	Isen	Germany	6	1	3	6	1	3	4	1.0	1.0	1.0	0.0	0.0	0.0	0.0	0.0	0.0	0.0	0.0	0.0	0.0	0.0	0.0	0.0	0	0	0	0	0	0	2.8	4.5	0.0	0.0	
1	6	Isen	Germany	12	1	4	12	1	4	6	1.0	1.0	1.0	0.0	0.0	0.0	0.0	0.0	0.0	0.0	0.0	0.0	0.0	0.0	0.0	0.0	0	0	0	0	0	0	2.8	3.9	0.0	0.0	
1	6	Isen	Germany	6	1	2	6	1	2	3	1.0	1.0	1.0	0.0	0.0	0.0	0.0	0.0	0.0	0.0	0.0	0.0	0.0	0.0	0.0	0.0	0	0	0	0	0	0	3.0	4.5	0.0	0.0	
1	7	Siret	Romania	53	2	0	11	3	2	1	0.5	1.9	0.2	0.0	0.1	0.0	0.0	0.0	0.0	0.2	0.0	0.0	0.0	0.0	0.0	0.0	0.0	1	1	5	0	0	1.1	1.5	0.0	0.0	
1	7	Siret	Romania	62	2	1	19	0	1	1	0.3	1.9	0.2	0.0	0.1	0.0	0.0	0.0	0.0	0.3	0.0	0.0	0.0	0.0	0.0	0.0	0.0	1	1	4	0	0	0.0	1.0	0.0	0.0	
1	7	Siret	Romania	81	2	1	##	1	1	1	0.3	1.8	0.7	0.0	0.0	0.0	0.0	0.0	0.0	0.3	0.0	0.0	0.0	0.0	0.0	0.0	0.0	2	9	3	0	0	0.7	1.1	0.0	0.0	
1	8	L'Oise	France	23	1	0	23	1	0	0	1.0	1.0	1.0	0.0	0.0	0.0	0.0	0.0	0.0	0.0	0.0	0.0	0.0	0.0	0.0	0.0	1	1	0	0	0	0	1.7	2.1	0.0	1.0	
1	8	L'Oise	France	23	1	0	23	1	0	0	1.0	1.0	1.0	0.0	0.0	0.0	0.0	0.0	0.0	0.0	0.0	0.0	0.0	0.0	0.0	0.0	0	0	0	0	0	0	6	9	0.0	0.0	
1	8	L'Oise	France	29	2	1	29	2	1	1	1.0	1.0	1.0	0.0	0.0	0.0	0.0	0.0	0.0	0.0	0.0	0.0	0.0	0.0	0.0	0.0	0	1	0	0	0	0	1.1	1.9	0.0	0.0	

Descriptions				Group 1 – Dimensions						Group 2 – Dim. ratio			Group 3 - Flow features						Group 4 - Bars and Benches						Group 5 - Floodplain Features						Group 6 - Vegetation							
Site	Reach no.	River Name	Country	Baseflow Median Width (m)	Baseflow Sinuosity	Baseflow Channel Slope (per mil)	Bankfull Median Width (m)	Bankfull Sinuosity	Bankfull Channel Slope (per mil)	Valley Gradient (per mil)	Baseflow_Bankfull Median Width	Baseflow_Bankfull Sinuosity	Baseflow_Bankfull Channel Slope	Pools	Riffles	Cascade	Waterfall and Steps	Boulders	Exposed Bedrock	Total Active Marginal Bars	Total Stabilising Marginal Bars	Total Active Mid-Channel Bars	Total Stabilising mid-channel bar	Total Active Bench	Total Stabilising Bench	Total Swamp-Wetland	Total Water-fille ponds	Total connected side channels	Total Dry depressions	Total Ridges and Swales	Total Oxbow	Total Stabilising arcuate bars	Total Stabilising Marginal bars (non-arcuate shape)	Vegetation Structure	Weighted Tree Distribution	Total Wood Jams	Emergent Macrophytes	
#	3	Malselv	Norway	136	1	1	188	1	1	1	0.7	1.1	1.0	0.0	0.0	0.0	0.0	0.0	0.0	0.13	0.03	0.01	0.01	0.00	0.00	0.00	0.00	0.00	0.00	0.00	0.00	0.00	0.00	0.00	2.59	4.47	0.00	0.00
#	1	Raba	Austria	25	2	0	32	2	0	1	0.8	1.0	0.0	0.0	0.0	0.0	0.0	0.0	0.0	0.00	0.00	0.00	0.00	0.00	0.00	0.00	0.00	0.00	0.00	0.00	0.00	0.00	0.00	2.25	3.69	0.00	0.00	
#	2	Raba	Austria	28	2	0	28	2	0	1	1.0	1.1	0.0	0.1	0.0	0.0	0.0	0.0	0.0	0.00	0.00	0.00	0.00	0.00	0.00	0.00	0.00	0.00	0.00	0.00	0.00	0.00	0.00	2.94	4.61	0.00	0.00	
#	3	Raba	Austria	27	2	1	27	2	1	2	1.0	1.1	0.0	0.0	0.0	0.0	0.0	0.0	0.0	0.04	0.01	0.02	0.00	0.00	0.00	0.00	0.00	0.00	0.00	0.00	0.00	0.00	2.83	3.50	0.00	0.00		
#	1	Subersach	Austria	11	1	4	31	1	1	4	0.3	1.1	0.0	0.0	0.0	0.0	0.0	0.15	0.04	0.02	0.01	0.03	0.01	0.00	0.00	0.00	0.00	0.00	0.00	0.00	0.00	0.00	3.05	4.75	0.24	0.00		
#	2	Subersach	Austria	9	1	3	33	1	1	8	0.3	1.1	0.0	0.0	0.0	0.0	0.0	0.18	0.04	0.02	0.01	0.00	0.00	0.00	0.00	0.00	0.00	0.00	0.00	0.00	0.00	0.00	3.04	4.40	0.24	0.00		
#	3	Subersach	Austria	18	1	1	64	1	1	4	0.3	1.1	0.0	0.0	0.0	0.0	0.1	0.06	0.02	0.00	0.01	0.00	0.00	0.00	0.00	0.00	0.00	0.00	0.00	0.00	0.00	3.04	4.40	0.40	0.00			
4	1	L'Aube	France	31	2	0	31	2	0	1	1.0	1.1	0.0	0.0	0.0	0.0	0.0	0.0	0.01	0.00	0.00	0.00	0.00	0.00	0.00	0.00	0.00	0.00	0.00	0.00	0.00	2.63	4.38	0.00	1.00			
4	1	L'Aube	France	24	2	0	24	2	0	1	1.0	1.1	0.0	0.0	0.0	0.0	0.0	0.0	0.01	0.00	0.00	0.00	0.00	0.00	0.00	0.00	0.00	0.00	0.00	0.00	0.00	2.28	4.09	0.00	0.00			
4	1	L'Aube	France	28	2	0	28	2	0	0	1.0	1.1	0.0	0.0	0.0	0.0	0.0	0.0	0.00	0.00	0.00	0.00	0.00	0.00	0.00	0.00	0.00	0.00	0.00	0.00	0.00	2.45	4.45	0.00	0.00			
#	1	Ljusnan	Sweedden	12	1	1	21	1	1	1	0.6	1.1	0.1	0.1	0.0	0.0	0.0	0.0	0.05	0.00	0.02	0.01	0.01	0.00	0.00	0.00	0.00	0.00	0.00	0.00	0.00	0.75	2.70	0.00	0.00			
#	2	Ljusnan	Sweedden	20	1	6	30	1	6	8	0.7	1.1	0.0	0.0	0.0	0.0	0.0	0.0	0.03	0.00	0.00	0.00	0.00	0.00	0.00	0.00	0.00	0.00	0.00	0.00	0.00	2.17	3.17	0.00	0.00			
#	3	Ljusnan	Sweedden	22	1	1	38	1	1	1	0.6	1.1	0.0	0.1	0.0	0.0	0.0	0.0	0.06	0.00	0.04	0.02	0.00	0.00	0.00	0.00	0.00	0.00	0.00	0.00	0.00	1.63	2.79	0.00	0.00			
#	1	Tywi	Wales	44	1	2	62	1	3	3	0.7	1.1	0.0	0.0	0.0	0.0	0.0	0.0	0.08	0.02	0.05	0.01	0.00	0.00	0.00	0.00	0.00	0.00	0.00	0.00	2.00	3.50	0.00	0.00				
#	2	Tywi	Wales	28	2	1	53	2	1	2	0.5	1.1	0.0	0.0	0.0	0.0	0.0	0.0	0.09	0.03	0.01	0.00	0.00	0.00	0.00	0.00	0.00	0.00	0.00	0.00	0.00	0.14	2.14	0.00	0.00			
#	3	Tywi	Wales	37	2	0	58	2	0	1	0.6	1.1	0.0	0.0	0.0	0.0	0.0	0.0	0.01	0.03	0.01	0.01	0.00	0.00	0.00	0.00	0.00	0.00	0.00	0.00	0.00	0.50	1.70	0.00	0.00			
#	1	Le Saux a Vitry en Perthois	France	20	2	1	20	2	1	1	1.0	1.1	0.0	0.0	0.0	0.0	0.0	0.0	0.01	0.00	0.00	0.00	0.00	0.00	0.00	0.00	0.00	0.00	0.00	0.00	0.00	3.00	4.17	0.00	0.00			
#	2	Le Saux a Vitry en Perthois	France	27	2	1	27	2	1	1	1.0	1.1	0.0	0.0	0.0	0.0	0.0	0.0	0.04	0.03	0.01	0.00	0.00	0.00	0.00	0.00	0.00	0.00	0.00	0.00	0.00	2.83	4.06	0.00	0.00			
#	3	Le Saux a Vitry en	France	35	1	1	35	1	1	1	1.0	1.1	0.0	0.0	0.0	0.0	0.0	0.0	0.04	0.01	0.00	0.00	0.00	0.00	0.00	0.00	0.00	0.00	0.00	0.00	0.00	3.00	4.50	0.00	0.00			

Descriptions				Group 1 – Dimensions						Group 2 – Dim. ratio			Group 3 - Flow features					Group 4 - Bars and Benches					Group 5 - Floodplain Features							Group 6 - Vegetation								
Site	Reach no.	River Name	Country	Baseflow Median Width (m)	Baseflow Sinuosity	Baseflow Channel Slope (per mil)	Bankfull Median Width (m)	Bankfull Sinuosity	Bankfull Channel Slope (per mil)	Valley Gradient (per mil)	Baseflow_Bankfull Median Width	Baseflow_Bankfull Sinuosity	Baseflow_Bankfull Channel Slope	Pools	Riffles	Cascade	Waterfall and Steps	Boulders	Exposed Bedrock	Total Active Marginal Bars	Total Stabilising Marginal Bars	Total Active Mid-Channel Bars	Total Stabilising mid-channel bar	Total Active Bench	Total Stabilising Bench	Total Swamp-Wetland	Total Water-fille ponds	Total connected side channels	Total Dry depressions	Total Ridges and Swales	Total Oxbow	Total Stabilising arcuate bars	Total Stabilising Marginal bars (non-arcuate shape)	Vegetation Structure	Weighted Tree Distribution	Total Wood Jams	Emergent Macrophytes	
		Perthois																																				
#	1	Endrick Water nr. Drymen	Scotland	13	1	4	13	1	4	6	1.0	1.0	1.0	0.0	0.0	0.0	0.0	0.0	0.0	0.0	0.0	0.0	0.0	0.0	0.0	0.0	0.0	0.0	0.0	0.0	0.0	0.0	0.0	0.0	1.2	3.0	0.0	0.0
#	2	Endrick Water nr. Drymen	Scotland	21	1	2	25	1	2	2	0.8	1.0	1.0	0.0	0.0	0.0	0.0	0.0	0.0	0.0	0.0	0.0	0.0	0.0	0.0	0.0	0.0	0.0	0.0	0.0	0.0	0.0	0.0	1.0	1.5	0.0	0.0	
#	3	Endrick Water nr. Drymen	Scotland	26	2	0	50	2	0	0	0.5	1.0	1.0	0.0	0.0	0.0	0.0	0.0	0.0	0.0	0.0	0.0	0.0	0.0	0.0	0.0	0.0	0.0	0.0	0.0	0.0	0.0	0.0	0.6	1.3	0.0	0.0	
#	1	Tweed	Scotland	7	1	2	7	1	2	3	1.0	1.0	1.0	0.0	0.0	0.0	0.0	0.0	0.0	0.0	0.0	0.0	0.0	0.0	0.0	0.0	0.0	0.0	0.0	0.0	0.0	0.0	0.0	0.3	1.3	0.0	4.0	
#	2	Tweed	Scotland	20	1	3	20	1	3	4	1.0	1.0	1.0	0.0	0.0	0.0	0.0	0.0	0.0	0.0	0.0	0.0	0.0	0.0	0.0	0.0	0.0	0.0	0.0	0.0	0.0	0.0	1.1	2.4	0.0	0.0		
#	3	Tweed	Scotland	32	1	2	35	1	2	2	0.9	1.0	1.0	0.0	0.0	0.0	0.0	0.0	0.0	0.0	0.0	0.0	0.0	0.0	0.0	0.0	0.0	0.0	0.0	0.0	0.0	0.0	0.0	1.6	2.2	0.0	0.0	
#	1	Spey	Scotland	51	1	3	51	1	3	4	1.0	1.0	1.0	0.0	0.0	0.0	0.0	0.0	0.0	0.0	0.0	0.0	0.0	0.0	0.0	0.0	0.0	0.0	0.0	0.0	0.0	0.0	2.0	4.0	0.0	0.0		
#	2	Spey	Scotland	51	1	3	95	1	3	3	0.5	1.0	1.0	0.0	0.0	0.0	0.0	0.0	0.0	0.0	0.0	0.0	0.0	0.0	0.0	0.0	0.0	0.0	0.0	0.0	0.0	0.0	0.0	2.5	3.8	0.0	0.0	
#	3	Spey	Scotland	50	1	3	13	1	3	4	0.4	1.0	1.0	0.0	0.0	0.0	0.0	0.0	0.0	0.0	0.0	0.0	0.0	0.0	0.0	0.0	0.0	0.0	0.0	0.0	0.0	0.0	0.0	2.2	4.0	0.0	0.0	
#	1	Feshie	Scotland	21	1	8	55	1	8	9	0.4	1.0	1.0	0.1	0.1	0.0	0.0	0.0	0.0	0.0	0.2	0.1	0.0	0.0	0.0	0.0	0.0	0.0	0.0	0.0	0.0	0.0	0.0	1.2	2.0	0.0	0.0	
#	2	Feshie	Scotland	22	1	6	10	1	7	8	0.2	1.0	1.0	0.0	0.0	0.0	0.0	0.0	0.0	0.0	0.5	0.0	0.2	0.0	0.0	0.0	0.0	0.0	0.0	0.0	0.0	0.0	0.0	1.6	2.7	0.0	0.0	
#	3	Feshie	Scotland	23	1	1	53	1	2	3	0.4	1.0	1.0	0.0	0.0	0.0	0.0	0.0	0.0	0.2	0.0	0.1	0.0	0.0	0.0	0.0	0.0	0.0	0.0	0.0	0.0	0.0	1.7	3.5	0.0	0.0		
#	1	Bollin	England	8	2	3	12	1	3	4	0.7	1.0	1.0	0.0	0.0	0.0	0.0	0.0	0.0	0.0	0.1	0.0	0.0	0.0	0.0	0.0	0.0	0.0	0.0	0.0	0.0	0.0	0.6	0.7	0.0	1.0		
#	2	Bollin	England	9	1	2	11	1	2	3	0.8	1.0	1.0	0.0	0.0	0.0	0.0	0.0	0.0	0.0	0.0	0.0	0.0	0.0	0.0	0.0	0.0	0.0	0.0	0.0	0.0	0.0	1.8	2.7	0.0	0.0		
#	3	Bollin	England	7	2	1	11	2	1	1	0.6	1.0	1.0	0.0	0.0	0.0	0.0	0.0	0.0	0.1	0.0	0.0	0.0	0.0	0.0	0.0	0.0	0.0	0.0	0.0	0.0	0.0	1.5	1.8	0.0	5.0		
#	1	Torr ridge	England	15	1	1	17	1	1	1	0.9	1.0	1.0	0.0	0.0	0.0	0.0	0.0	0.0	0.0	0.0	0.0	0.0	0.0	0.0	0.0	0.0	0.0	0.0	0.0	0.0	0.0	2.0	3.3	0.0	0.0		
#	2	Torr ridge	England	20	2	1	33	2	1	2	0.6	1.0	1.0	0.0	0.0	0.0	0.0	0.0	0.0	0.0	0.0	0.0	0.0	0.0	0.0	0.0	0.0	0.0	0.0	0.0	0.0	0.0	2.7	4.6	0.0	0.0		
#	3	Torr ridge	England	22	2	3	29	2	3	5	0.8	1.0	1.0	0.0	0.0	0.0	0.0	0.0	0.0	0.0	0.0	0.0	0.0	0.0	0.0	0.0	0.0	0.0	0.0	0.0	0.0	2.2	3.9	0.0	0.0			

Descriptions				Group 1 – Dimensions						Group 2 – Dim. ratio			Group 3 - Flow features					Group 4 - Bars and Benches					Group 5 - Floodplain Features							Group 6 - Vegetation								
Site	Reach no.	River Name	Country	Baseflow Median Width (m)	Baseflow Sinuosity	Baseflow Channel Slope (per mil)	Bankfull Median Width (m)	Bankfull Sinuosity	Bankfull Channel Slope (per mil)	Valley Gradient (per mil)	Baseflow_Bankfull Median Width	Baseflow_Bankfull Sinuosity	Baseflow_Bankfull Channel Slope	Pools	Riffles	Cascade	Waterfall and Steps	Boulders	Exposed Bedrock	Total Active Marginal Bars	Total Stabilising Marginal Bars	Total Active Mid-Channel Bars	Total Stabilising mid-channel bar	Total Active Bench	Total Stabilising Bench	Total Swamp-Wetland	Total Water-fille ponds	Total connected side channels	Total Dry depressions	Total Ridges and Swales	Total Oxbow	Total Stabilising arcuate bars	Total Stabilising Marginal bars (non-arcuate shape)	Vegetation Structure	Weighted Tree Distribution	Total Wood Jams	Emergent Macrophytes	
# 1	1	Coquet	England	18	1	5	43	1	6	6	0.4	1.0	1.0	0.0	0.0	0.0	0.0	0.0	0.0	0.18	0.03	0.10	0.00	0.01	0.00	0.00	0.00	0.21	0.01	0.00	0.01	0.00	0.01	0.00	1.50	2.33	0.00	0.00
# 2	2	Coquet	England	30	1	3	56	1	3	4	0.5	1.0	0.0	0.0	0.13	0.00	0.00	0.00	0.00	0.16	0.07	0.02	0.00	0.02	0.00	0.00	0.00	0.17	0.01	0.07	0.06	0.01	0.03	0.16	1.69	0.03	0.00	
# 3	3	Coquet	England	19	2	1	32	2	1	2	0.6	1.1	0.0	0.0	0.00	0.00	0.00	0.00	0.00	0.12	0.01	0.03	0.02	0.01	0.00	0.00	0.01	0.07	0.02	0.07	0.01	0.03	0.17	1.72	0.02	0.00		
# 1	1	Nairn	Scotland	5	1	5	12	1	5	7	0.5	1.1	0.0	0.0	0.02	0.00	0.00	0.00	0.00	0.10	0.00	0.02	0.01	0.01	0.00	0.00	0.00	0.01	0.00	0.00	0.00	0.00	0.00	0.07	0.00	0.00	0.00	
# 2	2	Nairn	Scotland	5	1	4	12	1	4	5	0.4	1.0	0.0	0.0	0.00	0.00	0.00	0.00	0.00	0.14	0.00	0.01	0.00	0.01	0.00	0.00	0.00	0.03	0.00	0.00	0.00	0.00	0.00	0.02	0.00	0.00	0.00	
# 3	3	Nairn	Scotland	5	1	2	14	1	2	2	0.4	1.1	0.0	0.0	0.00	0.00	0.00	0.00	0.00	0.09	0.00	0.01	0.00	0.00	0.00	0.00	0.00	0.01	0.00	0.00	0.00	0.00	0.01	0.00	0.00	0.00	0.00	
# 1	1	Annan	England	27	1	4	48	1	4	4	0.6	1.1	0.0	0.0	0.02	0.00	0.00	0.00	0.00	0.10	0.01	0.02	0.00	0.00	0.00	0.00	0.00	0.04	0.00	0.02	0.00	0.00	1.23	3.27	0.00	0.00		
# 2	2	Annan	England	25	1	2	33	1	2	3	0.8	1.0	0.0	0.0	0.01	0.00	0.00	0.00	0.00	0.06	0.00	0.00	0.00	0.00	0.00	0.00	0.00	0.02	0.00	0.00	0.00	0.00	0.66	2.40	0.00	0.00		
# 3	3	Annan	England	20	1	1	25	1	1	2	0.8	1.0	0.0	0.0	0.02	0.00	0.00	0.00	0.00	0.05	0.00	0.00	0.01	0.00	0.00	0.00	0.01	0.00	0.01	0.00	0.09	3.30	0.00	0.00				
# 1	1	Meig	Scotland	19	1	5	41	1	5	5	0.5	1.1	0.0	0.0	0.04	0.00	0.00	0.00	0.00	0.18	0.00	0.01	0.00	0.02	0.00	0.00	0.01	0.02	0.00	0.00	0.00	0.71	2.29	0.00	0.00			
# 2	2	Meig	Scotland	24	1	3	39	1	3	3	0.6	1.1	0.0	0.0	0.04	0.00	0.00	0.00	0.00	0.24	0.00	0.00	0.00	0.00	0.00	0.00	0.00	0.04	0.00	0.00	0.00	0.09	2.25	0.00	0.00			
# 3	3	Meig	Scotland	21	1	4	32	1	4	4	0.7	1.0	0.0	0.0	0.00	0.00	0.02	0.00	0.00	0.14	0.00	0.05	0.01	0.00	0.00	0.00	0.00	0.00	0.00	0.00	0.00	2.25	4.35	0.00	0.00			
# 1	1	Abhnainn	Scotland	10	1	5	24	1	5	7	0.4	1.1	0.0	0.0	0.00	0.00	0.00	0.00	0.00	0.23	0.00	0.01	0.01	0.02	0.00	0.00	0.04	0.04	0.04	0.03	0.02	0.00	1.00	0.00	0.00	0.00		
# 2	2	Abhnainn	Scotland	10	1	0	15	1	0	1	0.7	1.1	0.0	0.0	0.00	0.00	0.00	0.00	0.00	0.09	0.00	0.00	0.00	0.01	0.00	0.00	0.01	0.02	0.00	0.03	0.00	1.00	0.00	0.00	0.00			
# 3	3	Abhnainn	Scotland	15	1	2	16	1	2	3	0.9	1.1	0.0	0.0	0.00	0.00	0.00	0.00	0.00	0.06	0.00	0.00	0.00	0.00	0.00	0.00	0.01	0.00	0.00	0.00	0.00	1.00	0.70	0.00	0.00			
# 1	1	South Tyne	England	17	1	7	39	1	7	7	0.4	1.0	0.0	0.0	0.00	0.00	0.00	0.00	0.00	0.08	0.02	0.02	0.00	0.00	0.00	0.00	0.00	0.05	0.00	0.00	0.00	0.00	2.50	4.13	0.00	0.00		
# 2	2	South Tyne	England	18	1	9	25	1	0	1	0.7	1.1	0.0	0.0	0.01	0.00	0.00	0.00	0.02	0.10	0.00	0.00	0.00	0.00	0.00	0.01	0.00	0.01	0.00	0.00	0.00	2.08	4.08	0.00	0.00			
# 3	3	South Tyne	England	23	1	8	41	1	8	8	0.6	1.1	0.0	0.0	0.00	0.00	0.00	0.00	0.00	0.05	0.01	0.01	0.00	0.00	0.00	0.00	0.00	0.00	0.00	0.00	1.90	3.05	0.00	0.00				
7 1	1	Beaume	France	19	2	3	63	2	3	4	0.3	1.9	0.0	0.0	0.00	0.00	0.00	0.00	0.07	0.34	0.04	0.01	0.00	0.00	0.00	0.00	0.00	0.00	0.00	0.00	0.00	2.29	4.50	0.01	0.00			
7 1	2	Beaume	France	21	2	4	39	2	4	7	0.5	1.0	0.0	0.0	0.00	0.00	0.00	0.00	0.00	0.10	0.00	0.00	0.00	0.00	0.00	0.00	0.00	0.00	0.00	0.03	0.01	2.00	4.40	0.00	0.00			

